

ESTIMATED EDWARDS AQUIFER RECHARGE AND SPRING FLOWS UNDER FUTURE CLIMATE CONDITIONS

CHAPTER 1, FUTURE ESTIMATES OF EDWARDS AQUIFER RECHARGE USING CLIMATE DATA

Authors: H. Başağaoğlu and L. Schmidt

CHAPTER 2, PROJECTED SPRING FLOWS UNDER FUTURE CLIMATE CONDITIONS: MODFLOW MODELING ANALYSIS

Authors: C. Yang and L. Schmidt

Edwards Aquifer Authority
900 E Quincy Street
San Antonio, TX 78215

September 2024



Edwards Aquifer Authority. 2024. *Estimated Edwards Aquifer Recharge and Spring Flows Under Future Climate Conditions*. September. San Antonio, TX. Prepared with assistance from ICF, Austin TX.

Contents

List of Appendices.....	ii
List of Tables.....	ii
List of Figures.....	iii
List of Acronyms and Abbreviations.....	vii
Executive Summary.....	ES-1
Chapter 1 Future Estimates of Edwards Aquifer Recharge Using Climate Data	1-1
1.1 Current Recharge Estimates for the Edwards Aquifer	1-1
1.2 Artificial Intelligence/Machine Learning–Based Aquifer Recharge Models.....	1-3
1.3 Available Recharge Data.....	1-4
1.4 Historical Climate Data for the Edwards Aquifer Region	1-7
1.5 AI/ML-Based Aquifer Recharge Predictions	1-11
1.5.1 Recharge Model Testing	1-12
1.5.2 Importance of Features in Predicting Aquifer Recharge	1-14
1.5.3 AI/ML-Based Aquifer Recharge Predictions with Respect to Groundwater Levels at the Index Wells.....	1-15
1.5.4 AI/ML-Based Aquifer Recharge Predictions and Adjustments	1-18
1.6 Recharge Projections Under Future Climate Conditions.....	1-24
Chapter 2 Projected Spring Flows Under Future Climate Conditions: MODFLOW Modeling Analysis	2-1
2.1 Model Preparation	2-1
2.2 Modeling Procedure.....	2-3
2.3 Model Validation.....	2-5
2.3.1 Comparisons to the Archived EAHCP Phase II Model Runs	2-5
2.3.2 Modeling Analysis Using USGS, HSPF, and AI/ML Modeled Recharge for Historical Period 2001–2022	2-6
2.4 Results and Discussion	2-11
2.4.1 Modeled Projected Water Levels for the J17 Index Well	2-12
2.4.2 Modeled Projected Spring Flows	2-12
2.4.3 Protective Measures Triggered for Climate Projections.....	2-15
2.4.4 Potential Hydrological Droughts Under Future Climates	2-19
2.4.5 Selected Individual Model Results.....	2-21
2.5 Summary	2-28
Chapter 3 References	3-1
3.1 Chapter 1.....	3-1
3.2 Chapter 2.....	3-3

List of Appendices

Appendix A MODFLOW Jupyter Notebook Example

Appendix B Summary of Individual Model Results

Appendix C SAMP Model Runs Inputs and Assumptions

List of Tables

Table 2-1. Summary of VISPO and ASR related protective measures	2-16
Table 2-2. Summary of CPM stage occurrences in the models. Values indicate the number of time steps (total of 516) in each condition.....	2-17
Table 2-3. Summary of Lowest Spring Flow Events in the Low Flow Models.....	2-22

List of Figures

Figure 1-1. Map of the Edwards Aquifer region including the recharge basins described in Puente (1978). Basins are colored where they cross the recharge zone of the aquifer 1-2

Figure 1-2. Statistical correlation of monthly aquifer recharge from recharge basins within the EAR, using USGS estimated monthly recharge data from January 1934 to December 2022..... 1-5

Figure 1-3. Comparison of monthly variations in aquifer recharge estimated by the USGS for the Bexar basin for the period of November 1946 to December 2003 to groundwater levels recorded at the J17 index well and monthly precipitation totals recorded at the SAT 1-6

Figure 1-4. Comparison of monthly variations in aquifer recharge estimated by the USGS for the Nueces basin for the period of November 1946 to December 2003 to groundwater levels recorded at the J27 index well and monthly precipitation totals recorded at the SAT 1-6

Figure 1-5. Comparison of (a) monthly precipitation data recorded at the SAT to monthly precipitation data from TWDB’s Quadrant ID 809, encompassing the SAT, and (b) annual precipitation totals at the SAT and from the TWDB’s Quadrant ID 809..... 1-8

Figure 1-6. Comparison of monthly precipitation (a) and maximum temperature data (b) recorded at the SAT (local) to monthly precipitation data from Daymet for the Bexar basin..... 1-9

Figure 1-7. Polygons (black lines) delineating the nine major river basins comprising the contributing zone used to spatially average gridded weather datasets, superimposed over the mean daily precipitation (cm) from 1980 to 2022 from Daymet..... 1-9

Figure 1-8. Comparison of testing data comprising randomly shuffled monthly basin-average precipitation (top) and maximum temperature (bottom) data for the Bexar basin and their predictions by the ERT model 1-11

Figure 1-9. AI-based monthly recharge estimates for the Bexar basin. Recharge predictions by the ERT model are shown by the solid blue line, while the light blue shadow represents the uncertainty band formed by the recharge predictions by the ERT, RF, XGBoost, and HGBBoost models..... 1-13

Figure 1-10. AI-based monthly recharge estimates for the Nueces basin. Recharge predictions by the ERT model are shown by the solid blue line, while the light blue shadow represents the uncertainty band formed by the recharge predictions by the ERT, RF, XGBoost, and HGBBoost models..... 1-14

Figure 1-11. The global explanation from ERT-SHAP for aquifer recharge on the testing data. P and T represent monthly precipitation totals and monthly temperatures,

respectively. TRB, N1B, and N2B stand for the target recharge basin, neighboring recharge basin west, and neighboring recharge basin east, respectively 1-15

Figure 1-12. AI/ML-based monthly recharge estimates for the Bexar Basin, in comparison to monthly recharge estimates by the USGS model and HSPF model. Recharge predictions by the ERT model are shown by the solid blue line, while the light blue shadow represents the uncertainty band formed by the recharge predictions by the ERT, RF, XGBoost, and HGBBoost models. Temporal variations in groundwater levels at the J17 index well are shown as a reference 1-16

Figure 1-13. AI/ML-based monthly recharge estimates for the Nueces Basin, in comparison to monthly recharge estimates by the USGS model and HSPF model. Recharge predictions by the ERT model are shown by the solid blue line, while the light blue shadow represents the uncertainty band formed by the recharge predictions by the ERT, RF, XGBoost, and HGBBoost models. Temporal variations in groundwater levels at the J17 index well are shown as a reference 1-18

Figure 1-14. Cumulative aquifer recharge in the Bexar Basin during the 2012–2015 drought period (top panel) and for the entire testing period (2004–2022) (bottom panel) as estimated by the USGS (red), AI/ML (blue), and HSPF (green) models 1-19

Figure 1-15. Cumulative aquifer recharge in the Bexar Basin during the 2012–2015 drought period (top panel) and for the period 2004–2022 (bottom panel) as predicted by the USGS (red) and AI/ML (blue) models. A recharge threshold of 10,000 ac-ft is used to set monthly recharge values below 10,000 ac-ft in the Bexar Basin to zero 1-20

Figure 1-16. Comparison of cumulative aquifer recharge for the Nueces, Frio-Dry Frio, Sabinal, and Seco-Hondo Basins for the period from 2004–2022, after application of threshold values to reduce AI/ML modeled recharge during drought periods 1-21

Figure 1-17. Comparison of cumulative aquifer recharge for the Medina, Bexar, Cibolo Dry Comal, and Blanco Basins for the period from 2004–2022, after application of threshold values to reduce AI/ML modeled recharge during drought periods 1-22

Figure 1-18. Comparison of cumulative aquifer recharge for the entire EAR for the period from 2004 through 2022, when a threshold recharge, below which AI-predicted aquifer recharge is presumed to be zero to replicate the outcomes from the USGS recharge model 1-23

Figure 1-19. Box plot of annual recharge for each basin for the period 2004–2022. AI/ML model predictions are in gray and USGS calculated values are in blue 1-23

Figure 1-20. Projected aquifer recharge for the Bexar recharge basin using downscaled climate data from 2023 through 2065, sourced from two GCMs, including a CMIP5 (HadGEM2-CC) and CMIP6 (KIOST-ESM) models under intermediate- and high-emission scenarios. These are the AI-based recharge predictions, not incorporating recharge thresholds. Recharge predictions by the ERT model are shown by the solid

blue line, while the light blue shadow represents the uncertainty band formed by the recharge predictions by the ERT, RF, XGBoost, and HGBBoost models 1-25

Figure 1-21. Projected cumulative monthly total recharge from each GCM (colored lines) for the period 2023–2065. Cumulative monthly historical recharge for the period 1980–2022 is shown by the heavy black line..... 1-26

Figure 1-22. Box plots of projected total monthly recharge for the Edwards Aquifer from each GCM for the period 2023–2065. Measured historical recharge for the period 1934–2022 is also shown for comparison. Note the projections and historical recharge box plots are ordered by their median recharge values 1-27

Figure 2-1. Modeling Procedure with Projected Recharge to Simulate Spring Flows in the Edwards Aquifer..... 2-4

Figure 2-2. Comparison of J17 water levels (WL) simulated with the modeling procedure described in the previous section compared to the SAMP modeling result 2-5

Figure 2-3. Comparison of spring flow rates of Comal Springs (top) and San Marcos Springs (bottom) simulated with the current modeling procedure compared to the SAMP modeling result 2-6

Figure 2-4. Comparison of J17 water levels (top) and J27 water levels (bottom) simulated using the groundwater flow model with the USGS recharge, HSPF recharge, and AI/ML recharge models..... 2-8

Figure 2-5. Comparison of spring flow rates for Comal Springs (top) and San Marcos Springs (bottom) simulated using the groundwater flow model and the USGS recharge, HSPF recharge, and AI/ML recharge models 2-9

Figure 2-6. Comparison of monthly pumping from the output of the EAA 2017 model and the EAHCP Phase II model simulation using USGS recharge with protective measures. The bottom plot is focused on the period January 2014 to May 2015. Pumping extracted from the output of the EAA 2017 model represents estimated actual pumping from the aquifer 2-11

Figure 2-7. Modeled water levels for the J17 index well for the 19 GCM projections spanning (a) from 2023 to 2065 and (b) during the first 12 stress periods of the model runs..... 2-12

Figure 2-8. Modeled spring flow rates for a) Comal Springs and b) San Marcos Springs from 19 GCM projections spanning from 2023 to 2065..... 2-13

Figure 2-9. Summary of modeled spring flows for Comal Springs (top) and San Marcos Springs (bottom) using GCM projections spanning from 2023 to 2065. The dashed line is the median value of all models, and the shaded area is the range of the modeled spring flows..... 2-14

Figure 2-10. Cumulative probability of (a) modeled future Comal Springs flows from GCMs spanning from 2023 to 2065. The dashed dark line represents historical spring flows

for the period 1980–2023, and (b) a zoomed-in version of the plot focusing on flows of 100 cfs and below 2-15

Figure 2-11. Bar plots of the projected occurrences of VISPO, ASR Lease forbearances, and SAWS ASR forbearance triggered under the 19 climate projections..... 2-18

Figure 2-12. Stacked bar plots of frequency of CPM for the modeled climate projections. GCMs are sorted with decreasing frequency of Stage 5 from left to right..... 2-19

Figure 2-13. Comparison of the modeled projected Comal Springs flow rates (red) from the KACE-10-G ssp245 GCM during 2046–2057 to historical spring flow rate measurements (blue) during 1947–1958. 2-20

Figure 2-14. Comparison of the modeled projected Comal Springs flow rates (red) from the CMCC-CM rcp45 GCM during 2039–2047 to historical spring flow rate measurements (blue) during 2009–2017 2-21

Figure 2-15. Modeled Comal Springs (top) and San Marcos Springs (bottom) flows from the INM-CM4-9 ssp585 GCM for the period 2023–2065. This model is an example of a Neutral group model. The shaded area depicts the range of modeled spring flow rates for all 19 climate model projections. 2-23

Figure 2-16. Modeled Comal Springs (top) and San Marcos Springs (bottom) flows from the KIOST-ESM ssp245 GCM for the period 2023–2065. This model is an example of the Stressed group models. The shaded area depicts the range of modeled spring flow rates for all 19 climate model projections. 2-24

Figure 2-17. Modeled Comal Springs (top) and San Marcos Springs (bottom) flows from the KACE-1-0-G ssp245 GCM for the period 2023–2065. This model is an example of a Low Flow model. The shaded area depicts the range of modeled spring flow rates for all 19 climate model projections. 2-25

Figure 2-18. Projected Comal (top, blue) and San Marcos springs flows (bottom, blue) from the INM-CM4-8 ssp585 GCM (a Neutral group model) spanning from 2023 to 2065. Applied monthly pumping (brown), total monthly recharge (dark green line), annual recharge (green bar), and the 10-year moving annual average recharge (light green line) are shown. 2-26

Figure 2-19. Projected San Marcos Springs flows (blue) from the KIOST-ESM ssp245 GCM (a Stressed group model) spanning from 2023 to 2065. Applied monthly pumping (brown), total monthly recharge (dark green line), annual recharge (green bar), and the 10-year moving annual average recharge (light green line) are shown..... 2-27

Figure 2-20. Projected Comal Springs flows (blue) from the KACE-1-0-G ssp245 GCM (a Low Flow group model) spanning from 2023 to 2065. Applied monthly pumping (brown), total monthly recharge (dark green line), annual recharge (green bar), and the 10-year moving annual average recharge (light green line) are shown. 2-27

List of Acronyms and Abbreviations

°F	degrees Fahrenheit
ac-ft	acre-feet
AI	artificial intelligence
amsl	above mean sea level
ASR	Aquifer Storage and Recovery
cfs	cubic feet per second
CPM	critical period management
EAA	Edwards Aquifer Authority
EAHCP	Edwards Aquifer Habitat Conservation Plan
EAR	Edwards Aquifer region
ERT	Extremely Randomized Trees
ft	feet
GCM	global climate model
HGBoost	Histogram-based Gradient Boosting
HSPF	Hydrologic Simulation Program-Fortran
in	inches
ITP	Incidental Take Permit
ML	machine learning
MODFLOW	modular finite-difference groundwater flow
NAS	National Academy of Sciences
PET	potential evapotranspiration
RWCP	Regional Water Conservation Program
SAMP	Strategic Adaptive Management Program
SAT	San Antonio International Airport
SAWS	San Antonio Water System
SHAP	Shapley Additive Explanation
TRB	targeted recharge basin
TWDB	Texas Water Development Board
USGS	U.S. Geological Survey
VISPO	Voluntary Irrigation Suspension Program Option
XAI	explainable Artificial Intelligence
XGBoost	Extreme Gradient Boosting

Executive Summary

The Edwards Aquifer Habitat Conservation Plan (EAHCP) Incidental Take Permit (ITP) renewal process is evaluating the potential effects of climate change on covered species to support the information needed to apply for a proposed permit duration of 30 years. The goal of this report is to assess the potential effects of climate change on the Edwards Aquifer by characterizing changes in future recharge and estimating the effects of those changes on aquifer water levels and the spring flows that support covered species habitat. The Edwards Aquifer Authority (EAA) has previously utilized the U.S. Geological Survey's (USGS) modular finite-difference groundwater flow (MODFLOW) modeling program tailored for use for the Edwards Aquifer to simulate future spring flows; however, the method for estimating inputs (i.e., recharge) was based on streamflow data, and did not incorporate climate change indicators such as temperature and precipitation. Therefore, it was necessary to develop a method to evaluate the effect of future projected temperature and precipitation on aquifer recharge to model spring flows under potential future climate conditions.

This analysis describes the development of predictive models that generate future estimates of Edwards Aquifer recharge using downscaled temperature and precipitation projections from global climate models (GCMs). The report presents the results of modeled recharge from 2023 to 2065, which covers the proposed permit term (2028–2058). The recharge projections are then used within the EAA MODFLOW program to model future aquifer levels and spring flows.

Chapter 1, *Future Estimates of Edwards Aquifer Recharge Using Climate Data*, details the development of a recharge model at the basin scale to estimate future recharge in the Edwards Aquifer region based on temperature and precipitation projections derived from 19 GCMs. After evaluating several approaches to modeling recharge, an artificial intelligence (AI)/machine learning (ML) model based on extremely randomized trees (ERT) was selected. The AI/ML model was coupled with the Shapley Additive Explanation (SHAP) (Shapley 1953; Lundberg et al. 2020) to generate explainable Artificial Intelligence (XAI) models, which were used to identify the most influential hydroclimatic features in predicting recharge. The analysis identified previous month recharge as the most critical feature in determining monthly recharge, followed by precipitation in the target basin, precipitation in neighboring basins, and the previous month's precipitation in neighboring and target basins. Current and lagged precipitation were identified as more critical to the model than temperature.

Using this AI/ML model, the team predicted historical recharge and projected future recharge by month and year through 2065 across eight basins. USGS recharge data served as the ground truth for the predictive recharge analysis, and long-term climate data, including daily precipitation and temperature, were used to train the AI/ML models and test their predictive accuracy in forecasting aquifer recharge.

When compared to observed recharge, some models tended to overpredict recharge, which was most impactful during drought conditions. After post-training and post-adjustments, the resulting models are reasonably and statistically similar to USGS historical data and behave similarly to the USGS approach, the Puente (1978) method, making the estimated cumulative recharge consistent with the assessments of the effectiveness of various spring flow protection measures enumerated in the EAHCP. The results project recharge from most GCMs after 2030 to be lower than the recharge observed in the recent past, irrespective of various modeled emission scenarios. The ranges and magnitudes of the projections, however, are similar to those in the recent past, suggesting that the

associated groundwater modeling results are likely to vary in a manner similar to historical observations.

Chapter 2, *Projected Spring Flows Under Future Climate Conditions: MODFLOW Modeling Analysis*, utilizes the recharge outputs from the AI/ML model to simulate future spring flows using the MODFLOW modeling program as tailored for the Edwards Aquifer (Lindgren et al. 2004; Liu et al. 2017). This model was nearly identical to that used for previous EAHCP analyses, with only minor modifications to improve efficiency.

The simulation period spans from 2023 through 2065, totaling 43 years with 516 stress periods (months). The calculations occur at monthly time steps consistent with pumping and recharge data availability. The model includes the spring flow protection measures that exist in the current EAHCP. The model follows five steps in the simulation of spring flows via a Jupyter notebook (Kluyver et al. 2016). In Step 1, the monthly recharge generated from the climate models is converted and reformatted for use. In Step 2, the 10-year moving annual average of total recharge is calculated to determine any periods in which the 10-year moving average falls below 500,000 acre-feet, which is a trigger value for San Antonio Water System (SAWS) Aquifer Storage and Recovery (ASR)-related forbearance requirements. In Step 3, the model is run and the reduction of total pumping via the Regional Water Conservation Program (RWCP) is implemented; reductions in pumping are implemented from EAA forbearance of SAWS ASR leases in years following those years where the 10-year average is below the trigger level; the full range of critical period management (CPM) pumping reductions based on water levels and spring flow values is applied; and protective measures of RWCP, EAA forbearance, and CPM Stages 1–5 pumping reductions are implemented. In Step 4, the annual water level at the J17 index well for each year in the simulated period is checked; if the water level is below 635 feet above mean sea level, reductions in pumping covered by Voluntary Irrigation Suspension Program Option (VISPO) leases are applied in the year after VISPO is triggered. Step 4 includes another full model run and implements the protective measures in Step 3 and VISPO-related reductions if triggered. Step 5 is a full run of the model and applies pumping reductions related to SAWS ASR forbearance. Spring flow protection measures implemented in Steps 3 and 4 are also included in Step 5.

The Jupyter notebook and corresponding model were assessed by comparing its output for the historical drought of record and by using a range of realistic recharge inputs. The current model successfully reproduced the outcomes from previous drought modeling in the EAHCP and generated reasonable and anticipated results across three distinct recharge input tests. Quality assurance and control evaluations of the model provide confidence in its ability to project water levels and spring flows based on future recharge scenarios.

Separate model runs were then conducted for each of the projected recharge sequences associated with the 19 downscaled GCMs to project water levels and spring flows from 2023 to 2065. The model projects water levels for the J17 index well and spring flows for Comal and San Marcos Springs. The median modeled flow rates for Comal and San Marcos Springs were consistent with historical data, and the model effectively captured low flow conditions below 100 cubic feet per second without bias. The analysis confirmed that protective measures were triggered as expected and aligned with groundwater management criteria. The modeling results produced three drought sequences similar to the 1950s drought of record and more than 19 sequences similar to the 2011–2015 drought.

The 19 projections were categorized into three groups: Neutral, Stressed, and Low Flow. Neutral projections showed spring flows similar to the past 40 years, while Stressed scenarios had lower flows that remained above daily average minimum targets. The Low Flow scenarios, however, included two climate projections with one or more stress periods where flows dropped below the proposed minimum daily average spring flow discharge objectives.

For both spring systems, increases in spring flow rates correspond to the peaks of monthly recharge to the aquifer, while decreases reflect less recharge and greater applied pumping, particularly during the summer season. The exaggerated intra-annual sawtooth shape of the spring flow rates is likely due to the application of maximum allowed monthly groundwater pumping in the model; however, the modeled declines are consistent with seasonal pumping. The analysis also revealed that some protective measures, like ASR forbearance, were not triggered during Low Flow scenarios resulting in very low flows; however, under no scenario do spring flows cease.

This analysis successfully incorporated projected future temperature and precipitation data to estimate future recharge and produce future spring flow projections under varying climate scenarios. Several future spring flow projections produce drought sequences similar to those experienced in recent history but none that appear more severe than the drought of record. The majority of future spring flow projections indicate that existing spring flow protection measures would maintain spring flows above minimum average daily spring flow discharge objectives for the Comal and San Marcos Springs, but 2 of the 19 projections produce flow rate sequences over the course of 1 to 4 months that are below these objectives. No future spring flow projections result in zero flows in Comal or San Marcos Springs.



Chapter 1

Future Estimates of Edwards Aquifer Recharge Using Climate Data

Evaluation of future environmental effects, including climate change, is a necessary component of the application process for renewal of the Edwards Aquifer Habitat Conservation Plan (EAHCP) Incidental Take Permit (ITP). A thorough assessment of the potential effects of future climates on the Edwards Aquifer requires more than a review of future climate model projections and includes characterizing changes in future recharge and estimating effects of those changes on aquifer water levels and spring flows. The Edwards Aquifer Authority (EAA) has an available groundwater flow model that can simulate water levels and spring flows using recharge as input (Liu et al. 2017), but a method to estimate future recharge has not previously been developed.

The following sections describe the methodology used to generate predictive models of recharge for the Edwards Aquifer system using meteorological parameters output by global climate models (GCMs) and present the results of modeling recharge from 2023 to 2065, encompassing the proposed permit renewal period of 30 years (2028–2058).

1.1 Current Recharge Estimates for the Edwards Aquifer

Estimates of annual recharge to the San Antonio segment of the Edwards (Balcones Fault Zone) Aquifer are provided by the U.S. Geological Survey (USGS) using a methodology described in Puente (1978). Although there is some acknowledged additional uncertainty, the USGS also provides estimates of monthly recharge (Puente 1978; USGS 2023). Calculations have been made to quantify recharge from 1934 to the present, and the Puente method is specified in the EAHCP (RECON et al. 2012; U.S. Fish and Wildlife Service 2015) as the means for calculating recharge in the aquifer system.

The USGS method for estimating recharge is based on streamflow data (Puente 1978). Estimates for recharge are made monthly for eight individual river basins in the contributing zone (Figure 1-1). The basic approach is a water balance, in which recharge in a basin is the difference in streamflow measured at gaging sites upstream and downstream of the recharge zone, plus the estimated runoff generated in the recharge zone. This balance is applied directly in five of the nine basins that have stream gages located upstream and downstream of major contributing rivers. The other four basins either have gaging stations only downstream of the recharge zone or have no gaging sites at all. Recharge in these partially or ungaged basins is estimated based on assumptions relating the runoff characteristics from gaged areas to ungaged areas. Recharge in the Medina River basin also includes seepage losses from Medina Lake and Diversion Reservoir. One of the gaged basins, the Guadalupe River Basin, is not considered to contribute significant recharge. Total recharge to the system is the sum of the other eight basin recharge estimates.

The basins, from west to east, are:

- Nueces-West Nueces River Basin (Nueces)
- Frio-Dry Frio Basin and adjacent areas (Frio-Dry Frio)

- Sabinal River Basin and adjacent areas (Sabinal)
- Area between Sabinal River Basin and Medina River Basin (Seco-Hondo)
- Medina River Basin (Medina)
- Area between the Medina River Basin and Cibolo Creek Basin (Bexar)
- Cibolo Creek and Dry Comal Creek Basins (Cibolo Dry Comal)
- Blanco River Basin and adjacent areas (Blanco)

In general, we use the abbreviated names (in parentheses above) for each of these basins in this report. To perform the analyses, we used reported recharge data through 2022.

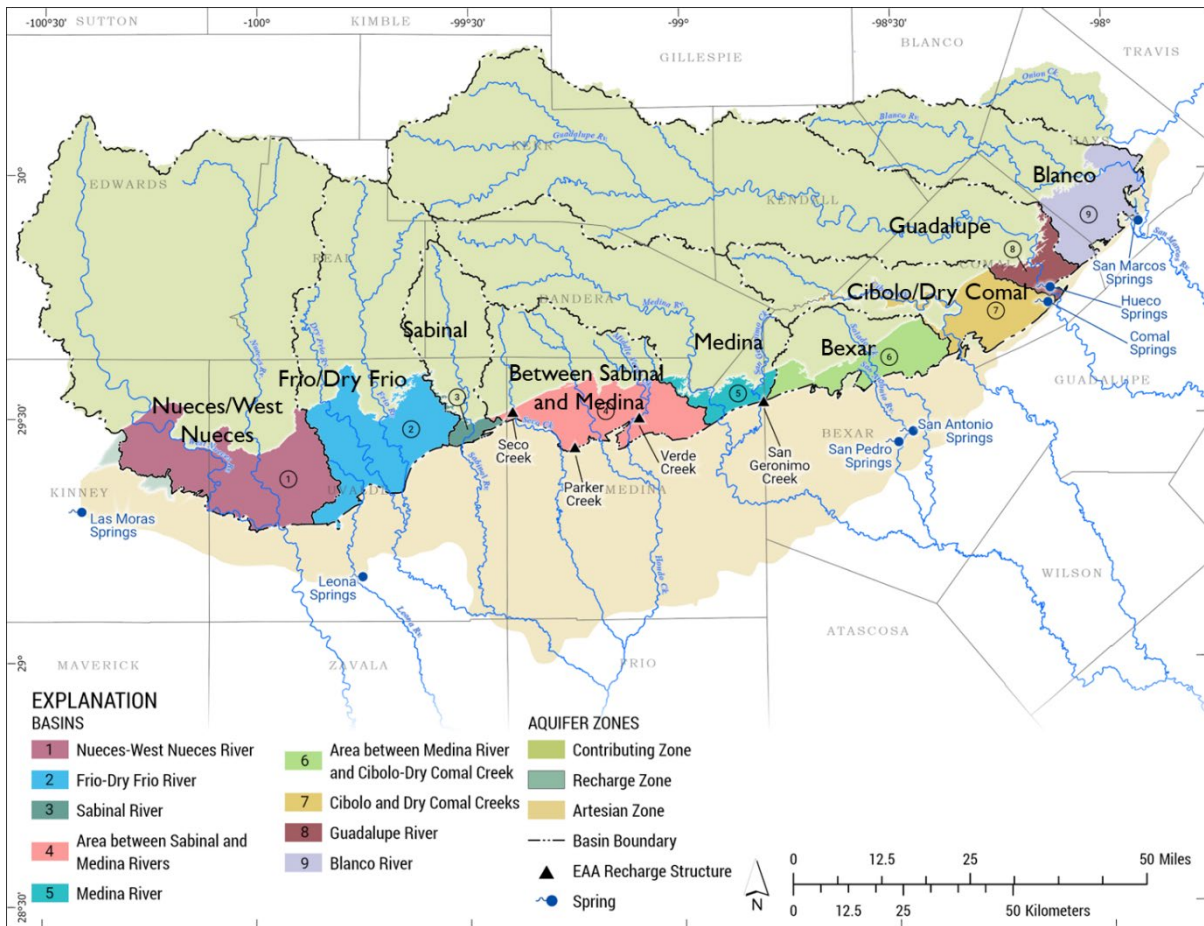


Figure 1-1. Map of the Edwards Aquifer region including the recharge basins described in Puente (1978). Basins are colored where they cross the recharge zone of the aquifer.

One major limitation of the current method for determining recharge is that it relies upon measured stream flows at gages above and below the recharge zone. Besides using precipitation data to calculate upstream and downstream rainfall ratios in basin segments to aid in the separation of baseflow, the Puente method does not incorporate temperature, precipitation, or other environmental factors in its calculation of recharge. As a result, the method is not suitable for calculating future recharge based solely on climate model data.

A surface water–based mechanistic model using Hydrologic Simulation Program–Fortran (HSPF) was developed by the EAA in the 2010s (e.g., Clear Creek Solutions 2012, 2013). HSPF explicitly incorporates precipitation and evapotranspiration data, but discrepancies between the HSPF model recharge estimates and the USGS estimates, especially at high and low flow extremes, resulted in shelving of the HSPF approach.

Thus, one of the major difficulties in assessing future climate-related impacts on spring flows and other aquifer components is the inability to directly estimate recharge from climate data. Further, it is important that methodologies to estimate future recharge be consistent with past measurements of recharge. That is, we would strongly prefer to have a recharge model for future projections that behaves similarly to the Puente method, which has been used extensively in assessments of the effectiveness of various spring flow protection measures enumerated in the EAHCP.

1.2 Artificial Intelligence/Machine Learning–Based Aquifer Recharge Models

After evaluating several approaches to modeling recharge, we used artificial intelligence (AI)/machine learning (ML) models based on ensemble decision tree algorithms encompassing monthly total precipitation, and monthly average minimum and maximum temperatures to develop recharge models for all eight recharge basins that predict historical recharge and project future recharge by month through the year 2065.

In our analyses, we examined four AI/ML models based on boosting and bagging algorithms that exhibited high predictive performance across diverse domains in our recent research (Chakraborty et al. 2021, 2024; Başağaoğlu et al. 2023; Nicolae et al. 2023). These AI/ML models are Extremely Randomized Trees (ERT) (Geurts et al. 2006), Random Forest (RF) (Breiman 2001), Extreme Gradient Boosting (XGBoost) (Chen and Guestrin 2016), and Histogram-based Gradient Boosting (HGBoost) (Guryanov 2019). Boosting algorithms reduce bias and sequentially train models that focus on errors of previous models, making them particularly effective for models with high bias. Complementary to this, bagging algorithms reduce variance and perform average predictions from models trained on different subsets of data, making them effective for models with high variance.

Compared to statistical models, the ensemble decision tree–based AI/ML models used in this study are non-parametric; thus, the model structure does not need to be specified *a priori*. The models can unfold nonlinear relationships and patterns between multidimensional predictors and predictands. Unlike statistical models, they do not rely on prespecified assumptions about the distribution of residuals and the functional form of the equation or non-collinearity among the predictors. Additionally, the tree-based AI/ML models are interpretable and offer better predictive accuracy than traditional statistical models (Chang et al. 2016; Dumitrescu et al. 2021).

The tree-based ensemble AI/ML models chosen for this study are also conducive to integration with explanatory methods, improving the explainability of AI/ML-based decisions (Başağaoğlu et al. 2022). Among the explanatory methods, we coupled the AI/ML models with the Shapley Additive Explanation (SHAP) (Shapley 1953; Lundberg et al. 2020) to generate explainable Artificial Intelligence (XAI) models. These XAI models were used in this study to identify the most influential hydroclimatic features in predicting the aquifer recharge for each basin.

We first assessed the predictive performance of the AI/ML models in generating basin-wide time-series of monthly precipitation totals and average minimum and maximum temperatures for the region. These results were used to supplement the temperature record from 1946 to 1980. Subsequently, we used AI/ML models to predict monthly aquifer recharge for each recharge basin as well as aggregated recharge across the Edwards Aquifer region (EAR) from 1946 to 2023. We then projected aquifer recharge from 2023 through 2065, considering potential future climatic conditions obtained from downscaled GCMs under intermediate- and high-emission scenarios.

1.3 Available Recharge Data

USGS monthly recharge estimates from 1934 to 2022 are complete for all basins with no missing values. These estimates represent the sole historical recharge data available for the EAR. However, due to inherent challenges in direct field measurements of aquifer recharge, these estimates entail uncertainties. As acknowledged in his report, Puente's method is susceptible to greater uncertainties during periods of exceptionally low or high stream flow because gage readings under these extreme conditions may lack precision. Given the absence of direct recharge measurements or alternative recharge estimates in the region, USGS recharge data is regarded as ground-truth data for the AI/ML-based predictive recharge analysis in this study. For the development of the AI/ML recharge model, we selected a subset of the USGS recharge data to focus on the period from November 1946 to December 2022. This period is purposely limited to better correspond with available historical climate data (discussed in the following sections). Moreover, the recharge dataset is split into two parts. One set, from November 1946 to December 2003, is used to train the AI/ML models, while the remainder, from January 2004 to December 2022, is used for validation testing of the models.

Aquifer recharge from the basins within the San Antonio pool, including Seco-Hondo, Bexar, and Cibolo Dry Comal exhibits statistically weaker correlations with recharge from the basins within the Uvalde pool, including Sabinal, Frio-Dry Frio, and Nueces (Figure 1-2), due to different geographical setting of the two pools. Additionally, the Uvalde pool experiences warmer and drier conditions compared to the San Antonio pool. Figure 1-2 further illustrates that recharge from the Medina Basin shows no statistically significant correlation with recharge from other basins within the EAR.

Historically larger recharge peaks, with at least one peak exceeding 100,000 acre-feet (ac-ft)/month, have been estimated for Frio-Dry Frio, Seco-Hondo, Cibolo Dry Comal, and Nueces basins. Lower recharge, with all recharge values falling below 50,000 ac-ft/month, have been estimated for Sabinal, Medina, and Blanco. Notably, aquifer recharge in the Guadalupe River Basin is reportedly considered negligible and is therefore not included in the list of recharge basins in the calculations.

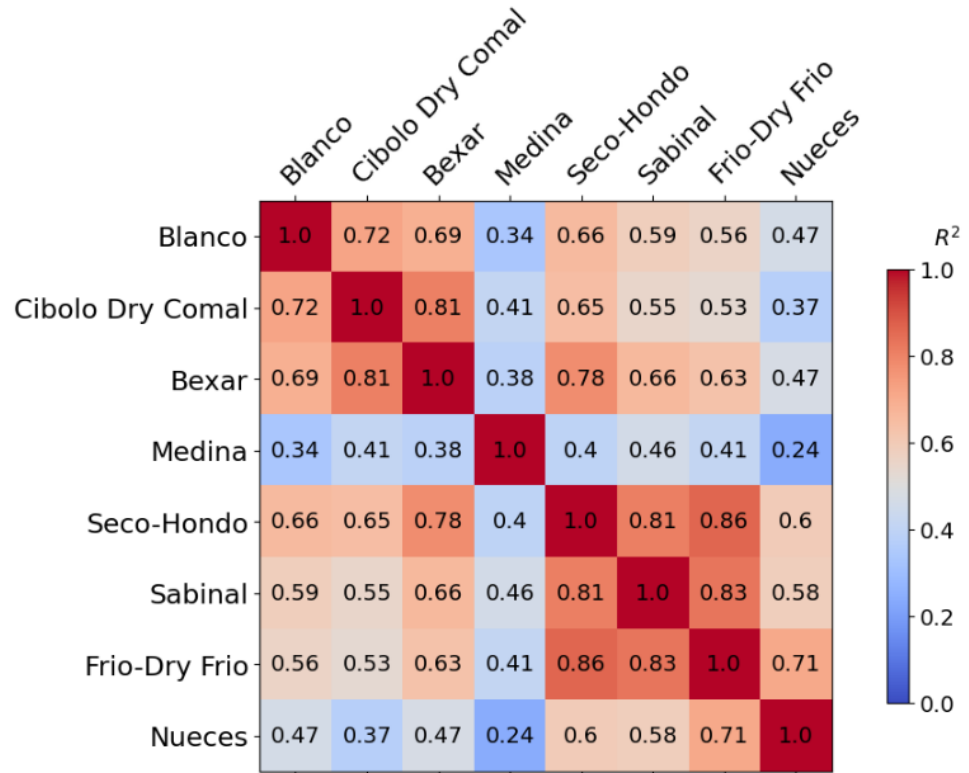


Figure 1-2. Statistical correlation of monthly aquifer recharge from recharge basins within the EAR, using USGS estimated monthly recharge data from January 1934 to December 2022

Temporal variations in recharge estimates within each basin are highly irregular, characterized by multiple isolated large recharge peaks surrounded by lower recharge events, which present challenges for recharge prediction using statistical or AI/ML-based models. These large peaks coincide with major storm events and show close correlations with monthly fluctuations in groundwater levels at the J17 and J27 index wells (Figure 1-3 and Figure 1-4). Large recharge peaks are typically associated with heavy storms and the resulting focused recharge within the EAR. For instance, the 1950s drought of record, which is marked by the longest and most intense meteorological and hydrological droughts in the past century, was ended by back-to-back heavy storm events in 1957 and 1958. This is exemplified by the groundwater response at the J17 well, where groundwater levels rose from 625.2 feet (ft) above mean sea level (amsl) in December 1956 to 650.1 ft amsl in December 1957 and further to 678.0 ft amsl in December 1958, marking an increase of approximately 53 ft over 2 years in response to heavy storm events (Figure 1-3). The rapid recovery of groundwater levels to high-recharge peaks following consecutive heavy storm events is consistently observed in the historical data for the Bexar Basin as well as in other recharge basins within the EAR.

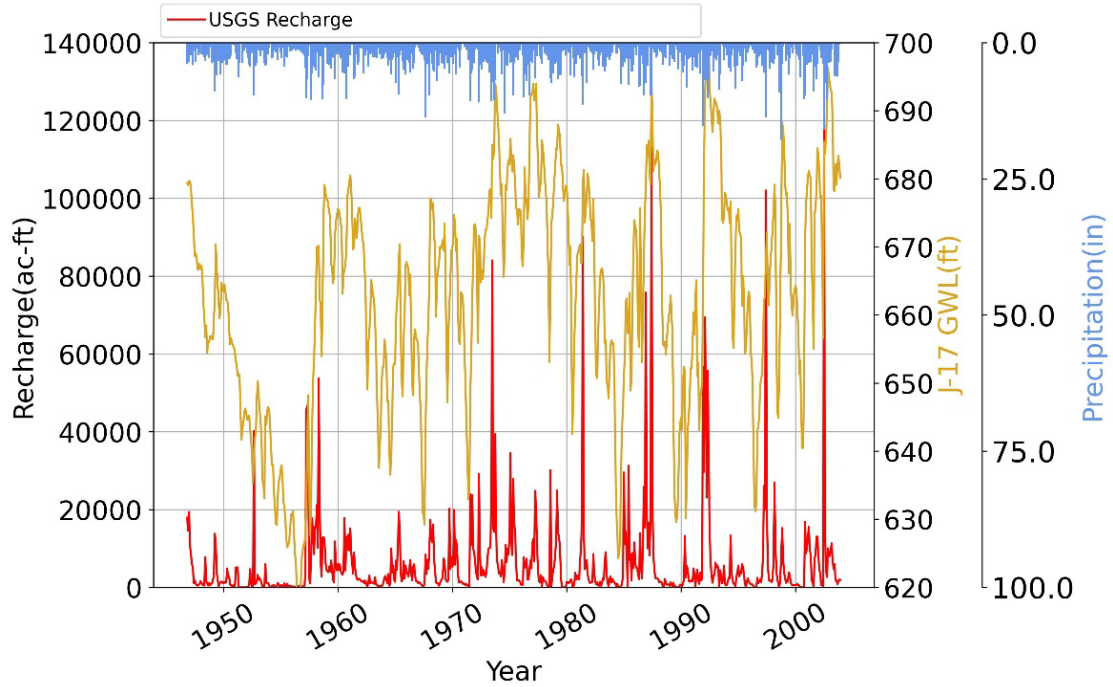


Figure 1-3. Comparison of monthly variations in aquifer recharge estimated by the USGS for the Bexar basin for the period of November 1946 to December 2003 to groundwater levels recorded at the J17 index well and monthly precipitation totals recorded at the SAT

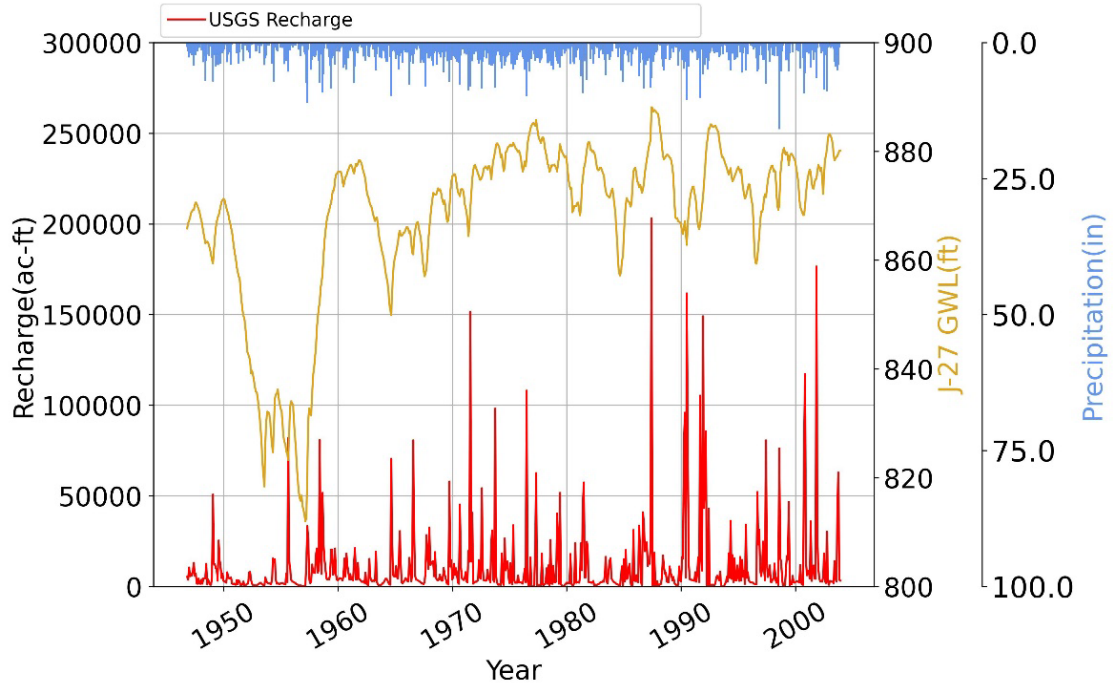


Figure 1-4. Comparison of monthly variations in aquifer recharge estimated by the USGS for the Nueces basin for the period of November 1946 to December 2003 to groundwater levels recorded at the J27 index well and monthly precipitation totals recorded at the SAT

While increases in groundwater levels at the J27 index well correlate with increases in aquifer recharge in the Nueces Basin, the impact of larger recharge peaks on groundwater levels after the year 1960 is less pronounced compared to 1950 through 1956 (Figure 1-4). Groundwater levels at the J27 well did not exhibit extreme declines, comparable to those observed during the drought of record between 1960 and 2003. Interestingly, estimated large recharge peaks in the late 1980s, early 1990s, and early 2000s within the Nueces Basin were associated with considerably smaller recovery in groundwater levels, in comparison to relatively smaller recharge peaks and resulting significantly higher recovery in groundwater levels in the late 1950s.

1.4 Historical Climate Data for the Edwards Aquifer Region

In our predictive and projective recharge analyses, we relate aquifer recharge to climatic forcings, including monthly minimum and maximum average temperatures, and monthly total precipitation, as the same set of climatic variables are available from GCMs. Therefore, it is essential to acquire or generate long-term climate data in each recharge basin for aquifer recharge predictions and projections.

The only comprehensive observed long-term daily climate dataset in the EAR including daily precipitation totals and daily minimum and maximum temperatures is available for the San Antonio International Airport (SAT) location. Climate data for the SAT location have been available since September 1, 1946, and thus cover the period of the drought of record. In addition, gridded daily precipitation totals, daily minimum and maximum temperature at a spatial resolution of 1 kilometer \times 1 kilometer are available across the EAR from Daymet version 4 (hereafter Daymet) (Thornton et al. 2022) back to January 1, 1980. The Daymet dataset is the same as was used in our GCM downscaling effort (Wootten et al. 2024).

Also available are monthly precipitation totals at a relatively coarser spatial-scale ($1^\circ \times 1^\circ$) beginning in January 1940 from the Texas Water Development Board (TWDB) website (<https://waterdatafortexas.org/lake-evaporation-rainfall>). In our analyses, monthly precipitation data for Quadrant ID 807 was used for the Nueces Basin, Quadrant ID 808 was used for the Frio-Dry Frio, Sabinal, Seco-Hondo, and Medina Basins, and Quadrant ID 809 was used for the Bexar, Cibolo Dry Comal, and Blanco Basins. Figure 1-5a illustrates that monthly precipitation recorded at the SAT is statistically correlated with monthly precipitation from TWDB Quadrant ID 809, which covers the SAT. The correlation measures, based on the coefficient of determination, $R^2=0.76$, and root-mean square error of $RMSE=1.11$ in, reveal a decent correlation, considering the point measurement nature of precipitation data at the SAT compared to precipitation data from the TWDB at its $1^\circ \times 1^\circ$ spatial resolution and the spatial variability of precipitation. Figure 1-5b demonstrates that annual precipitation trends recorded at the SAT and those obtained from the TWDB are well aligned. The annual precipitation plot is preferred for enhanced clarity over the monthly precipitation plot.

The availability of such long-term climate data is imperative for effectively training AI/ML models to learn about the relationship between climate forcings and aquifer recharge and to test the predictive accuracy of the AI/ML models in forecasting aquifer recharge before using them for recharge projections. To maintain consistency with the temporal resolution of the historical recharge data, we converted the daily climate data at the SAT to monthly data. Because none of the basins in the EAR have extensive local or regional climate data measurements, the initial step involves constructing basin-averaged long-term climate data for each recharge basin with the help of external data

available for the region. Although precipitation measurements display significant spatial variability, the temperature data at the SAT is indicative of temperatures in the San Antonio pool of the EAR. This region is relatively cooler and wetter than the area represented by the Uvalde pool of the EAR.

Because the climate data at the SAT is representative for the San Antonio pool of the EAR, a good statistical correlation between the recorded precipitation at the SAT and precipitation data from the TWDB (Figure 1-5) justifies the use of precipitation data from the TWDB quadrants as analogs for the recharge basins within the EAR. This extends the available historical data beyond the start date of the Daymet data (January 1980). Consequently, the TWDB database furnishes long-term precipitation data prior to 1980 and dating back to 1946 for all recharge basins.

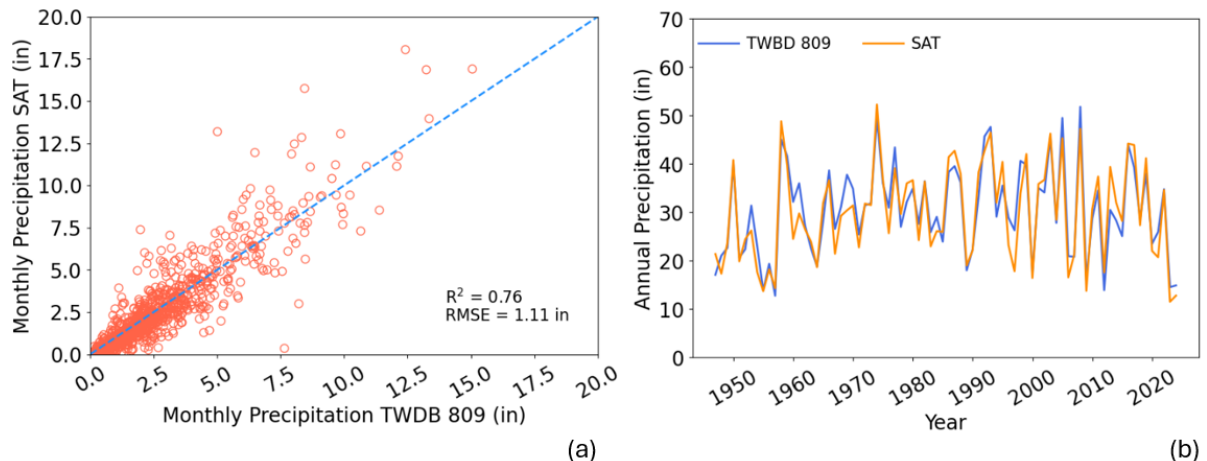


Figure 1-5. Comparison of (a) monthly precipitation data recorded at the SAT to monthly precipitation data from TWDB's Quadrant ID 809, encompassing the SAT, and (b) annual precipitation totals at the SAT and from the TWDB's Quadrant ID 809

The next step involves generating long-term temperature data for all recharge basins. The gridded Daymet temperature data are only available from January 1, 1980, while long-term temperature data that goes back to the 1940s are available only at the SAT. Therefore, we characterized the relationship between basin-specific daily climate data from Daymet and daily climate data from SAT from January 1, 1980, to present (2022) for all basins. In this analysis, we constructed basin-averaged gridded monthly precipitation totals in addition to basin-averaged minimum and maximum temperatures (as described in the following paragraph). Local daily climate data at the SAT were upscaled to monthly data. Figure 1-6 illustrates that the local climate data is statistically well-correlated with the basin-average Daymet climate data using the Bexar basin as an example.

To develop the basin averaged data, three-dimensional—two spatial and one temporal dimension—daily gridded weather datasets were processed to obtain one-dimensional, spatially averaged, monthly time series for input to recharge models. Two gridded weather products were used: Daymet for model training and downscaled GCM outputs for recharge projections. Three variables from each gridded weather product were used for model input: precipitation, minimum temperature, and maximum temperature. The gridded datasets for each variable were spatially averaged to the eight individual river basins associated with USGS recharge estimates (Figure 1-7). To compute the spatial averages, the gridded datasets were masked to the river basins, delineated by vector polygons, using the `mask_3D_geopandas()` method in the `regionmask` Python (<https://pypi.org/project/regionmask/>) package, and the spatial average of the masked data was

computed using the *xarray* Python package. The resulting one-dimensional, daily timeseries was then resampled to a monthly timestep to match the frequency of USGS recharge estimates. The monthly sum was taken for precipitation and the monthly mean was taken for minimum and maximum temperature. Prior to spatial averaging, all gridded datasets with non-standard calendars were converted to standard calendars using the *convert_calendar()* method in *xarray*. Precipitation units were converted to inches (in) and temperature units were converted to degrees Fahrenheit (°F).

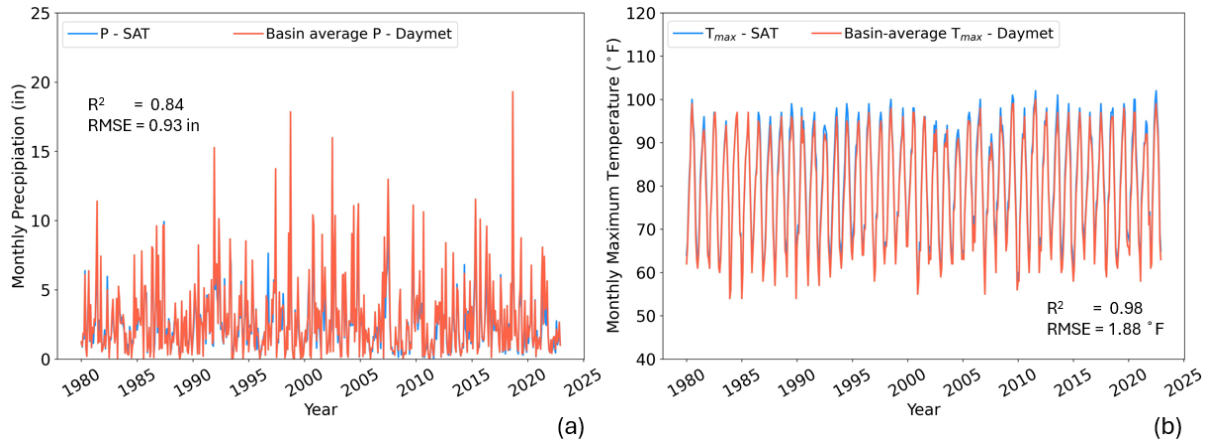


Figure 1-6. Comparison of monthly precipitation (a) and maximum temperature data (b) recorded at the SAT (local) to monthly precipitation data from Daymet for the Bexar basin

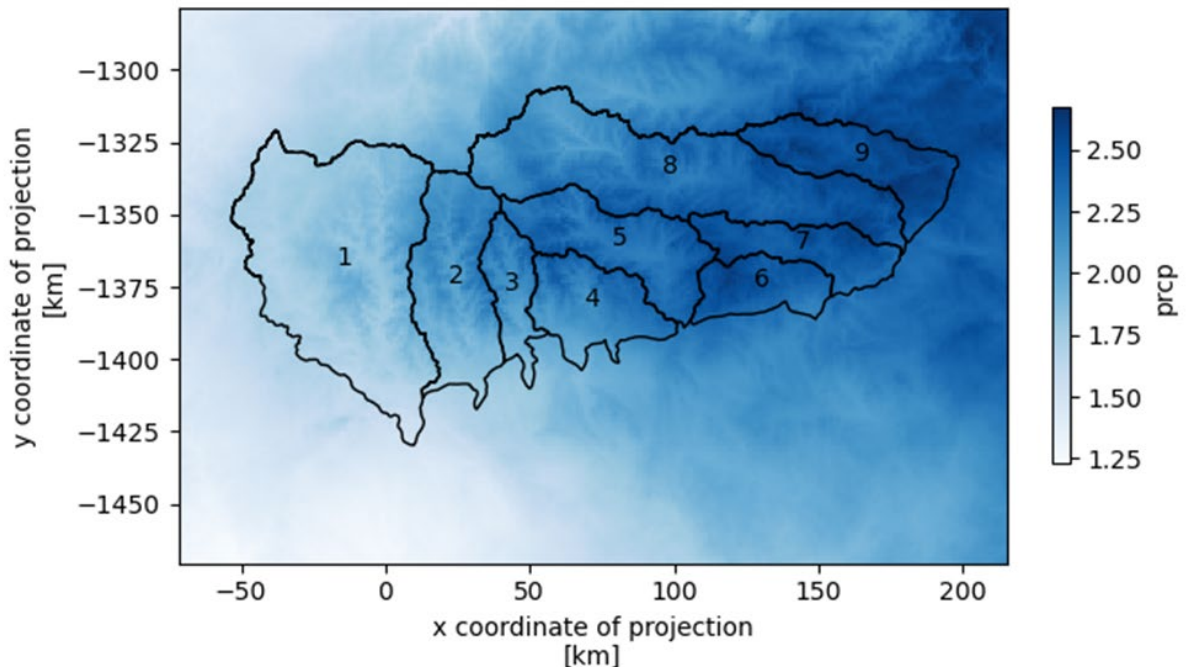


Figure 1-7. Polygons (black lines) delineating the nine major river basins comprising the contributing zone used to spatially average gridded weather datasets, superimposed over the mean daily precipitation (cm) from 1980 to 2022 from Daymet

The relationship between the Daymet climate data and local climate data at the SAT was established next using the AI/ML modeling framework. In this framework, Daymet climate variables are treated as target variables, while local climate variables at the SAT are treated as predictors. We randomly allocated 80% of the data, including the predictors and target variables in a tabular form, for training the AI/ML models and used the remaining 20% of the data, unseen by the AI/ML models during the training phase, to assess their predictive performance. All the models displayed high prediction accuracy relative to the test data. For example, R^2 and RMSE between the local data at the SAT and basin-averaged precipitation data for the Bexar Basin varied in the range of 0.88 to 0.92 and 0.99 to 1.02 in, respectively; for monthly maximum temperature the R^2 and RMSE were 0.994 to 0.995 and 0.97 to 1.42°F, respectively; and for monthly minimum temperature, 0.994 and 0.93 to 0.95°F, respectively.

A comparison of testing data, which encompasses randomly shuffled monthly precipitation totals and monthly maximum temperatures from the Daymet database and the AI/ML-based (using the ERT model) prediction of Daymet data from the SAT is shown in Figure 1-8. The data in the training and testing sets were randomly shuffled to ensure that data from extreme and non-extreme events are included in the training and testing of the AI/ML models in an unbiased fashion. In the end, all the AI/ML models exhibited high prediction accuracy. The ERT model closely matched the timing and magnitude of the peak precipitation values (Figure 1-8). Therefore, it is used in subsequent AI/ML-based analysis as the primary model.

We implemented the same procedure for all the recharge basins, generating an ERT model for each basin using basin-specific climatic data. The trained and tested model for each basin was then used to extrapolate basin-averaged Daymet climate data from 1980 back to 1946, using climate data from SAT as the predictors. In the end, we generated basin-averaged climate data for each basin from September 1946 to December 1979 to supplement the Daymet data. Monthly basin-scale precipitation totals were drawn from the TWDB database, and monthly basin-average minimum and maximum temperatures were extrapolated from basin-average Daymet data using the ERT model. AI/ML-modeled temperatures and TWDB precipitation data from September 1946 to December 1979 were combined with the basin-scale Daymet temperature data and precipitation data from January 1980 through December 2022 to generate climate data for each basin from September 1946 through December 2022.

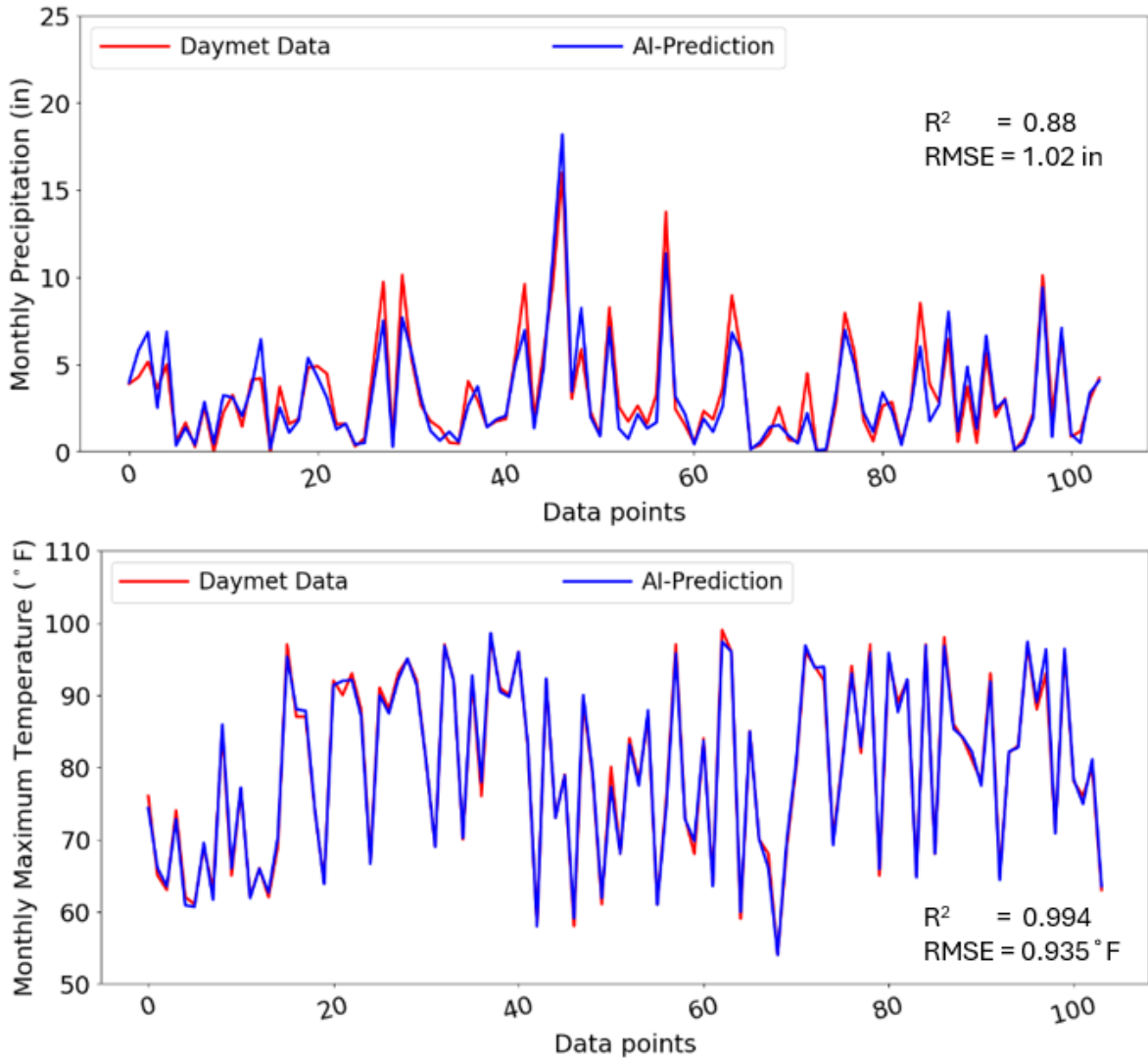


Figure 1-8. Comparison of testing data comprising randomly shuffled monthly basin-average precipitation (top) and maximum temperature (bottom) data for the Bexar basin and their predictions by the ERT model

1.5 AI/ML-Based Aquifer Recharge Predictions

Following the climate data assembly, we next constructed AI/ML models to predict aquifer recharge for a particular basin (i.e., targeted basin) using hydroclimatic variables and their lagged values from the targeted basin, along with those from the neighboring basin to the west and neighboring basin to the east. The AI/ML models in this analysis differ from those used in generating long-term climate data for each basin. Due to lagged variables in the AI/ML-based recharge predictions, the data for the training and testing data sets cannot be randomly shuffled. Recharge predictions must be executed sequentially because the recharge estimate for the current month would be influenced by the estimates for the climatic variables and aquifer recharge for the preceding month. Our analyses indicated that lags exceeding 1 month had insignificant impacts on recharge predictions; therefore, we used only 1-month lag in hydroclimatic variables in the models.

We used hydroclimatic features for the AI/ML model, including monthly precipitation totals, monthly minimum and maximum temperatures, along with their 1-month lags for the targeted basin (e.g., Bexar Basin). Additionally, we included the same climatic features from the adjacent basin to the west (e.g., the Medina Basin for the Bexar Basin) and the adjacent basin to the east (e.g., Cibolo Dry Comal for the Bexar Basin), as well as the recharge value in the targeted basin from the previous month in addition to month as the engineered feature in the AI/ML models. We used the hydroclimatic data from November 1946 to December 2003 to train the AI/ML models and the data from January 2004 through December 2022 to assess the predictive performance of the AI/ML models. In this set-up, 75% of the data was allocated to the training dataset and the remaining 25% was allocated to the testing dataset.

1.5.1 Recharge Model Testing

Using the Bexar recharge basin as an example, the AI/ML model closely captured the time-series of the aquifer recharge and overall trend (Figure 1-9). Similar results were obtained for other basins. Despite highly irregular patterns in the USGS recharge data, the AI/ML-based predictions reproduce the data quite closely. However, there were instances where the USGS model predicted zero recharge during dry periods, whereas the AI/ML models predicted non-zero recharges. For example, during the period of August, September, and October in 2006, while the USGS model predicted zero recharge, the ERT model predicted 204 ac-ft, 507 ac-ft, and 1,886 ac-ft during these 3 months, respectively (Figure 1-9).

The ERT model predictions are in close agreement with the timing and magnitude of monthly aquifer recharge peaks. While the AI/ML models accurately represented temporal fluctuations in aquifer recharge until 2016, they did not entirely reproduce the significant recharge peak in November 2004 (Figure 1-9). For instance, the USGS recharge estimate was 71,171 ac-ft, while the ERT model predicted 31,498 ac-ft and XGBoost model predicted 53,573 ac-ft, which was the closest to the USGS estimate. Two non-zero peaks consistently predicted by the AI/ML models for October 2009 and September 2018 were not captured by the USGS model. In the following section, we delve into these differences in reference to temporal monthly fluctuations at the J17 well and recharge predictions using additional HSPF simulations.

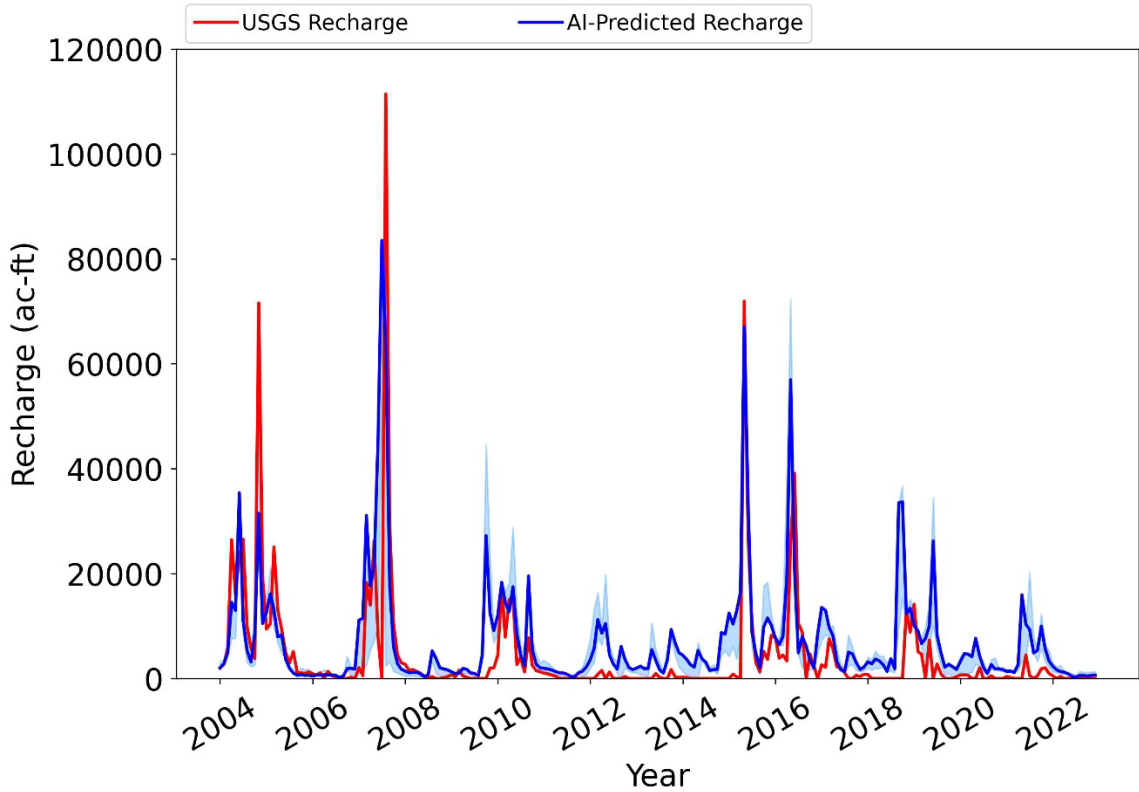


Figure 1-9. AI-based monthly recharge estimates for the Bexar basin. Recharge predictions by the ERT model are shown by the solid blue line, while the light blue shadow represents the uncertainty band formed by the recharge predictions by the ERT, RF, XGBoost, and HGBost models

We also compare AI/ML-based recharge estimates to USGS recharge estimates for the Nueces Basin in Figure 1-10. Like the Bexar Basin, the significant recharge peaks estimated by the USGS model are well captured by the AI/ML models. Although the magnitudes of the most significant recharge peaks differ (e.g., May 2015), the timing of the recharge peaks is consistent between the two models. In the following section, we delve into these differences in reference to temporal monthly fluctuations in groundwater levels at the J27 well and recharge predictions by HSPF simulations.

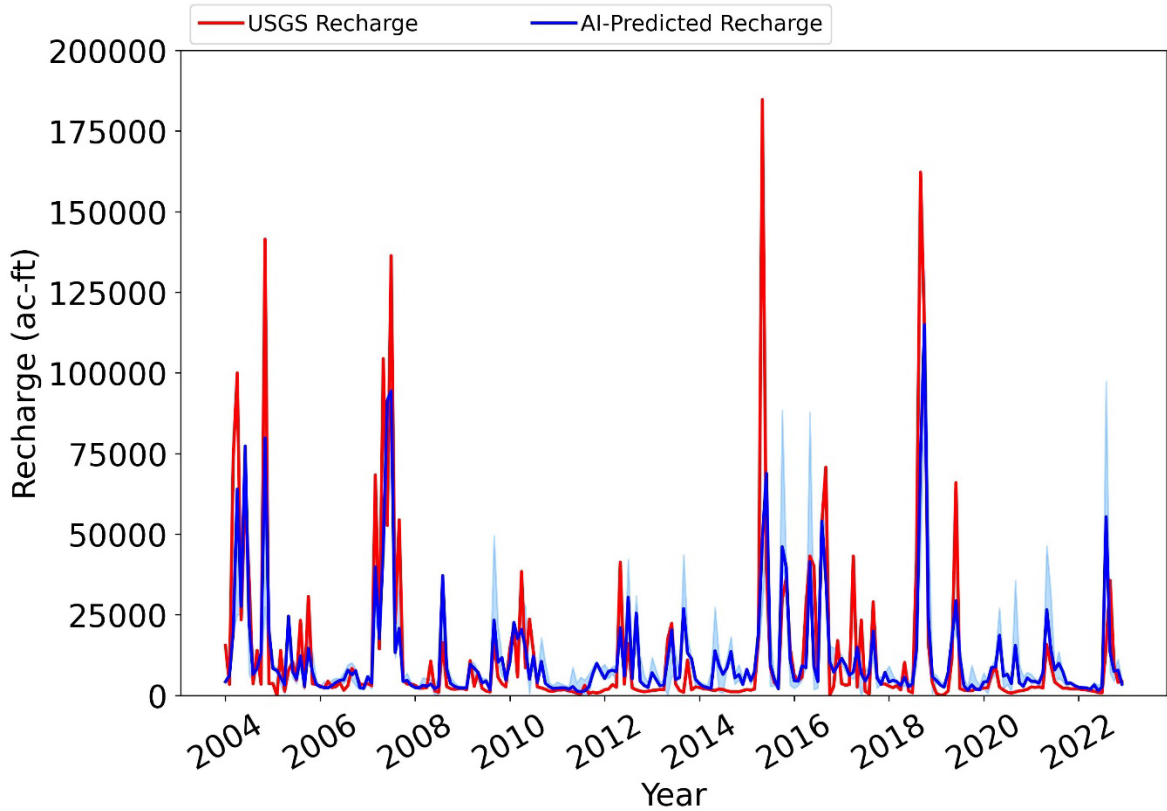


Figure 1-10. AI-based monthly recharge estimates for the Nueces basin. Recharge predictions by the ERT model are shown by the solid blue line, while the light blue shadow represents the uncertainty band formed by the recharge predictions by the ERT, RF, XGBoost, and HGBost models

1.5.2 Importance of Features in Predicting Aquifer Recharge

The ERT model was coupled with the SHAP method to create an XAI model. The Shapley value represents the average marginal contribution of each predictor value across all possible combinations of predictors. The global explanation from SHAP, as depicted by the beeswarm plot in Figure 1-11, identifies the most influential features, ranked by importance, for accurately predicting aquifer recharge. Predictors with large absolute Shapley values are deemed most important. In Figure 1-11, the importance of the predictors is presented in descending order, with the most influential predictors listed at the top. Hot-colored (red) and cold-colored (blue) dots correspond to the high and low predictor values. Positive and negative of SHAP values on the x-axis correspond to increased or reduced recharge, respectively. For example, increases in precipitation in the targeted recharge basin (TRB), depicted by red dots, are associated with enhanced recharge, as represented by positive SHAP values on the x-axis. Conversely, higher maximum temperatures, denoted by red dots, are associated with reduced recharge, as indicated by negative SHAP values on the x-axis.

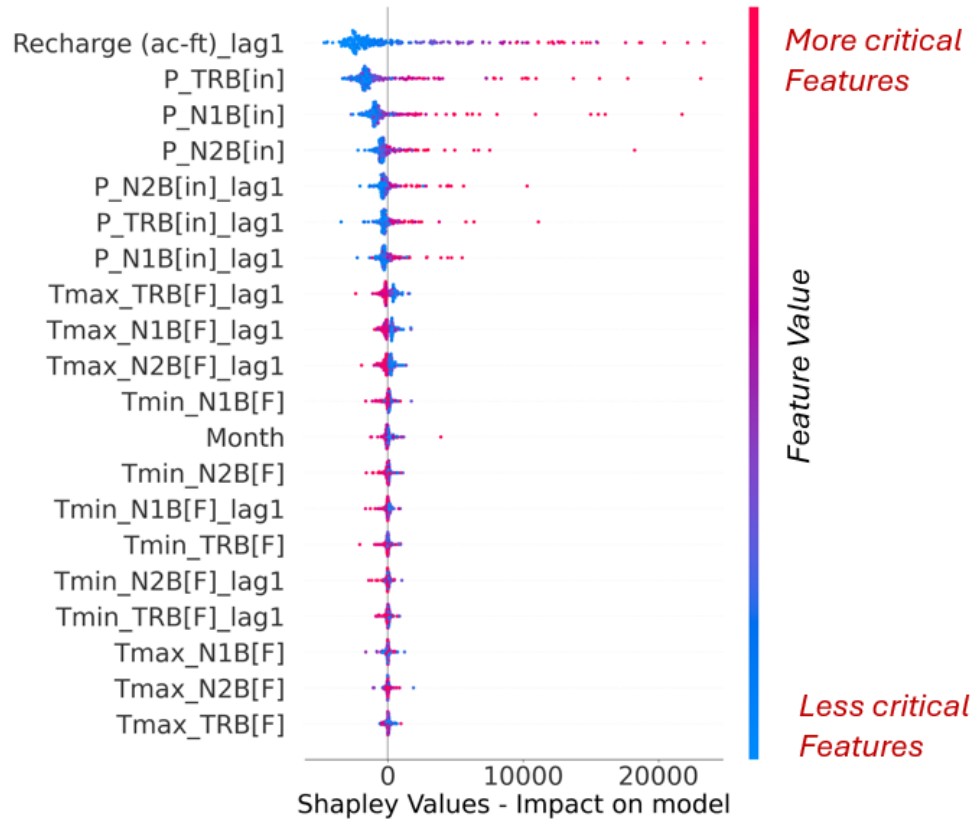


Figure 1-11. The global explanation from ERT-SHAP for aquifer recharge on the testing data. P and T represent monthly precipitation totals and monthly temperatures, respectively. TRB, N1B, and N2B stand for the target recharge basin, neighboring recharge basin west, and neighboring recharge basin east, respectively

The information gained in Figure 1-11 underscores the significance of recharge from the previous month, potentially reflecting antecedent soil moisture conditions, in forecasting recharge in the current month. Moreover, current and lagged values of monthly precipitation totals are more critical than monthly temperatures in predicting aquifer recharge. These findings are applicable to all basins in the EAR.

1.5.3 AI/ML-Based Aquifer Recharge Predictions with Respect to Groundwater Levels at the Index Wells

We examined the disparities in the magnitude and timing of the peak aquifer recharge as estimated by the ERT model and the USGS model. To support this analysis, we used previously developed HSPF models to simulate streamflow and recharge for the Edwards Aquifer system (Clear Creek Solutions 2012, 2013). There are 12 HSPF models comprising nine recharge basins. Groundwater recharge calculated for the Guadalupe River Basin is excluded from the HSPF results to be consistent with the manner in which the Guadalupe River Basin is handled in the Puente (1978) method. Time-series of precipitation and potential evapotranspiration (PET) data are required inputs for the HSPF models. Precipitation and temperature data for the period 2001 through 2022 were extracted from the DayMet V4 dataset (<https://daymet.ornl.gov/overview>) for use in the HSPF recharge calculations.

Calculation of PET is simplified in the HSPF simulations because of limited data availability. PET is obtained from the reference evapotranspiration (ET_0) using a crop coefficient of 0.85 uniformly distributed across the region. ET_0 was calculated with the Hargreaves-Samani method. HSPF estimated recharge for each basin was then used as a check for the AI/ML models.

Using the Bexar Basin as an example (Figure 1-12), the most notable distinctions include: zero aquifer recharge estimated by the USGS for April 2006 is not predicted by the AI/ML models, the non-zero recharge peak predicted by the AI/ML models for October 2009 is not accounted for in the USGS recharge estimation, and the non-zero recharge peak predicted by the AI/ML models for September 2018 is not included in the USGS recharge estimation.

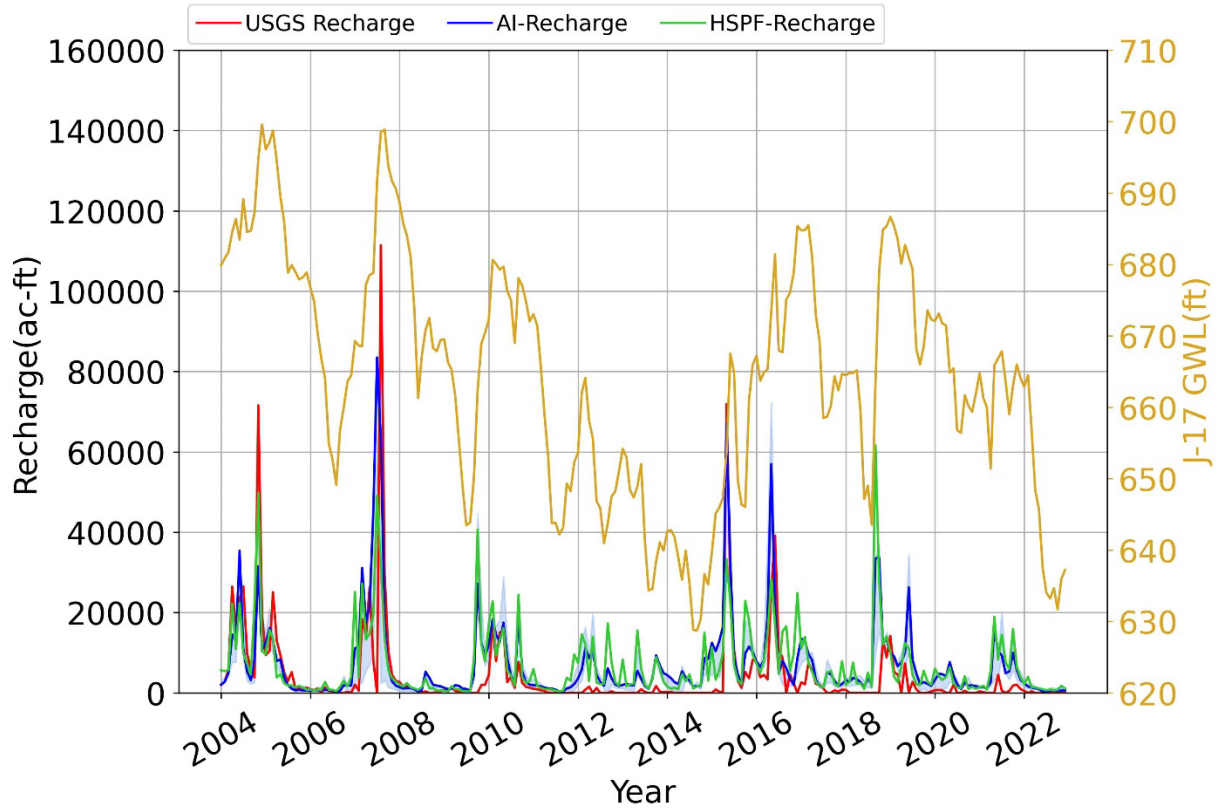


Figure 1-12. AI/ML-based monthly recharge estimates for the Bexar Basin, in comparison to monthly recharge estimates by the USGS model and HSPF model. Recharge predictions by the ERT model are shown by the solid blue line, while the light blue shadow represents the uncertainty band formed by the recharge predictions by the ERT, RF, XGBoost, and HGBost models. Temporal variations in groundwater levels at the J17 index well are shown as a reference

We explore these discrepancies by incorporating simulation results from the HSPF model, alongside estimates from the data-driven AI/ML models and USGS model in Figure 1-12. Additionally, we incorporate temporal fluctuations in groundwater levels at the J17 well, which is representative of the groundwater system in the San Antonio pool to provide further insight. The AI/ML models do not use groundwater levels at the index wells as a modeling feature, and hence, they are unaware of groundwater conditions at these wells during the prediction process.

As seen in Figure 1-12, during April 2006, groundwater levels at the J17 well rise following a period of decline earlier in the year. This relative change is not consistent with zero recharge recorded for the Bexar Basin in that month. Our in-house HSPF simulations also indicate non-zero recharge in April 2006, consistent with the estimates from the AI/ML models. Similarly, in October 2009, a sharp rise in groundwater levels coincide seamlessly with non-zero recharge predicted by both the AI/ML and HSPF models. Similarly, the larger recharge event in September 2018 identified by the AI/ML and HSPF models correlates well with the significant rise in groundwater levels at the J17 well, but is not consistent with estimates from the USGS model. A confounding factor is that precipitation, while often regionally correlated, can be significantly variable spatially. Thus, the response at J17 may also be influenced by recharge contributions from other basins. However, while not zero, there is low recharge recorded in the other seven basins during these periods—at levels that appear to be insufficient to fully account for the level changes at J17.

These discrepancies between groundwater levels at the index well and recharge predictions by the USGS model for recent years for the Bexar Basin could lead to disparities in annual and cumulative recharge estimates from each of the recharge models. Zero recharge predicted by the USGS model, contrasted with small non-zero recharge responses to small precipitation events during relatively dry periods as predicted by the AI/ML and HSPF models, may also contribute to disparities.

As shown in Figure 1-13, increases in groundwater levels at the J27 index well, representative of groundwater conditions in the Uvalde pool of the Edwards Aquifer, exhibit strong correlation with aquifer recharge events estimated for the Nueces Basin by the USGS, AI/ML, and HSPF models. Although the timing of the significant recharge events is well aligned from all models, aquifer recharge peaks predicted by the USGS are, in general, larger than the estimates by the AI/ML and HSPF models. However, the relative magnitudes of recharge peaks within each model remain consistent in relation to changes in groundwater levels at J27. In essence, greater Nueces Basin recharge in the USGS model is required to produce increases in groundwater levels at the J27 well when compared to AI/ML and HSPF modeled recharge. In contrast to the Bexar Basin, fewer instances of zero recharge events are predicted for the Nueces Basin by the USGS model, which better aligns with predictions of the AI/ML and HSPF models—as might be expected, there are reduced uncertainties under a perennial flow regime compared to the ephemeral streams in the Bexar Basin. Consequently, the AI/ML models trained on historical data at the Nueces Basin predict recharge more consistently, and the predictions are well aligned with the fluctuations in groundwater levels at the J27 index well.

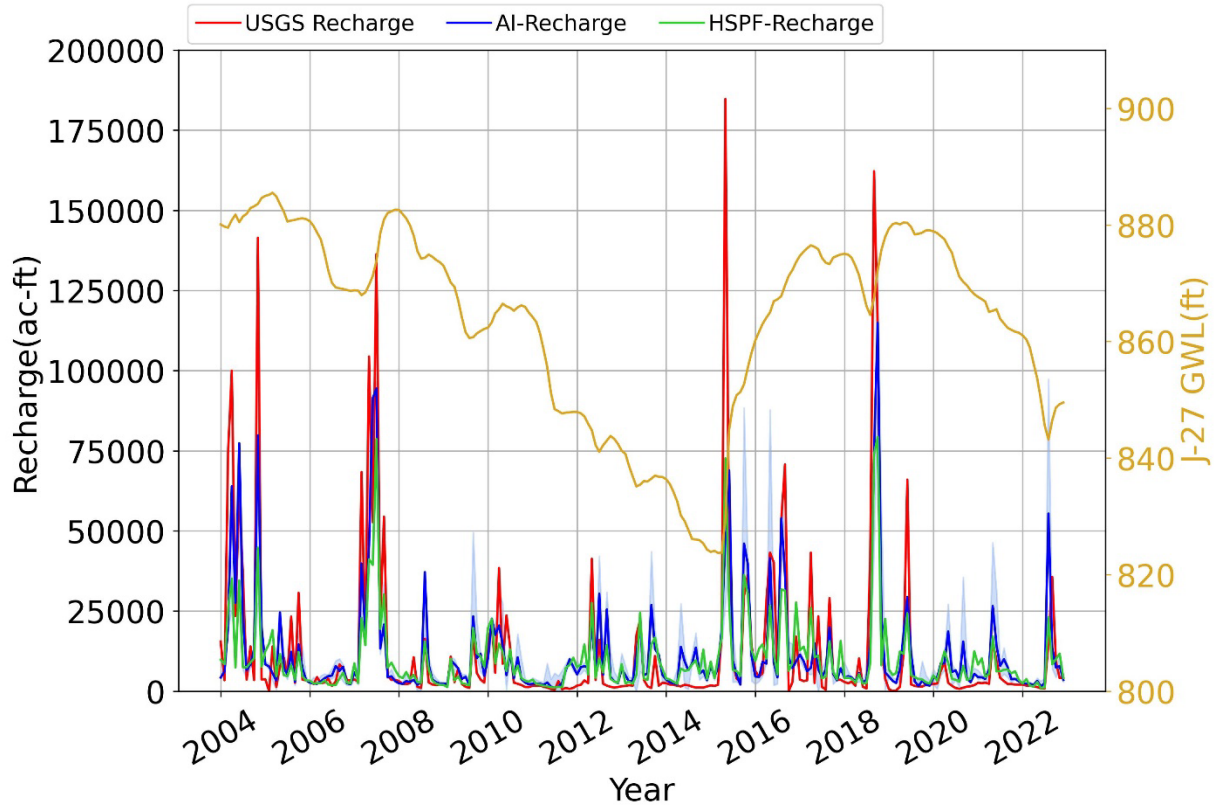


Figure 1-13. AI/ML-based monthly recharge estimates for the Nueces Basin, in comparison to monthly recharge estimates by the USGS model and HSPF model. Recharge predictions by the ERT model are shown by the solid blue line, while the light blue shadow represents the uncertainty band formed by the recharge predictions by the ERT, RF, XGBoost, and HGBost models. Temporal variations in groundwater levels at the J17 index well are shown as a reference

1.5.4 AI/ML-Based Aquifer Recharge Predictions and Adjustments

As discussed in the previous sections, the USGS model often attributes zero recharge during dry periods, whereas the AI/ML and HSPF models often predict non-zero recharge values during these same periods, partly in response to small precipitation events within a basin. Consequently, cumulative recharge values diverge as the AI/ML and HSPF models aggregate non-zero recharge values. This is evident in Figure 1-14.

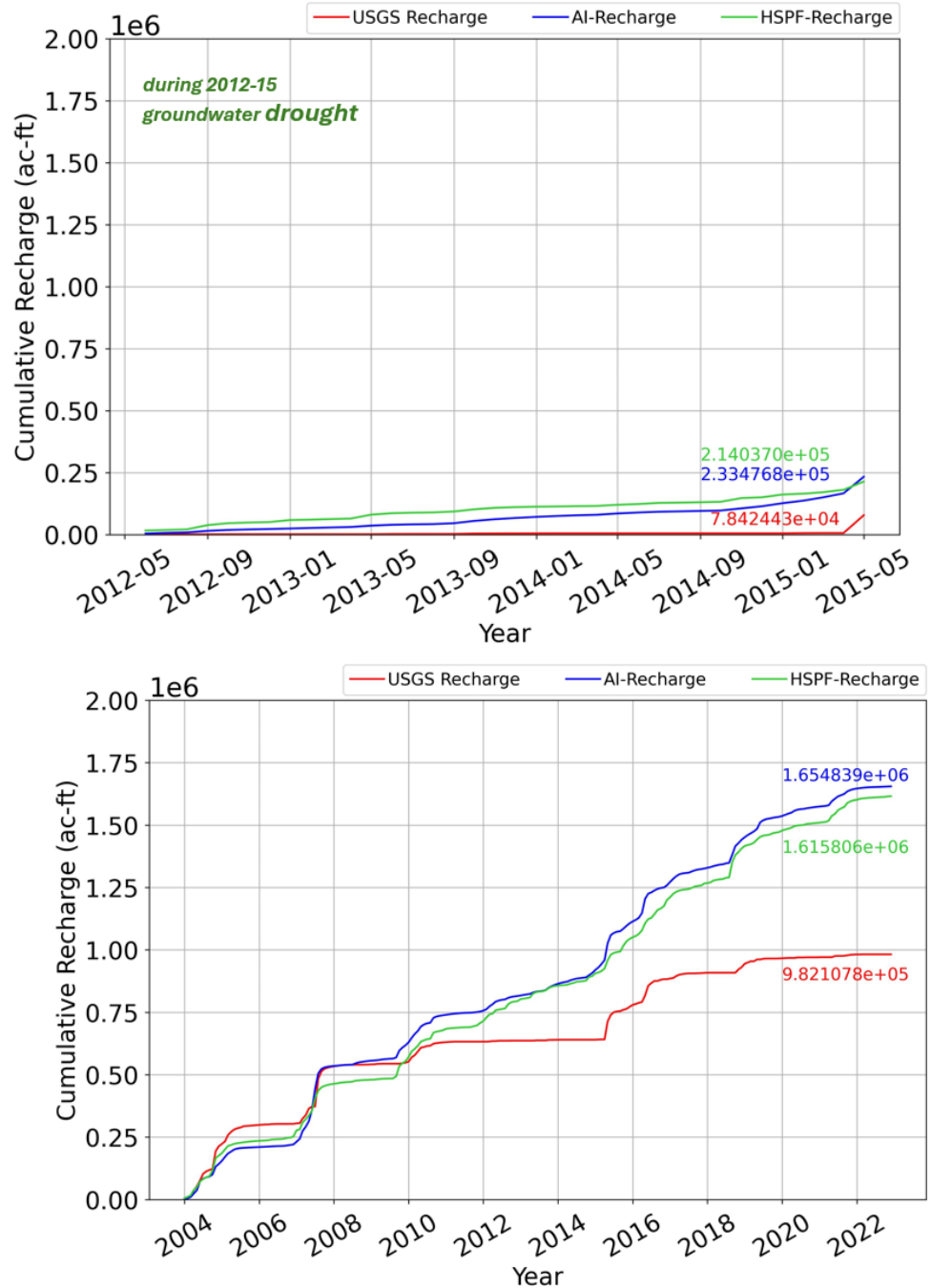


Figure 1-14. Cumulative aquifer recharge in the Bexar Basin during the 2012–2015 drought period (top panel) and for the entire testing period (2004–2022) (bottom panel) as estimated by the USGS (red), AI/ML (blue), and HSPF (green) models

Figure 1-14 (top panel) presents calculated recharge estimates for the Bexar basin as estimated by the USGS, AI/ML, and HSPF models. Both the AI/ML and HSPF models predict greater cumulative recharge relative to the USGS model during the 2012 through 2015 drought period. These differences occur for many basins during short-term drought events and contribute to divergence between USGS and AI/ML model recharge predictions. If we introduce a threshold for the AI/ML-

based predictions, below which aquifer recharge during drought periods is set to zero to mimic the USGS model estimates, we obtain results like those shown in Figure 1-15 in which the AI/ML model correlation with the USGS model is much improved.

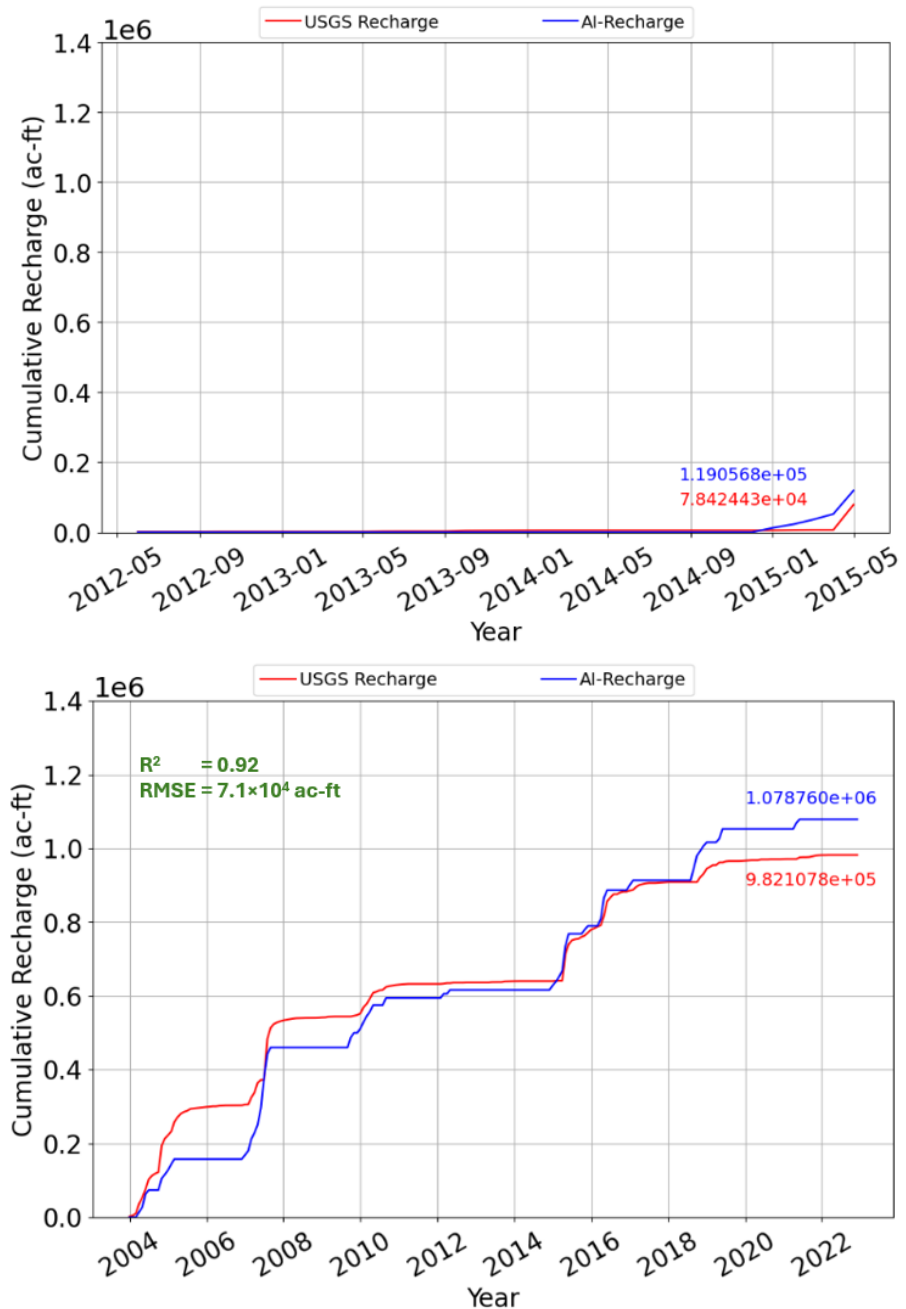


Figure 1-15. Cumulative aquifer recharge in the Bexar Basin during the 2012–2015 drought period (top panel) and for the period 2004–2022 (bottom panel) as predicted by the USGS (red) and AI/ML (blue) models. A recharge threshold of 10,000 ac-ft is used to set monthly recharge values below 10,000 ac-ft in the Bexar Basin to zero

We determined recharge threshold values for AI/ML-based recharge predictions for each basin, below which aquifer recharge is presumed to be zero, to mirror the outcomes from the USGS model. The values were selected by maximizing the R² values of the model relative to the USGS estimates. Threshold recharge values range from 0 (for the Nueces Basin) to 20,000 ac-ft (for the Seco-Hondo Basin). By implementing these threshold values, the USGS estimated aquifer recharge and AI/ML-predicted aquifer recharge in each basin displayed improved correlations with R²= 0.88–0.98 and RMSE= 3.7×10^4 – 1.92×10^5 ac-ft for the period of 2004 through 2022. Figure 1-16 and Figure 1-17 present the final recharge model results after implementation of the threshold values.

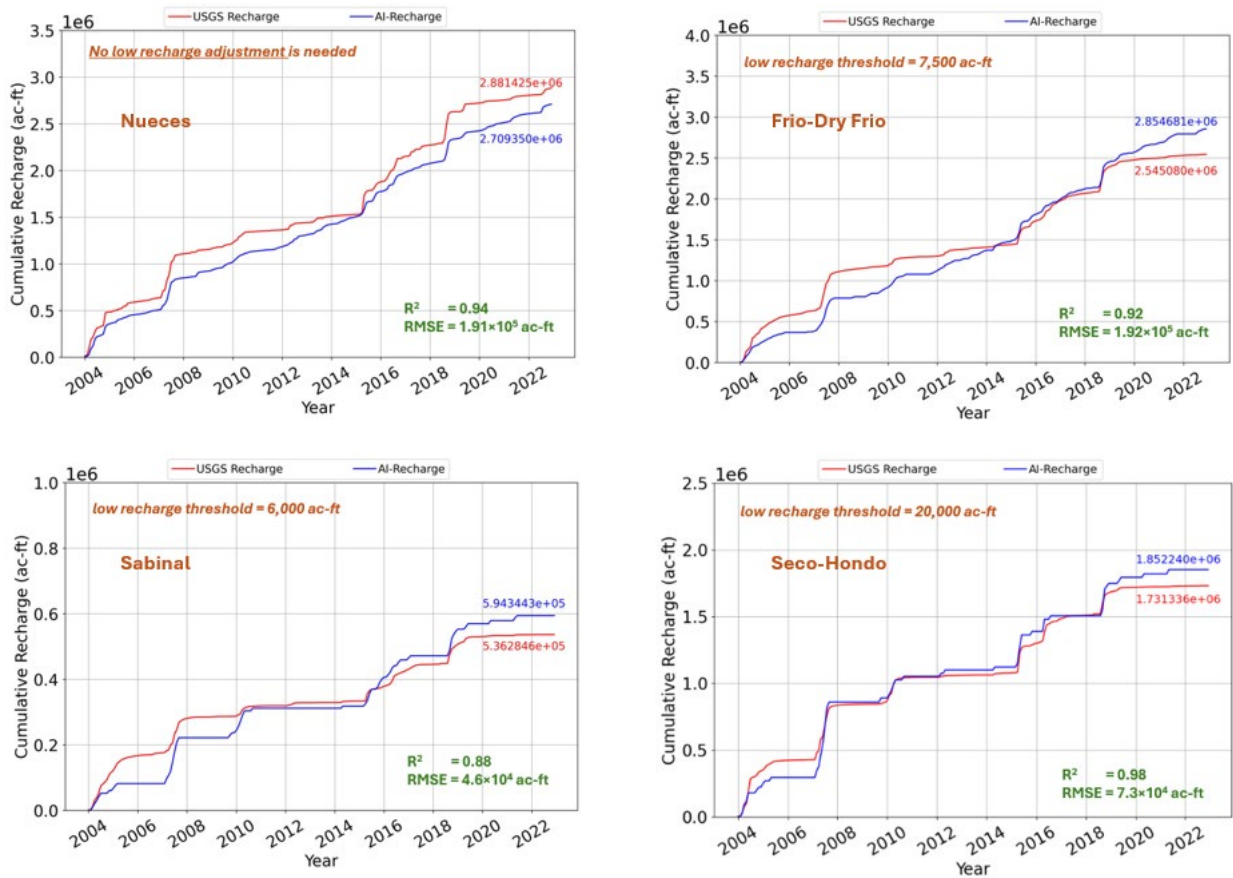


Figure 1-16. Comparison of cumulative aquifer recharge for the Nueces, Frio-Dry Frio, Sabinal, and Seco-Hondo Basins for the period from 2004–2022, after application of threshold values to reduce AI/ML modeled recharge during drought periods

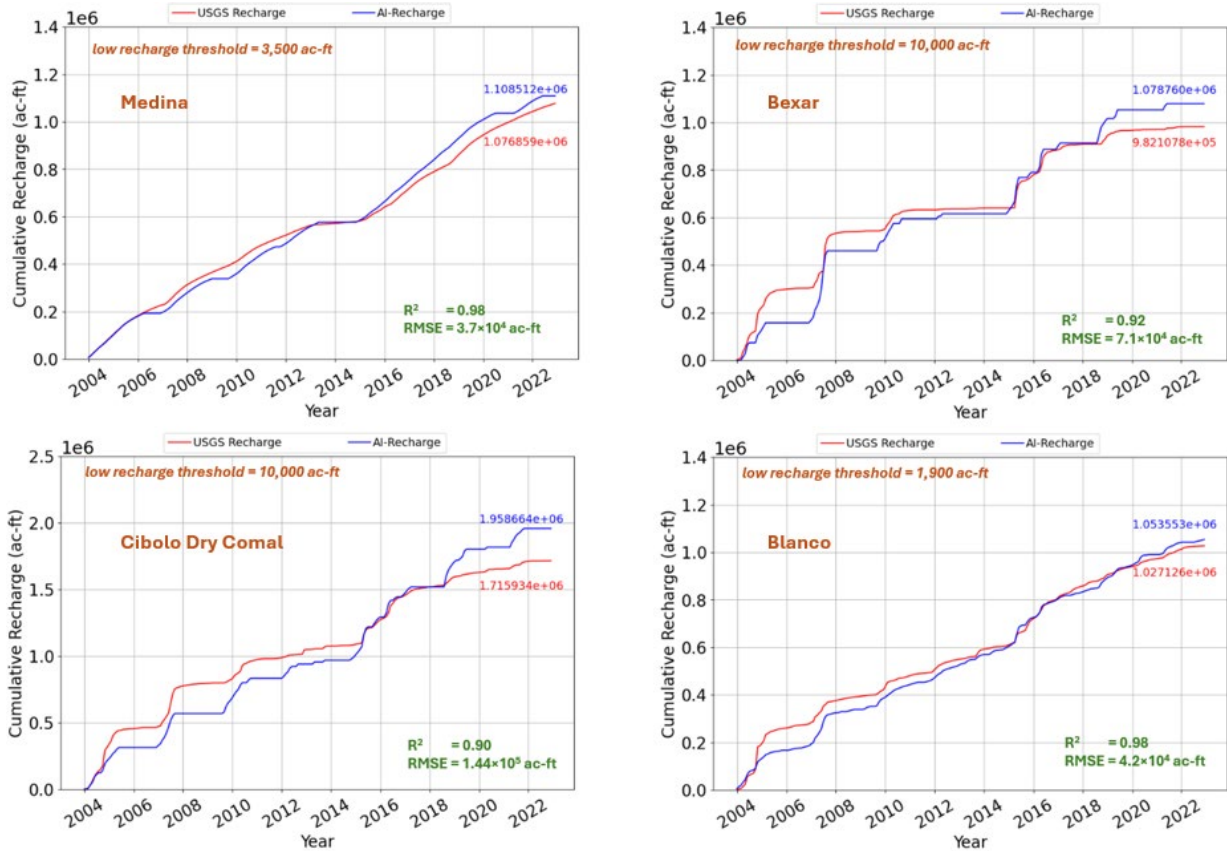


Figure 1-17. Comparison of cumulative aquifer recharge for the Medina, Bexar, Cibolo Dry Comal, and Blanco Basins for the period from 2004–2022, after application of threshold values to reduce AI/ML modeled recharge during drought periods

Total cumulative recharge predicted by the ERT model across the EAR, after implementing basin-specific recharge thresholds, is presented in comparison to USGS recharge estimates in Figure 1-18. The AI/ML model estimate, for which the 2004 through 2022 USGS recharge was not used to train the model, reproduces the USGS values quite well. The total difference in cumulative recharge between the two models for the entire EAR over the 18-year test period is about 6%.

As confirmed by comparison to values during the test period from 2004 through 2022, the AI/ML models for each recharge basin reasonably reproduce the timing and magnitude of recharge consistent with the Puente (1978) approach. Figure 1-19 shows a comparison of USGS estimated annual recharge and the ERT model predicted annual recharge for each basin. Median values of recharge and the range of recharge values for each basin during the test period (2004–2022) compare favorably.

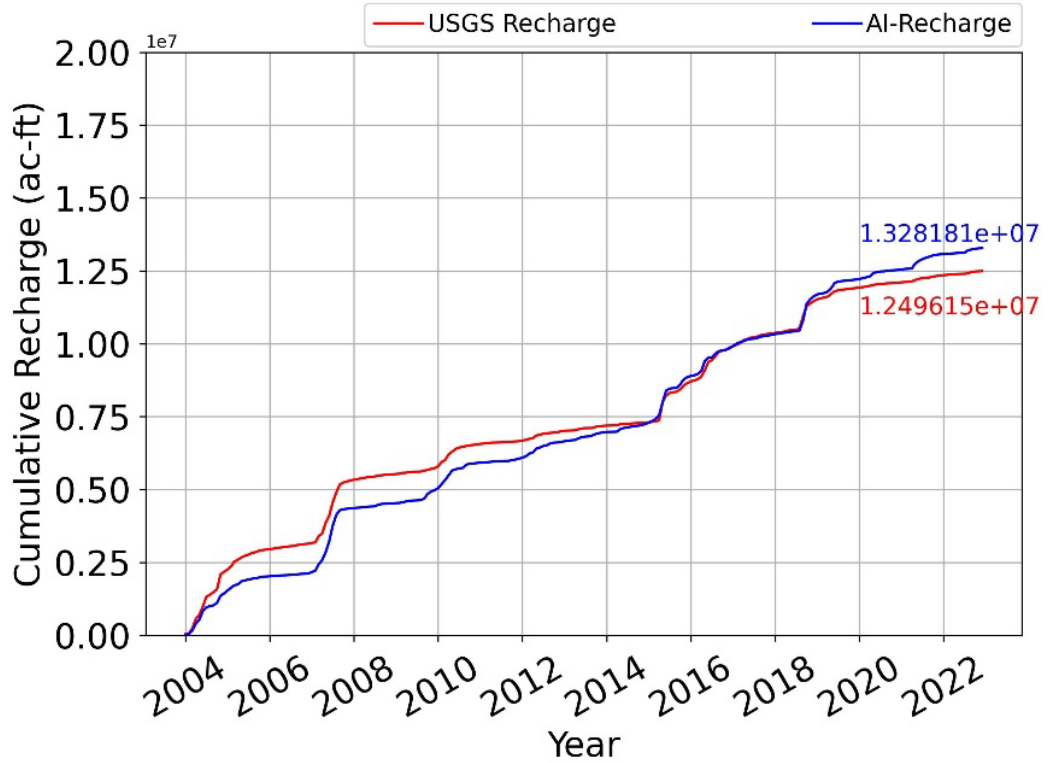


Figure 1-18. Comparison of cumulative aquifer recharge for the entire EAR for the period from 2004 through 2022, when a threshold recharge, below which AI-predicted aquifer recharge is presumed to be zero to replicate the outcomes from the USGS recharge model

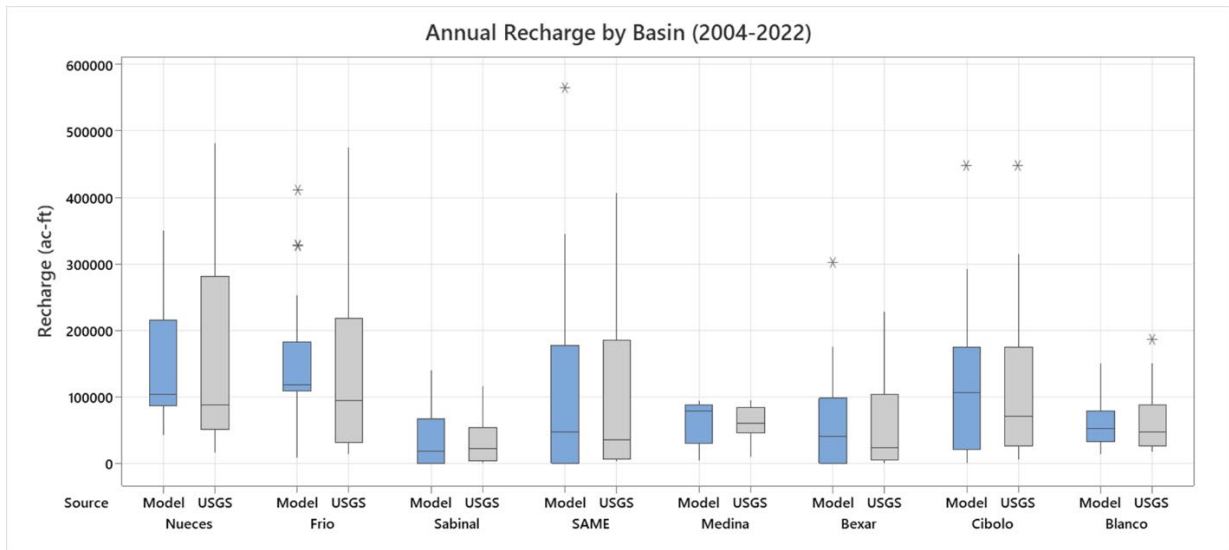


Figure 1-19. Box plot of annual recharge for each basin for the period 2004–2022. AI/ML model predictions are in gray and USGS calculated values are in blue

1.6 Recharge Projections Under Future Climate Conditions

Scenario-based future climatic conditions were derived from GCMs, using a statistical downscaling method focused on the EAR (Wootten et al. 2024). Time-series data for temperature and precipitation from each of the 19 GCMs assessed in our downscaling effort were used in combination with the AI/ML recharge models to produce projections of recharge for the Edwards Aquifer for the period 2023 through 2065. Recharge projections were generated by month for each basin and organized for input to subsequent groundwater flow modeling.

An example of projected aquifer recharge generated from two GCMs under differing emissions scenarios (i.e., four of the 19 GCMs) for the Bexar recharge basin is shown in Figure 1-20. The variability in projected recharge rates based on different GCM models and the emission scenarios is evident in the figure. For example, while aquifer recharge projections for the Bexar Basin are high when using the data from HadGEM2-CC under the intermediate emissions scenario, projections derived from the KIOST-ESM under the intermediate emission scenario are lower. Notably, these lower projections from the KIOST-ESM are comparable to projected recharge from the HadGEM2-CC under the high-emission scenario. Among the four projections in Figure 1-20, the most concerning recharge conditions, potentially posing a higher risk to groundwater sustainability, are observed in the future recharge projection using data from KIOST-ESM under the high-emission scenario. However, while basin-scale recharge estimates are informative, the actual effects on groundwater levels and spring flows requires evaluation in a flow model.

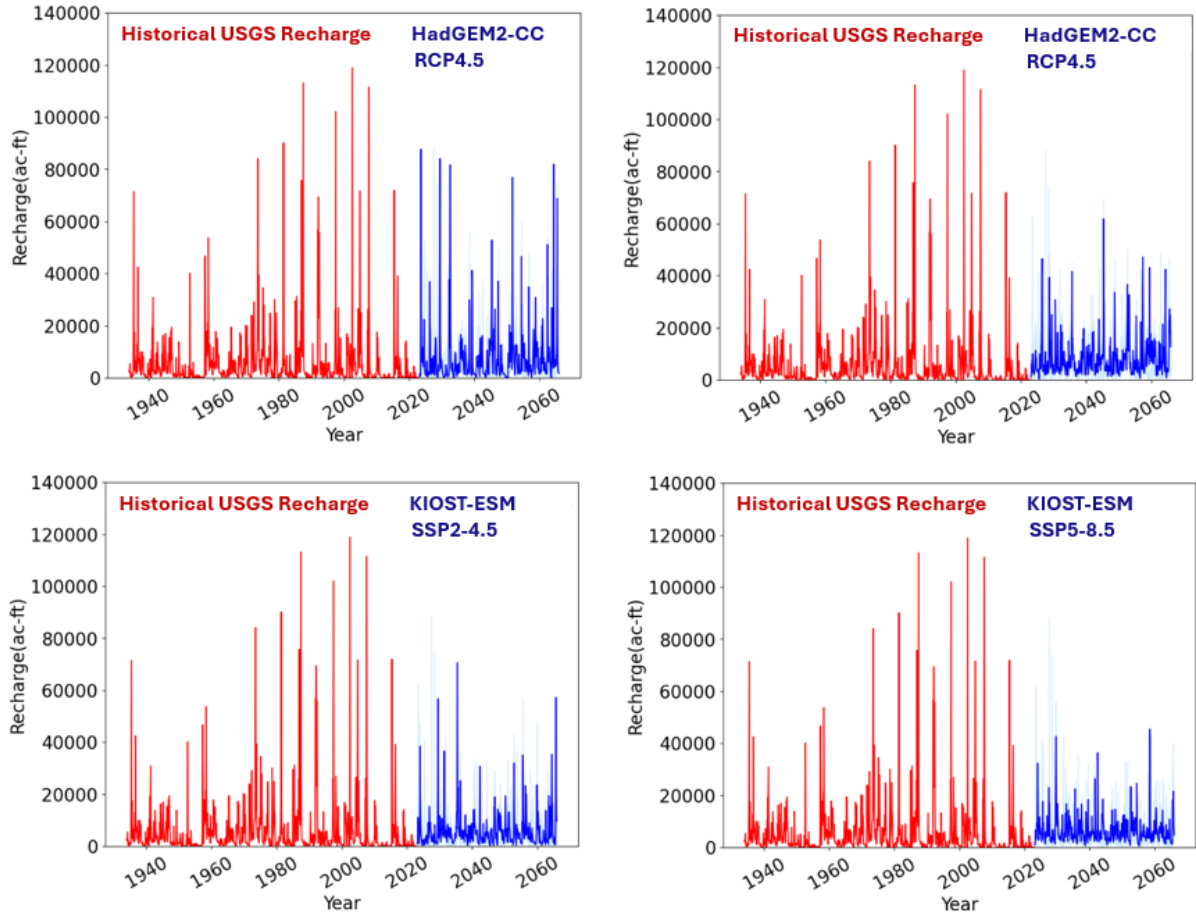


Figure 1-20. Projected aquifer recharge for the Bexar recharge basin using downscaled climate data from 2023 through 2065, sourced from two GCMs, including a CMIP5 (HadGEM2-CC) and CMIP6 (KIOST-ESM) models under intermediate- and high-emission scenarios. These are the AI-based recharge predictions, not incorporating recharge thresholds. Recharge predictions by the ERT model are shown by the solid blue line, while the light blue shadow represents the uncertainty band formed by the recharge predictions by the ERT, RF, XGBoost, and HGBost models

The cumulative total projected monthly recharge across all basins from 2023 through 2065 are shown in Figure 1-21. Also shown is the cumulative historical total monthly recharge for the period 1980 through 2022. Projected recharge from most GCMs is less than the recharge observed in the recent past, irrespective of the modeled emission scenario (Figure 1-21).

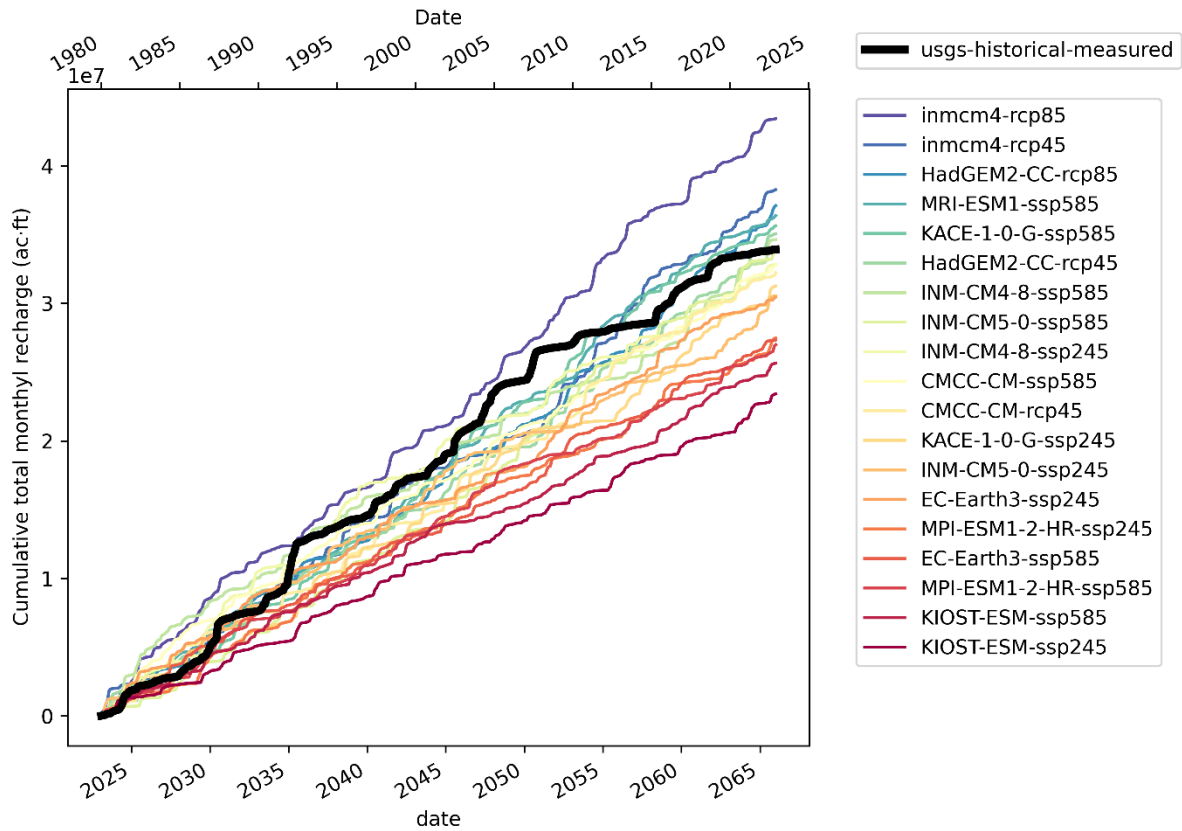


Figure 1-21. Projected cumulative monthly total recharge from each GCM (colored lines) for the period 2023–2065. Cumulative monthly historical recharge for the period 1980–2022 is shown by the heavy black line

A box plot summary of the projected (2023–2065) total monthly recharge for each GCM is shown in Figure 1-22. Also shown is a box plot of total monthly historical recharge for the period 1934 through 2022. Projected values of recharge bracket historical recharge for the Edwards Aquifer. The ranges and magnitudes of the projections are not dissimilar to the range of recharge experienced in the past, which suggests that the associated groundwater modeling results are likely to vary in range and magnitude that are similar to historical observations.

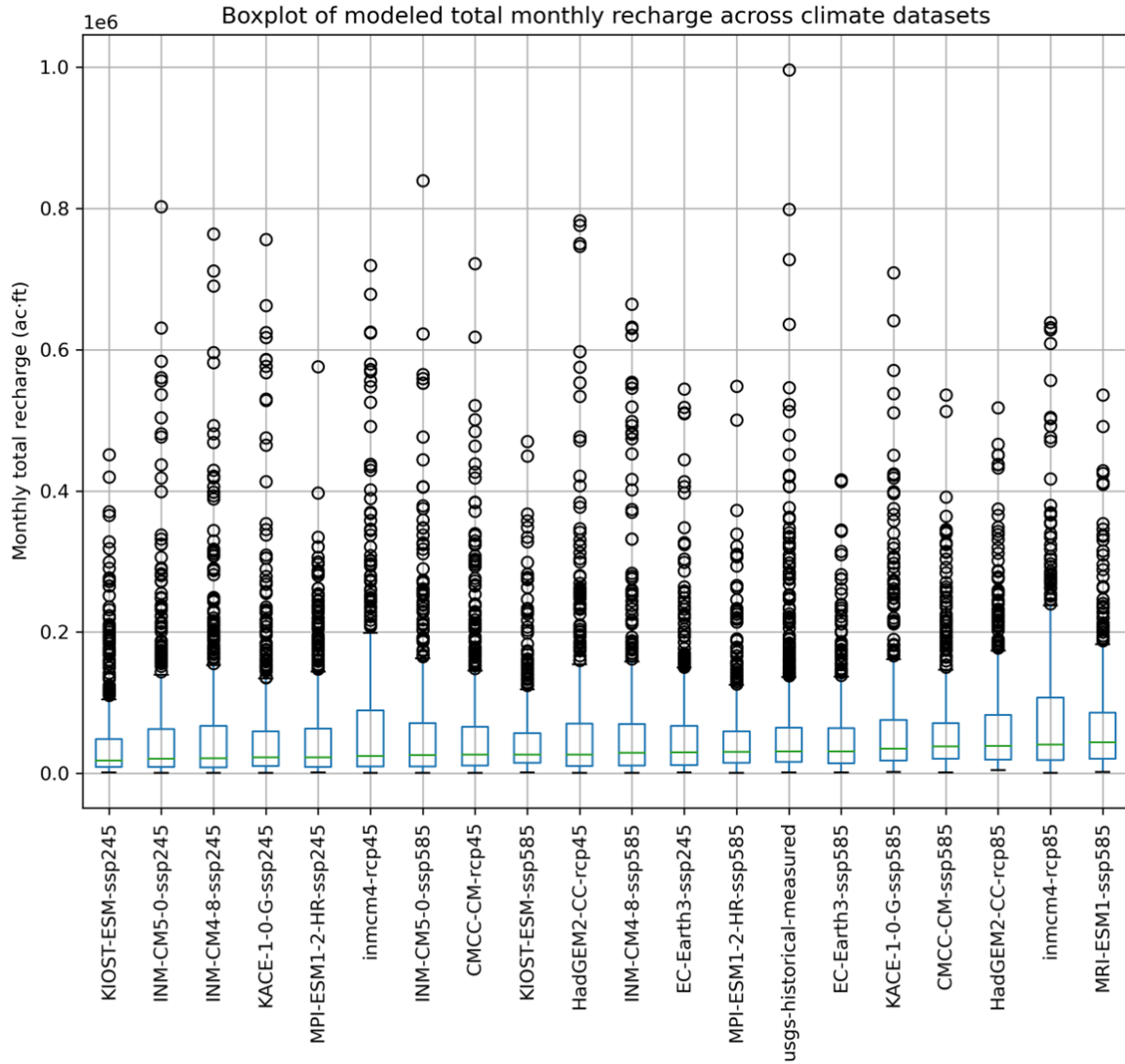


Figure 1-22. Box plots of projected total monthly recharge for the Edwards Aquifer from each GCM for the period 2023–2065. Measured historical recharge for the period 1934–2022 is also shown for comparison. Note the projections and historical recharge box plots are ordered by their median recharge values



Chapter 2

Projected Spring Flows Under Future Climate Conditions: MODFLOW Modeling Analysis

The USGS modular finite-difference groundwater flow (MODFLOW) modeling program was used to estimate groundwater levels and spring flow under varying recharge and discharge conditions for the Edwards Aquifer (Lindgren et al. 2004). This hydrogeologic numerical simulation model has served as the basis for subsequent evaluations of critical period management (CPM) measures and options for spring flow protection during development of the EAHCP (RECON et al. 2012; HDR 2011). The HDR (2011) version of the model is informally referred to as the “Bottom-Up package” or “Bottom-Up model.” The Lindgren et al. (2004) model was updated in 2017 to add conceptual features and improve model calibration using more recent pumping and recharge data (Liu et al. 2017). The updated model of Liu et al. was then used in conjunction with the management modules created for the earlier EAHCP analyses (HDR 2011) to run the EAHCP Phase II model simulations. Model construction, modifications, simulations, and the associated results are thoroughly documented in the model reports (Lindgren et al. 2004; Liu et al. 2017) and technical memoranda associated with the EAHCP Phase II analyses (Appendix C; Furl 2019) including the review by the EAA-appointed Groundwater Model Advisory Panel (Liu et al. 2017:Appendix), the National Academy of Sciences (NAS) Reports 1–3 covering the EAHCP (NAS 2015, 2017, 2018), and technical presentations delivered to the NAS panel and EAHCP Science Committee (www.eachp.org).

The information provided in the following sections summarizes work to update and verify model files used in this analysis and to incorporate recharge projections developed from the climate model data that are described in Chapter 1. We also provide a brief outline of model results to highlight various trends in projected spring flows.

2.1 Model Preparation

The EAHCP Phase II version of the MODFLOW model used in these simulations was not substantively changed from the previous calibrated version developed by Liu et al. (2017). Some modifications to input files and the execution of the model were required to incorporate a longer period of analysis, reduce potential errors in generating input files, and to simplify and make the running of each simulation more efficient.

The EAHCP Phase II model is configured for a 12-year numerical simulation that includes the drought of record period (1947–1958) with a total of 144 stress periods (months). To accommodate a proposed ITP renewal period of 30 years (i.e., 2028–2058), and to be consistent with the mid-century timeframe commonly used in future climate modeling, a simulation period spanning from 2023 through 2065, totaling 43 years with 516 stress periods (months), was established for this modeling effort. The period from 2023 through 2027 is included to minimize the impacts of the initial aquifer conditions on the simulated spring flows. However, sensitivity analysis suggests that the initial aquifer conditions exhibit minor impacts on simulated spring flows only within the first 3 to 7 stress periods (months) of any model run.

Several MODFLOW-specific packages were revised to simulate the additional stress periods. These packages include the DIS package for spatial and temporal discretization, the DRN package for the

parameters of the spring drainage features, the OC package for controlling model output, the MPW package for implementing well pumping management, the RCH package for distributing recharge, and the WEL package for the well pumping. No modifications are made to the other MODFLOW packages, including the BAS package that specifies the locations of active and inactive cells and the initial heads in all cells, the LPF package for the aquifer parameters, and the HFB package for horizontal barriers.

Updates to the DIS package are made solely for the time discretization section, which includes a total of 516 stress periods. No modifications are made to the spatial discretization section defined in the DIS package, such as the top and bottom elevations of the Edwards Aquifer. Updates to the DRN package are made to repeat the parameters of the springs over the 516 stress periods because the spring conductivity parameters, as established in the EAHCP Phase II model analysis, do not vary over time. The OC package is also updated to output the results of the 516 stress periods. The initial water heads, defined in the BAS package for the EAHCP Phase II model analysis, are used in the current modeling simulation under climate projections. The initial aquifer condition (heads) has only minor impacts on the modeling results, and the values are similar to long-term average water levels for the aquifer.

The configuration of groundwater pumping has been previously discussed in the HDR (2011) report and the two technical memos (Appendix C; Furl 2019). In the current modeling analysis, the configuration of groundwater pumping that was used in the EAHCP Phase II model analysis is not modified. The WEL package is used to represent groundwater pumping of both the permitted and exempt wells, implement the reduction of protective measures such as the Voluntary Irrigation Suspension Program Option (VISPO), the Regional Water Conservation Program (RWCP), and the EAA Forbearance of San Antonio Water System (SAWS) Aquifer Storage and Recovery (ASR) Leases. Two other packages are related to the implementation of CPM Stages 1–5. Details of the procedure to implement spring flow protective measures through pumping reduction are discussed in the next section. CPM is implemented in the TRF package (implementation of the CPM rules) and the MPW package, which contains information on the pool (i.e., San Antonio or Uvalde pool) and use of each managed pumping well in the aquifer (HydroGeoLogic, Inc. 2004, 2005). The TRF package is irrelevant to stress periods; therefore, no modifications are made. Modifications are made for the MPW package and data of the pool and use of each managed pumping well in the aquifer is repeated at each of the 516 stress periods.

Groundwater recharge is implemented in the RCH package. The EAHCP Phase II model is calibrated and validated with the input of USGS recharge estimates with adjustments (Lindgren et al. 2004; Liu et al. 2017). USGS monthly groundwater recharge estimates provided at each of the eight recharge basins are distributed to recharge zones defined in the model (Lindgren et al. 2004; Liu et al. 2017). The current modeling analysis follows the same procedure used for calibration and validation of the EAHCP Phase II model (Liu et al. 2017) to distribute monthly recharge estimated with the AI/ML models. The procedure of distribution of monthly USGS groundwater recharge in basins to the recharge zones was previously implemented via an Excel worksheet. After carefully reviewing the worksheet, the EAA modeling team found two minor errors: 1) the recharge from the Cibolo Dry Comal Basin was overreduced relative to the methods used in Lindgren et al. (2004), and 2) the cap of the USGS recharge from the Blanco Basin was not enabled. These errors did not affect the previous drought of record analyses conducted as part of the EAHCP Phase II work because the accepted historical recharge values for that period were included directly in the model (i.e., no intervening spreadsheet calculation was required). The minor errors could have affected the quality of the 2017 model calibration, but subsequent uncertainty analyses of model performance did not

identify a more suitable set of calibration parameters (White et al. 2020). After correcting the minor errors, the EAA modeling team decided to implement the procedure to distribute monthly recharge via a Python-based script (<https://www.python.org/>) to avoid manual mistakes, improve efficiency of numerical simulations, and more easily integrate recharge input into an automatic procedure for running the modeling analysis.

2.2 Modeling Procedure

Figure 2-1 summarizes the main steps of the procedure used to run the EAA model with projected recharge (Winterle pers. comm. 2023). In Step 1, the monthly recharge generated from the climate models is converted and reformatted for use in the RCH package. In Step 2, the 10-year moving annual average of total recharge is calculated to determine any periods in which the 10-year moving average falls below 500,000 ac-ft, which is a trigger value for ASR-related forbearance requirements. Because the monthly recharge estimates from the AI/ML models are provided for the period of 2023–2065, USGS reported annual total recharge values for the period of 2014–2022 are used to calculate the 10-year moving average annual average through 2031.

Step 3 consists of several parts and includes the first full run of the model. Reduction of total pumping via the RWCP is implemented in Step 3. Step 3 also implements reductions in pumping from EAA forbearance of SAWS ASR leases in years following those years where the 10-year average is below the trigger level calculated in Step 2. Step 3 also applies the full range of CPM pumping reductions based on water levels and spring flow values. Step 3 implements protective measures of RWCP, EAA forbearance, and CPM Stages 1–5 pumping reductions “on the fly” through the Groundwater Management Module (HDR 2011; HydroGeoLogic, Inc. 2004, 2005).

The calculated water level at the J17 index well on October 1 of each year in the simulated period is checked in Step 4. If the water level in the J17 index well is below 635 ft amsl on that date, then reductions in pumping covered by VISPO leases are applied in the year after VISPO is triggered. Step 4 includes another full model run and implements the protective measures in Step 3 and VISPO-related reductions if triggered.

Step 5 is a full run of the model and applies pumping reductions related to SAWS ASR forbearance, which is triggered based on two conditions: 1) the 10-year moving annual average recharge is below 500,000 ac-ft, and 2) the water level in J17 index well is below 630 ft amsl (based on results from of Step 4). A Python script is implemented to check the two conditions for all stress periods. In a month when the two conditions are met, reduction in groundwater pumping following the scheme listed in Table 4 in the report by Furl (2019) is applied. Implementation of the SAWS ASR forbearance is accomplished via the RCH package (HDR 2011; Liu et al. 2017; Winterle 2019). Spring flow protection measures implemented in Steps 3 and 4 are also included in Step 5.

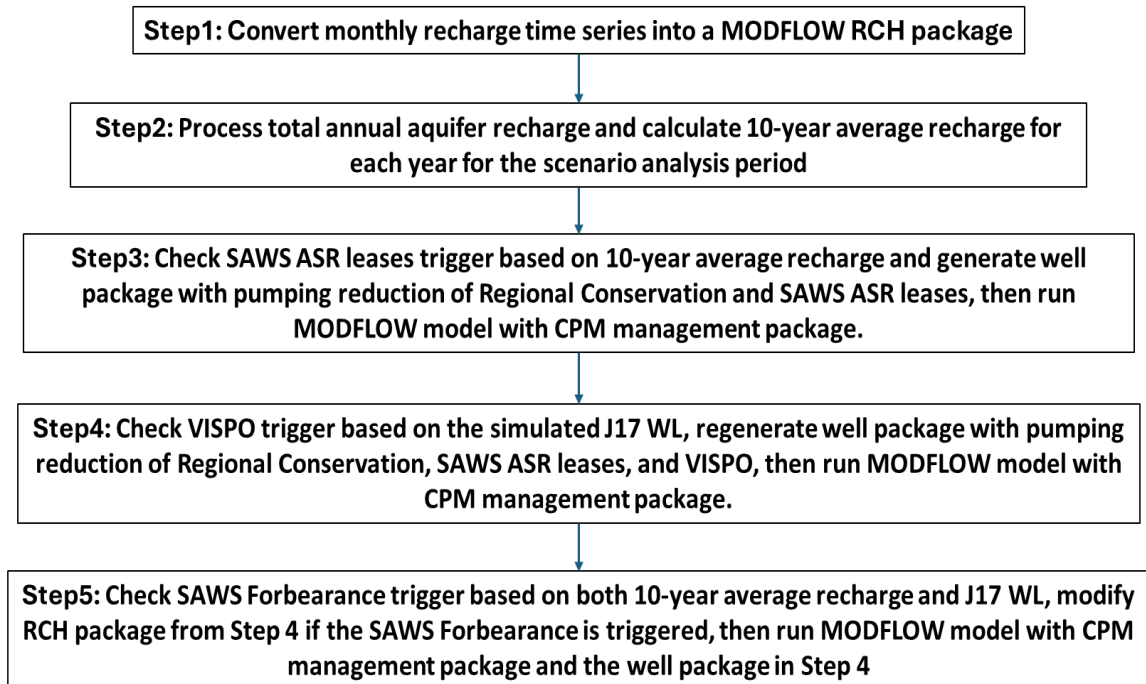


Figure 2-1. Modeling Procedure with Projected Recharge to Simulate Spring Flows in the Edwards Aquifer

The five steps of the modeling procedure depicted in Figure 2-1 are implemented via a Jupyter notebook (<https://jupyter.org>) (Kluyver et al. 2016) that includes several Python programming language modules. While the EAHCP Phase II model was also previously run in part using a Jupyter notebook interface, the new and revised Python modules and scripts in the updated Jupyter notebook constitute the main changes to the modeling process in this analysis. Most of the changes were made to reduce the potential for data entry errors and to streamline the running of the model. Scripts were developed to: 1) properly distribute the monthly recharge per basin output from the recharge model into the RCH package, 2) automate identification and implementation of VISPO reductions, 3) automate the identification and implementation of SAWS ASR forbearance in the RCH package, and 4) create visualizations and user-friendly output files for post-processing and inspection of results. Appendix A provides an example of the Jupyter notebook for the modeling analysis with example input of recharge from the KIOST-ESM ssp245 GCM.

The modeling procedure in the Jupyter notebook has several advantages. First, modeling efficiency is significantly increased. The time required to complete a model run for each climate model input was reduced from 3–7 days using the manual procedure to 8–14 hours with the newly automated procedure. This reduced the time required to complete the full range of models by several weeks. Second, the scripting helps to avoid potential data entry and other transcription errors that can occur when updating recharge and well packages manually. Only the projected basin-scale recharge values are needed to initiate a complete model run. Finally, post-processing and quality checks are improved because of added control of output file types and locations. Intermediate results and final results are saved and available for inspection without additional file type conversion or the need for proprietary software.

2.3 Model Validation

2.3.1 Comparisons to the Archived EAHCP Phase II Model Runs

The EAA model was previously run as part of the EAHCP Strategic Adaptive Management Program (SAMP). Model runs were conducted for the drought of record period from 1947 to 1958 with a total of 144 stress periods (months). One of the archived EAHCP SAMP model runs was repeated with the new automatic modeling procedure in the Jupyter notebook to test the new modeling procedure. For this test run, no updates are made in the SAMP model. The recharge package in the SMAP model was used without modification, and no changes were applied to the SAWS ASR forbearance scheme implemented in the SAMP model.

Figure 2-2 and Figure 2-3 show results from the archived SAMP model and the current model as run with the automated procedure. Water levels in the J17 index well and spring flow rates for both Comal Springs and San Marcos Spring produced by the two models are nearly indistinguishable. The results indicate the current model and the associated Jupyter notebook procedure are equivalent to previous models used to assess spring flow protection measures for the EAHCP Phase II.

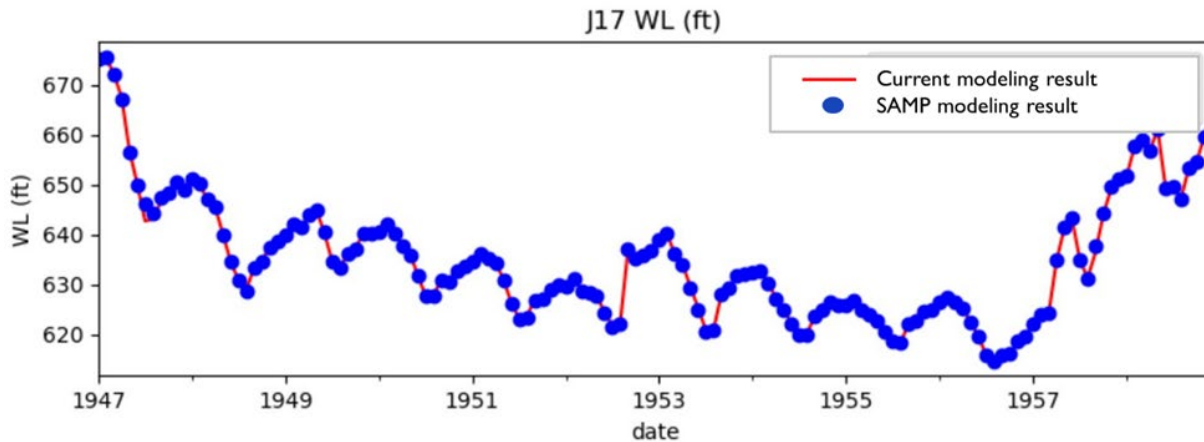


Figure 2-2. Comparison of J17 water levels (WL) simulated with the modeling procedure described in the previous section compared to the SAMP modeling result

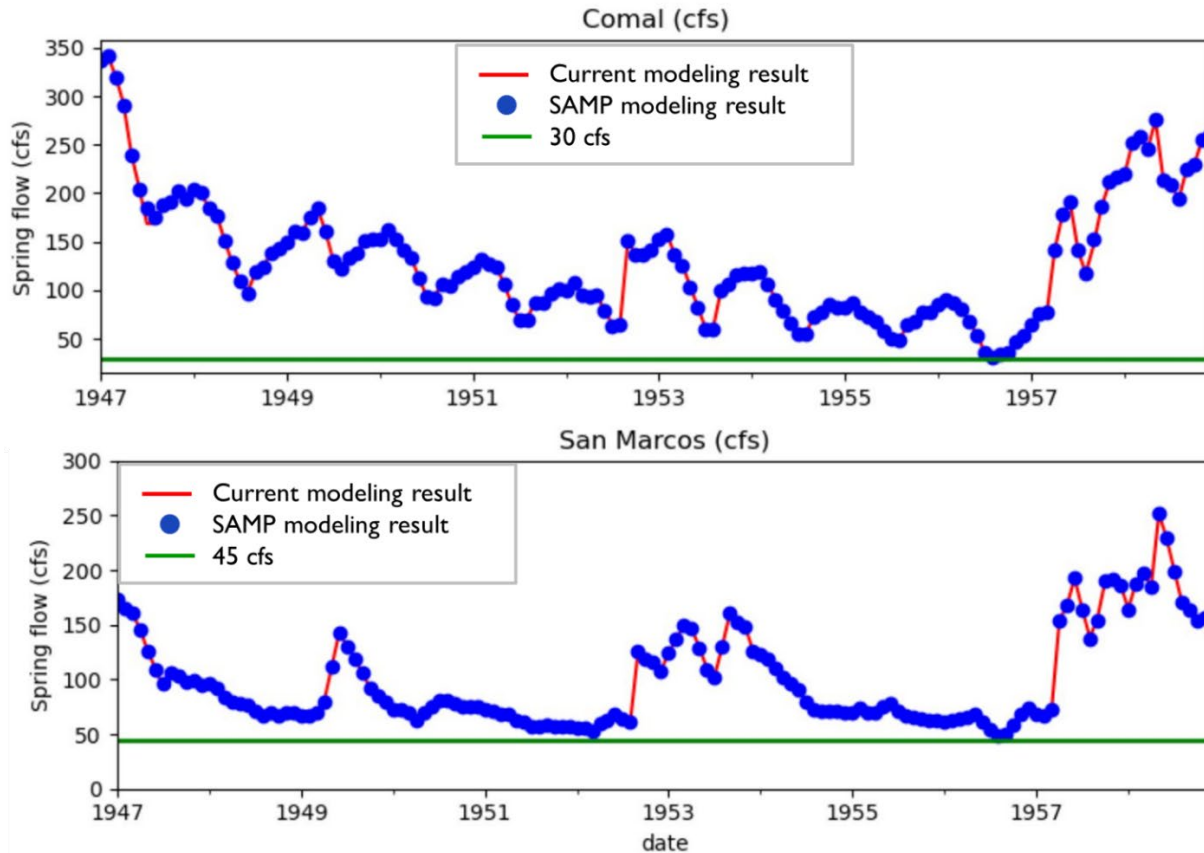


Figure 2-3. Comparison of spring flow rates of Comal Springs (top) and San Marcos Springs (bottom) simulated with the current modeling procedure compared to the SAMP modeling result

2.3.2 Modeling Analysis Using USGS, HSPF, and AI/ML Modeled Recharge for Historical Period 2001–2022

As discussed in previous sections, the MODFLOW model used to produce the projected water levels and spring flows is the same as has been used in earlier HCP-related analyses. The Lindgren et al. (2004) and the updated Liu et al. (2017) models were calibrated using best available aquifer data and the results are provided in the respective reports. Because the focus of the current modeling effort is to assess performance of spring flow protection measures, maximum permitted pumping is always applied. This limits our ability to directly compare model outputs to actual historical water levels and spring flows. One way of testing the model is to conduct a set of analyses with known recharge inputs and compare model output(s) for appropriate magnitude and scale of water levels and spring flow. Three modeling analyses were performed using reported USGS recharge, recharge calculated using an existing HSPF model (described in Section 1.5.3), and the AI/ML recharge model for the historical period of 2001–2022. These model runs provide a means to compare model output using reasonable, but differing recharge input variables.

Because the validation period is 22 years (2001–2022) with a total of 264 stress periods (months), the model’s MODFLOW packages described previously were updated accordingly to accommodate

264 stress periods. In addition, the initial aquifer conditions for the EAA model calibration of Liu et al. (2017) were applied by updating the BAS package. The Liu et al. (2017) model calibration was conducted for 2001–2011, so the initial heads used in that simulation are appropriate.

The AI/ML recharge from the GCMs is provided for the period 2004–2022 (19 years). Details of the AI/ML modeling are found in Chapter 1. As a result, data from USGS reported recharge in 2001–2003 was appended to the AI/ML recharge input so that these three model evaluation runs had the same number of stress periods.

The three modeling runs were conducted using the Jupyter notebook with the automatic modeling procedure. The modeling results are shown in Figure 2-4 and Figure 2-5. The results for this set of tests may not correlate well with actual water levels and spring flows observed from 2001–2022 because of the continuous application of maximum permitted pumping in the model. Nonetheless, we can use information from the three recharge estimations (e.g., Chapter 1, Figure 1-13) to assess the results. Simulated water levels in the J17 index well are generally higher with the HSPF recharge than with the USGS and the AI/ML recharge (Figure 2-4). This result is consistent with the relatively greater recharge estimated by the HSPF models, especially during dry periods. Simulated flow rates for Comal Springs and San Marcos Springs are consistent with variations in water levels at J17 for each recharge model (Figure 2-5). The HSPF recharge generally produces higher flow rates of both springs than the USGS recharge and the AI/ML recharge, particularly during the low flow periods (Figure 2-5).

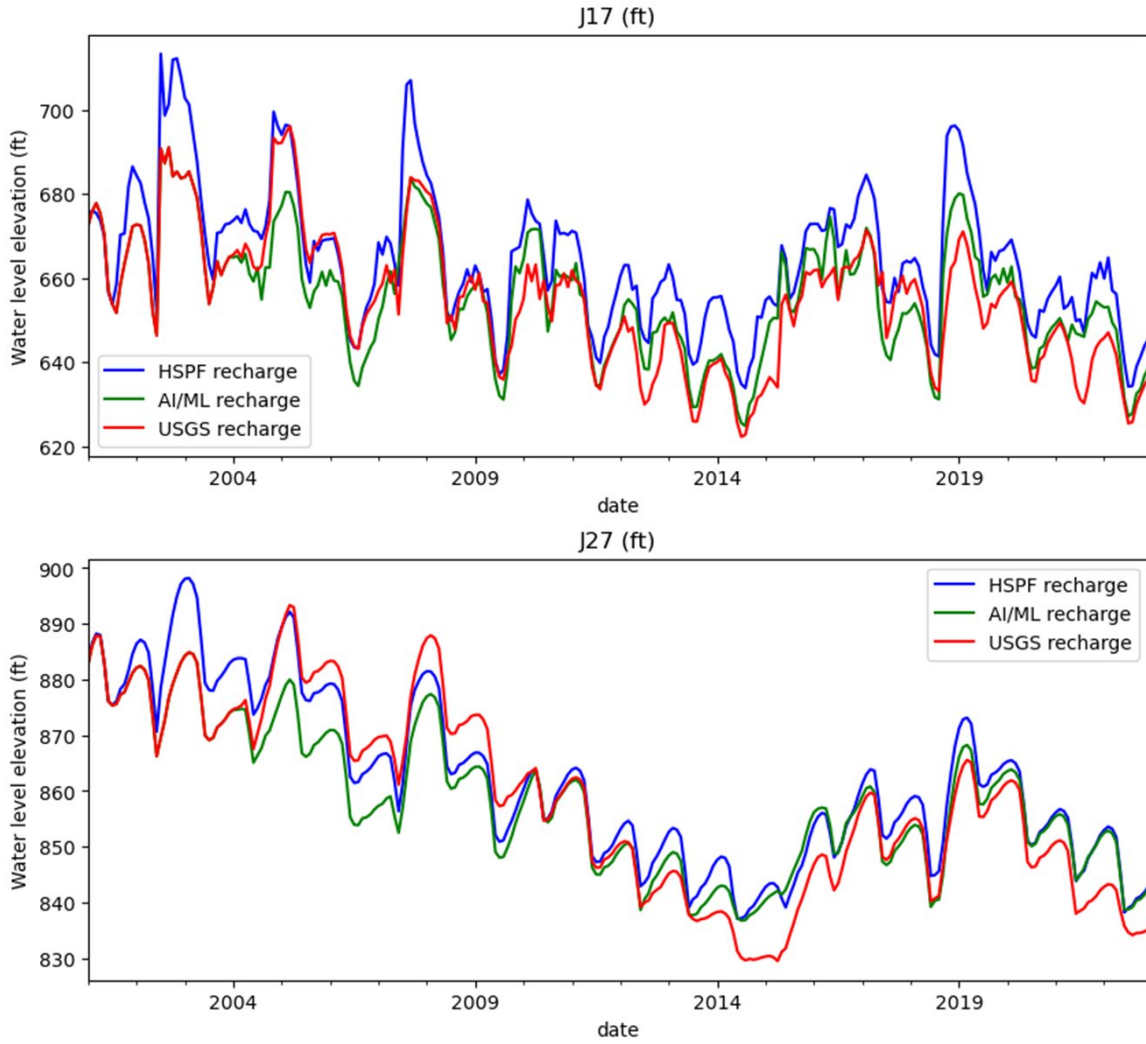


Figure 2-4. Comparison of J17 water levels (top) and J27 water levels (bottom) simulated using the groundwater flow model with the USGS recharge, HSPF recharge, and AI/ML recharge models

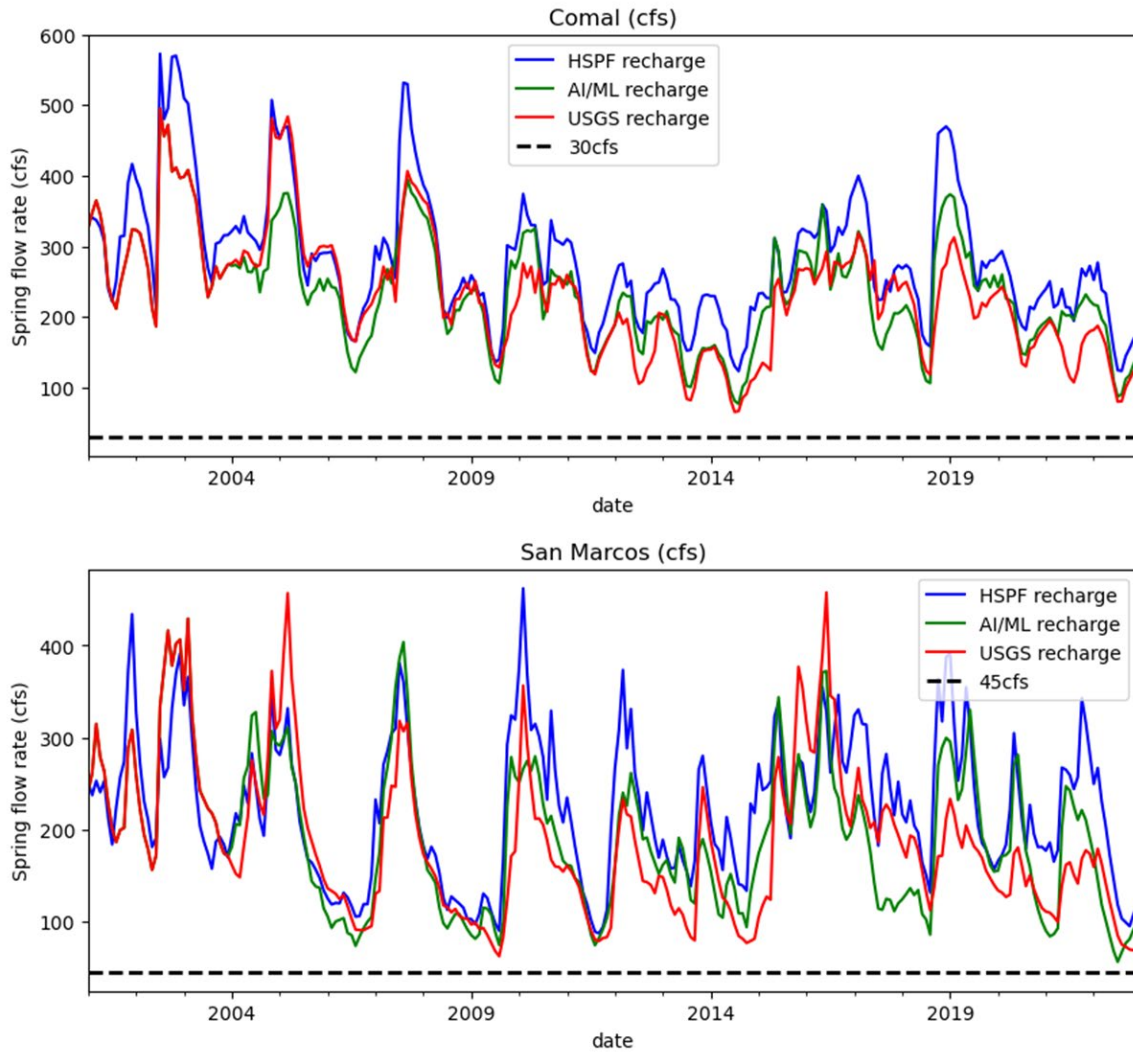


Figure 2-5. Comparison of spring flow rates for Comal Springs (top) and San Marcos Springs (bottom) simulated using the groundwater flow model and the USGS recharge, HSPF recharge, and AI/ML recharge models

Simulated water levels in the J27 index well show more agreement between the HSPF and the AI/ML recharge estimates (Figure 2-4). One reason for this is that the Uvalde pool recharge is dominated by inputs from the Nueces and West Nueces rivers (a single basin recharge calculation) so there is less variation in the estimates of the two models relative to other outputs, which represent inputs from multiple basins.

An important observation can be made regarding the variation or sensitivity in model output relative to the recharge model used. Minimum spring flows produced by the USGS recharge estimates and the associated AI/ML recharge model are quite similar (Figure 2-4). In some cases, the AI/ML recharge model produces lower flows, and in other cases, the USGS recharge produces lower flows. With the exception of a few instances (e.g., 2018 at San Marcos and 2022 at Comal), the pattern displayed by the AI/ML recharge model is a reasonable facsimile of the results produced by historical recharge data. This provides added confidence that the AI/ML recharge model is a good representation of recharge for the aquifer system and can be used in the projections of future water

levels and spring flows. The differences also make clear the relative changes in model output that result from differences in recharge input.

As mentioned previously, direct comparison of model output and observed historical water levels and spring flows is not particularly relevant because of the strict way in which maximum permitted pumping and other mitigation measures are applied in the model. Groundwater pumping in the model simulations is generally higher than the actual pumping from the Edwards Aquifer. Figure 2-6 compares the estimated monthly total pumping in the Edwards Aquifer used in the Liu et al. (2017) model and the monthly pumping input in the current model analysis for the period 2001–2015. Clearly groundwater pumping in the current model is greater than the actual estimated monthly pumping (top plot of Figure 2-6). However, as might be expected during severe drought conditions, estimated pumping from January 2014 to January 2015 is very similar in both models (bottom plot of Figure 2-6). We can use this period to conduct a spot check on model performance. We evaluated the output of the model using the USGS estimated recharge as input for September 2014 when aquifer levels at J17 and spring flows at Comal Springs were at their lowest. The minimum water level at J17 as calculated by the bottom-up model is 623 ft amsl while the actual level was 627 ft amsl. Similarly, the minimum spring flow at Comal Springs in September 2014 is calculated by the model to be 65 cubic feet per second (cfs) while the actual measured low spring flow at Comal Springs for that period was also 65 cfs. Results are different for San Marcos Springs. Low flows in San Marcos did not fall below 100 cfs in September 2014, but the bottom-up model estimates flows of about 80 cfs. Thus, for a specific timeframe in which we can compare withdrawals and conditions between observed data and conditions used in the model, the model performs reasonably well and is consistent with its performance during the EAHCP Phase II drought of record analysis (Furl 2019).

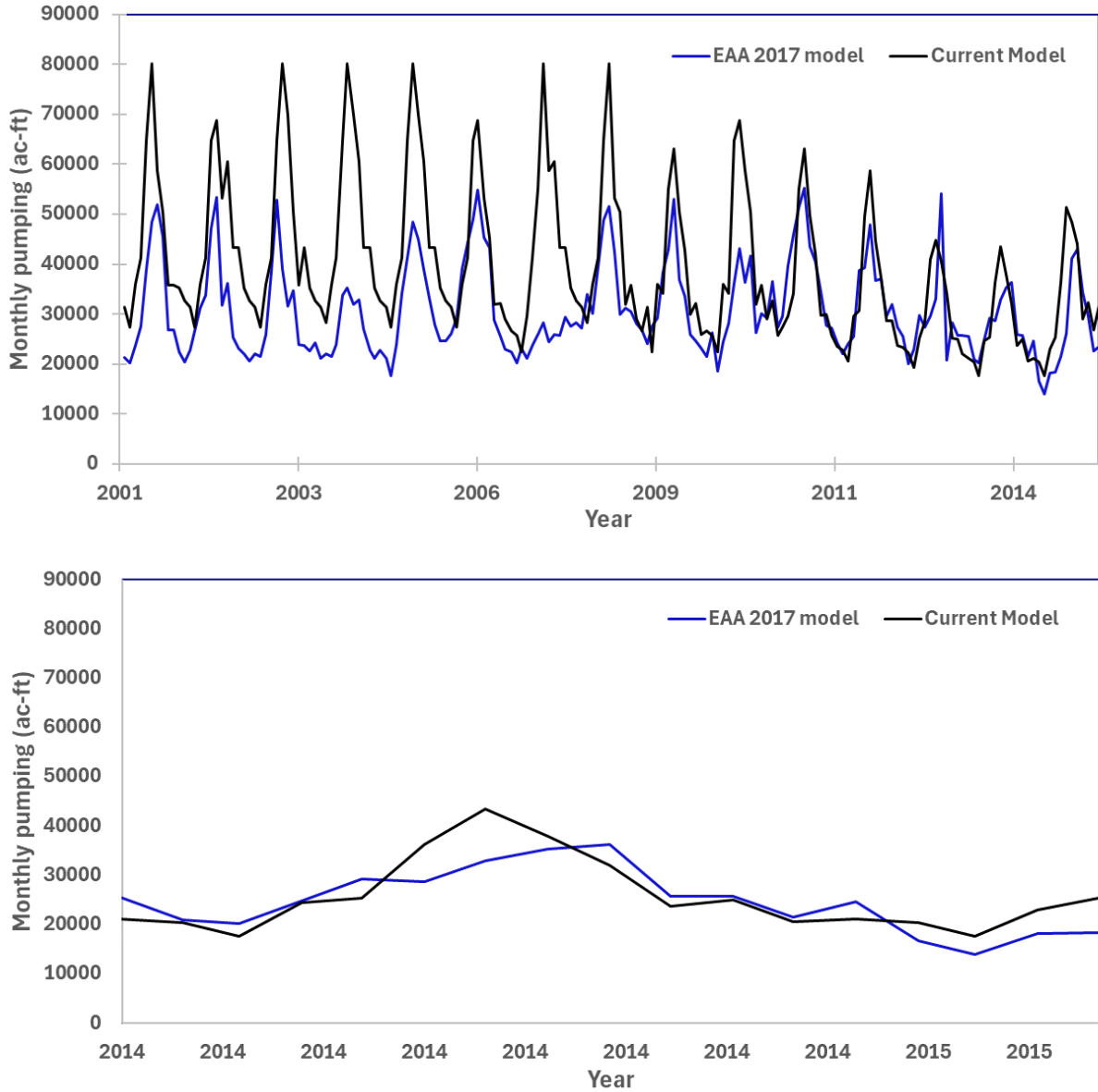


Figure 2-6. Comparison of monthly pumping from the output of the EAA 2017 model and the EAHCP Phase II model simulation using USGS recharge with protective measures. The bottom plot is focused on the period January 2014 to May 2015. Pumping extracted from the output of the EAA 2017 model represents estimated actual pumping from the aquifer

2.4 Results and Discussion

Separate model runs were conducted for each of the projected recharge sequences associated with the 19 downscaled GCMs (Wootten et al. 2024). Simulating a single climate projection with the Jupyter notebook and the automatic modeling procedure typically required about 8–14 hours. Three of the 19 simulations faced numerical convergence issues, but by adjusting the convergence criteria specified for solving nonlinear groundwater flow equations, these issues were effectively resolved.

2.4.1 Modeled Projected Water Levels for the J17 Index Well

Figure 2-7 displays modeled water levels in the J17 index well for all 19 climate projections spanning from 2023 to 2065. Modeled water levels in J17 exhibit a range from 614 ft amsl to 698 ft amsl. Figure 2-7 (bottom) illustrates the modeled water levels in the J17 index well specifically during the first 12 stress periods (months). The influence of the initial aquifer conditions on modeling results is primarily confined to the first three to seven stress periods.

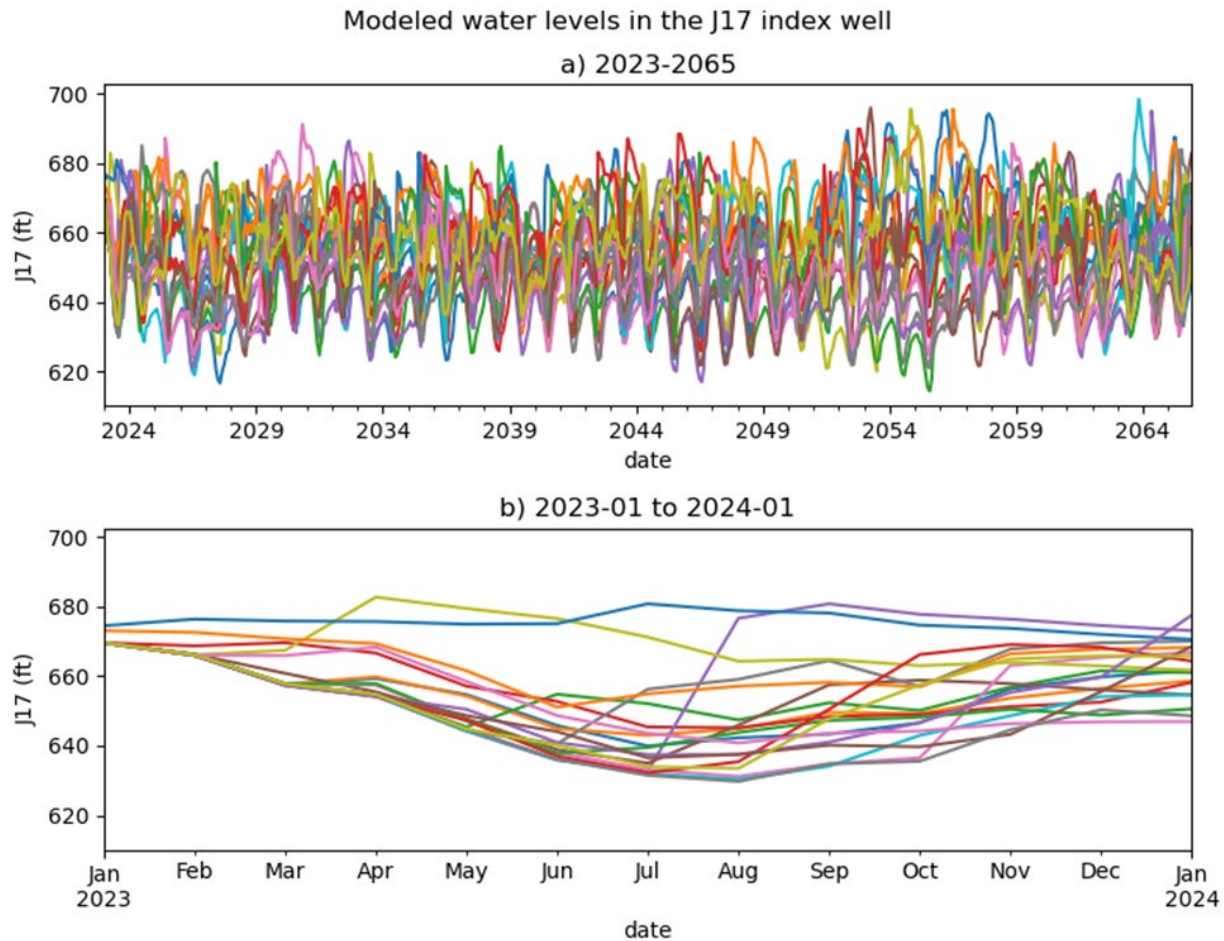


Figure 2-7. Modeled water levels for the J17 index well for the 19 GCM projections spanning (a) from 2023 to 2065 and (b) during the first 12 stress periods of the model runs

2.4.2 Modeled Projected Spring Flows

Modeled spring flow rates for Comal Springs and San Marcos Springs for all 19 climate projections are presented in Figure 2-8 and Figure 2-9. Across all models, simulated flow rates range from 24 cfs to 516 cfs for Comal Springs and from 27.6 cfs to 498.7 cfs for San Marcos Springs. The model is known to be sensitive to large values of recharge, especially for San Marcos Springs, and was purposely calibrated to perform better at low flow conditions, so the higher modeled spring flows have the greatest uncertainty.

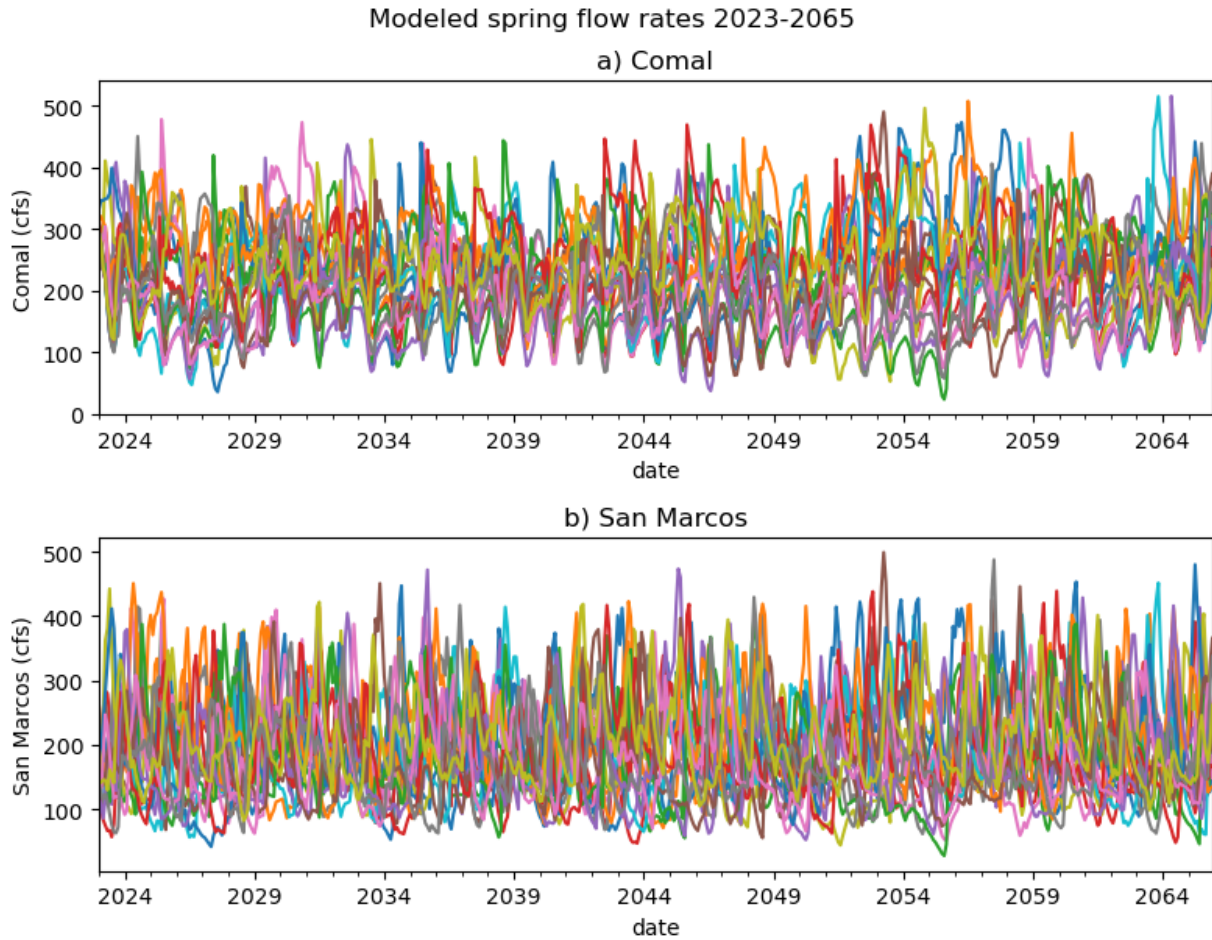


Figure 2-8. Modeled spring flow rates for a) Comal Springs and b) San Marcos Springs from 19 GCM projections spanning from 2023 to 2065

Figure 2-9 recasts the model results to depict the range of spring flow values (maximum to minimum) for all models combined. Also shown are the median values of the modeled spring flow rates over the simulation period. While informative, it is difficult to assess long-term flow conditions because of the applied maximum allowed pumping regime used in the model; however, the projections indicate long-term median flow values of about 210 cfs and 180 cfs for Comal and San Marcos springs, respectively.

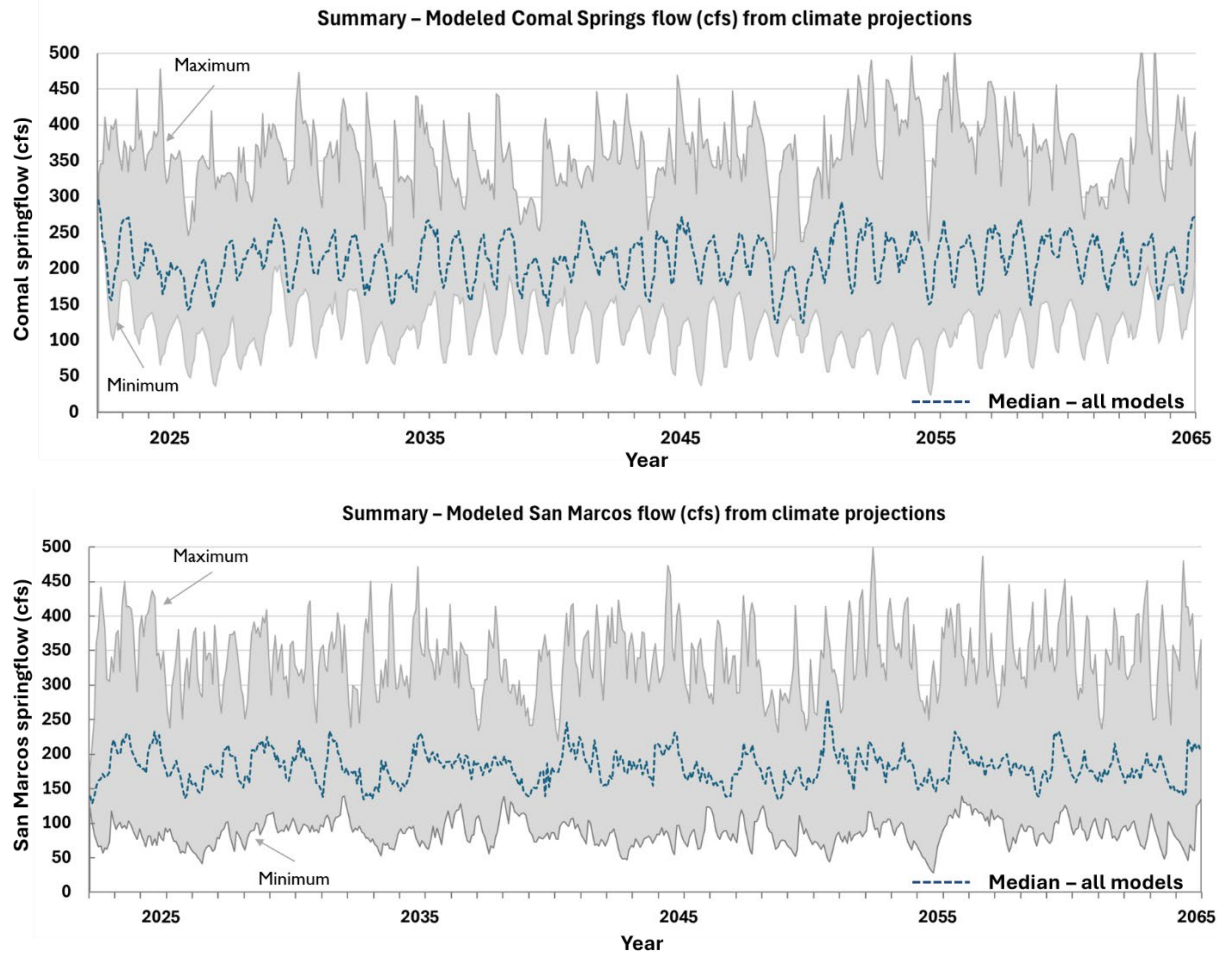


Figure 2-9. Summary of modeled spring flows for Comal Springs (top) and San Marcos Springs (bottom) using GCM projections spanning from 2023 to 2065. The dashed line is the median value of all models, and the shaded area is the range of the modeled spring flows

The cumulative probability distributions of all 19 model projections of flow at Comal Springs from 2023 to 2065 are shown in Figure 2-10. Also shown in Figure 2-10 is the cumulative probability distribution of historical Comal Springs flow rates from 1980 to 2023. The modeled spring flow rates are generally lower than the historical spring flow rates and are influenced by: 1) generally lower projected cumulative recharge relative to historical recharge (Figure 1-21), and 2) the effects of high pumping stress. A detailed look at lower spring flow rates (Figure 2-10b) indicates the cumulative probability distribution of historical spring flow rates below 100 cfs is effectively bracketed by the cumulative probability distributions of the modeled spring flow rates. This suggests that the projected recharge values and current spring flow protection measures in the model result in low flow distributions that are similar to historical observations.

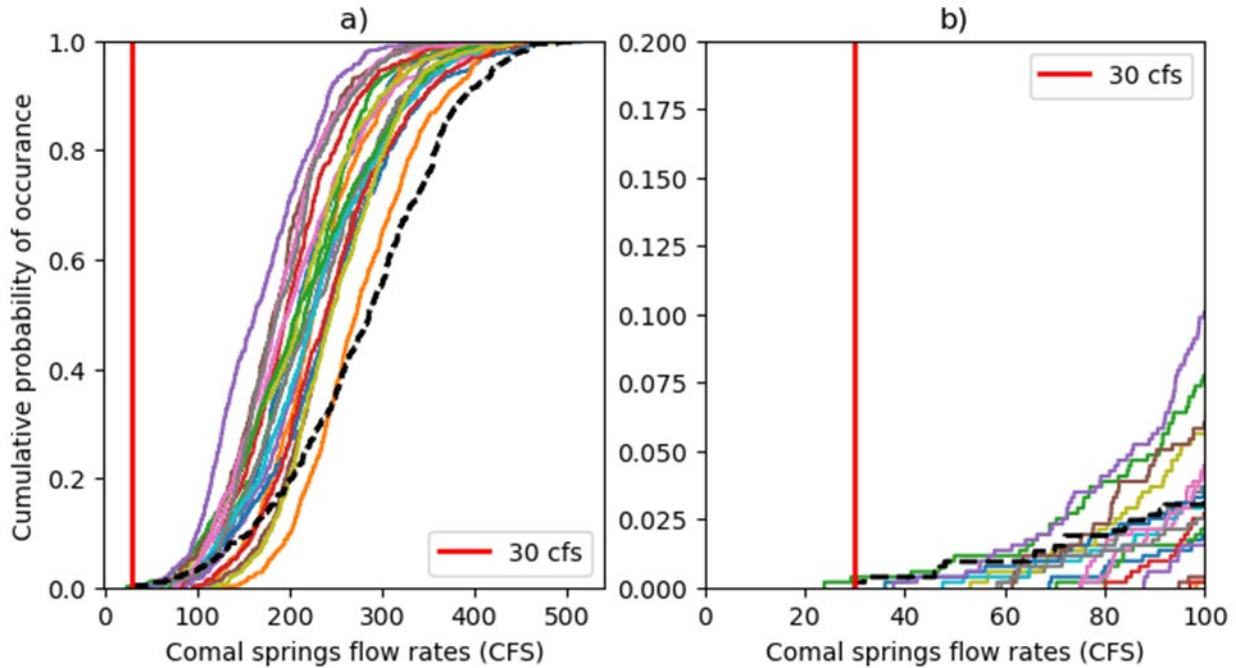


Figure 2-10. Cumulative probability of (a) modeled future Comal Springs flows from GCMs spanning from 2023 to 2065. The dashed dark line represents historical spring flows for the period 1980–2023, and (b) a zoomed-in version of the plot focusing on flows of 100 cfs and below

2.4.3 Protective Measures Triggered for Climate Projections

Table 2-1 summarizes the occurrences of three protective measures: VISPO, ASR lease forbearance, and SAWS ASR forbearance for each of the 19 climate projections. Information in Table 2-2 is presented graphically in Figure 2-11, which shows the frequency of these protective measures triggered across the 19 climate projections. Key findings include: 1) VISPO is triggered at least once in 14 out of 19 climate projections, and the frequency of VISPO implementation varies from 5 to 19 years among those 14 climate projections; 2) both the SAWS ASR forbearance and the ASR lease forbearance are triggered in 9 of the 19 climate projections; and 3) one projection, KIOST-ESM ssp245, dominates the number of times these protection measures are implemented.

Table 2-2 lists the occurrence frequency of the CPM stages for each of the 19 climate projections. Figure 2-12 shows stacked bar plots illustrating CPM frequency in the San Antonio pool for each of the 19 climate model projections. Key findings include: 1) 12 of the 19 model projections trigger CPM Stage 5 in the San Antonio Pool at least once; 2) projections KACE-1-0-G ssp245 and KIOST-ESM ssp245 have the most occurrences of CPM Stages of 4 and 5 both in the San Antonio and Uvalde pools; and 3) in contrast, the inmcm4 rcp85 scenario has about 90% of its modeled periods in normal (no restrictions) or Stage 1 for the San Antonio pool.

Table 2-1. Summary of VISPO and ASR related protective measures

Climate projection	VISPO		ASR Lease Forbearance		SAWS ASR Forbearance	
	Year Applied	Number of Years	Year Applied	Number of Years	Period Applied (year-month)	Number of periods
CMCC-CM_rcp45	2034, 2037, 2043, 2045, 2060	5				
CMCC-CM_ssp585						
EC-Earth3_ssp245	2038, 2045, 2049, 2050, 2051, 2064, 2065	7				
EC-Earth3_ssp585	2035, 2039, 2043, 2044, 2048, 2049, 2050, 2056, 2057, 2063	10				
HadGEM2-CC_rcp45	2032, 2041, 2044, 2050, 2051	5				
HadGEM2-CC_rcp85						
INM-CM4-8_ssp245	2024, 2043, 2044, 2048, 2049, 2050, 2056, 2059, 2060	9				
INM-CM4-8_ssp585	2042, 2043, 2048, 2055, 2056, 2057	6	2056, 2057, 2059	3	2056-04, 2056-05, 2056-06, 2056-08	4
INM-CM5-0_ssp245	2027, 2028, 2041, 2051, 2052, 2053, 2060, 2061, 2062	9	2056, 2060	2	2060-06, 2060-07, 2060-08	3
INM-CM5-0_ssp585	2024, 2025, 2027, 2028, 2031, 2034, 2044, 2045, 2063	9	2027, 2028, 2029, 2030, 2031	5	2027-07, 2027-08, 2030-07, 2030-08	4
inmcm4_rcp45	2027, 2028, 2047, 2048, 2051	5	2028	1	2028-01, 2028-02	2
inmcm4_rcp85						
KACE-1-0-G_ssp245	2027, 2035, 2042, 2053, 2054, 2055, 2056	7	2027, 2029, 2030	3	2027-06, 2027-07	2
KACE-1-0-G_ssp585			2029	1		
KIOST-ESM_ssp245	2026, 2027, 2028, 2029, 2034, 2035, 2039, 2040, 2046, 2047, 2048, 2050, 2051, 2053, 2055, 2059, 2060, 2062, 2063	19	2027, 2028, 2029, 2030, 2031, 2032, 2034, 2035, 2048, 2051, 2053, 2054, 2055, 2062, 2063	15	2027-07, 2027-08, 2028-06, 2028-07, 2028-08, 2028-09, 2028-10, 2028-11, 2028-12, 2029-01, 2029-03, 2029-04, 2029-05, 2029-06, 2030-07, 2032-07, 2034-06, 2034-07, 2034-08, 2034-09, 2034-10, 2053-08, 2054-07, 2054-08, 2054-09, 2054-10, 2055-04, 2062-06, 2062-07, 2062-08	30
KIOST-ESM_ssp585	2027, 2029, 2046, 2047, 2048, 2050, 2056, 2058	8	2029, 2030, 2053, 2054, 2055	5	2029-05, 2029-06, 2055-07, 2055-08	4
MPI-ESM1-2-HR_ssp245	2026, 2027, 2029, 2034, 2041, 2053, 2056, 2062	8	2027, 2028, 2029, 2030	4	2027-04, 2027-05, 2028-06, 2028-07, 2028-08, 2028-09, 2028-10	7
MPI-ESM1-2-HR_ssp585	2024, 2029, 2034, 2036, 2053, 2054, 2056, 2061	8	2027, 2028, 2029, 2059, 2060, 2061	6	2028-06, 2028-07, 2028-08, 2060-08	4
MPI-ESM1-ssp585						

Table 2-2. Summary of CPM stage occurrences in the models. Vaues indicate the number of time steps (total of 516) in each condition.

Climate projection	San Antonio Pool Stage						Uvalde Pool Stage				
	Normal	1	2	3	4	5	Normal	2	3	4	5
CMCC-CM_rcp45	125	149	162	69	9	2	188	47	28	19	234
CMCC-CM_ssp585	145	195	129	46	1		347	85	46	19	19
EC-Earth3_SSP585	73	157	176	93	17		58	71	60	51	276
EC-Earth3_ssp245	130	165	128	78	14	1	170	89	60	41	156
HadGEM2-CC_rcp45	173	152	124	59	8		233	31	41	33	178
HadGEM2-CC_rcp85	215	171	103	25	2		362	57	31	20	46
INM-CM4-8_ssp245	125	125	141	99	21	5	269	91	69	28	59
INM-CM4-8_ssp585	187	113	128	69	11	8	357	80	33	14	32
INM-CM5-0_ssp245	126	152	116	92	21	9	161	88	59	46	162
INM-CM5-0_ssp585	174	153	106	66	10	7	267	44	19	25	161
KACE-1-0-G_ssp245	168	104	122	81	22	19	143	58	39	7	269
KACE-1-0-G_ssp585	217	136	122	39	2		366	25	20	13	92
KIOST-ESM_ssp245	29	109	149	174	36	19	4	13	10	4	485
KIOST-ESM_ssp585	48	119	195	115	28	11	37	54	34	33	358
MPI-ESM1-2-HR_ssp245	58	137	172	123	23	3	54	69	50	38	305
MPI-ESM1-2-HR_ssp585	65	137	177	122	9	6	126	109	72	34	175
MRI-ESM1_SSP585	222	177	98	19			347	52	38	21	58
inmcm4_rcp45	221	151	76	47	13	8	250	55	37	36	138
inmcm4_rcp85	323	136	52	5			484	23	8	1	

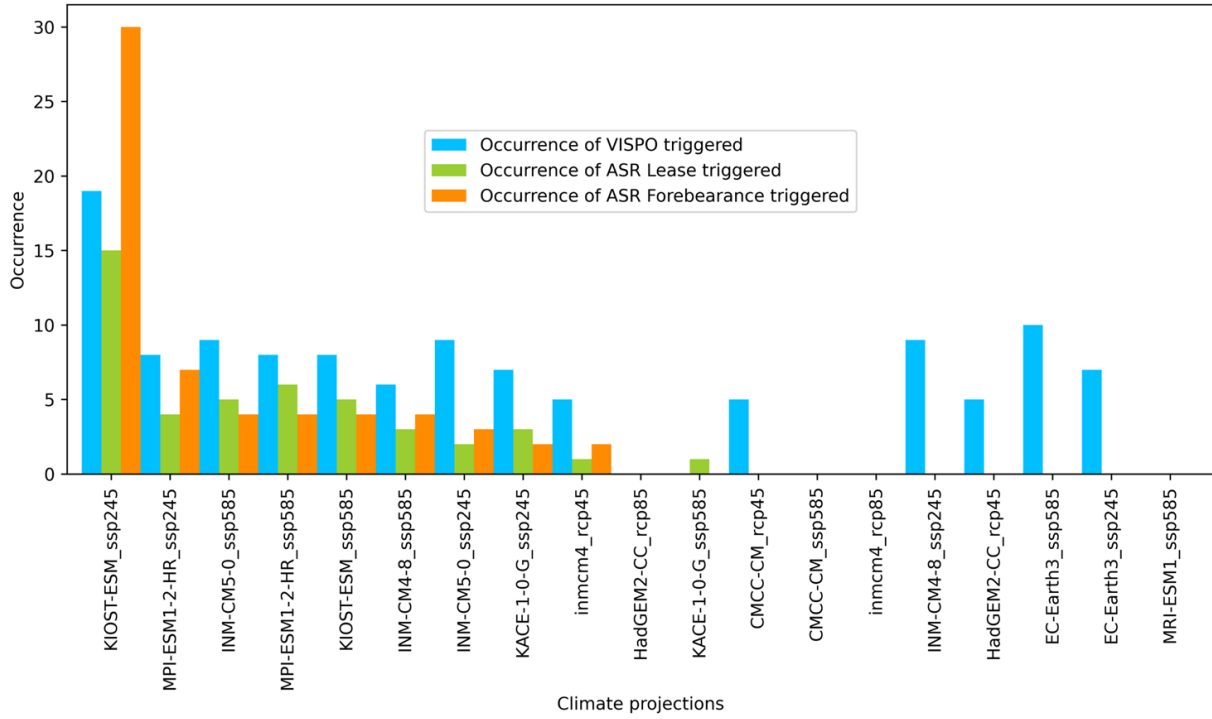


Figure 2-11. Bar plots of the projected occurrences of VISPO, ASR Lease forbearances, and SAWS ASR forbearance triggered under the 19 climate projections

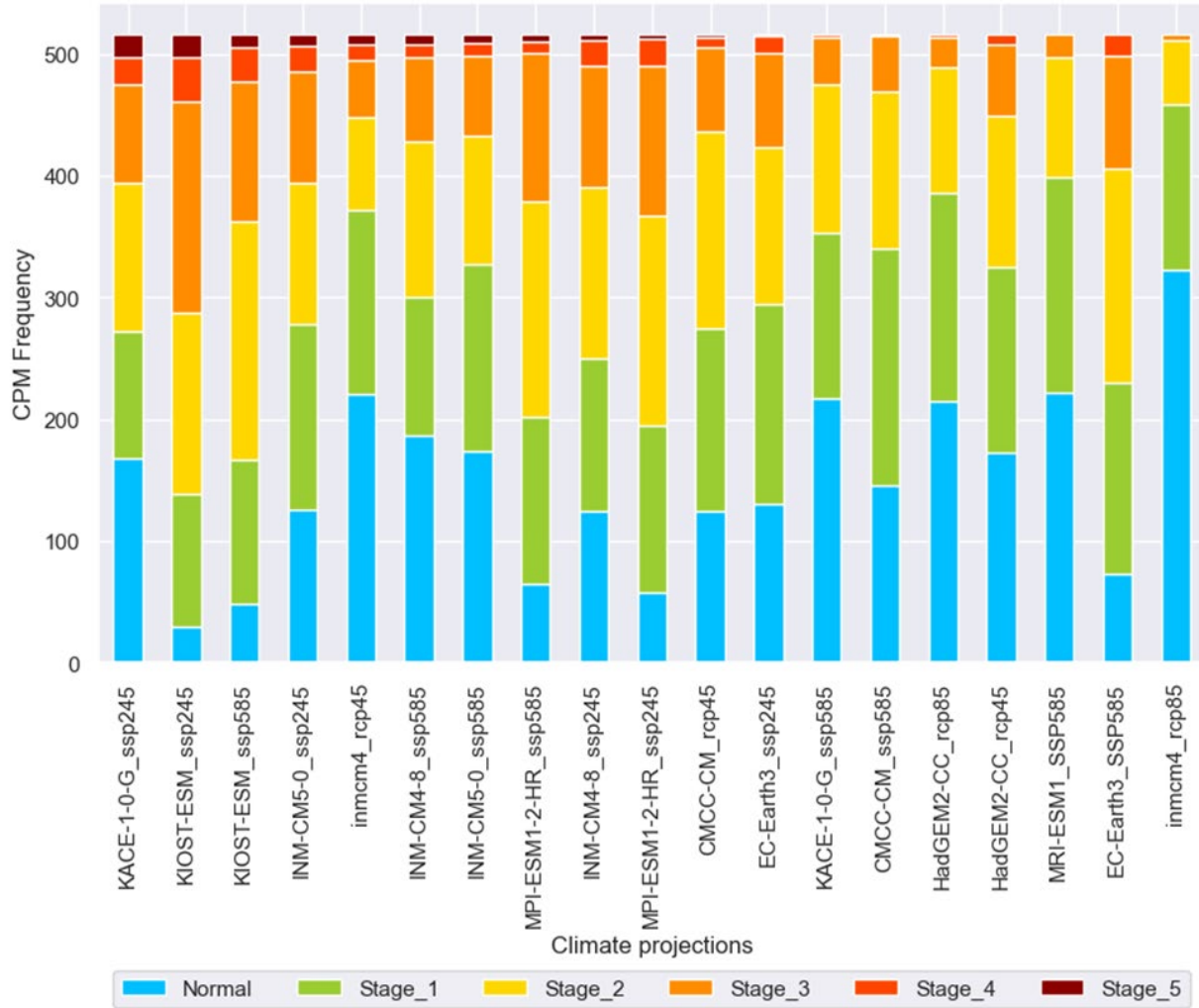


Figure 2-12. Stacked bar plots of frequency of CPM for the modeled climate projections. GCMs are sorted with decreasing frequency of Stage 5 from left to right

2.4.4 Potential Hydrological Droughts Under Future Climates

The 1950s drought of record for the EAR stands out as the most severe in the past century. The EAHCP Phase II and Bottom-Up modeling focused on the period from 1947 to 1958 to assess spring flow protection measures (Appendix C; HDR 2011; Furl 2019). Comal Springs flows reached historically low levels during this time. The 2010–2015 drought is the most recent severe drought in the Edwards Aquifer region, and until very recently (2022–2024) it was the only severe drought when at least some of the spring flow protection measures were enabled.

We inspected the results for projected Comal Springs flows from the 19 models to identify sequences that may be similar or worse than the drought of record and to identify sequences that may be equivalent to the drought of 2011–2015. Figure 2-13 shows modeled Comal Springs flow rates from 2046 to 2057 for the KACE-1-0-G ssp245 model projection compared to the observed Comal Springs flow rates during 1947–1958. The plot suggests the modeled spring flow rates from 2046 to 2057 are quite similar to what was observed during the drought of record. Importantly,

projected springs flows do not cease during this projected severe drought sequence. Although one or two other modeled flow sequences for Comal Springs are also similar to the drought of record, we found no examples of sequences that were more severe (e.g., lower flow for longer periods) than the drought of record in any of the 19 model runs.

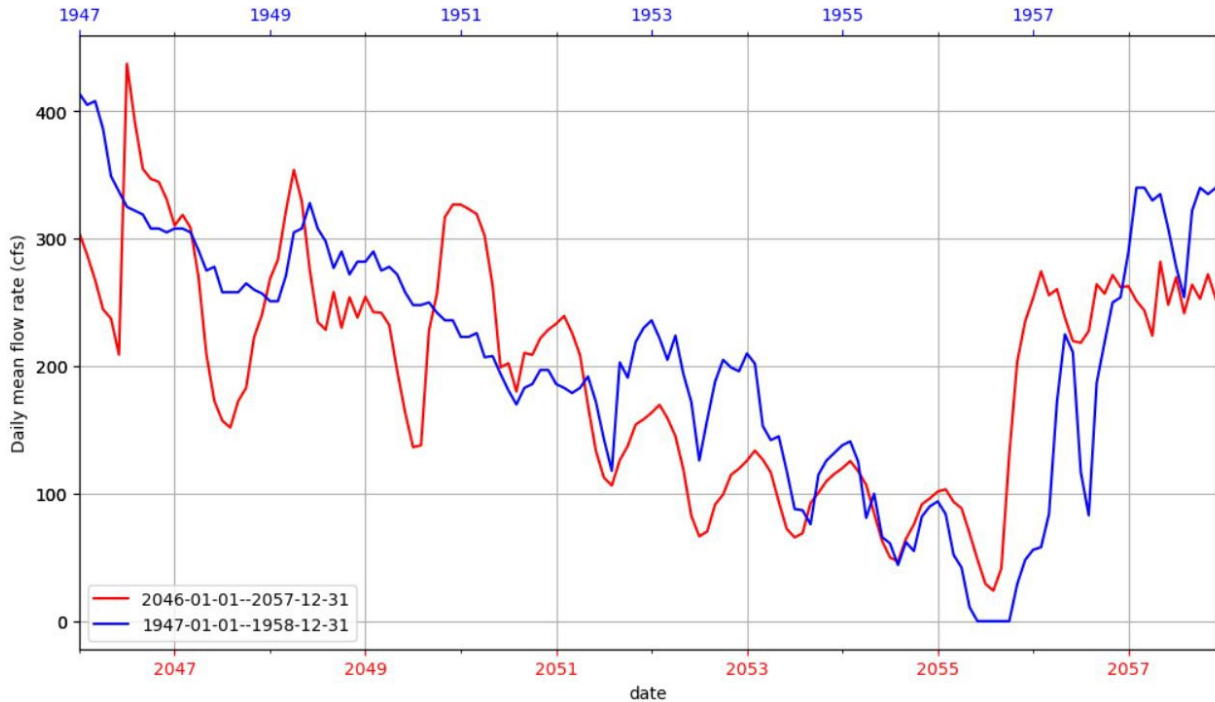


Figure 2-13. Comparison of the modeled projected Comal Springs flow rates (red) from the KACE-10-G ssp245 GCM during 2046–2057 to historical spring flow rate measurements (blue) during 1947–1958.

Figure 2-14 displays the modeled Comal Springs flow rates from the CMCC-CM rcp45 climate projection for the period 2039–2046 as compared to observed Comal Springs flows during 2009–2016. Clearly, the modeled spring flow rate sequence shows a similar pattern to the 2011–2015 drought. There are more than 19 instances of spring flow rate sequences from the various climate projections that display a similar pattern to the 2011–2015 drought. However, in each of those instances Comal Springs flows do not fall below goals set in the EAHCP. This pattern suggests droughts like the one experienced in 2011–2015 will not be uncommon in the future but are likely to be manageable using the current spring flow protection measures.

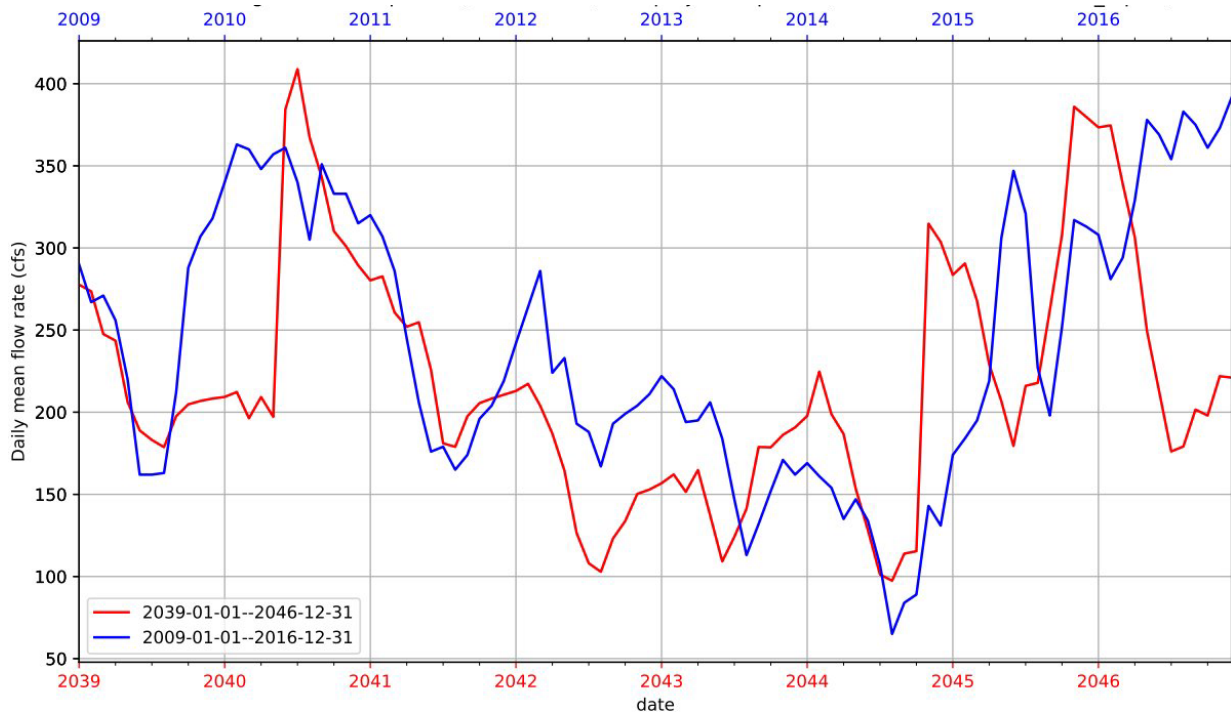


Figure 2-14. Comparison of the modeled projected Comal Springs flow rates (red) from the CMCC-CM rcp45 GCM during 2039–2047 to historical spring flow rate measurements (blue) during 2009–2017

2.4.5 Selected Individual Model Results

The ensemble characteristics of modeled spring flow rates for both Comal Springs and San Marcos Springs, as depicted in Figure 2-9, indicate the range of flows and minimum flows in nearly all model projections are similar to conditions experienced in the past few decades. This strongly suggests that for the 19 climate projections assessed, the established spring flows protection measures for the aquifer system are suitable for the proposed renewal period of 2028 to 2058. However, it is important to assess modeled spring flow rates under each individual climate projection to evaluate when flow minima occur and what factors may contribute to the model projection results.

Graphical results for projected Comal and San Marcos springs flows for all 19 models are provided in Appendix B. Comparing statistics of water levels and the modeled spring flow rates with historical measurements, we can qualitatively group the 19 climate projections into three broad categories. We label these categories as Neutral, Stressed, and Low Flow. Neutral model results have projected water level and spring flow values that are similar to recent historical trends in the aquifer. For example, Neutral model results have projected J17 water levels below CPM Stage 3 in less than 18% of the 516 stress periods (months) of the modeled period. Approximately 10 of the models fit into this category. Stressed model results have projected J17 water levels that are in CPM Stage 3 more than 18% of the time and generally have sustained lower than median flows at the springs. Nine of the models fit into the category. Low flow models exhibit the lowest flows at either Comal Springs or San Marcos Springs during the period 2028–2058. These flows are below minimum daily average spring flow discharge objectives, 30 cfs for Comal and 45 cfs for San Marcos, as proposed in the technical memorandum, *Recommended Biological Goals and Objectives for the Permit Renewal*

(Kunkel et al. 2024). Two models fit into this category—one is in the Neutral group and the other is in the Stressed group.

A set of example results from a Neutral model, INM-CM4-8 ssp585, is shown in Figure 2-15 for both Comal and San Marcos springs. The projected spring flows include high and low flow periods with average flows near the median for the 19 models. The lowest projected flows during drought sequences are also well above the minimum daily average spring flow discharge objective for either spring.

Figure 2-16 depicts an example of results that represent a Stressed model, KIOST-ESM ssp245. At Comal Springs, results from this model dominate the lowest flows (of all model runs) for many years. The KIOST-ESM ssp245 results represent projected conditions that would suggest CPM Stage 3 conditions or more in the San Antonio pool nearly 35% of the time between 2028 and 2058. As seen in Figure 2-11, this climate projection model also has the highest frequency of VISPO- and ASR-related triggers.

An example of a Low Flow model, KACE-1-0-G ssp245, is shown in Figure 2-17. When inspecting projected flows at San Marcos Springs, this model would generally fit into the Neutral category, but there is one drought sequence in the early 2050s in which the minimum projected flow is less than 45 cfs. Similarly, flow at Comal Springs in the same time period is projected to decrease below 30 cfs. All modeled stress periods (months) between 2028 and 2058 with low flows are listed in Table 2-3.

Table 2-3 lists the timing and periods when the modeled spring flow rates are below minimum daily average spring flow objectives at Comal or San Marcos springs. It should be noted that among the 19 climate projections, only two produce very low spring flow rate sequences and these are limited to one to four stress periods (months) with no sequences that produce zero flows. For several models, the period from the mid-2040s to mid-2050s appears to be associated with lower recharge and lower spring flows.

Table 2-3. Summary of Lowest Spring Flow Events in the Low Flow Models

Low Flow Condition	Model	When	Periods	Cause?
Comal Springs below 30 cfs	KACE-1-0-G ssp245	Jul–Aug 2055	2	Not all measures applied (no ASR trigger)
San Marcos Springs below 45 cfs	KACE-1-0-G ssp245	May–Aug 2055	4	Not all measures applied (no ASR trigger)
San Marcos Springs below 45 cfs	INM-CM5-0 ssp245	Aug 2051	1	Not all measures applied (no ASR trigger)

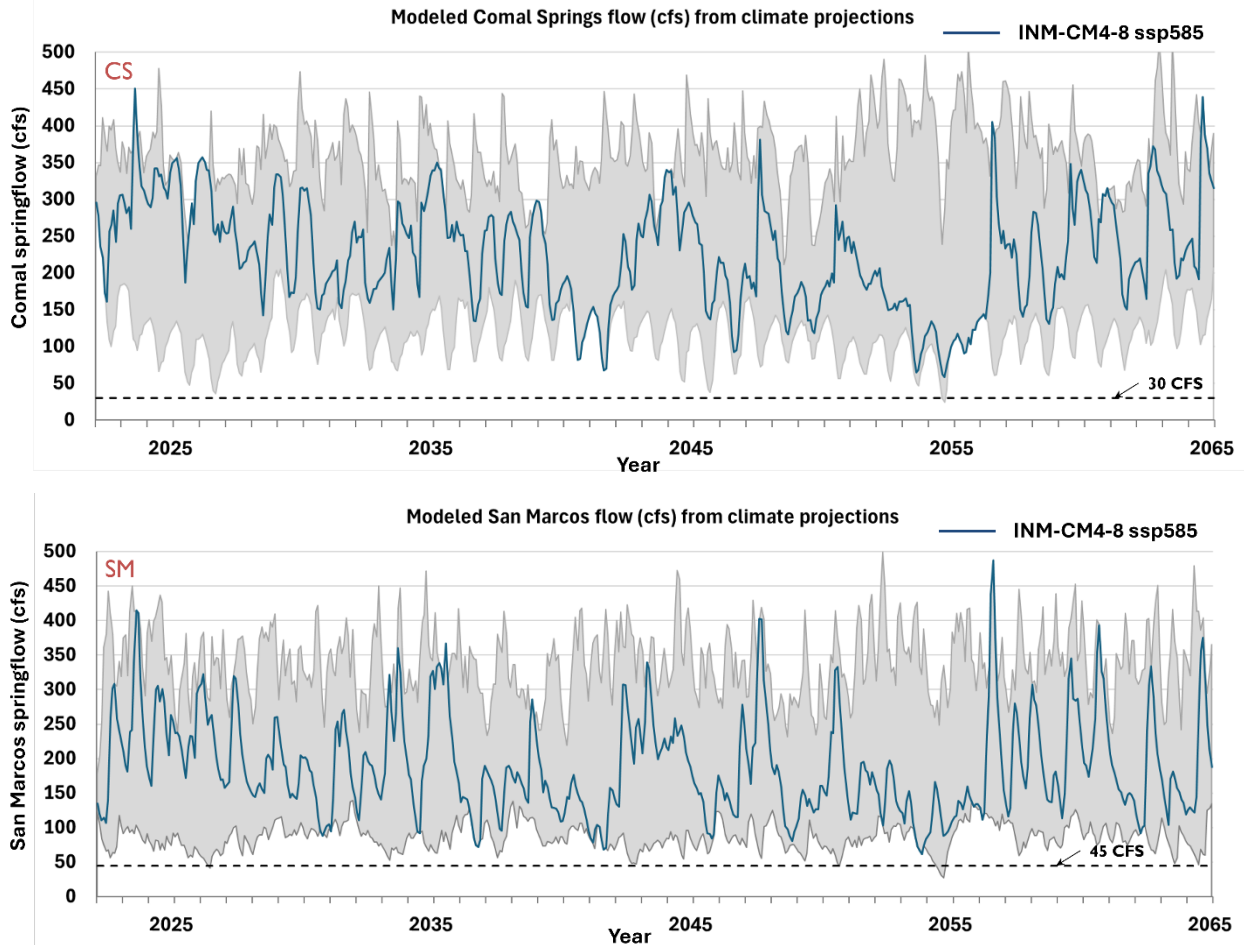
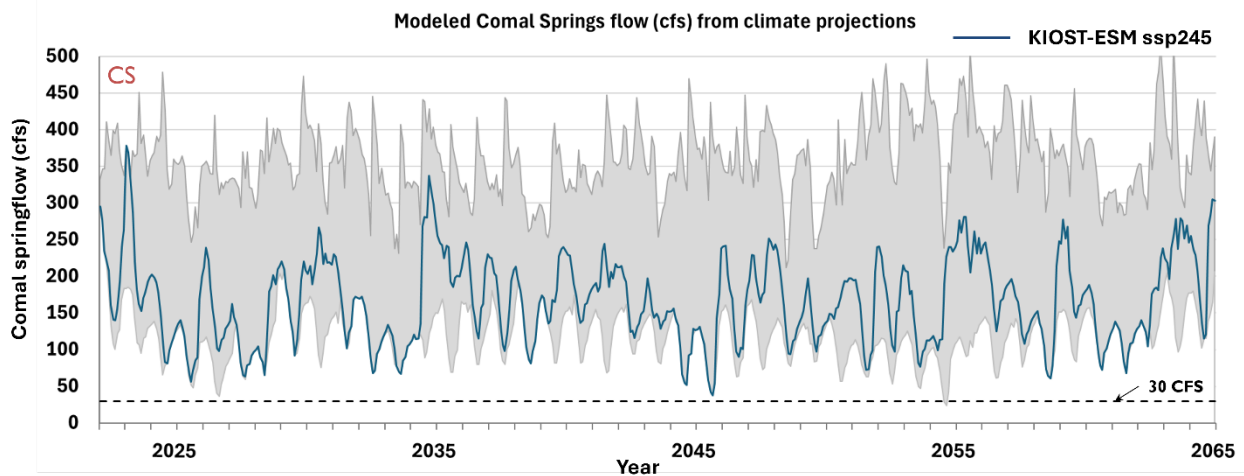


Figure 2-15. Modeled Comal Springs (top) and San Marcos Springs (bottom) flows from the INM-CM4-9 ssp585 GCM for the period 2023–2065. This model is an example of a Neutral group model. The shaded area depicts the range of modeled spring flow rates for all 19 climate model projections.



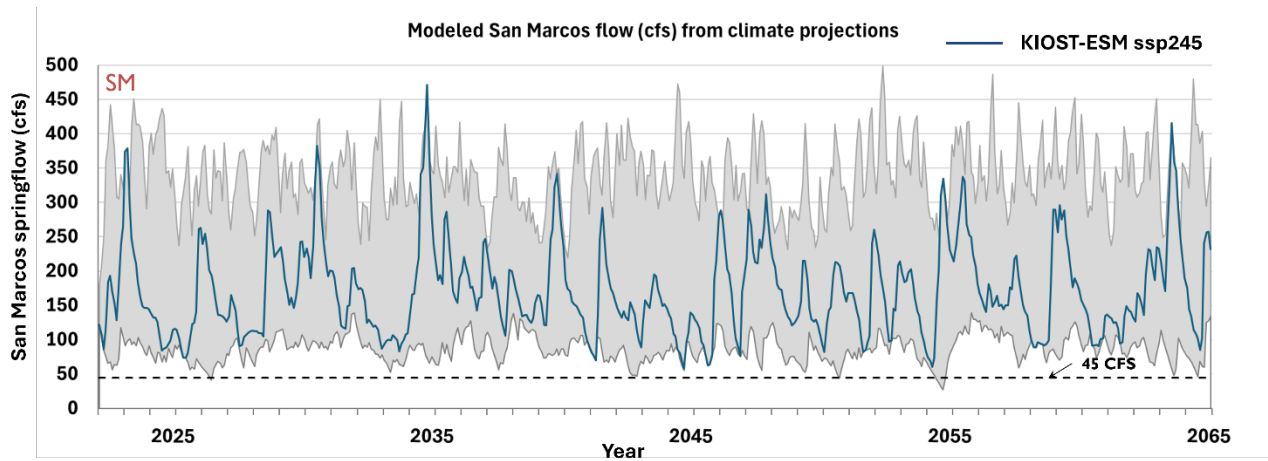


Figure 2-16. Modeled Comal Springs (top) and San Marcos Springs (bottom) flows from the KIOST-ESM ssp245 GCM for the period 2023–2065. This model is an example of the Stressed group models. The shaded area depicts the range of modeled spring flow rates for all 19 climate model projections.

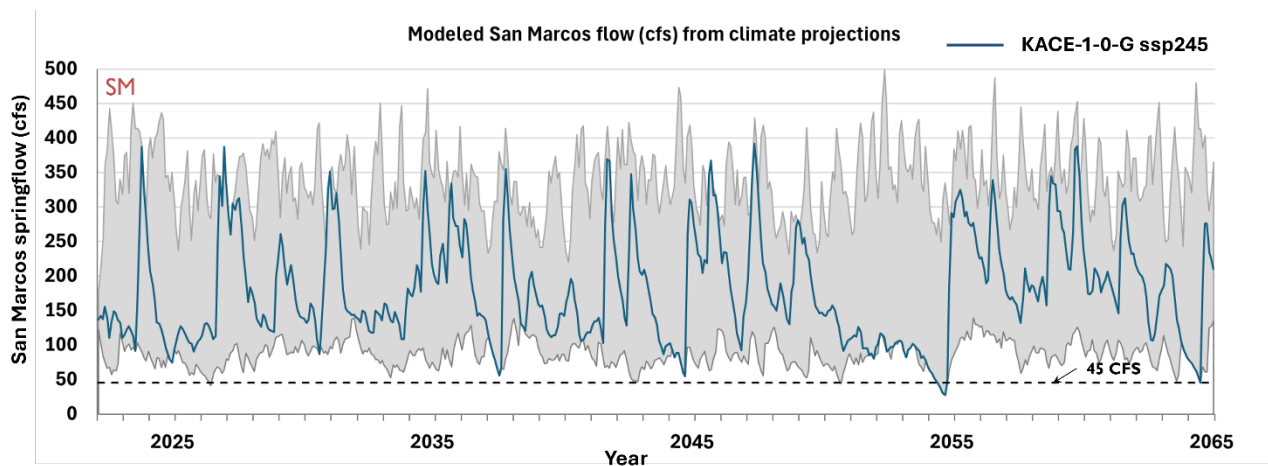
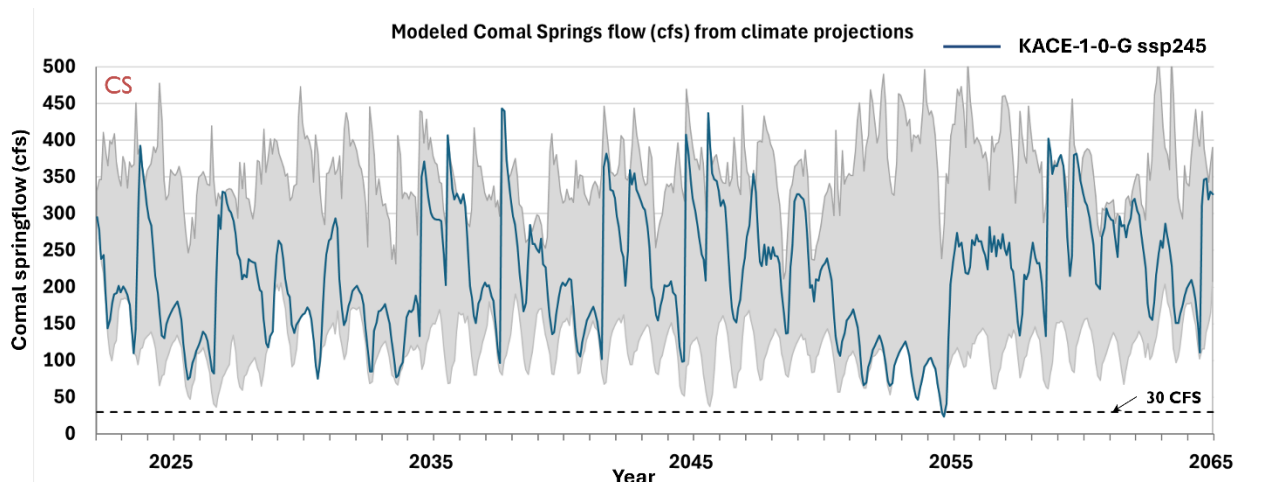


Figure 2-17. Modeled Comal Springs (top) and San Marcos Springs (bottom) flows from the KACE-1-0-G ssp245 GCM for the period 2023–2065. This model is an example of a Low Flow model. The shaded area depicts the range of modeled spring flow rates for all 19 climate model projections.

Water levels and spring flow rates are generally affected by complex interactions between groundwater recharge and groundwater pumping in the Edwards Aquifer. Numerical models of the aquifer system explicitly incorporate these interactions, and the model's response to system inputs and withdrawals is also sensitive to the application of spring flow protection measures. Figure 2-18 illustrates the range of factors that contribute to projected model flow rates at Comal Springs and San Marcos Springs from the climate model INM-CM4-8 ssp245 (a Neutral group model). The figures are complex but reveal some of the components controlling the magnitude of flow at either spring system. Shown in the figures are: 1) monthly applied pumping, adjusted for CPM conditions and VISPO and ASR triggers, 2) monthly and annual applied recharge, the dark green line and green bars, respectively, 3) the 10-year moving average of annual recharge as indicated by the light green line, 4) the 500,000 ac-ft ASR-related trigger value for 10-year average annual recharge, and 5) the resulting projected spring flow rate in dark blue.

For both spring systems, increases in spring flow rates correspond to the peaks of monthly recharge to the aquifer (Figure 2-18), while decreases are a reflection of less recharge and greater applied pumping, especially during each summer. The exaggerated intra-annual sawtooth shape of the spring flow rates is likely caused by application of maximum allowed monthly groundwater pumping in the model, but the periodicity of declines is consistent with seasonal pumping. The short-term trend (within a couple of years) of the spring flow rates follows projected annual recharge, while the longer-term trend correlates with the 10-year moving average annual recharge. Variations in groundwater pumping are easily correlated with CPM restrictions during lower flow periods and application of VISPO- and ASR-related measures. For example, reduced pumping in the 2054–2058 timeframe (Figure 2-18) is associated with application of CPM restrictions and ASR forbearance.

Figure 2-19 shows an example of modeled spring flow rates of San Marcos Springs from the KIOST-ESM ssp245 model (a Stressed group member). For this model projection, 10-year moving average annual recharge falls below 500,000 ac-ft in several periods. When combined with CPM restrictions, there is a noticeable difference in maximum permitted pumping across the range of the simulation period.

Figure 2-20 depicts an example of projected spring flows for Comal Springs from a Low Flow model, KACE-1-0-G ssp245. During the significant drought period that occurs from 2051–2055, there is exceptionally low annual recharge, and pumping is reduced in accordance with applied CPM restrictions. However, the timing of this drought sequence is such that the 10-year moving average of annual recharge does not fall below 500,000 ac-ft during the drought. Thus, ASR-related forbearance is not triggered. The net result is that as flows at Comal Springs and San Marcos Springs reach their lowest, not all spring flow protection measures are implemented. Both Low Flow models are affected in the same manner—intense short-term droughts do not trigger all available spring flow protection measures, which results in very low flows.

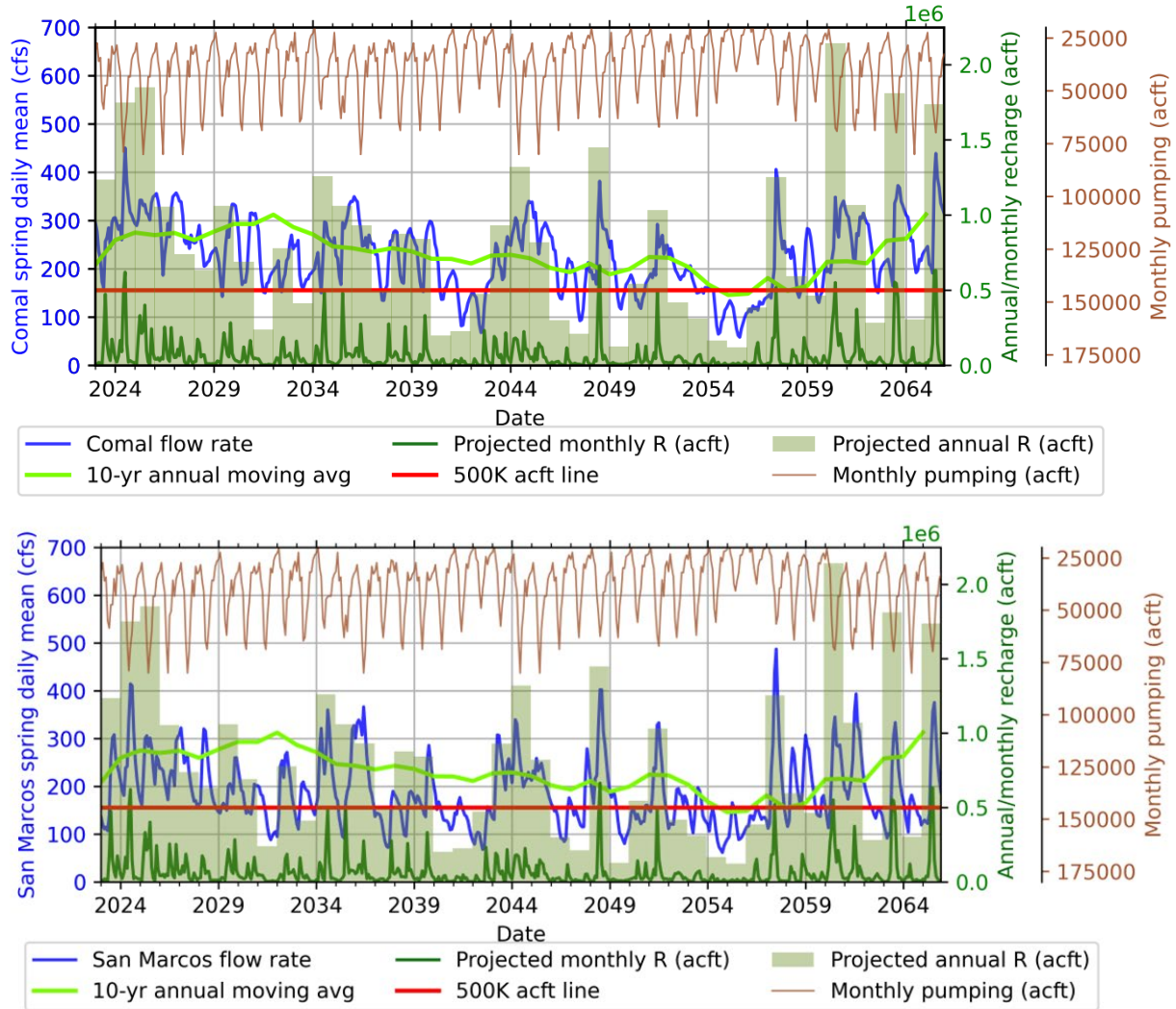


Figure 2-18. Projected Comal (top, blue) and San Marcos springs flows (bottom, blue) from the INM-CM4-8 ssp585 GCM (a Neutral group model) spanning from 2023 to 2065. Applied monthly pumping (brown), total monthly recharge (dark green line), annual recharge (green bar), and the 10-year moving annual average recharge (light green line) are shown.

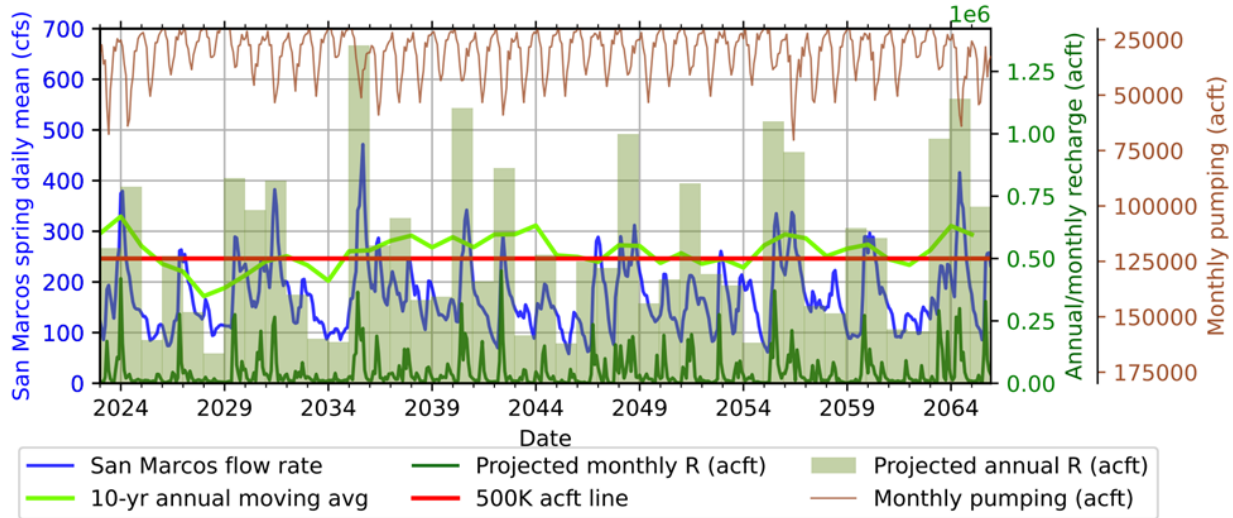


Figure 2-19. Projected San Marcos Springs flows (blue) from the KIOST-ESM ssp245 GCM (a Stressed group model) spanning from 2023 to 2065. Applied monthly pumping (brown), total monthly recharge (dark green line), annual recharge (green bar), and the 10-year moving annual average recharge (light green line) are shown.

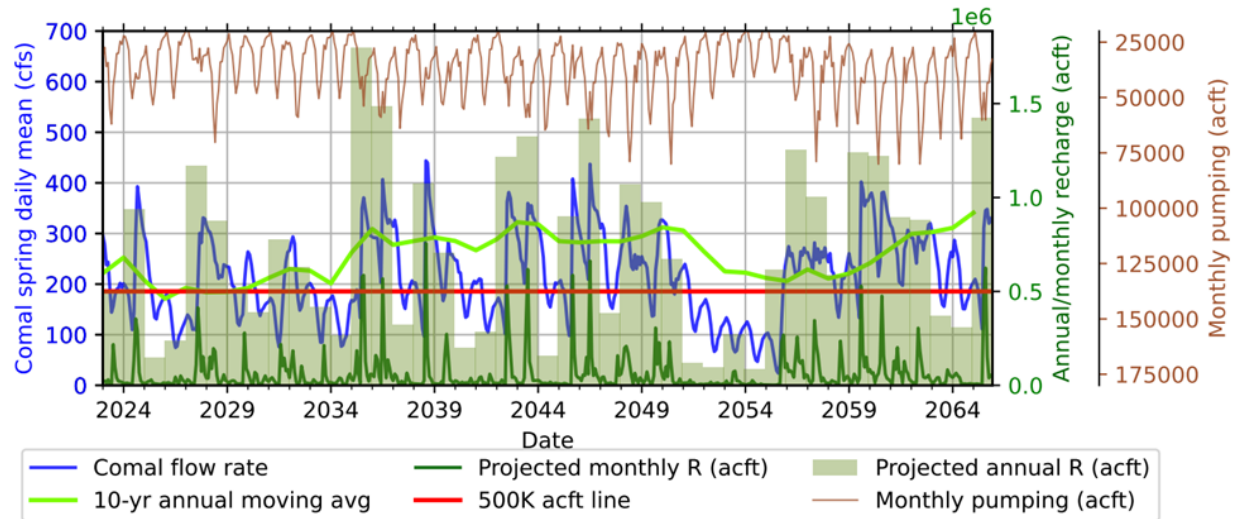


Figure 2-20. Projected Comal Springs flows (blue) from the KACE-1-0-G ssp245 GCM (a Low Flow group model) spanning from 2023 to 2065. Applied monthly pumping (brown), total monthly recharge (dark green line), annual recharge (green bar), and the 10-year moving annual average recharge (light green line) are shown.

2.5 Summary

Projections of future recharge, developed from downscaled GCMs, were used with an existing numerical groundwater model for the Edwards Aquifer to produce projections of future water levels and spring flows for the period 2023–2065. The MODFLOW model used in the simulations is the same as used in previous EAHCP Phase II simulations but was updated to include: 1) a capability to model 516 stress periods instead of the originally modeled 144 stress periods, 2) modifications to the Jupyter notebook and Python-based scripting package to automate running of the model, and 3) addition of features to produce more user-friendly output files. Pumping and spring flow protection measures in the model were the same as in the EAHCP Phase II analyses.

The Jupyter notebook and associated model were evaluated by comparing model output for the drought of record and by comparing model output using a range of realistic recharge inputs. The current model replicated results from previous modeling of drought of record, and the model successfully produced reasonable and expected output from the three separate recharge input tests. Results of the quality assurance and quality control checks of the model provide confidence in the model's performance for projecting of water levels and spring flows given projections of future recharge.

MODFLOW modeling analysis of spring flow rates was performed using a total of 19 GCM climate projections. Median values of the combined modeled spring flow rates for 2023–2065 are in the range of those historically observed for both the Comal Springs and San Marcos Springs. The cumulative distributions of the Comal Springs flows suggests that historical flow rates below 100 cfs are enveloped by the spring flow rates simulated from the climate projections; thus, the model outputs appear to be unbiased relative to low flow conditions. Analysis of the modeling results confirms that the protective measures are triggered appropriately and correspond to the groundwater management criteria. By comparing sequence patterns of the modeled Comal Spring flows to those of the historical drought periods, we found the modeling results produce a few (~3) sequences similar to the pattern of the 1950s drought of record and more than 19 sequences similar to the recent 2011–2015 drought.

Results of the 19 model projections can be qualitatively classified into three groups: Neutral, Stressed, and Low Flow. Neutral model results have water levels and spring flows that are reasonably similar to aquifer conditions over the past 4 decades. Stressed model results have generally lower spring flows and water levels but do not have minimum flows below proposed minimum average daily spring flow discharge objectives. The Low Flow includes two climate projections with one or more stress periods producing modeled spring flow rates that are lower than the proposed minimum average daily spring flow objectives.

Analysis of the impacts on modeled spring flow rates indicate that the exaggerated intra-annual sawtooth pattern is due to application of maximum permitted monthly pumping. As expected, the peaks of the modeled spring flow rates are associated with monthly recharge. Short-term and long-term trends in water levels and spring flows follow the trends in annual recharge and 10-year moving average of annual recharge, respectively. Further analysis of the lowest modeled spring flow rates indicate that some protective measures (ASR forbearance measures) are not triggered during those periods.

Some observations from the modeling analysis of projected groundwater levels and spring flows: 1) the EAHCP Phase II MODFLOW model successfully incorporated projected future recharge to

produce estimates of future spring flows under varying climate scenarios; 2) several model projections produce drought sequences similar to those experienced in recent history but none that appear more severe than the drought of record; 3) the majority of GCM projections indicate that existing spring flow protection measures would maintain spring flows above minimum average daily spring flow discharge objectives for the Comal and San Marcos springs, but 2 of the 19 projections produce flow rate sequences over the course of one to four months that are below these objectives; and 4) no projections result in zero flows in Comal or San Marcos springs.

3.1 Executive Summary

- Kluyver T, Ragan-Kelley B, Pérez F, Granger B, Bussonnier M, Frederic J, Kelley K, Hamrick J, Grout J, Corlay S, Ivanov P, Avila D, Abdalla S, Willing C, and Jupyter development team. 2016. Jupyter Notebooks – a publishing format for reproducible computational workflows. Loizides, Fernando and Schmidt, Birgit (eds.) In *Positioning and Power in Academic Publishing: Players, Agents and Agendas*. IOS Press. pp. 87-90. (doi:10.3233/978-1-61499-649-1-87).
- Lindgren RJ, Dutto AR, Hovorka SD, Worthington SRH, and Painter S. 2004. Conceptualization and simulation of the Edwards Aquifer, San Antonio region, Texas, U.S. Geological Survey Scientific Investigations Report 2004-5277, 143 p.
- Liu A, Troshanov N, Winterle J, Zhang A, Eason S. 2017. Updates to the MODFLOW Groundwater Model of the San Antonio Segment of the Edwards Aquifer. 78 p.
<https://www.edwardsaquifer.org/science-and-maps/research-and-scientific-reports/science-document-library>
- Lundberg SM, Erion G, Chen H, DeGrave A, Prutkin JM, Nair B, Katz R, Himmelfarb J, Bansal N, Lee SI. 2020. From local explanations to global understanding with explainable AI for trees. *Nature Machine Intelligence* 2, 2522–5839.
- Puente C. 1978. Method of estimating natural recharge to the Edwards Aquifer in the San Antonio area, Texas, U.S. Geological Survey Water-Resources Investigations 78-10, 38 p.
- Shapley L. 1953. A value for n-person games. *Contributions to the Theory Games II*, 307–317.

3.2 Chapter 1

- Başağaoğlu H, Chakraborty D, Lago CD, Gutierrez L, Şahinli MA, Giacomoni M, Furl C, Mirchi A, Moriasi D, Şengör SS. 2022. A Review on Interpretable and Explainable Artificial Intelligence in Hydroclimatic Applications. *Water*, 14, 1230. <https://doi.org/10.3390/w14081230>.
- Başağaoğlu H, Sharma C, Chakraborty D, Yoosefdoost I, Bertetti FP. 2023. Heuristic data-inspired scheme to characterize meteorological and groundwater droughts in a semi-arid karstic region under a warming climate, *Journal of Hydrology: Regional Studies*, 48, 101481, <https://doi.org/10.1016/j.ejrh.2023.101481>.
- Breiman L. 2001. Random forests. *Machine Learning* 45, 5–32.
<https://doi.org/10.1023/A:1010933404324>.
- Chakraborty D, Başağaoğlu H, Winterle J. 2021. Interpretable vs. noninterpretable machine learning models for data-driven hydro-climatological process modeling, *Expert Systems with Applications*, 170, 114498, <https://doi.org/10.1016/j.eswa.2020.114498>.
- Chakraborty D, Gutierrez-Chakraborty E, Rodriguez-Aguayo C, Başağaoğlu H, Lopez-Berestein G, Amero P. 2024. Discovering genetic biomarkers for targeted cancer therapeutics with

- eXplainable Artificial Intelligence. *Cancer Communications*, 44: 584-588. <https://doi.org/10.1002/cac2.12530>
- Chang Y.-C., Chang K-H., Chu H-H., Tong, L-I, 2016. Establishing decision tree-based short-term default credit risk assessment models. *Communications in Statistics-Theory and Methods*, 45, 6803–6815.
- Chen T, and Guestrin C. 2016. XGBoost: A scalable tree boosting system In Proceedings of the 22Nd ACM SIGKDD International Conference on Knowledge Discovery and Data Mining, (pp. 785–794). New York, NY, USA: ACM 10.
- Clear Creek Solutions, Inc. 2012. Edwards Aquifer recharge HSPF subbasins models modifications for Nueces River and tributaries calibration and recharge report. 473p.
- Clear Creek Solutions, Inc. 2013. HSPF model updates to Nueces and Blanco sub-basins of the Edwards Aquifer for Nueces River and tributaries, Texas feasibility study. 191p.
- Dumitrescu E, Hué S, Hurlin C, Tokpavi S. 2021. Machine learning for credit scoring: Improving logistic regression with non-linear decision-tree effects. *European Journal of Operational Research*, 297(3), 1178–1192. <https://doi.org/https://doi.org/10.1016/j.ejor.2021.06.053>.
- Geurts P, Ernst D, Wehenkel L. 2006. Extremely randomized trees. *Machine Learning* 63, 3–42. <https://doi.org/10.1007/s10994-006-6226-1>.
- Guryanov A. 2019. Histogram-Based Algorithm for Building Gradient Boosting Ensembles of Piecewise Linear Decision Trees. In: van der Aalst, W., *et al.* Analysis of Images, Social Networks and Texts. AIST 2019. Lecture Notes in Computer Science, vol 11832. Springer, Cham. https://doi.org/10.1007/978-3-030-37334-4_4.
- Liu A, Troshanov N, Winterle J, Zhang A, Eason S. 2017. Updates to the MODFLOW Groundwater Model of the San Antonio Segment of the Edwards Aquifer. 78 p. <https://www.edwardsaquifer.org/science-and-maps/research-and-scientific-reports/science-document-library>
- Lundberg SM, Erion G, Chen H, DeGrave A, Prutkin JM, Nair B, Katz R, Himmelfarb J, Bansal N, Lee SI. 2020. From local explanations to global understanding with explainable AI for trees. *Nature Machine Intelligence* 2, 2522–5839.
- Nicolae S, Başağaoğlu H, Chakraborty D, Ben Jabeur S. 2023. Does institutional quality affect CO2 emissions? Evidence from explainable artificial intelligence models, *Energy Economics*, 124, 106822, <https://doi.org/10.1016/j.eneco.2023.106822>.
- Puente C. 1978. Method of estimating natural recharge to the Edwards Aquifer in the San Antonio area, Texas, U.S. Geological Survey Water-Resources Investigations 78-10, 38 p.
- RECON Environmental, Inc., Hicks & Company, Zara Environmental, LLC, and BIO-WEST. 2012. Edwards Aquifer Recovery Implementation Program Habitat Conservation Plan. Available: <https://www.edwardsaquifer.org/wp-content/uploads/2022/07/Edwards-Aquifer-Recovery-Implementation-Program-Nov-2021.pdf>
- Shapley L. 1953. A value for n-person games. *Contributions to the Theory Games II*, 307–317.

- Thornton MM, Shrestha R, Wei Y, Thornton PE, Kao S-C, Wilson BE. 2022. Daymet: Daily Surface Weather Data on a 1-km Grid for North America, Version 4 R1. ORNL Distributed Active Archive Center. <https://doi.org/10.3334/ORNLDAAC/2129>
- U.S. Fish and Wildlife Service. 2015. Fish and Wildlife Service–Endangered Species Act– Incidental Take Permit amendment (TE63663A-1). Available: https://www.edwardsaquifer.org/wp-content/uploads/2019/02/USFWS_response_to_Refugia_amendment.pdf
- U.S. Geological Survey. 2023. Estimated annual recharge to the Edwards aquifer in the San Antonio area, by stream basin or ungaged area, 1934–2022. Available at: <https://www.sciencebase.gov/catalog/item/641cafc4d34e807d39b654db>
- Wootten A, Başağaoğlu H, Bertetti FP, Chakraborty D, Sharma C, Samimi M, Mirchi A. 2024. Customized Statistically Downscaled CMIP5 and CMIP6 Projections: Application in the Edwards Aquifer Region in South-Central Texas, *in review* Earth's Future.

3.3 Chapter 2

- Furl C. 2019. Scientific Evaluation Report: Nonroutine Adaptive Management Proposal for the EAHCP VISPO, 16p, Memo to EAHCP Committees. <https://www.edwardsaquifer.org/wp-content/uploads/2023/06/VISPO-AMP-Scientific-Evaluation-Report-April-2019.pdf>.
- HDR. 2011. Evaluation of Water Management Programs and Alternatives for Springflow Protection of Endangered Species at Comal and San Marcos Springs. 157 p. https://www.edwardsaquifer.org/doc_publications/evaluation-of-water-management-programs-and-alternatives-for-springflow-protection-of-endangered-species-at-comal-and-san-marcos-springs/
- HydroGeoLogic, Inc. 2004. Reference Manual for the Groundwater Management Package for MODFLOW-2000: Prepared for Edwards Aquifer Authority.
- HydroGeoLogic, Inc. 2005. User's Manual for the Groundwater Management Package for MODFLOW-2000: Prepared for Edwards Aquifer Authority
- Kluyver T, Ragan-Kelley B, Pérez F, Granger B, Bussonnier M, Frederic J, Kelley K, Hamrick J, Grout J, Corlay S, Ivanov P, Avila D, Abdalla S, Willing C, and Jupyter development team. 2016. Jupyter Notebooks – a publishing format for reproducible computational workflows. Loizides, Fernando and Schmidt, Birgit (eds.) In Positioning and Power in Academic Publishing: Players, Agents and Agendas. IOS Press. pp. 87-90. (doi:10.3233/978-1-61499-649-1-87).
- Kunkel C, Sullivan K, Oborny E, Littrell B, Williams C, Pintar M, Bare L. 2024. *Memorandum: Revised Recommended Biological Goals and Objectives for the Permit Renewal*. March 7, 2024.
- Lindgren RJ, Dutto AR, Hovorka SD, Worthington SRH, and Painter S. 2004. Conceptualization and simulation of the Edwards Aquifer, San Antonio region, Texas, U.S. Geological Survey Scientific Investigations Report 2004-5277, 143 p.
- Liu A, Troshanov N, Winterle J, Zhang A, Eason S. 2017. Updates to the MODFLOW Groundwater Model of the San Antonio Segment of the Edwards Aquifer. 78 p. <https://www.edwardsaquifer.org/science-and-maps/research-and-scientific-reports/science-document-library>

- National Academy of Sciences (NAS). 2015. *Review of the Edwards Aquifer Habitat Conservation Plan: Report 1.*
- National Academy of Sciences (NAS). 2017. *Review of the Edwards Aquifer Habitat Conservation Plan: Report 2.*
- National Academy of Sciences (NAS). 2018. *Review of the Edwards Aquifer Habitat Conservation Plan: Report 3.*
- RECON Environmental, Inc., Hicks & Company, Zara Environmental, LLC, and BIO-WEST. 2012. Edwards Aquifer Recovery Implementation Program Habitat Conservation Plan. Available: <https://www.edwardsaquifer.org/wp-content/uploads/2022/07/Edwards-Aquifer-Recovery-Implementation-Program-Nov-2021.pdf>
- White, J.T., L.K. Foster, M.N. Fienen, M.J. Knowling, B. Hemmings, and J.R. Winterle. 2020. Toward Reproducible Environmental Modeling for Decision Support: A Worked Example, *Frontiers in Earth Science*, Vol. 8. <https://doi.org/10.3389/feart.2020.00050>
- Winterle J. 2019. How to Run a Bottom-Up Analysis, Edwards Aquifer Authority internal report, 11p, Available on request.
- Winterle, J. 2023. A draft of Steps to Run a Future Climate Scenario Analysis with a MODFLOW model, 5p. Personal communication. Available on request.
- Wootten A, Başağaoğlu H, Bertetti FP, Chakraborty D, Sharma C, Samimi M, Mirchi A. 2024. Customized Statistically Downscaled CMIP5 and CMIP6 Projections: Application in the Edwards Aquifer Region in South-Central Texas, *in review Earth's Future*.

Appendix A

MODFLOW Jupyter Notebook Example

Introduction

- This jupyter notebook should work together with the following subfolders
 - baseModel
 - GenerateWellPackage
 - postprocessingLogFiles
 - recharge
 - updateRCH_SAWsForbearance
 - documentation folder includes documents related to this type of simulations.
- Copy all files in those folders with this Jupyter notebook together. Do not change the names of the subfolders
- The projected recharge should be copied to the subfolder of recharge, `.\recharge\rechargeprocessing`

User Interface

- `projectedR_filename`: the file name for the projected recharge
- `scenario`: a string to combine GCM and rcp which is used for saving the WL of J17 and J27 and Q

```
In [ ]: projectedR_filename = 'formatted_ProjRech_KIOST-ESM_ssp245_adjusted.csv'  
        scenario = 'KIOST-ESM_ssp245'
```

No need to change after this cell

```
In [ ]:
```

```
In [ ]:
```

```
In [ ]: import pandas as pd  
        import numpy as np  
        import matplotlib.pyplot as plt
```

```
In [ ]: import os  
        from pathlib import Path
```

```
In [ ]: import shutil  
        import subprocess
```

Step 1, Convert monthly recharge time series into a Modflow.RCH file

- Estimates based on the Puente method will require adjustment prior to input into the Modflow model (Lindgren et al, 2004; Liu et al., 2017).
- EAA previously developed a spreadsheet to load in the Puente method numbers and apply the necessary corrections. A python script was also developed by Logan to convert the corrected recharge numbers from the spreadsheet into a .RCH file.
- Use these tools to create the .RCH file with the appropriate number of stress periods for the desired scenario.

```
In [ ]: ## Load the python module to generate the RCH package from the projected recharge  
## the allocatingRCH requires two input parameters:  
##     The folder for the data (including the input and output)  
##     The name of the projected recharge  
##     the projected recharge should be placed within the folder of the data.  
## The output of the module is the RCH package with added "Allocated_" to the name of  
  
from recharge.AllocateRecharge import allocatingRCH
```

```
In [ ]: help(allocatingRCH)  
  
Help on function allocatingRCH in module recharge.AllocateRecharge:  
  
allocatingRCH(data_directory, recharge_filename)
```

```
In [ ]: cwd = os.getcwd()
```

```
In [ ]: iRCH = True ## for processing recharge
```

```
In [ ]: recharge_folder = os.path.join(cwd, 'recharge', 'rechargeprocessing')  
if iRCH == True:  
    allocatingRCH(recharge_folder, projectedR_filename)
```

```
In [ ]:
```

Step 2, Process Future Recharge Scenario to get total annual aquifer recharge and then calculate 10-year average recharge for each year of the scenario analysis period

- The 10-year average recharge numbers should be based on the raw Puente method numbers, not the corrected numbers used for the model input. Make note of all the years when the 10-year average recharge is below 500,000 acre-feet.
- Note that the USGS recharge before 2023 was used together with the projected recharge (2023-2065) to calculate 10-year average annual recharge

In []:

```
usgsRechFile = os.path.join( cwd, 'recharge', 'rechargeprocessing', 'USGSmonthlyRecharge'
rchUSGS = pd.read_csv(usgsRechFile, parse_dates=True, index_col='date')
```

In []:

```
projRechFile = os.path.join( cwd, 'recharge', 'rechargeprocessing', projectedR_filename)
rchProj = pd.read_csv(projRechFile, parse_dates=True, index_col='date')
rchProj.head()
```

Out []:

	Nueces	Frio	Sabinal	SAME	Medina	MECI	Cibolo
date							
2023-01-31	2798.968647	0.000000	0.000000	0.000000	0.00	0.000000	0.000000
2023-02-28	5005.608405	0.000000	0.000000	0.000000	0.00	0.000000	0.000000
2023-03-31	3795.695989	0.000000	0.000000	0.000000	0.00	0.000000	0.000000
2023-04-30	10280.794869	9174.712058	0.000000	0.000000	0.00	0.000000	0.000000
2023-05-31	33475.853824	38231.247307	17352.01556	41347.264558	4394.32	11112.642139	11124.194112

```
# rchProj.resample('Y').sum().to_csv('IPSL-CM5A-MR-RCP85-projectedHSPFrechargeScaledWi
```

In []:

```
totalRchUSGS = rchUSGS.resample('Y').sum().sum(axis=1)
totalRchProj = rchProj.resample('Y').sum().sum(axis=1)
```

```
totalR = pd.concat([totalRchUSGS, totalRchProj], axis=0)
totalR.head()
```

```
Out[ ]: date
1934-12-31    179601.0
1935-12-31    1258139.0
1936-12-31     909578.0
1937-12-31     400588.0
1938-12-31     432702.0
Freq: A-DEC, dtype: float64
```

```
In [ ]: totalR.tail()
```

```
Out[ ]: date
2061-12-31    2.148216e+05
2062-12-31    2.081732e+05
2063-12-31    9.801406e+05
2064-12-31    1.138691e+06
2065-12-31    7.062272e+05
Freq: A-DEC, dtype: float64
```

```
In [ ]: totalR_10yr_movingAvg = totalR.rolling(10).mean()
```

```
In [ ]: totalR_10yr_movingAvg = pd.DataFrame(totalR_10yr_movingAvg)
totalR_10yr_movingAvg.columns=['totalR']
```

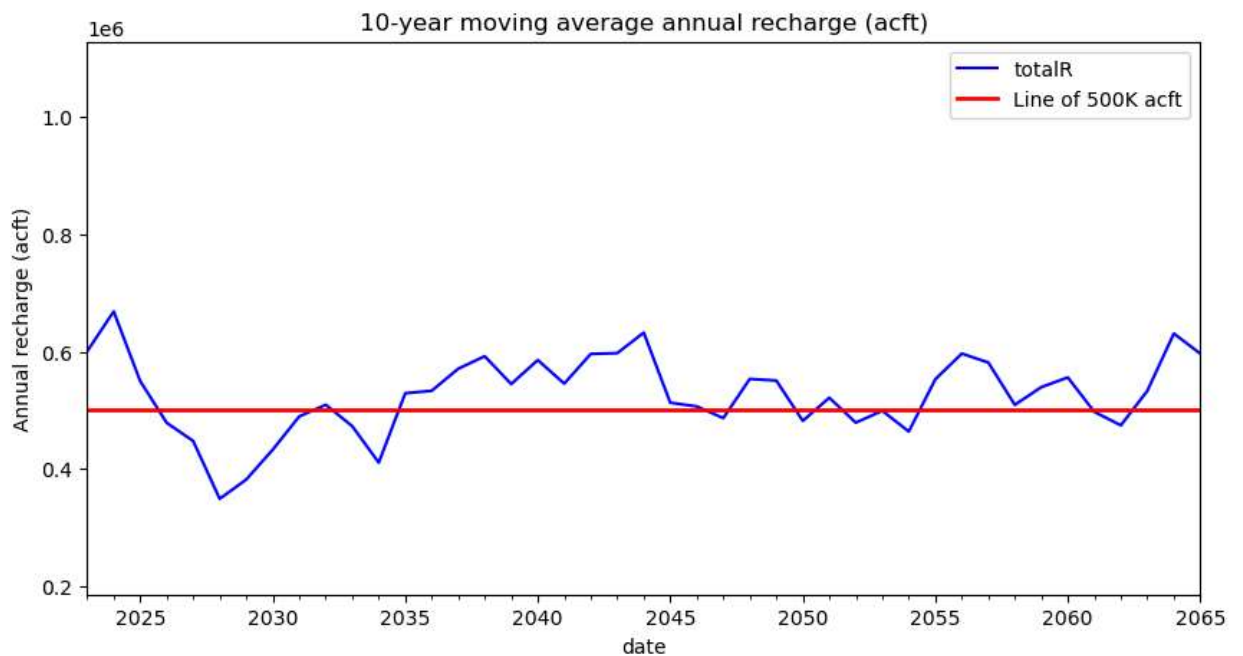
```
In [ ]:
```

```
In [ ]: cond = (totalR_10yr_movingAvg.index.year>2022) & (totalR_10yr_movingAvg['totalR']<500000)
years_totalR_below500K = totalR_10yr_movingAvg.loc[cond,:].index.year.tolist()
years_totalR_below500K
```

```
Out[ ]: [2026,
2027,
2028,
2029,
2030,
2031,
2033,
2034,
2047,
2050,
2052,
2053,
2054,
2061,
2062]
```

```
In [ ]: fig,ax =plt.subplots(figsize=(10,5))
totalR_10yr_movingAvg.plot(ax=ax,style='b-',label = '10-year moving average (acft)')
R_belwo500K = pd.DataFrame({'date':[totalRchProj.index[0],totalRchProj.index[-1]],'Lir
R_belwo500K = R_belwo500K .set_index('date')
#J17WL635.plot(ax=ax[0,1])
R_belwo500K .plot(ax=ax,style='r-',lw=2)
ax.set_ylabel('Annual recharge (acft)')
ax.set_xlim('2023-01-01','2065-12-31')
ax.set_title('10-year moving average annual recharge (acft)')
```

```
Out[ ]: Text(0.5, 1.0, '10-year moving average annual recharge (acft)')
```



In []:

Step 3, Create the first run

- Use the Jupyter script "GenerateWellFiles.py" to create the .WEL files. This script uses a .csv file called "Pumping Regime Types" to determine the conservation measures that are triggered for each year of the scenario analysis. Because it is not yet known which conservation measures will be triggered during the analysis, we first need to run it with only the conservation measures that are known.
- Regional Conservation. This conservation measure assumes that a reduction of 10,000 af out of the 578,000 af of total permitted pumping will not be pumped. The 10k af reduction is implemented for any year where CON is specified in column C of the Pumping Regime Types .csv file. For most scenario analysis, this should be specified for every year
- SAWS ASR Leases. The SAWS ASR program actually includes two parts. The first part is 50,000 af of permits that fall under lease options. In most years, when the 10-yr average recharge is above 500,000 af, this water will be pumped as normal. These years are known in advance based on the analysis of recharge estimates done in Step 2 above. For these years with 10-yr average recharge greater than 500,000 af, the number 1 should be specified in column D of the Pumping Regime Types file. For those years when the 10-yr average recharge falls below 500,000 af, enter the number 3 in column D. (Note: the number 2 in column D should not be used, as it is part of an obsolete program and no longer used.
- VISPO Leases. The VISPO program includes 41,795 af of leased water that is pumped in most years, but is not pumped in years when, on October 1 of the previous year, the 10-day average water level in Index Well J-17 was below 635 ft. For future scenario analyses, these years are not yet known. Therefore, the model has to be run without VISPO forbearance and the results analyzed to see which years meet the VISPO trigger. Therefore, for this first

run through the analysis, the word NORMAL should be entered in column B of the Pumping Regime Types file.

In []:

Step 3.1 Make a new folder for conducting Step 3 analysis

In []:

```
In [ ]: ## Create a folder with a name of Step3
folderStep3 = os.path.join(cwd, 'step3')
if not os.path.exists(folderStep3):
    os.makedirs(folderStep3)
```

```
In [ ]: ## Create a subfolder for conducting model simulations
folderStep3Simulation = os.path.join(folderStep3, 'simulation')
if not os.path.exists(folderStep3Simulation):
    os.makedirs(folderStep3Simulation)
```

```
In [ ]: ## Need to copy the model files from the basemodel folder into the simulation folder
baseModelFolder = os.path.join(cwd, 'baseModel')
files = os.listdir(baseModelFolder)
for file in files:
    file = os.path.join(baseModelFolder, file)
    shutil.copy2(file, folderStep3Simulation)
```

```
In [ ]: ## Copy the rch Pacakge to the simulation folder
fileRCH = os.path.join(recharge_folder, 'allocated_'+projectedR_filename[:-3]+'rch')
shutil.copy2(fileRCH, folderStep3Simulation)
```

```
Out [ ]: 'C:\\Users\\cyang\\Desktop\\BottomUp Analysis\\KIOST-ESM_ssp245\\step3\\simulation\\a
llocated_formatted_ProjRech_KIOST-ESM_ssp245_adjusted.rch'
```

In []:

Step 3.2 create well package

```
In [ ]: ## Create a subfolder of genWellPacakge with the folder of Step 3:
```

```
folderStep3Well = os.path.join(folderStep3, 'genWellPack')
if not os.path.exists(folderStep3Well):
    os.makedirs(folderStep3Well)
```

```
In [ ]: ## Copy the pumping type file to the folderStep3Well
PRTfile = os.path.join(cwd, 'GenerateWellPackage', 'Pumping Regime Types.csv')
shutil.copy2(PRTfile, folderStep3Well)
```

```
Out [ ]: 'C:\\Users\\cyang\\Desktop\\BottomUp Analysis\\KIOST-ESM_ssp245\\step3\\genWellPack
\\Pumping Regime Types.csv'
```

```
In [ ]: # Now we need to update the PRT file based on the recharge
PRTfile = os.path.join(folderStep3Well, 'Pumping Regime Types.csv')
pumping_regime=pd.read_csv(PRTfile)
pumping_regime
```

```
In [ ]: years_totalR_below500K
```

```
Out[ ]: [2026,  
2027,  
2028,  
2029,  
2030,  
2031,  
2033,  
2034,  
2047,  
2050,  
2052,  
2053,  
2054,  
2061,  
2062]
```

```
In [ ]: ## Set initial value for VISPO column to be Normal  
pumping_regime['VISPO'] = 'NORMAL'
```

```
In [ ]: pumping_regime['SAWS'] = ['3' if pumping_regime.loc[i,'Year']-1 in years_totalR_below5
```

```
In [ ]: pumping_regime
```

```
In [ ]:
```

```
In [ ]: _,pumpRegimeFile = os.path.split(PRTfile)  
PRTfile_updatedStep3 = os.path.join(folderStep3Well,pumpRegimeFile[:-4]+'_step3.csv' )  
pumping_regime.to_csv(PRTfile_updatedStep3,index=False)
```

```
In [ ]: PRTfile_updatedStep3
```

```
Out[ ]: 'C:\\Users\\cyang\\Desktop\\BottomUp Analysis\\KIOST-ESM_ssp245\\step3\\genWellPack  
\\Pumping Regime Types_step3.csv'
```

```
In [ ]: ## Copy the L1normal_2023_2065.wel to the folder of genwellpackage
```

```
In [ ]: ## Copy the L1normal_2023_2065.wel from the folder of genwellpackage to the folderStep  
fileL1norm = os.path.join(cwd,'GenerateWellPackage','L1normal_2023_2065.wel')  
shutil.copy2(fileL1norm,folderStep3Well)
```

```
Out[ ]: 'C:\\Users\\cyang\\Desktop\\BottomUp Analysis\\KIOST-ESM_ssp245\\step3\\genWellPack  
\\L1normal_2023_2065.wel'
```

```
In [ ]: ## Load the python module to generate the Well  
from GenerateWellPackage.GenerateWellFiles import updateWellPackage
```

```
In [ ]: help(updateWellPackage)
```

Help on function updateWellPackage in module GenerateWellPackage.GenerateWellFiles:

```
updateWellPackage(pathWell, pumpingRegimeFile, startingDate, endingDate, oriWellFile,  
iRunSplitWell=True, iCheckNewWel=True)
```

- After editing the Pumping Regime Types file, the Generate_Pumping_Files Jupyter script is ready to run. The script will generate a .WEL file called L3ASR3.wel.
- This is the .WEL file that should be run through the Groundwater Management Module for the first run.

In []:

```
In [ ]: iWell = True
_,pumpingRegimeFile = os.path.split(PRTfile_updatedStep3)
startingDate = '2023-01-01'
endingDate = '2065-12-31'
oriWellFile = 'L1normal_2023_2065.wel'
if iWell == True:
    targetWellFile = updateWellPackage(folderStep3Well, pumpingRegimeFile, startingDate)
```

```
In [ ]: ## Copy the generated file to the simulation folder
shutil.copy2(targetWellFile, folderStep3Simulation)
```

```
Out[ ]: 'C:\\Users\\cyang\\Desktop\\BottomUp Analysis\\KIOST-ESM_ssp245\\step3\\simulation\\L3ASR3.wel'
```

Step 3.3 Prepare input files for model simulations

```
In [ ]: ### Need to update the RCH and well package names in the MODFLOW nam file
namFile = os.path.join(folderStep3Simulation, 'itprenewal2023.nam')
with open(namFile, 'r') as namF:
    namLines = namF.readlines()
    namF.close()

newLines = []
_, wellPackName = os.path.split(targetWellFile)
_, rchpackName = os.path.split(fileRCH)
for line in namLines:
    newline = line
    if 'WEL 12' in line:
        print(line)
        newline = line[:7] + ' ' + wellPackName + '\n'
        print(newline)
    if 'RCH 18 ' in line:
        newline = line[:7] + ' ' + rchpackName + '\n'
        newLines.append(newline)

with open(namFile, 'w') as namF:
    for line in newLines:
        namF.write(line)
    namF.close()
```

```
WEL 12 L4STG5_new-41795vspo.wel
```

```
WEL 12 L3ASR3.wel
```

Step 3.4 Run the simulation of Step 3

```
In [ ]: ## Change the current dir to the folder of simulation
os.chdir(folderStep3Simulation)
exec_cmd = ['mfnr12_525.exe', 'itprenewal2023.nam']
proc = subprocess.Popen(exec_cmd, stdout=subprocess.PIPE, stderr=subprocess.STDOUT)

while proc.poll() is None:
    txt = proc.stdout.readline()
    txt = txt.decode('utf-8')
    if len(txt.strip())>0:
        print(txt)

if proc.returncode == 0:
    print("Simulation executed successfully")
else:
    print("Simulation encountered an error")
    print("Error:", proc.returncode)

## make sure change the current dir to main folder with this Jupyter notebook
os.chdir(cwd)
```

In []:

In []:

Step 3.5 Postprocess the results of Step 3 simulation

- After running the Groundwater Management Modul batch file from Step 3, evaluate the output water levels for J-17.

```
In [ ]: from postProcessingLogFiles.logstat6 import extractingSimulationResults
```

In []:

```
In [ ]: ## Postprocessing the results
logFile = os.path.join(folderStep3Simulation, 'itprenewal2023.log')
step3OutputF = os.path.join(folderStep3Simulation, 'Step3_log.csv')
extractingSimulationResults(logFile, step3OutputF)
```

Step 3.6 Check the results

```
In [ ]: dates = pd.date_range('2023-01-01', '2065-12-31', freq='M')
```

```
In [ ]: len(dates)
```

Out[]: 516

```
In [ ]: logStep3 = pd.read_csv(step3OutputF)
```

```
In [ ]: logStep3
```

```
In [ ]: logStep3['date'] = dates
logStep3 = logStep3.set_index('date')
```

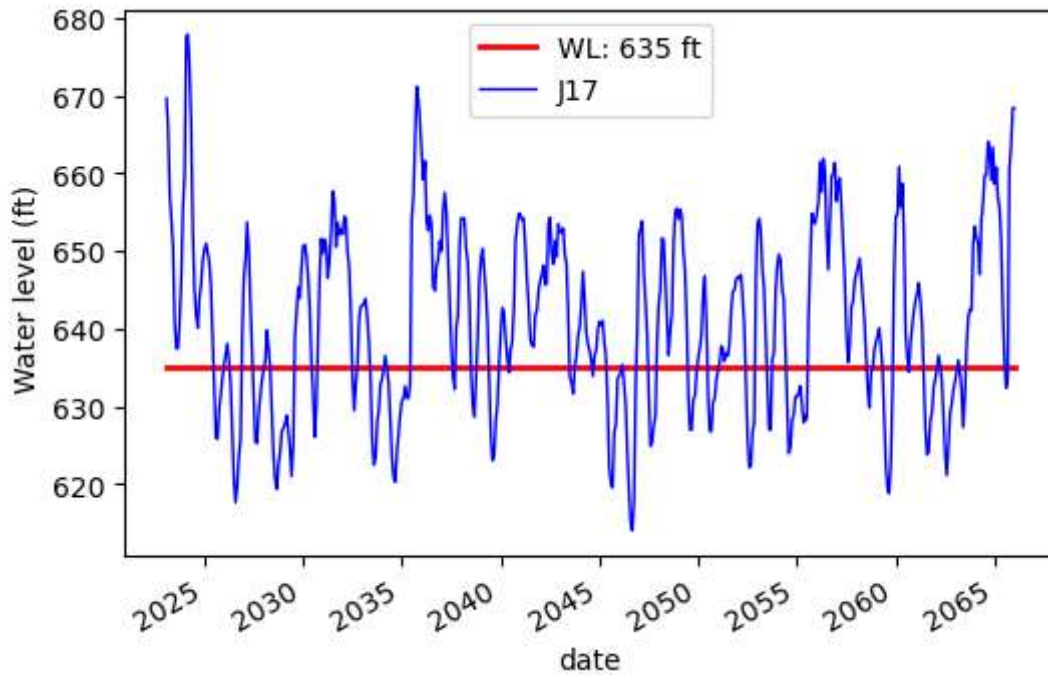
```
In [ ]: logStep3.columns
```

```
Out[ ]: Index(['SP', 'days', 'Comal', 'San Marcos', 'J17', 'J27'], dtype='object')
```

```
In [ ]: fig,ax =plt.subplots(figsize=(6,4))
```

```
J17WL635 = pd.DataFrame({'date':[logStep3.index[0],logStep3.index[-1]],'WL: 635 ft':[635,635]})  
J17WL635 = J17WL635.set_index('date')  
#J17WL635.plot(ax=ax[0,1])  
J17WL635.plot(ax=ax,style='r-',lw=2)  
logStep3[['J17']].plot(ax=ax,style='b-',lw=1)  
ax.set_ylabel('Water level (ft)')
```

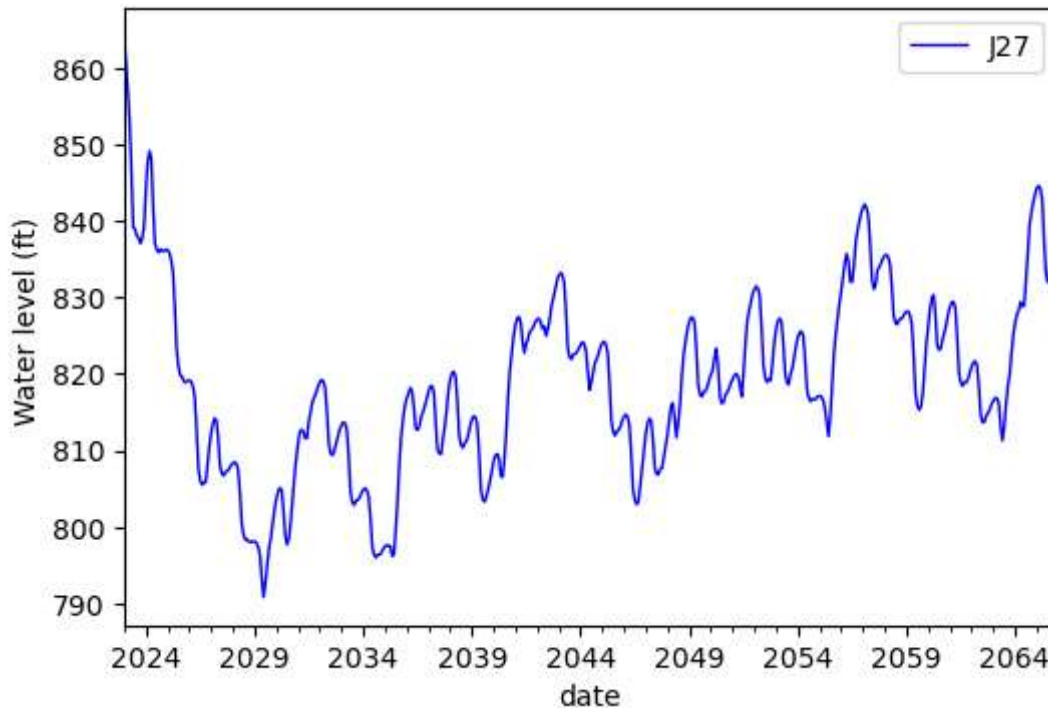
```
Out[ ]: Text(0, 0.5, 'Water level (ft)')
```



```
In [ ]: fig,ax =plt.subplots(figsize=(6,4))
```

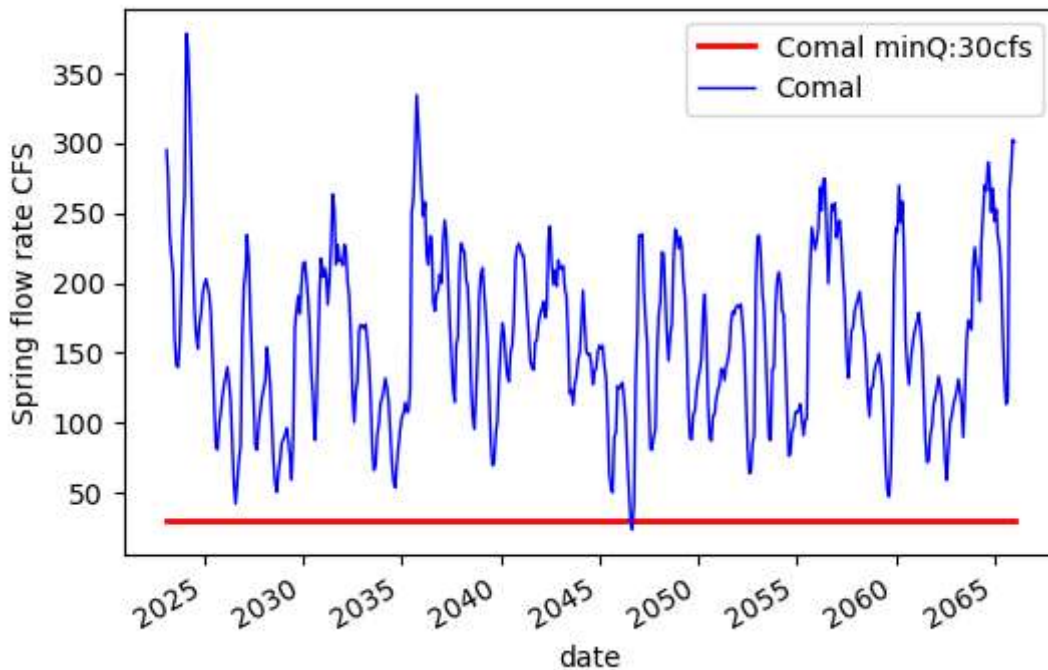
```
logStep3[['J27']].plot(ax=ax,style='b-',lw=1)  
ax.set_ylabel('Water level (ft)')
```

```
Out[ ]: Text(0, 0.5, 'Water level (ft)')
```



```
In [ ]: fig,ax =plt.subplots(figsize=(6,4))
minColmal = pd.DataFrame({'date':[logStep3.index[0],logStep3.index[-1]],'Comal minQ:30cfs':minColmal})
minColmal = minColmal.set_index('date')
minColmal.plot(ax=ax,style='r-',lw=2)
logStep3[['Comal']].plot(ax=ax,style='b-',lw=1)
ax.set_ylabel('Spring flow rate CFS')
```

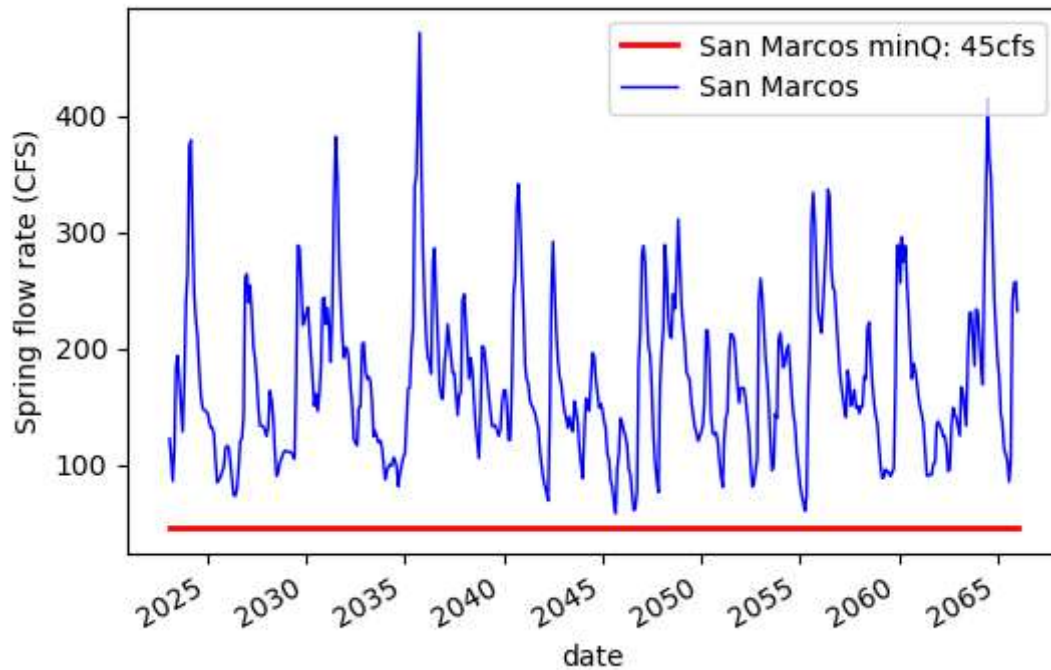
```
Out[ ]: Text(0, 0.5, 'Spring flow rate CFS')
```



```
In [ ]: fig,ax =plt.subplots(figsize=(6,4))
minSM = pd.DataFrame({'date':[logStep3.index[0],logStep3.index[-1]],'San Marcos minQ:30cfs':minSM})
minSM = minSM.set_index('date')
minSM.plot(ax=ax,style='r-',lw=2)
```

```
logStep3[['San Marcos']].plot(ax=ax,style='b-',lw=1)
ax.set_ylabel('Spring flow rate (CFS)')
```

```
Out[ ]: Text(0, 0.5, 'Spring flow rate (CFS)')
```



```
In [ ]: ## Output the WL of J17 and J27 and Q of two springs to a folder of outputWLQ

outputLogStep3 = logStep3.loc[:,['Comal', 'San Marcos', 'J17', 'J27']]
outputLogStep3.columns = ['Comal (cfs)', 'San Marcos (cfs)', 'J17 (ft)', 'J27 (ft)']
outputPath = os.path.join(os.getcwd(), 'outputWLQ')
if not os.path.exists(outputPath):
    os.makedirs(outputPath)
outputLogStep3.to_csv(os.path.join(outputPath, scenario+'_Step3_results.csv'))
```

```
In [ ]:
```

Step 4, Create the second run and update .WEL file

- After running the Groundwater Management Modul batch file from Step 3, evaluate the output water levels for J-17.
- Identify all the instances when the level is below 635 acre feet on October 1 (end of 9th Stress Period in each year).
- Whenever this occurs, Column B of the Pumping Regime Types file should be edited to change from Normal to Dry in the next year .
- This change will specify the VISPO forbearance is implemented for that year.
- Run the Generate_Pumping_Files Jupyter script again using this modified input.
- Then run the resulting L3ASR3.wel file through the Groundwater Management Module.
- By Jim Winterle

Step 4.1, Create a folder and copy the files for Step4 simulation

```
In [ ]: ## Create a folder with a name of Step4  
folderStep4 = os.path.join(cwd, 'step4')  
if not os.path.exists(folderStep4):  
    os.makedirs(folderStep4)
```

```
In [ ]: ## Create a subfolder for conducting model simualtions  
folderStep4Simulation = os.path.join(folderStep4, 'simulation')  
if not os.path.exists(folderStep4Simulation):  
    os.makedirs(folderStep4Simulation)
```

```
In [ ]: ## Need to copy the model files from the basemodel folder into the simualtion folder  
baseModelFolder = os.path.join(cwd, 'baseModel')  
files = os.listdir(baseModelFolder)  
for file in files:  
    file = os.path.join(baseModelFolder, file)  
    shutil.copy2(file, folderStep4Simulation)
```

```
In [ ]: ## Copy the rch Pacakge to the simulation folder  
fileRCH = os.path.join(recharge_folder, 'allocated_'+projectedR_filename[:-3]+'rch')  
shutil.copy2(fileRCH, folderStep4Simulation)
```

```
Out[ ]: 'C:\\Users\\cyang\\Desktop\\BottomUp Analysis\\KIOST-ESM_ssp245\\step4\\simulation\\a  
llocated_formatted_ProjRech_KIOST-ESM_ssp245_adjusted.rch'
```

```
In [ ]:
```

Step 4.2, Update well package

```
In [ ]: ## Create a subfolder of genWellPacakge with the folder of Step 3:  
  
folderStep4Well = os.path.join(folderStep4, 'genWellPack')  
if not os.path.exists(folderStep4Well):  
    os.makedirs(folderStep4Well)
```

- Identify all the instances when the level is below 635 acre feet on October 1 (end of 9th Stress Period in each year).

```
In [ ]: cond = (logStep3.index.month == 9) & (logStep3['J17'] < 635)  
logStep3.loc[cond, 'J17']
```

```
In [ ]: vispoYears = list(logStep3.loc[cond, 'J17'].index.year+1)  
vispoYears
```

```
Out[ ]: [2026,
         2027,
         2028,
         2029,
         2034,
         2035,
         2039,
         2040,
         2046,
         2047,
         2048,
         2050,
         2051,
         2053,
         2055,
         2059,
         2060,
         2062,
         2063]
```

```
In [ ]: PRTfile_updatedStep3
```

```
Out[ ]: 'C:\\Users\\cyang\\Desktop\\BottomUp Analysis\\KIOST-ESM_ssp245\\step3\\genWellPack
        \\Pumping Regime Types_step3.csv'
```

```
In [ ]: ## Load the pumping regime types file generated previously
        pumping_regime=pd.read_csv(PRTfile_updatedStep3)
        pumping_regime.head(2)
```

```
Out[ ]:   Year  VISPO  CON  SAWS  Layer 1 ID  Layer 2 ID  Layer 3 ID
0  2023  NORMAL  CON    1      NaN      NaN      NaN
1  2024  NORMAL  CON    1      NaN      NaN      NaN
```

```
In [ ]: pumping_regime['VISPO'] = ['DRY' if pumping_regime.loc[i,'Year'] in vispoYears else 'N
        pumping_regime.head()
```

```
Out[ ]:   Year  VISPO  CON  SAWS  Layer 1 ID  Layer 2 ID  Layer 3 ID
0  2023  NORMAL  CON    1      NaN      NaN      NaN
1  2024  NORMAL  CON    1      NaN      NaN      NaN
2  2025  NORMAL  CON    1      NaN      NaN      NaN
3  2026    DRY   CON    1      NaN      NaN      NaN
4  2027    DRY   CON    3      NaN      NaN      NaN
```

```
In [ ]: ## Save the updated pumping regime types to a new file for step 4
        _, rgtFile4 = os.path.split(PRTfile_updatedStep3)
        rgtFile4 = rgtFile4.replace('step3','step4')
        rgtFile4path = os.path.join(folderStep4Well,rgtFile4)
        pumping_regime.to_csv(rgtFile4path,index=False)
```

```
In [ ]: rgtFile4path
```

```
Out [ ]: 'C:\\Users\\cyang\\Desktop\\BottomUp Analysis\\KIOST-ESM_ssp245\\step4\\genWellPack
\\Pumping Regime Types_step4.csv'
```

```
In [ ]:
```

```
In [ ]: ## Copy the pumping type file to the folderStep3Well
fileL1norm = os.path.join(cwd, 'GenerateWellPackage', 'L1normal_2023_2065.wel')
shutil.copy2(fileL1norm, folderStep4Well)
```

```
Out [ ]: 'C:\\Users\\cyang\\Desktop\\BottomUp Analysis\\KIOST-ESM_ssp245\\step4\\genWellPack
\\L1normal_2023_2065.wel'
```

```
In [ ]:
```

```
In [ ]: iWell = True
_, pumpingRegimeFile = os.path.split(rgtFile4path)
startingDate = '2023-01-01'
endingDate = '2065-12-31'
oriWellFile = 'L1normal_2023_2065.wel'
if iWell == True:
    targetWellFile = updateWellPackage(folderStep4Well, pumpingRegimeFile, startingDate)
```

```
In [ ]: ## Copy the generated file to the simulation folder
shutil.copy2(targetWellFile, folderStep4Simulation)
```

```
Out [ ]: 'C:\\Users\\cyang\\Desktop\\BottomUp Analysis\\KIOST-ESM_ssp245\\step4\\simulation\\L
3ASR3.wel'
```

```
In [ ]:
```

Step 4.3, Prepare model simulation

```
In [ ]: ### Need to update the RCH and well package names in the MODFLOW nam file
namFile = os.path.join(folderStep4Simulation, 'itprenewal2023.nam')
with open(namFile, 'r') as namF:
    namLines = namF.readlines()
    namF.close()

newLines = []
_, wellPackName = os.path.split(targetWellFile)
_, rchpackName = os.path.split(fileRCH)
for line in namLines:
    newline = line
    if 'WEL 12' in line:
        print(line)
        newline = line[:7] + ' ' + wellPackName + '\n'
        print(newline)
    if 'RCH 18 ' in line:
        newline = line[:7] + ' ' + rchpackName + '\n'
        newLines.append(newline)

with open(namFile, 'w') as namF:
    for line in newLines:
        namF.write(line)
    namF.close()
```

WEL 12 L4STG5_new-41795vspo.wel

WEL 12 L3ASR3.wel

Step 4.4, Run the simulation of Step 4

```
In [ ]: ## Run the model
## Change the current dir to the folder of simulation
os.chdir(folderStep4Simulation)
exec_cmd = ['mfnr12_525.exe', 'itprenewal2023.nam']
proc = subprocess.Popen(exec_cmd, stdout=subprocess.PIPE, stderr=subprocess.STDOUT)

while proc.poll() is None:
    txt = proc.stdout.readline()
    txt = txt.decode('utf-8')
    if len(txt.strip())>0:
        print(txt)

if proc.returncode == 0:
    print("Simulation executed successfully")
else:
    print("Simulation encountered an error")
    print("Error:", proc.returncode)
## make sure change the current dir to main folder with this Jupyter notebook
os.chdir(cwd)
```

Step 4.5 PostProcess results of the Step 4 Simulation

```
In [ ]: ## Postprocess LOG file
logFile = os.path.join(folderStep4Simulation, 'itprenewal2023.log')
step4OutputF = os.path.join(folderStep4Simulation, 'Step4_log.csv')
extractingSimulationResults(logFile, step4OutputF)
```

In []:

Step 4.6 Check the results of Step 4

In []:

```
In [ ]: logStep4 = pd.read_csv(step4OutputF)
logStep4['date'] = dates
logStep4 = logStep4.set_index('date')
```

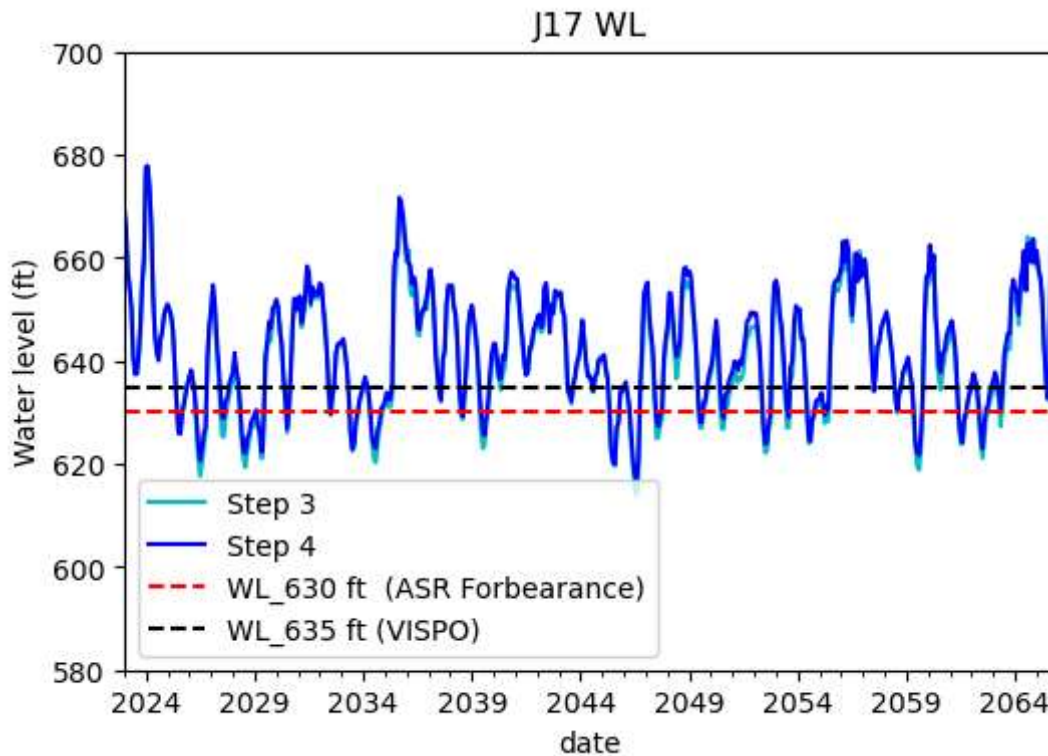
```
In [ ]: fig, ax = plt.subplots(figsize=(6,4))
logStep3['J17'].plot(ax=ax, style=['c-'], label='Step 3')
logStep4['J17'].plot(ax=ax, style=['b-'], label='Step 4')
#logStep5['J17'].plot(ax=ax, style=['go'], Label='Step 5', markersize = 3)
#logStat6_Jim['J17'].plot(ax=ax, style=['g-'], Label='Jim Archive')

df1 = pd.DataFrame({'date':logStep4.index, 'WL_630':[630]*len(logStep4.index)})
df1 = df1.set_index('date')
df1['WL_635'] = [635]*len(logStep4.index)

df1['WL_630'].plot(ax=ax, style='r--', label='WL_630 ft (ASR Forbearance)')
```

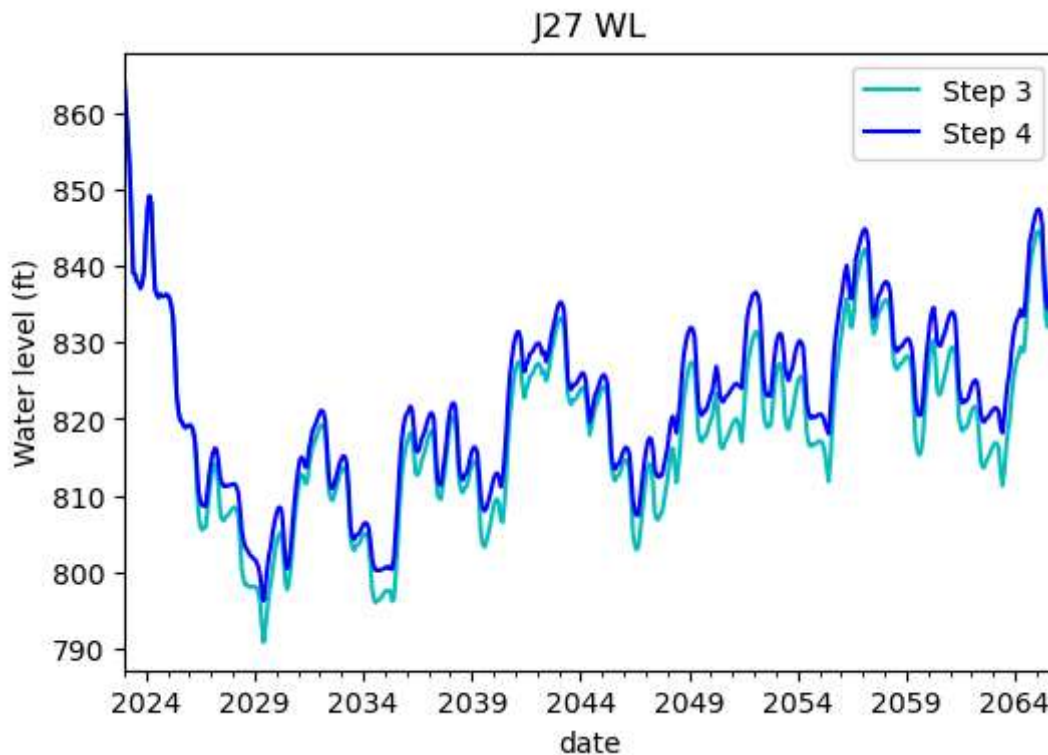
```
df1['WL_635'].plot(ax=ax,style='k--',label='WL_635 ft (VISPO)')
ax.set_ylim(580,700)
ax.set_ylabel('Water level (ft)')
ax.set_title('J17 WL')
ax.legend(loc='best')
```

Out[]: <matplotlib.legend.Legend at 0x1c75afaf610>



```
In [ ]: fig,ax =plt.subplots(figsize=(6,4))
logStep3['J27'].plot(ax=ax,style=['c-'],label='Step 3')
logStep4['J27'].plot(ax=ax,style=['b-'],label='Step 4')
#logStep5['J27'].plot(ax=ax,style=['go'],Label='Step 5',markersize = 3)
#LogStat6_Jim['J27'].plot(ax=ax,style=['g-'],label='Jim Archive')
df1 = pd.DataFrame({'date':logStep4.index,'WL_630':[630]*len(logStep4.index)})
df1 =df1.set_index('date')
#df1['WL_635'] = [635]*len(logStep4.index)
#df1['WL_630'].plot(ax=ax,style='r--',label='WL_630')
#df1['WL_635'].plot(ax=ax,style='k--',label='WL_635')
#ax.set_ylim(580,700)
ax.set_ylabel('Water level (ft)')
ax.set_title('J27 WL')
ax.legend(loc='best')
```

Out[]: <matplotlib.legend.Legend at 0x1c74d6a1b90>

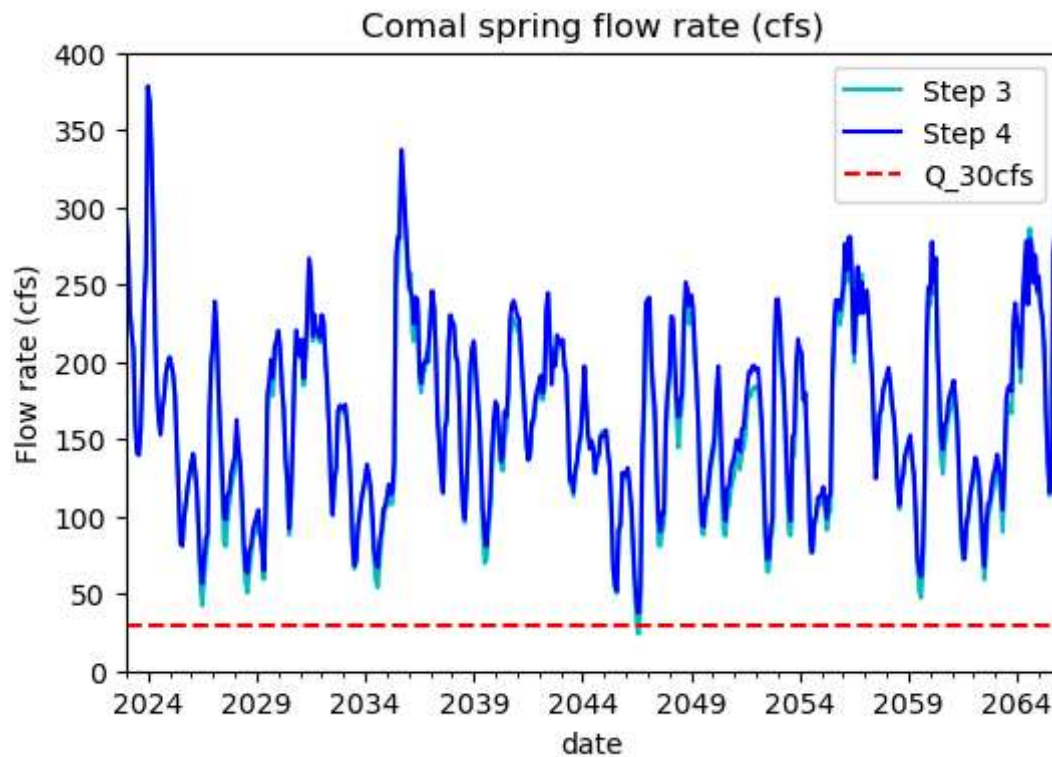


```
In [ ]: fig,ax =plt.subplots(figsize=(6,4))
logStep3['Comal'].plot(ax=ax,style=['c-'],label='Step 3')
logStep4['Comal'].plot(ax=ax,style=['b-'],label='Step 4')
#LogStep5['Comal'].plot(ax=ax,style=['go'],Label='Step 5',markersize=3)
#LogStat6_Jim['Comal'].plot(ax=ax,style=['g-'],Label='Jim Archive')

df1 = pd.DataFrame({'date':logStep4.index,'Q_30cfs':[30]*len(logStep4.index)})
df1 =df1.set_index('date')
#df1['Q_30cfs'] = [30]*len(logStep4.index)

df1['Q_30cfs'].plot(ax=ax,style='r--',label='Q_30cfs')
ax.set_ylim(0,400)
ax.set_ylabel('Flow rate (cfs)')
ax.set_title('Comal spring flow rate (cfs)')
#df1['Q_30cfs'].plot(ax=ax,style='k--',Label='WL_635')
ax.legend(loc='best')
```

```
Out[ ]: <matplotlib.legend.Legend at 0x1c75aac5090>
```

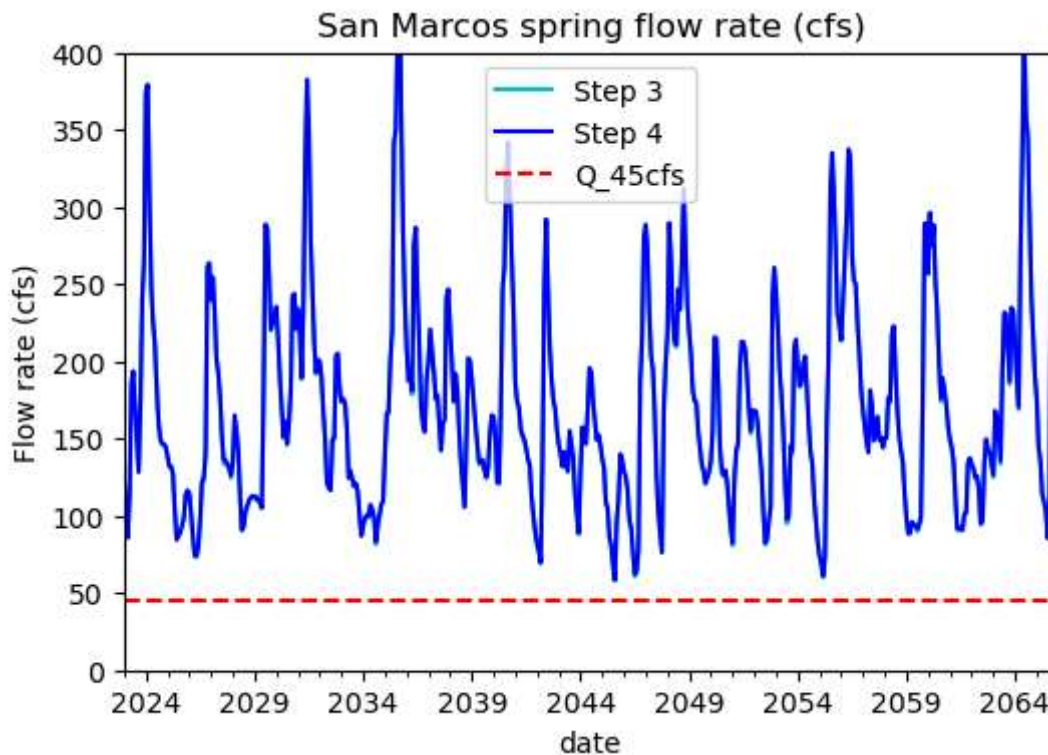


```
In [ ]: fig,ax =plt.subplots(figsize=(6,4))
logStep3['San Marcos'].plot(ax=ax,style='c-',label='Step 3')
logStep4['San Marcos'].plot(ax=ax,style='b-',label='Step 4')

df1 = pd.DataFrame({'date':logStep4.index, 'Q_45cfs':[45]*len(logStep4.index)})
df1 =df1.set_index('date')
#df1['Q_30cfs'] = [30]*len(logStep4.index)

df1['Q_45cfs'].plot(ax=ax,style='r--',label='Q_45cfs')
ax.set_ylim(0,400)
ax.set_ylabel('Flow rate (cfs)')
ax.set_title('San Marcos spring flow rate (cfs)')
#df1['Q_30cfs'].plot(ax=ax,style='k--',label='WL_635')
ax.legend(loc='best')
```

```
Out [ ]: <matplotlib.legend.Legend at 0x1c75adb98d0>
```



```
In [ ]: ## Output the WL of J17 and J27 and Q of two springs to a folder of outputWLQ

outputLogStep4 = logStep4.loc[:,['Comal', 'San Marcos', 'J17', 'J27']]
outputLogStep4.columns = ['Comal (cfs)', 'San Marcos (cfs)', 'J17 (ft)', 'J27 (ft)']
outputPath = os.path.join(os.getcwd(), 'outputWLQ')
if not os.path.exists(outputPath):
    os.makedirs(outputPath)
outputLogStep4.to_csv(os.path.join(outputPath, scenario+'_Step4_results.csv'))
```

In []:

Step 5: Modify the .RCH file for a third run, if needed

Step 5.1, Create a folder and copy the files for Step5 simulation

```
In [ ]: ## Create a folder with a name of Step5
folderStep5 = os.path.join(cwd, 'step5')
if not os.path.exists(folderStep5):
    os.makedirs(folderStep5)
```

```
In [ ]: ## Create a subfolder for conducting model simulations
folderStep5Simulation = os.path.join(folderStep5, 'simulation')
if not os.path.exists(folderStep5Simulation):
    os.makedirs(folderStep5Simulation)
```

```
In [ ]: ## Copy files from the folder of simulation at Step 4 to Simulation of Step 5
fileLst = os.listdir(folderStep4Simulation)

for fl in fileLst:
    ext = fl[-3:]
    if 'rch' in fl:
```

```

rchFileNameStep5= f1
if ext not in ['csv','cbb','cbd','cbw','crc','glo','hds','lg2','log','lst']:
    file =os.path.join(folderStep4Simulation,f1)
    shutil.copy2(file,folderStep5Simulation)

```

In []: rchFileNameStep5

Out[]: 'allocated_formatted_ProjRech_KIOST-ESM_ssp245_adjusted.rch'

Table 4. SAWS ASR forbearance representation in MODFLOW Drought of Record simulations.

Month In 1956	HDR (2011) (ac-ft)	Nonroutine AMP Runs (ac-ft)
January	1700	3200
February	1400	3500
March	1100	4500
April	2200	4500
May	3800	5600
June	5600	5600
July	5600	5600
August	5600	5600
September	5600	3000
October	5200	2000
November	4700	1700
December	3800	1500

Step 5.2, Calculate injection rate at four cells with Nonroutine AMP (Table above)

(1) the 10-yr average recharge is below 500,000 af, and (2) the 10-day average water level at J-17 is below 630 ft

```

In [ ]: def calc_inj_rate(x,years_below500K):
        ## acft-month
        ASRInj_month = [3200,3500,4500,4500,5600,5600,5600,5600,3000,2000,1700,1500]
        month = [i+1 for i in range(12)]
        SAWS_ASR_month =dict(zip(month,ASRInj_month))
        acre_sqft=43559.9 ## acre to square ft
        area_grid = 1320*1320 # sqare ft
        #print(x.name)
        rate = 0.0
        # check if 10-year average of annual recharge in the the previous year fall in the
        if (x.name.year-1 in years_below500K) and (x['J17']<630.0):
            rate = SAWS_ASR_month[x.name.month] # acft
            rate = rate/x.name.daysinmonth*acre_sqft # convert ft3/day

```

```

    rate = rate/(4*area_grid)    # convert ft/day at 4 grids
    #print(rate)
else:
    rate = 0.0
return rate

```

In []: years_totalR_below500K

Out[]: [2026,
2027,
2028,
2029,
2030,
2031,
2033,
2034,
2047,
2050,
2052,
2053,
2054,
2061,
2062]

```

In [ ]: updateSawsASR = logStep4[['J17']]
updateSawsASR['RCH_inj'] = updateSawsASR.apply(lambda x: calc_inj_rate(x,years_totalR_
updateSawsASR

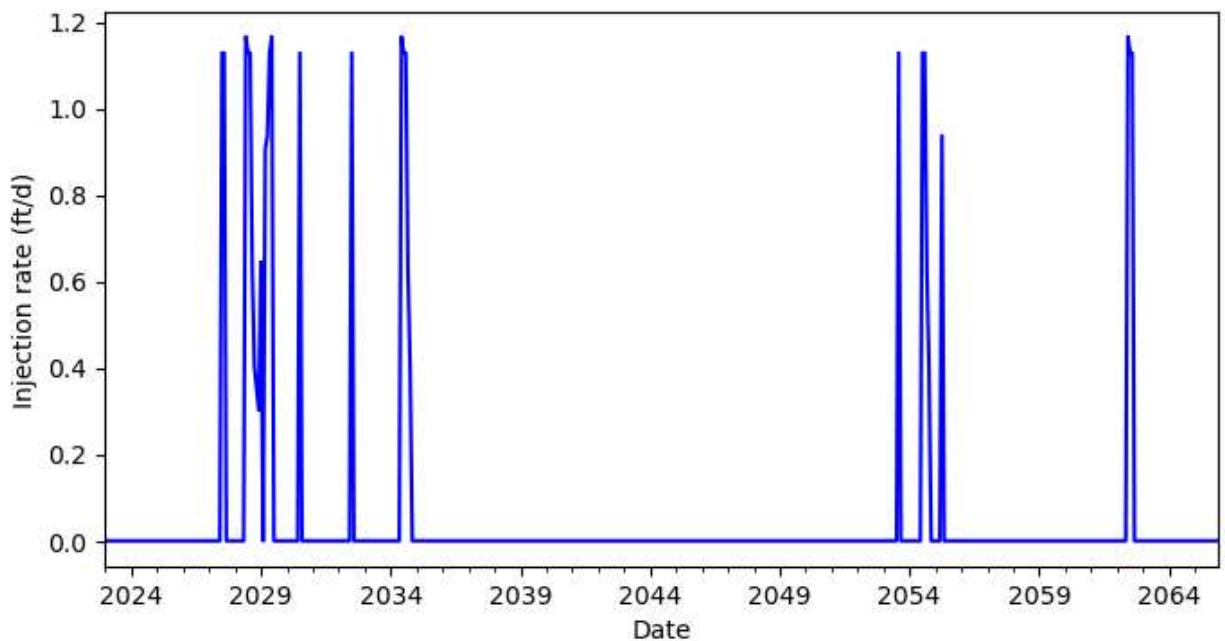
```

```

In [ ]: fig, ax = plt.subplots(figsize=(8,4))
updateSawsASR['RCH_inj'].plot(ax=ax,linestyle='-',color='b')
ax.set_ylabel('Injection rate (ft/d)')
ax.set_xlabel('Date')

```

Out[]: Text(0.5, 0, 'Date')



```

In [ ]: updateSawsASR.to_csv(os.path.join(folderStep5,'injected_ASR_forbearance.csv'))

```

In []:

Step 5.3, Update the recharge package at the four cells with the injection rate (ft/day) previously calculated

```
In [ ]: from updateRCH_SAWSasrForbearance.readingWritingRch import updatingRCH
```

```
In [ ]: rchFileNameStep5
```

```
Out[ ]: 'allocated_formatted_ProjRech_KIOST-ESM_ssp245_adjusted.rch'
```

```
In [ ]: rchFileOri = os.path.join(folderStep5Simulation, rchFileNameStep5)
        ## the new file name to be saved after the updating
        outRchFile = rchFileOri.replace('allocated_', 'step5_')
        ### the recharge of each stress period at a cell

        newR = updateSawsASR['RCH_inj'].values
        ### If true the RCH file will be updated with the the newR, otherwise, no update and s
        iUpdated = True
        # Four injection cells
        cells = [(269, 469), (270, 461), (279, 457), (267, 435)] # Base 0
        oriDataDict = updatingRCH(rchFileOri, outRchFile, newR, cells, iUpdated)
```

Step 5.4, Prepare the files for model simulation of Step 5

```
In [ ]: ### Need to update the RCH and well pacakge names in the MODFLOW nam file
        namFile = os.path.join(folderStep5Simulation, 'itprenewal2023.nam')
        with open(namFile, 'r') as namF:
            namLines = namF.readlines()
            namF.close()

        newLines = []
        _, rchpackName = os.path.split(outRchFile)
        for line in namLines:
            newline = line
            if 'RCH 18 ' in line:
                newline = line[:7] + ' ' + rchpackName + '\n'
            newLines.append(newline)

        with open(namFile, 'w') as namF:
            for line in newLines:
                namF.write(line)
            namF.close()
```

In []:

Step 5.5, Run the simulation of Step 5

```
In [ ]: ## Run the model
        ## Change the current dir to the folder of simulation
        os.chdir(folderStep5Simulation)
        exec_cmd = ['mfnr12_525.exe', 'itprenewal2023.nam']
        proc = subprocess.Popen(exec_cmd, stdout=subprocess.PIPE, stderr=subprocess.STDOUT)
```

```

while proc.poll() is None:
    txt = proc.stdout.readline()
    txt = txt.decode('utf-8')
    if len(txt.strip())>0:
        print(txt)

if proc.returncode == 0:
    print("Simulation executed successfully")
else:
    print("Simulation encountered an error")
    print("Error:", proc.returncode)

## make sure change the current dir to main folder with this Jupyter notebook
os.chdir(cwd)

```

In []:

Step 5.6 Postprocess the modeling results

```

folderStep5Simulation = r'E:\projects\EAA_All_modflows\Rerun_RCP85_IPSL-CM5A-
MR_20240116\step5\simulation'
logFile = os.path.join(folderStep5Simulation,'itprenewal2023.log')
step5OutputF = os.path.join(folderStep5Simulation,'Step5_log.csv')
extractingSimulationResults(logFile,step5OutputF)

```

```

In [ ]: ## Postprocess LOG file
logFile = os.path.join(folderStep5Simulation,'itprenewal2023.log')
step5OutputF = os.path.join(folderStep5Simulation,'Step5_log.csv')
extractingSimulationResults(logFile,step5OutputF)

```

In []:

In []:

Step 5.6 Check the modeling results of the Step 5 simulation

```

In [ ]: logStep5 = pd.read_csv(step5OutputF)
if len(logStep5) != len(dates):
    print(" Step 5 simulation has a convergence issue! Please check the run!")
else:

    logStep5['date'] = dates
    logStep5 = logStep5.set_index('date')

```

In []:

In []:

```

In [ ]: fig,ax =plt.subplots(figsize=(6,4))
logStep3['J17'].plot(ax=ax,style=['c-'],label='Step 3')
logStep4['J17'].plot(ax=ax,style=['b-'],label='Step 4')
logStep5['J17'].plot(ax=ax,style=['g-'],label='Step 5',markersize = 3)
#LogStat6_Jim['J17'].plot(ax=ax,style=['g-'],label='Jim Archive')

df1 = pd.DataFrame({'date':logStep4.index,'WL_630':[630]*len(logStep4.index)})
df1 =df1.set_index('date')

```

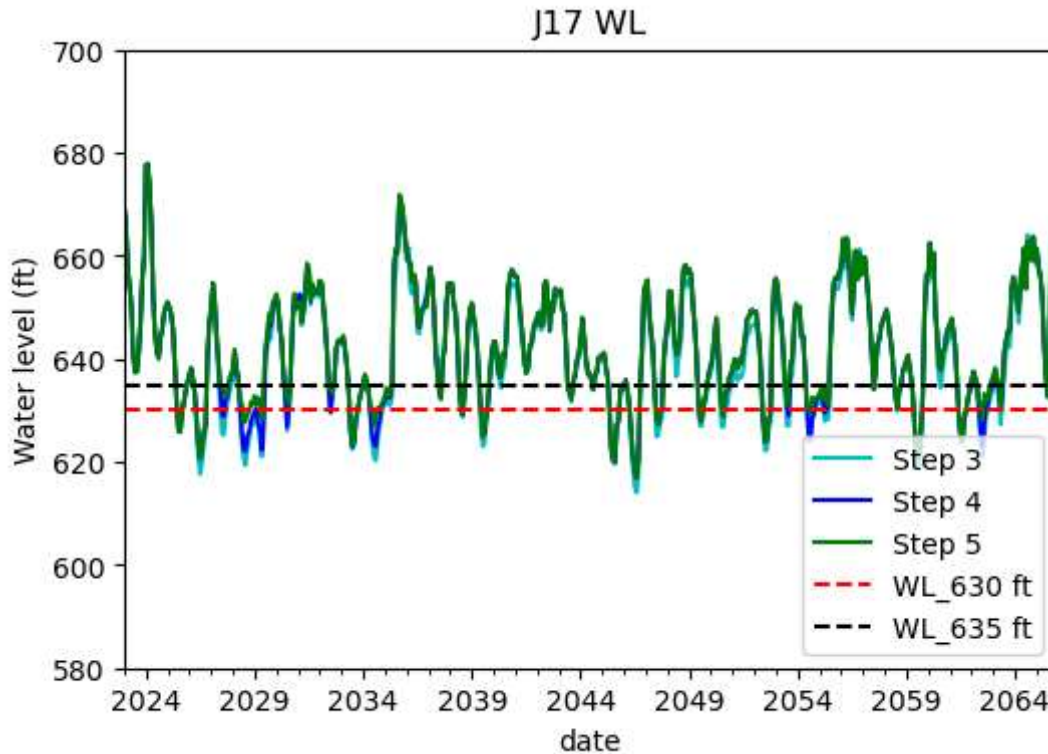
```

df1['WL_635'] = [635]*len(logStep4.index)

df1['WL_630'].plot(ax=ax,style='r--',label='WL_630 ft')
df1['WL_635'].plot(ax=ax,style='k--',label='WL_635 ft')
ax.set_ylim(580,700)
ax.set_ylabel('Water level (ft)')
ax.set_title('J17 WL')
ax.legend(loc='best')

```

Out[]: <matplotlib.legend.Legend at 0x1c75acc0cd0>

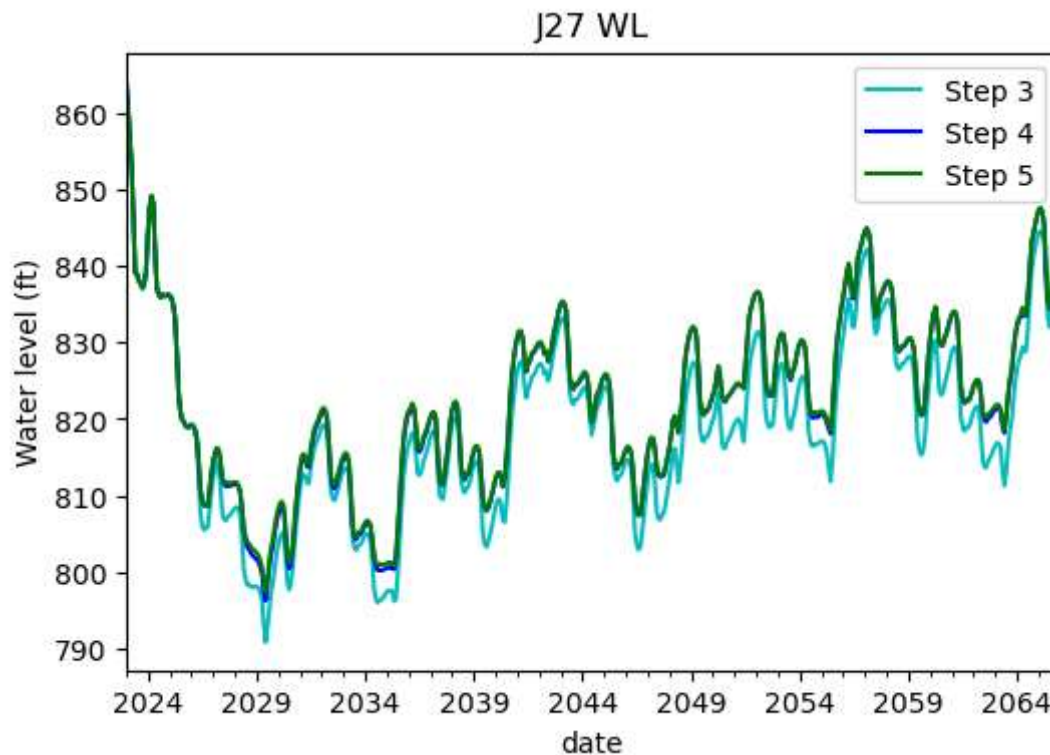


```

In [ ]: fig,ax =plt.subplots(figsize=(6,4))
logStep3['J27'].plot(ax=ax,style=['c-'],label='Step 3')
logStep4['J27'].plot(ax=ax,style=['b-'],label='Step 4')
logStep5['J27'].plot(ax=ax,style=['g-'],label='Step 5',markersize = 3)
#logStat6_Jim['J27'].plot(ax=ax,style=['g-'],label='Jim Archive')
df1 = pd.DataFrame({'date':logStep4.index,'WL_630':[630]*len(logStep4.index)})
df1 =df1.set_index('date')
#df1['WL_635'] = [635]*len(logStep4.index)
#df1['WL_630'].plot(ax=ax,style='r--',label='WL_630')
#df1['WL_635'].plot(ax=ax,style='k--',label='WL_635')
#ax.set_ylim(580,700)
ax.set_ylabel('Water level (ft)')
ax.set_title('J27 WL')
ax.legend(loc='best')

```

Out[]: <matplotlib.legend.Legend at 0x1c75ab22550>

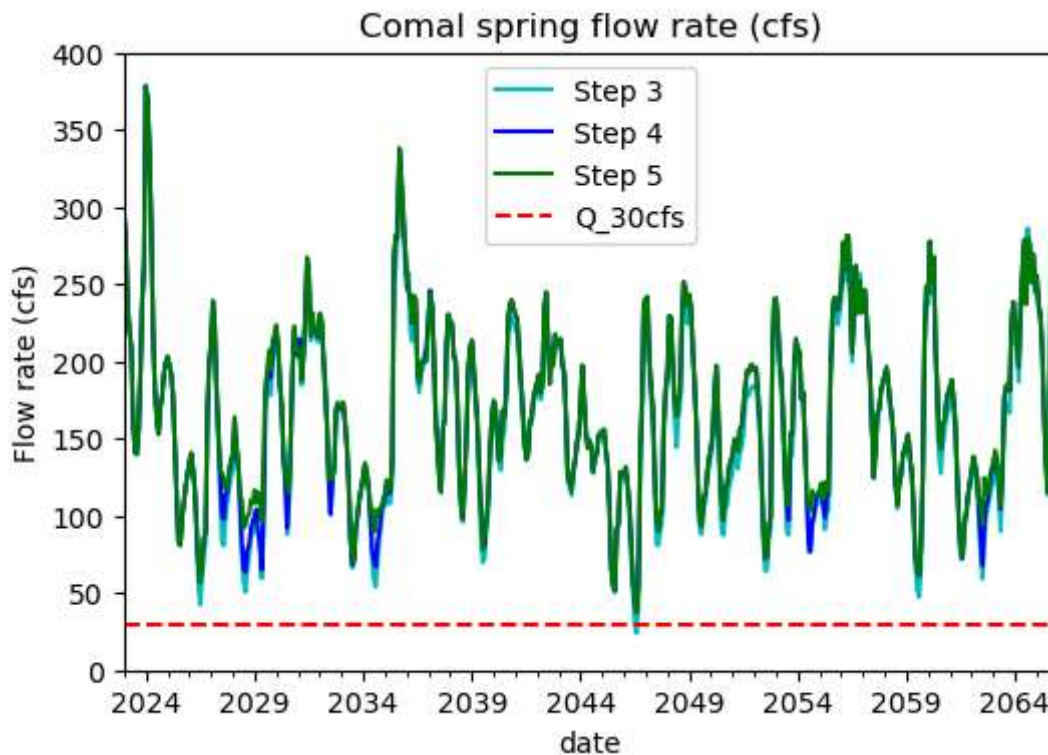


```
In [ ]: fig,ax =plt.subplots(figsize=(6,4))
logStep3['Comal'].plot(ax=ax,style=['c-'],label='Step 3')
logStep4['Comal'].plot(ax=ax,style=['b-'],label='Step 4')
logStep5['Comal'].plot(ax=ax,style=['g-'],label='Step 5',markersize=3)
#LogStat6_Jim['Comal'].plot(ax=ax,style=['g-'],label='Jim Archive')

df1 = pd.DataFrame({'date':logStep4.index,'Q_30cfs':[30]*len(logStep4.index)})
df1 =df1.set_index('date')
#df1['Q_30cfs'] = [30]*len(logStep4.index)

df1['Q_30cfs'].plot(ax=ax,style='r--',label='Q_30cfs')
ax.set_ylim(0,400)
ax.set_ylabel('Flow rate (cfs)')
ax.set_title('Comal spring flow rate (cfs)')
#df1['Q_30cfs'].plot(ax=ax,style='k--',label='WL_635')
ax.legend(loc='best')
```

```
Out[ ]: <matplotlib.legend.Legend at 0x1c7b5088590>
```



```
In [ ]: logStep5[logStep5['Comal']<30]
```

```
Out[ ]:      SP days Comal San Marcos J17 J27
```

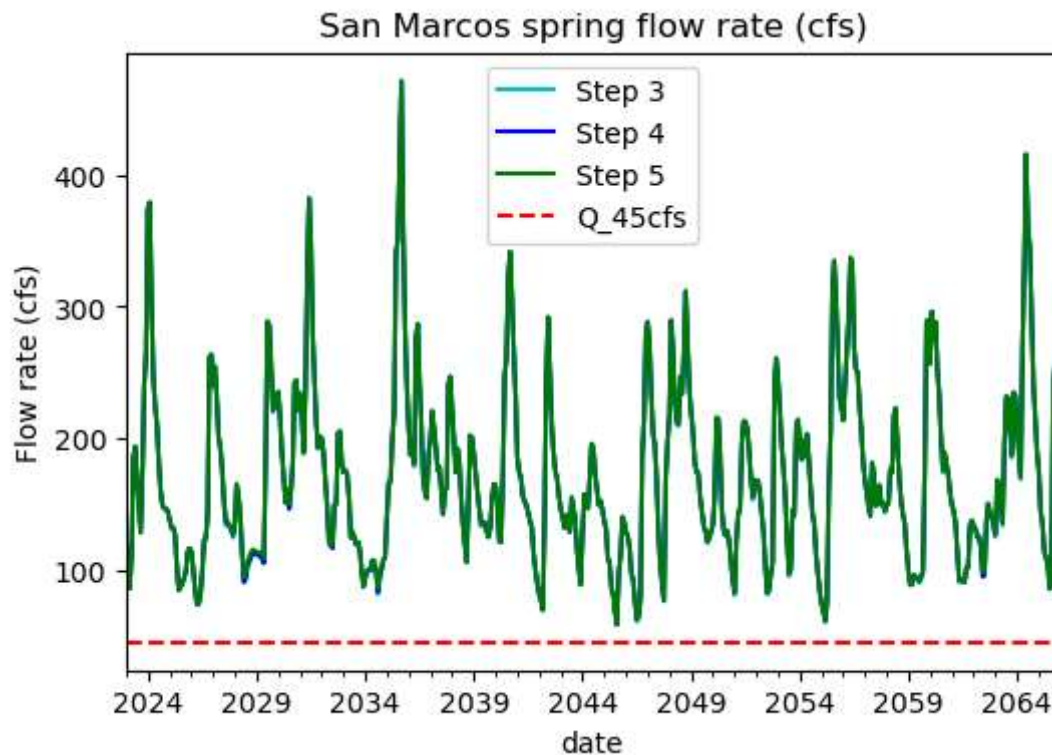
```
date
```

```
In [ ]: fig,ax =plt.subplots(figsize=(6,4))
logStep3['San Marcos'].plot(ax=ax,style=['c-'],label='Step 3')
logStep4['San Marcos'].plot(ax=ax,style=['b-'],label='Step 4')
logStep5['San Marcos'].plot(ax=ax,style=['g-'],label='Step 5',markersize=3)
#LogStat6_Jim['San Marcos'].plot(ax=ax,style=['g-'],label='Jim Archive')

df1 = pd.DataFrame({'date':logStep4.index,'Q_45cfs':[45]*len(logStep4.index)})
df1 =df1.set_index('date')
#df1['Q_30cfs'] = [30]*len(logStep4.index)

df1['Q_45cfs'].plot(ax=ax,style='r--',label='Q_45cfs')
#ax.set_ylim(0,600)
ax.set_ylabel('Flow rate (cfs)')
ax.set_title('San Marcos spring flow rate (cfs)')
#df1['Q_30cfs'].plot(ax=ax,style='k--',label='WL_635')
ax.legend(loc='best')
```

```
Out[ ]: <matplotlib.legend.Legend at 0x1c7b49b5090>
```



```
In [ ]: logStep5.loc[logStep5['San Marcos']<45,'San Marcos']
```

```
Out[ ]: Series([], Name: San Marcos, dtype: float64)
```

```
In [ ]: ## Output the WL of J17 and J27 and Q of two springs to a folder of outputWLQ
```

```
outputLogStep5 = logStep5.loc[:,['Comal', 'San Marcos', 'J17', 'J27']]
outputLogStep5.columns = ['Comal (cfs)', 'San Marcos (cfs)', 'J17 (ft)', 'J27 (ft)']
outputPath = os.path.join(os.getcwd(), 'outputWLQ')
if not os.path.exists(outputPath):
    os.makedirs(outputPath)
outputLogStep5.to_csv(os.path.join(outputPath, scenario+'_Step5_results.csv'))
```

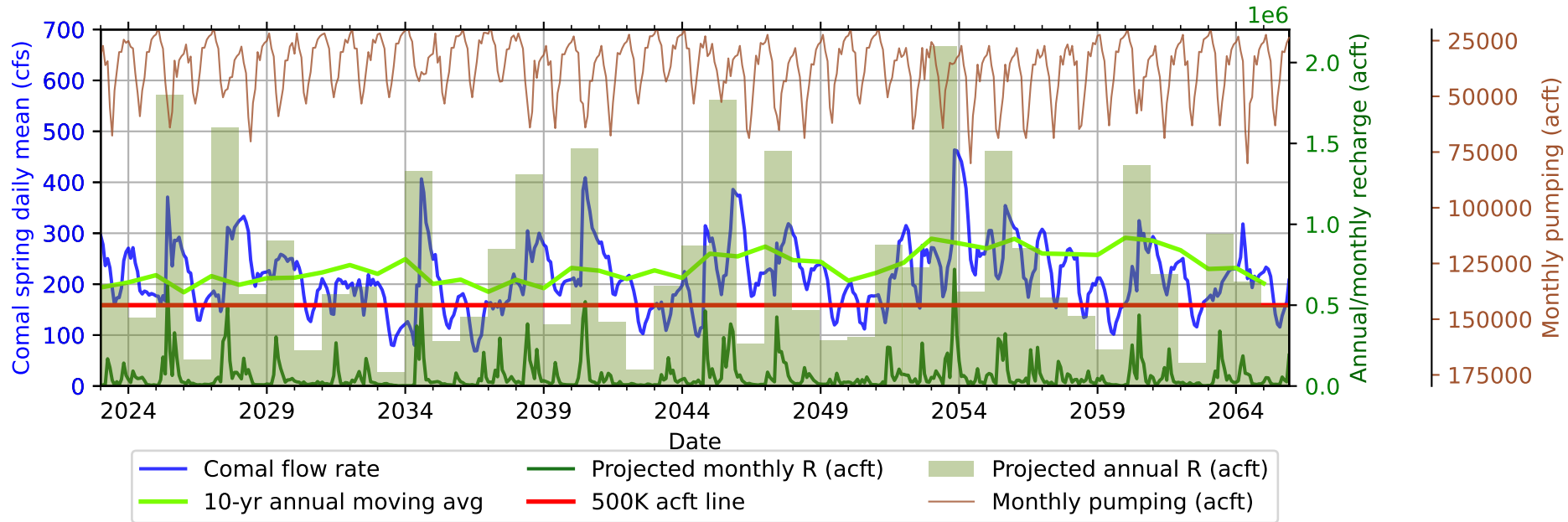
```
In [ ]:
```

The end

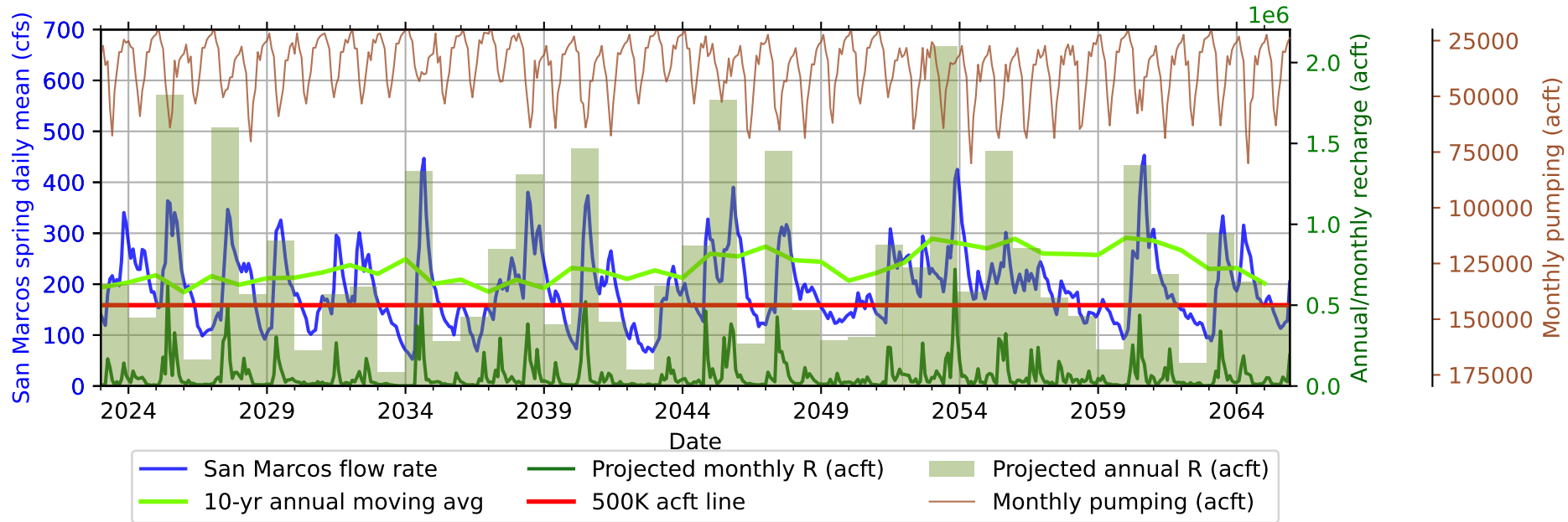
```
In [ ]:
```

Appendix B
Summary of Individual Model Results

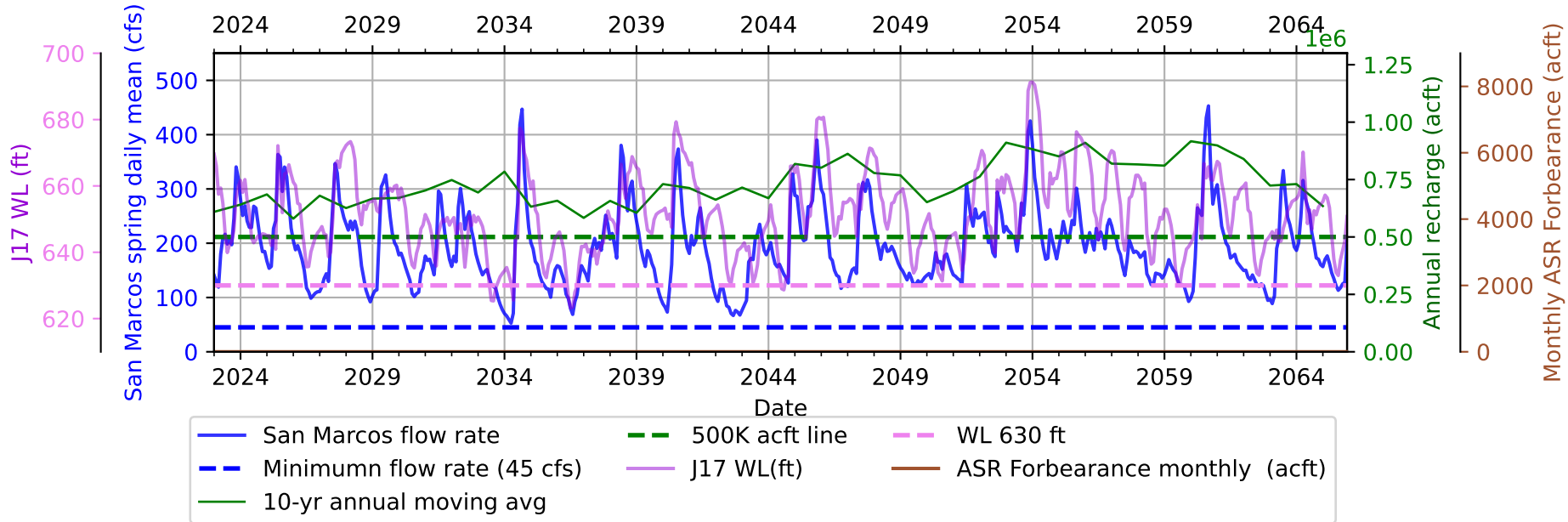
CMCC-CM_rcp45



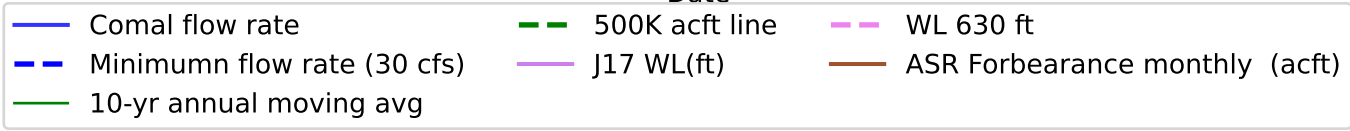
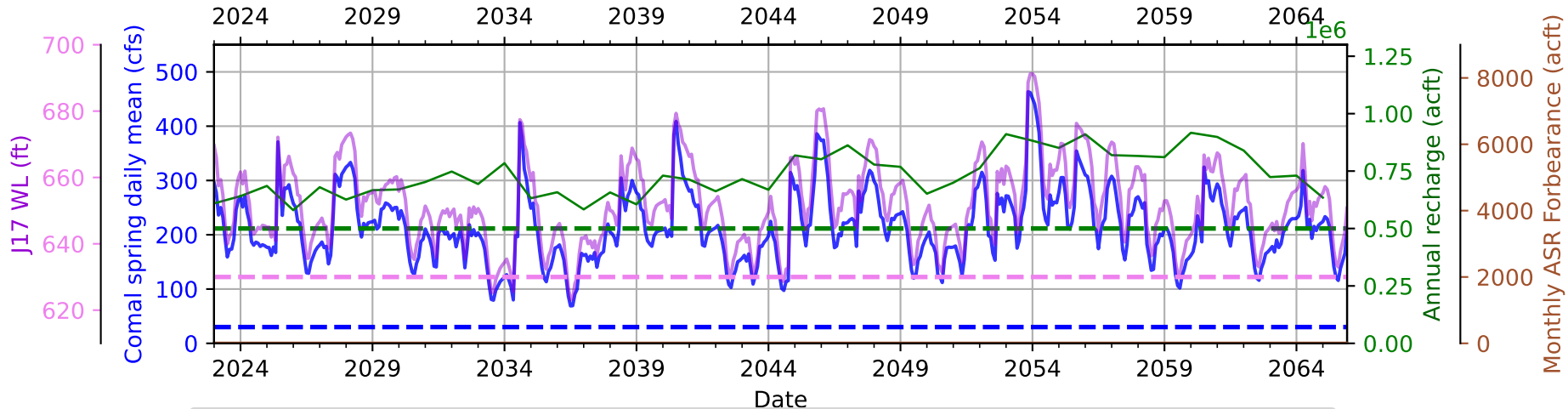
CMCC-CM_rcp45



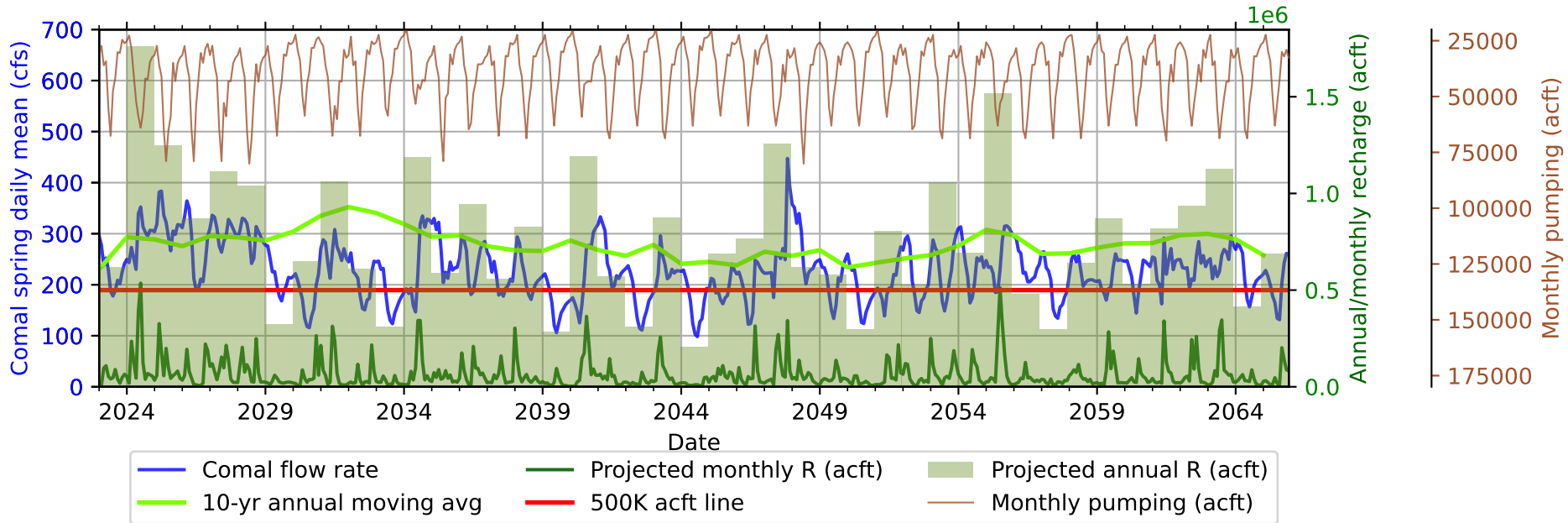
CMCC-CM_rcp45



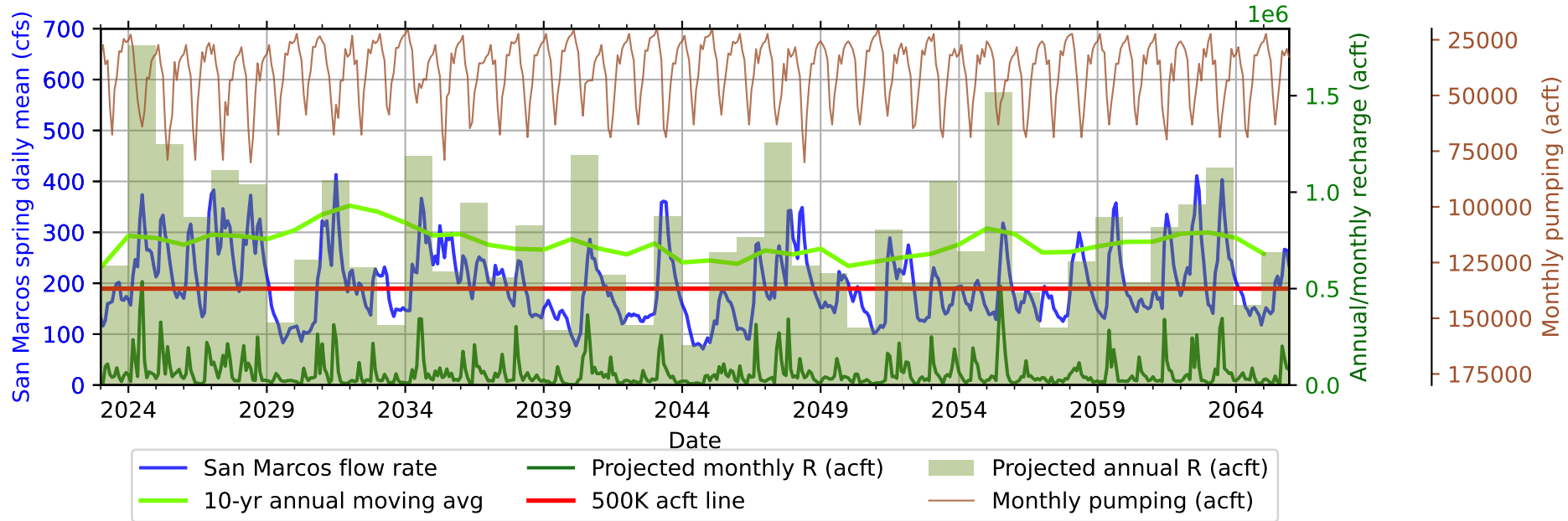
CMCC-CM_rcp45



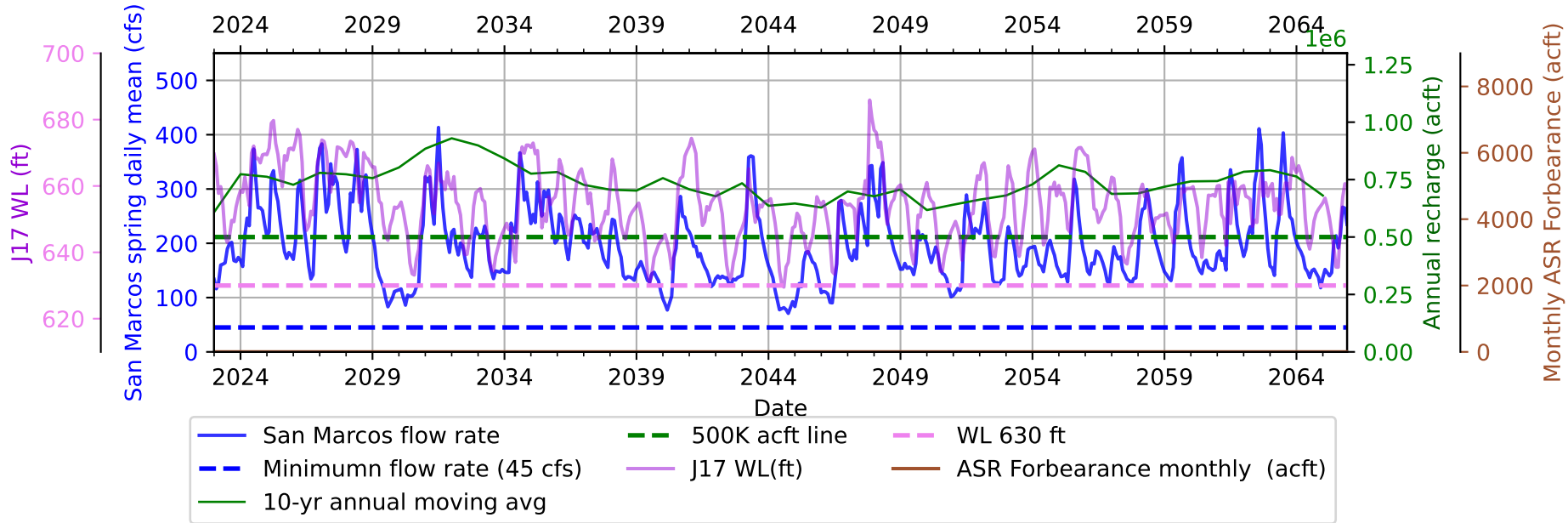
CMCC-CM_rcp85



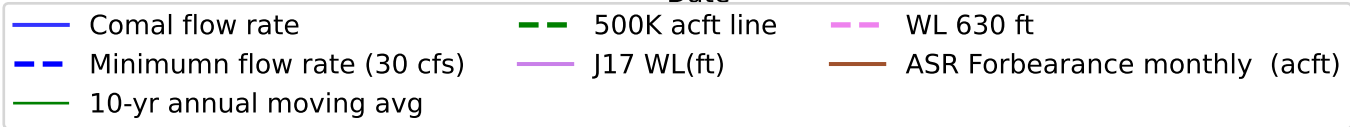
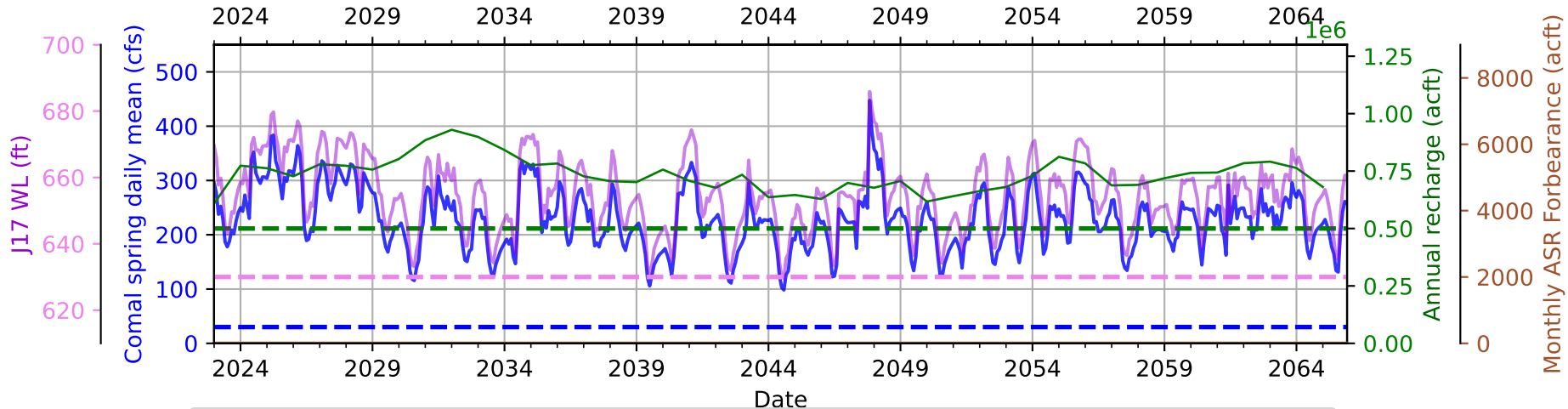
CMCC-CM_rcp85



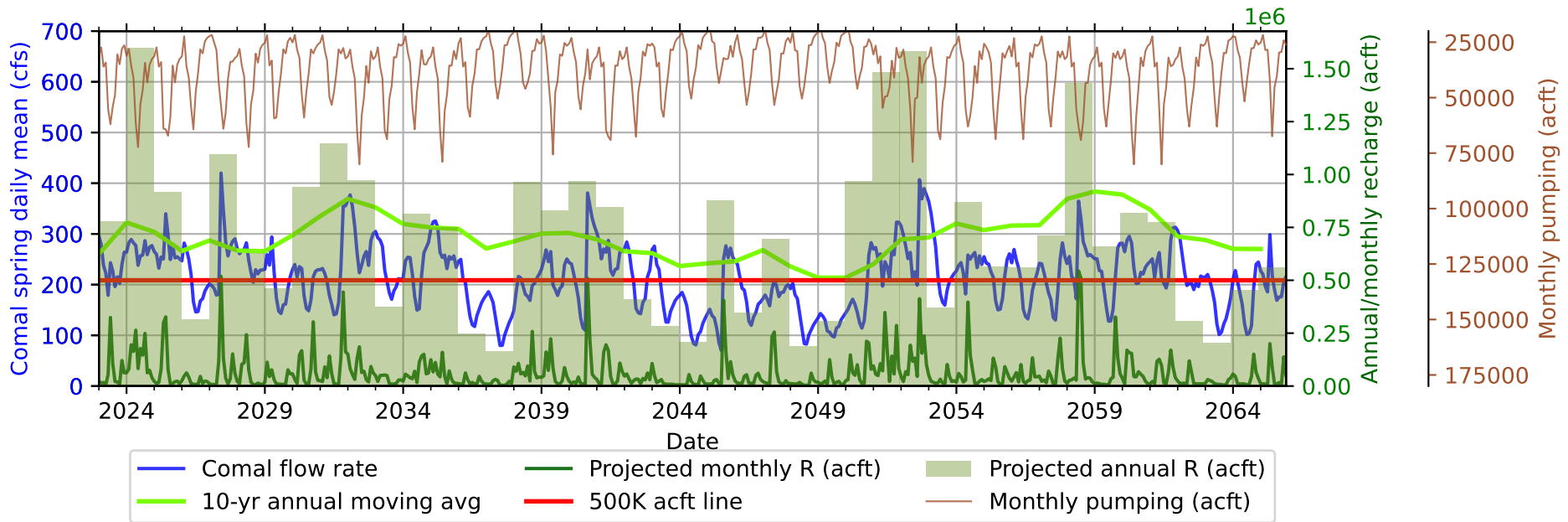
CMCC-CM_rcp85



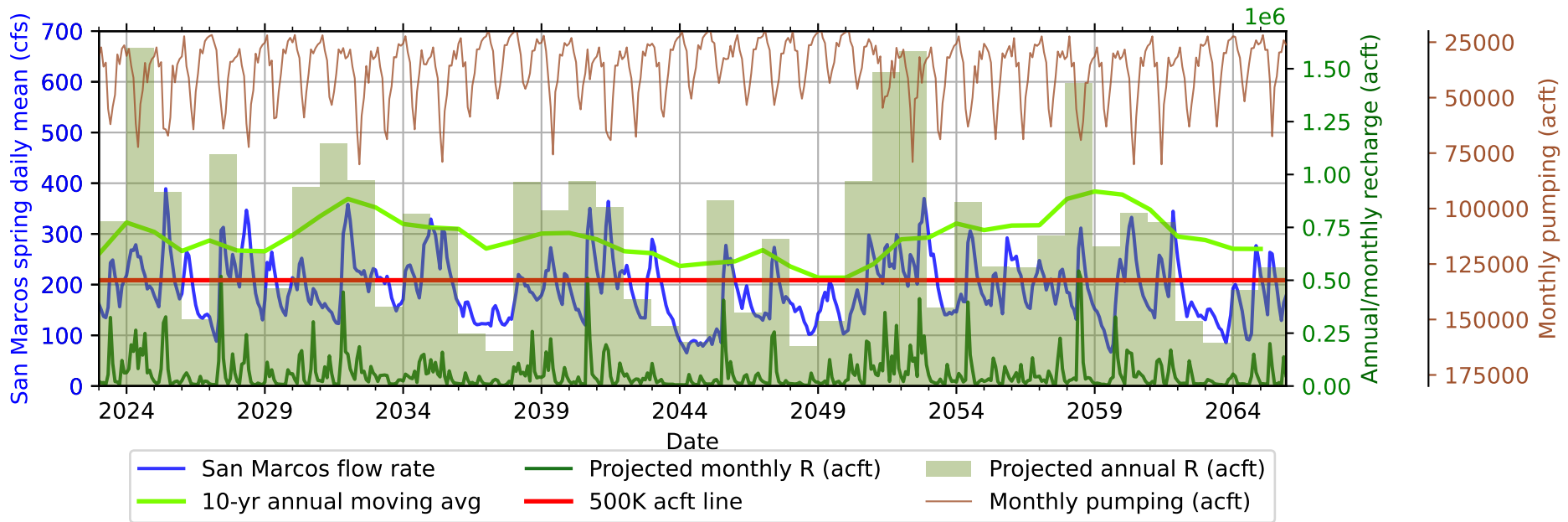
CMCC-CM_rcp85



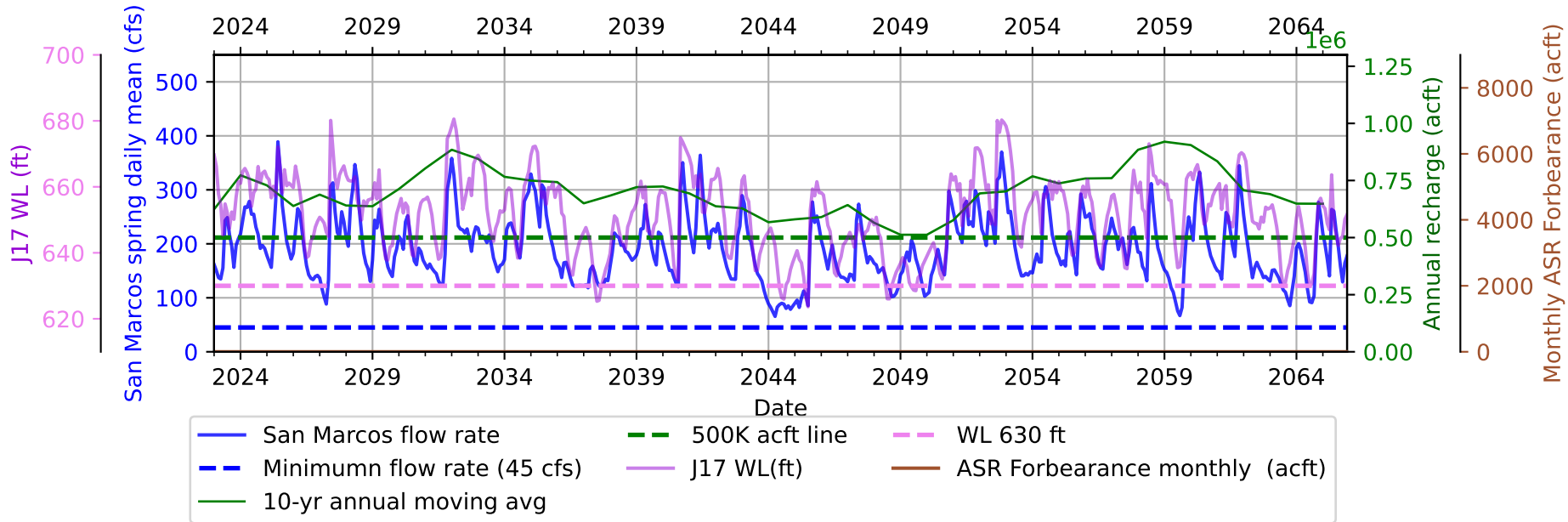
EC-Earth3_ssp245



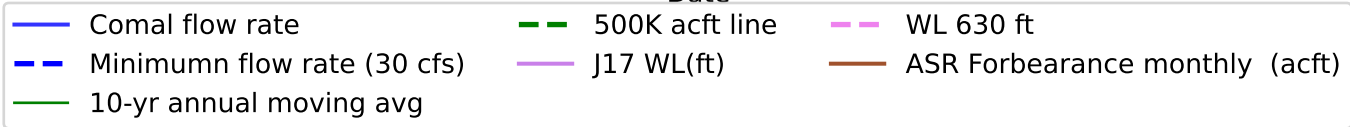
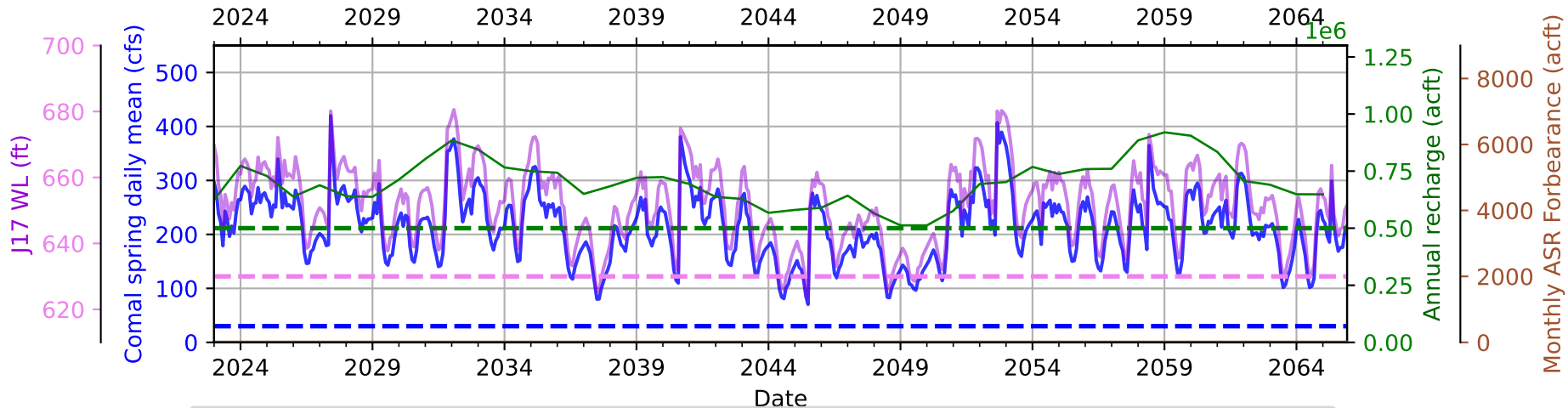
EC-Earth3_ssp245



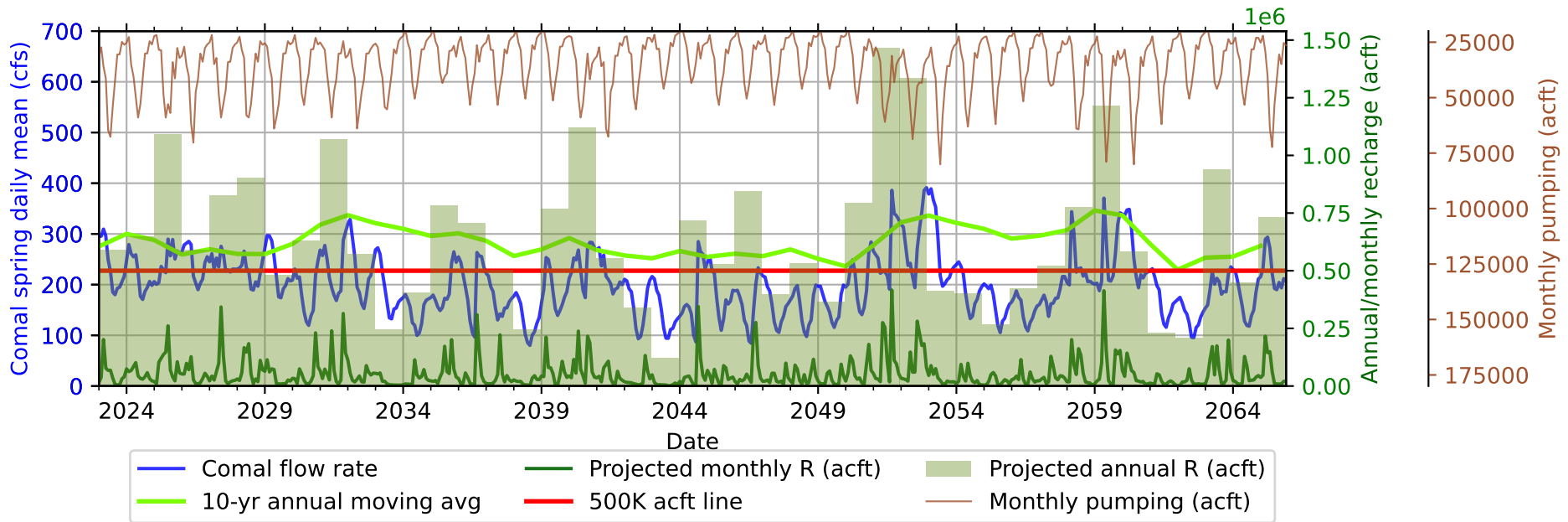
EC-Earth3_ssp245



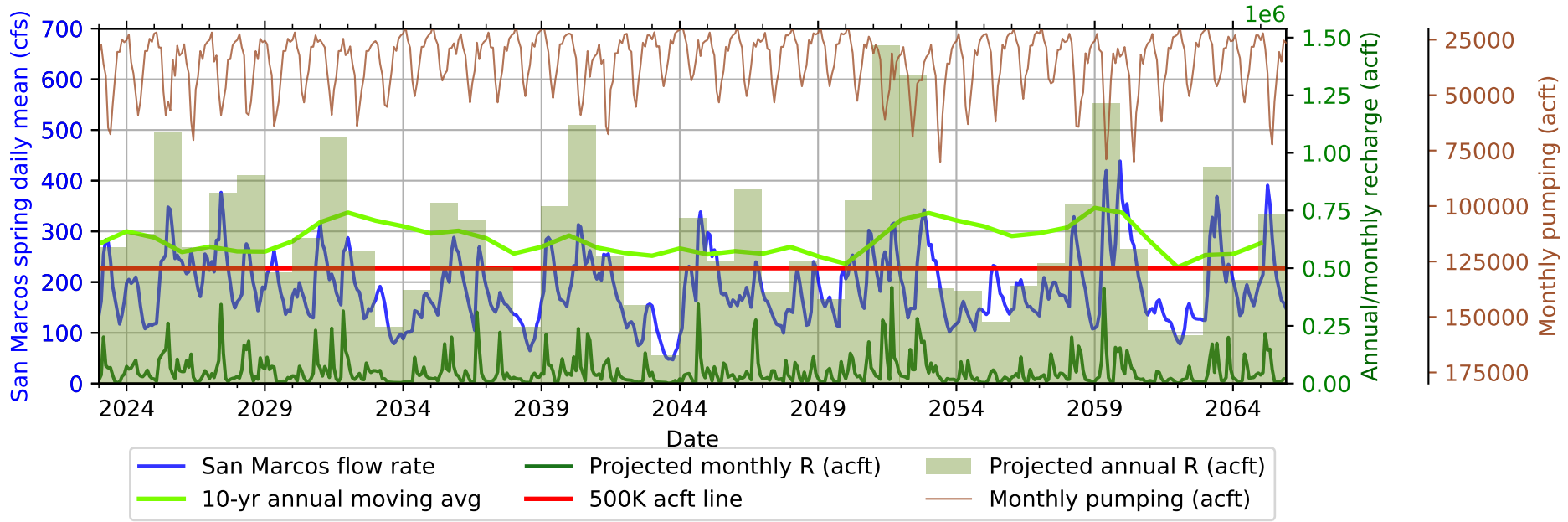
EC-Earth3_ssp245



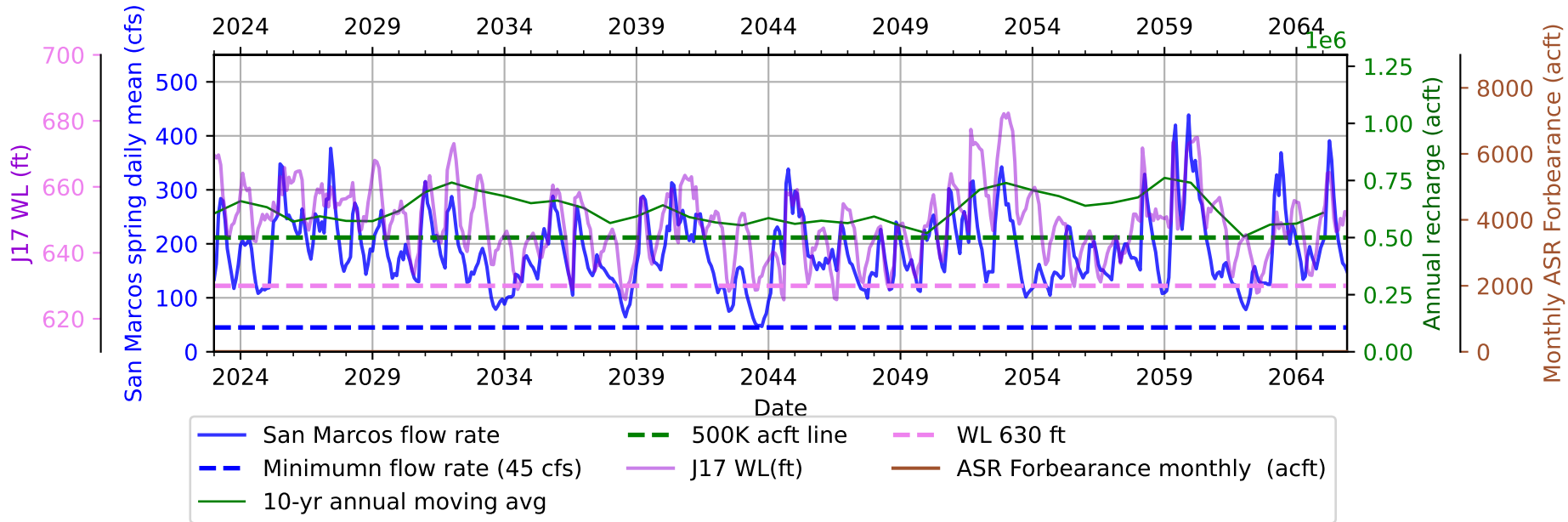
EC-Earth3_ssp585



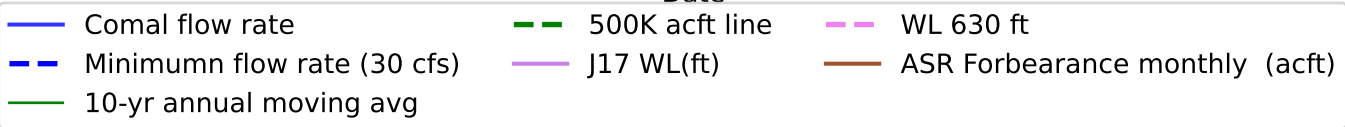
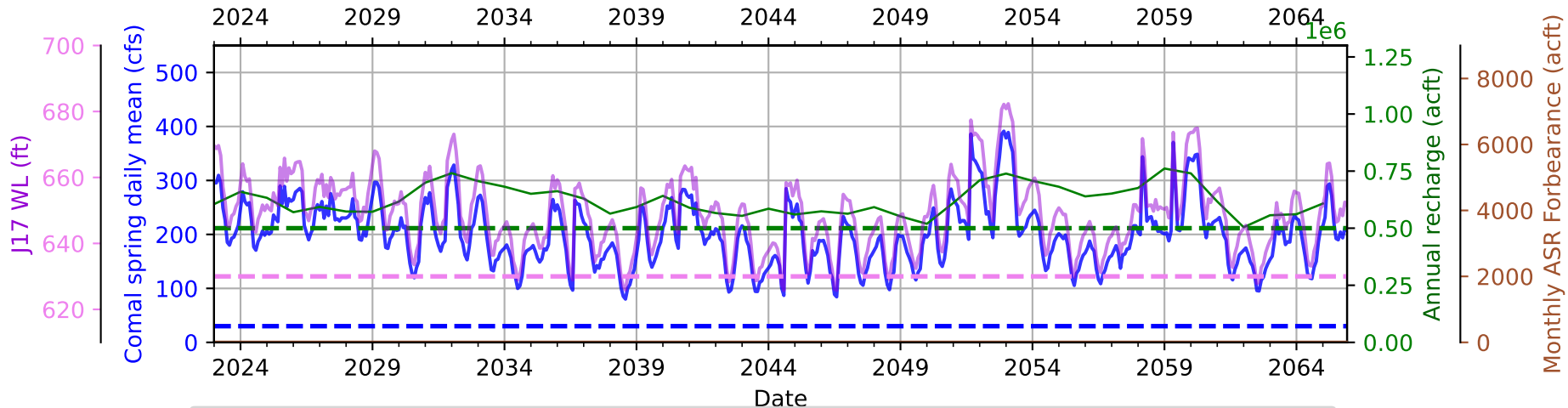
EC-Earth3_ssp585



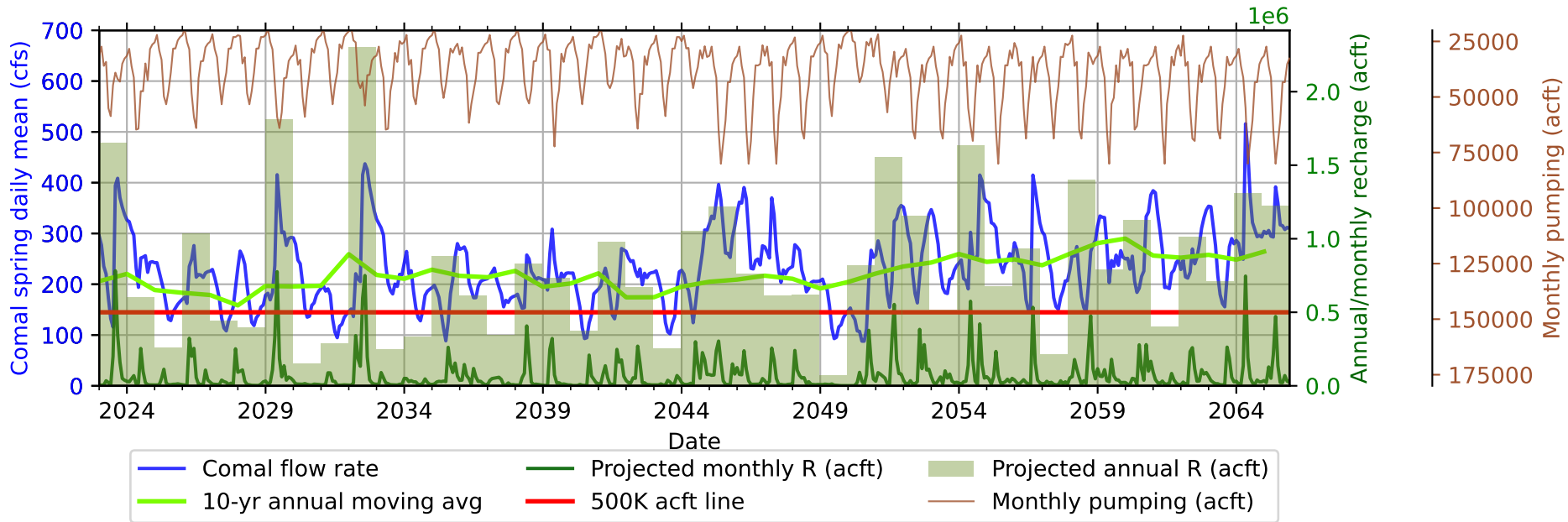
EC-Earth3_ssp585



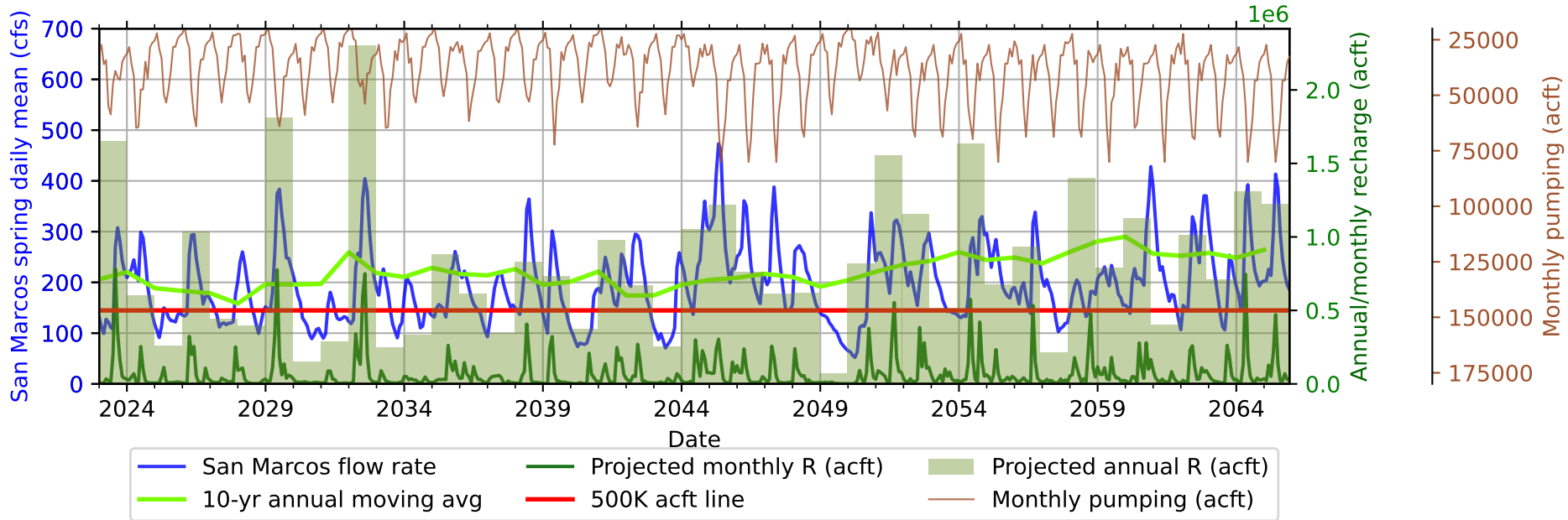
EC-Earth3_ssp585



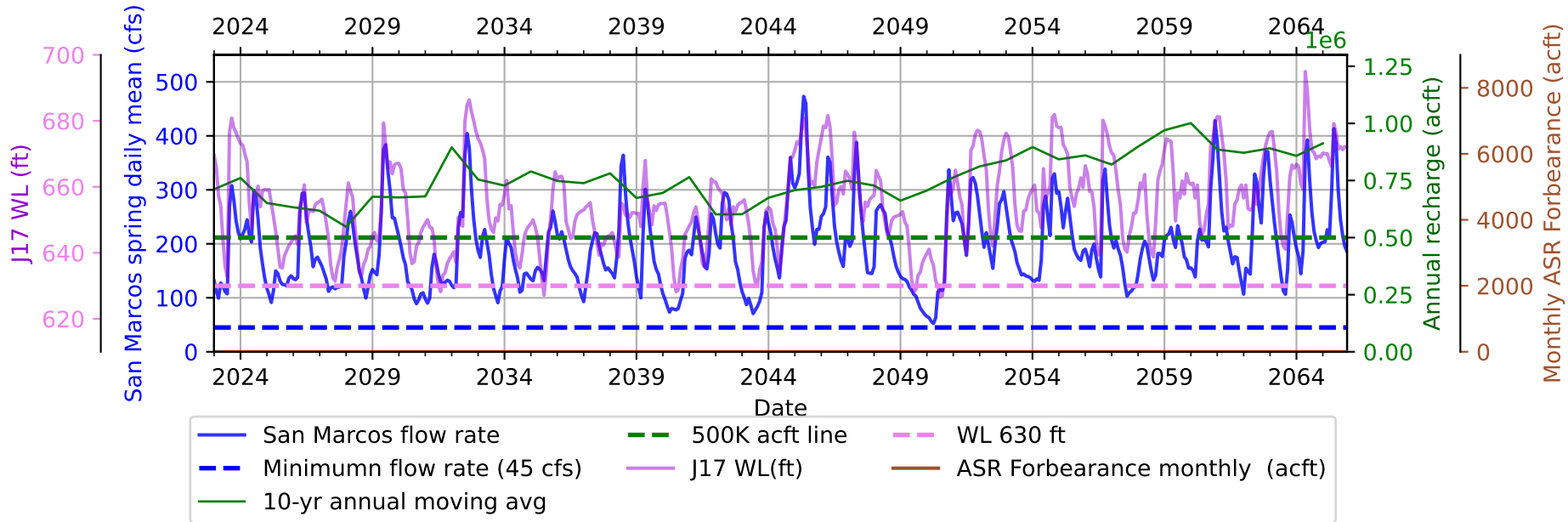
HadGEM2-CC_rcp45



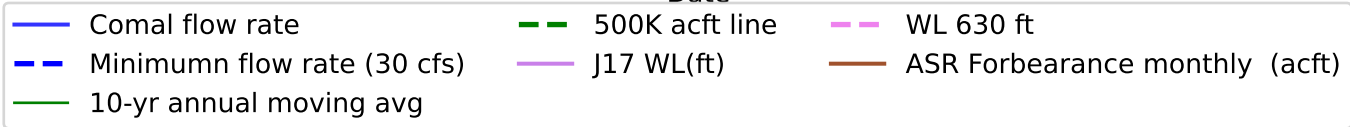
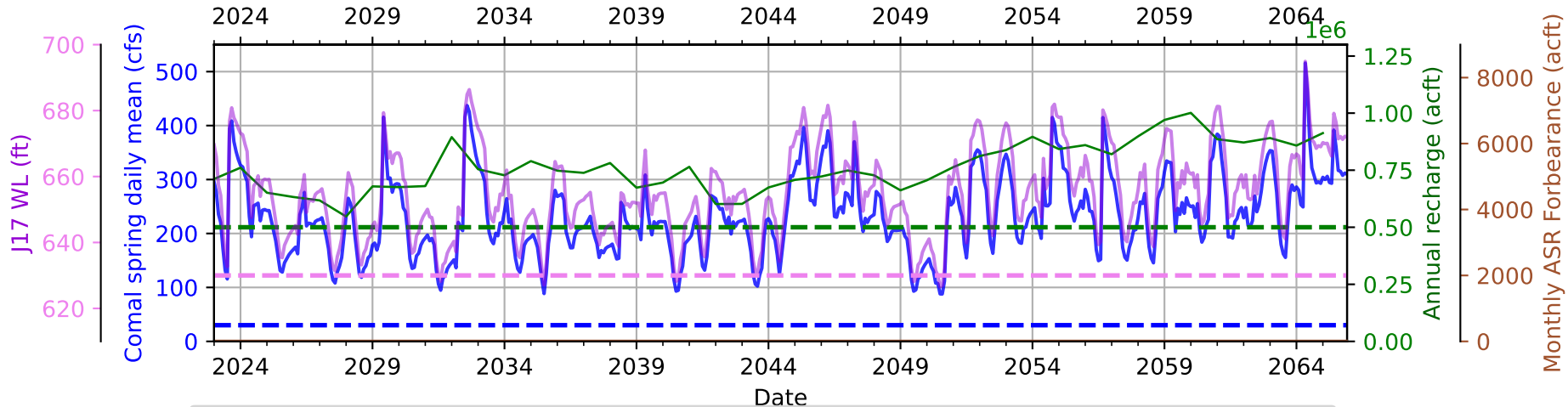
HadGEM2-CC_rcp45



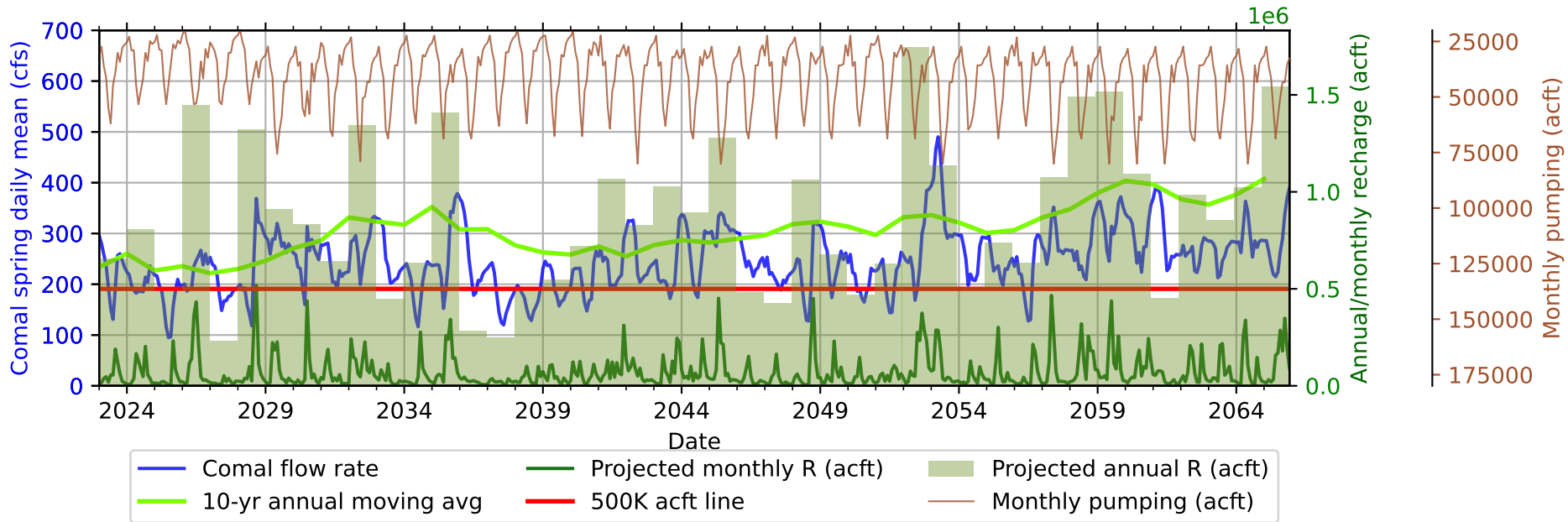
HadGEM2-CC_rcp45



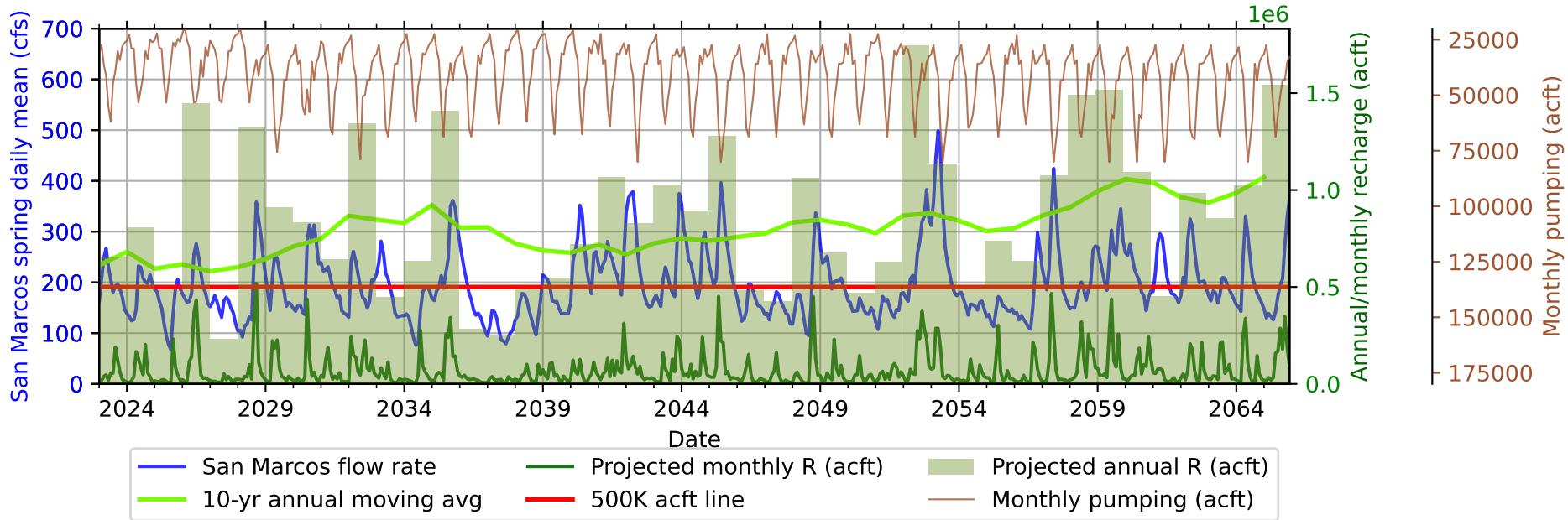
HadGEM2-CC_rcp45



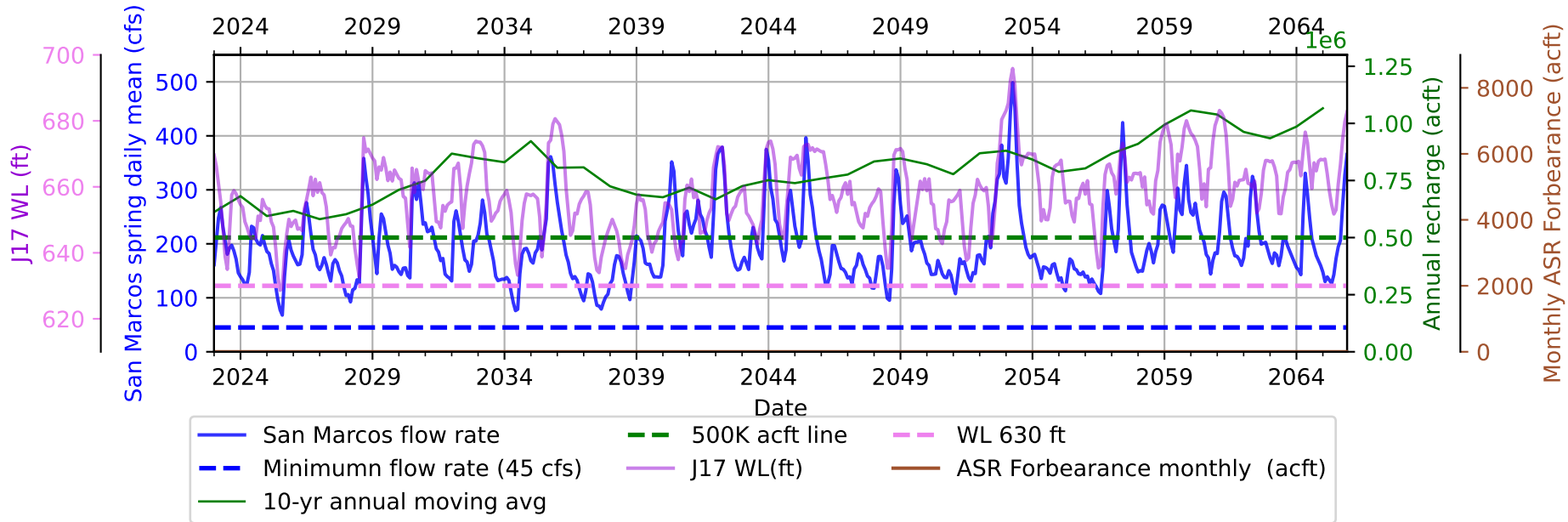
HadGEM2-CC_rcp85



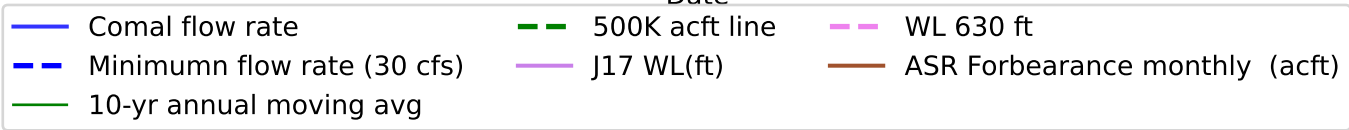
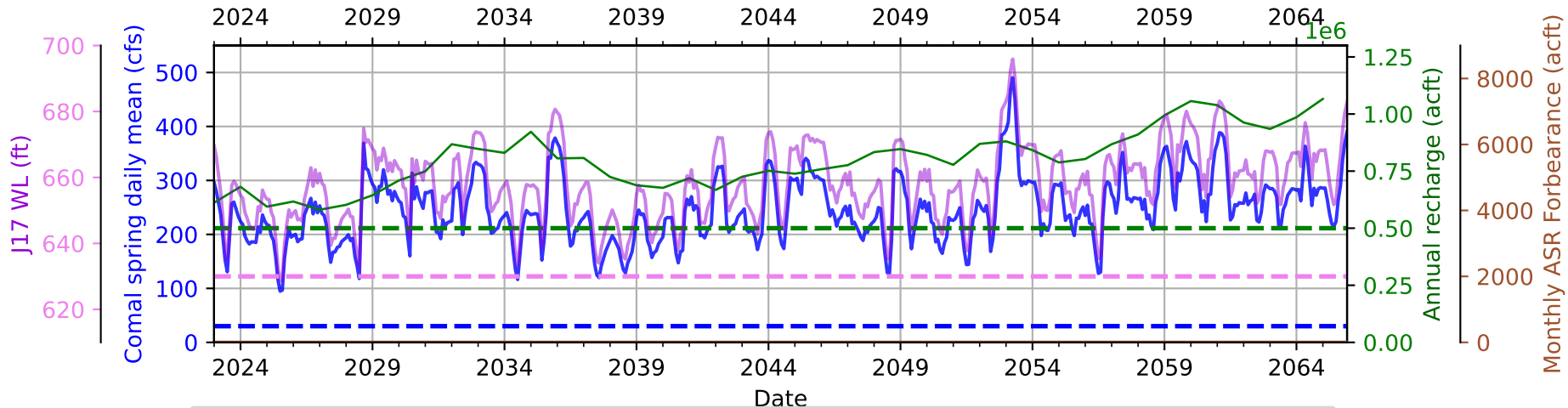
HadGEM2-CC_rcp85



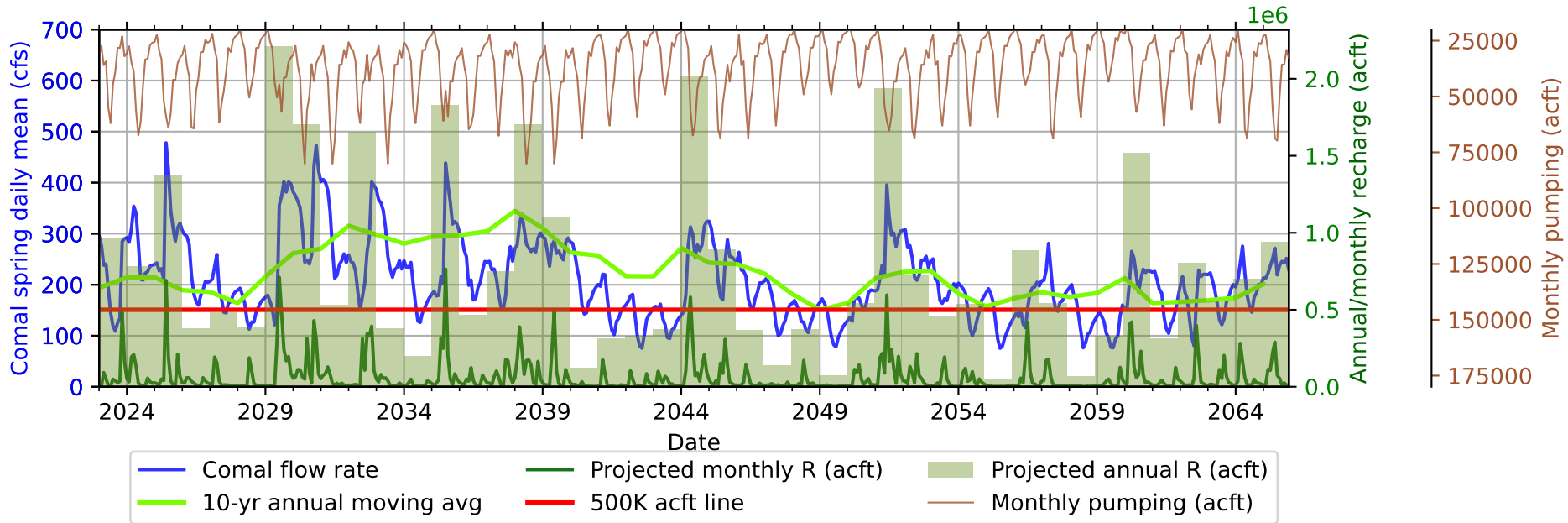
HadGEM2-CC_rcp85



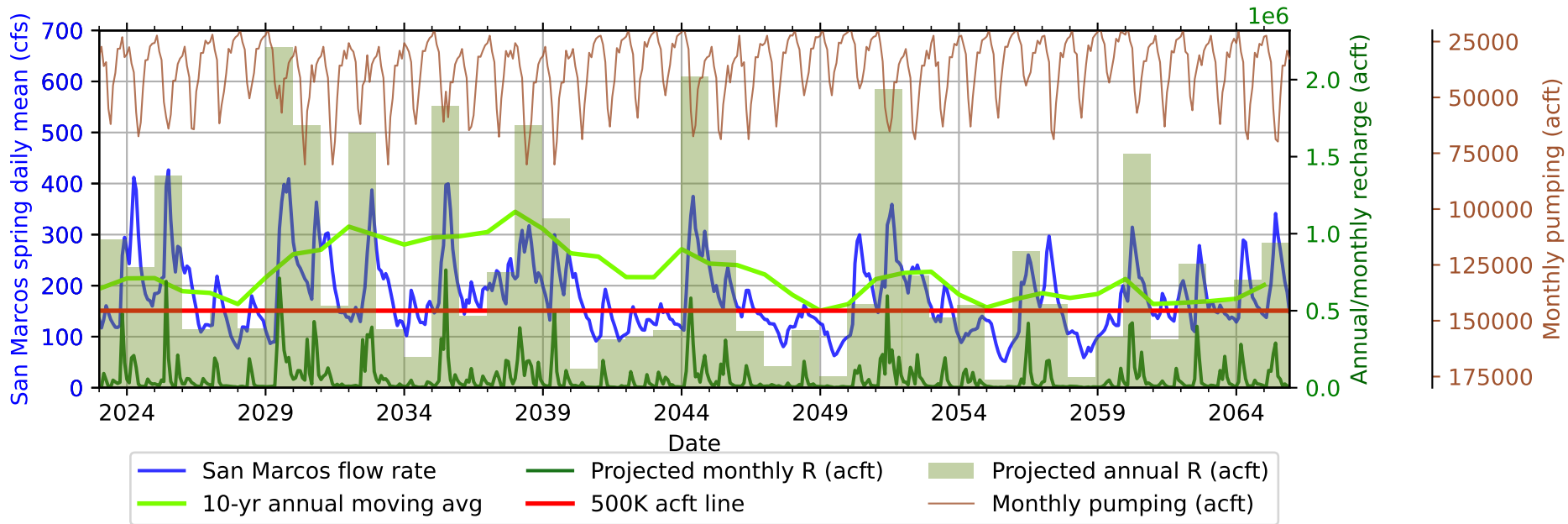
HadGEM2-CC_rcp85



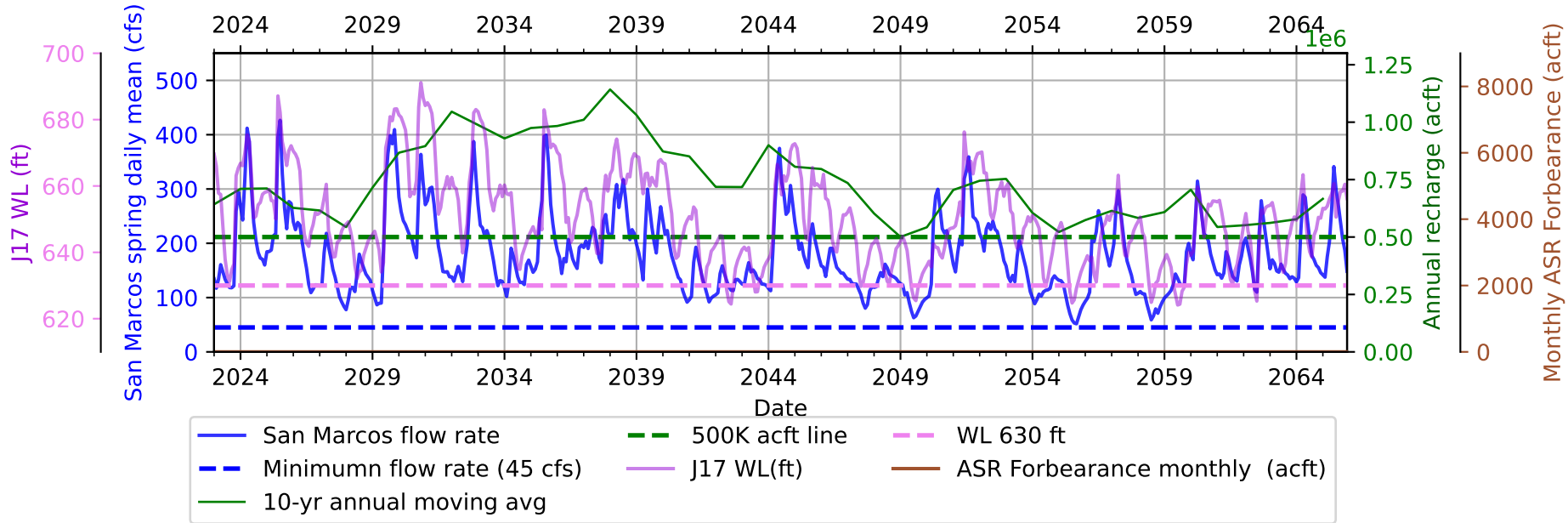
INM-CM4-8_ssp245



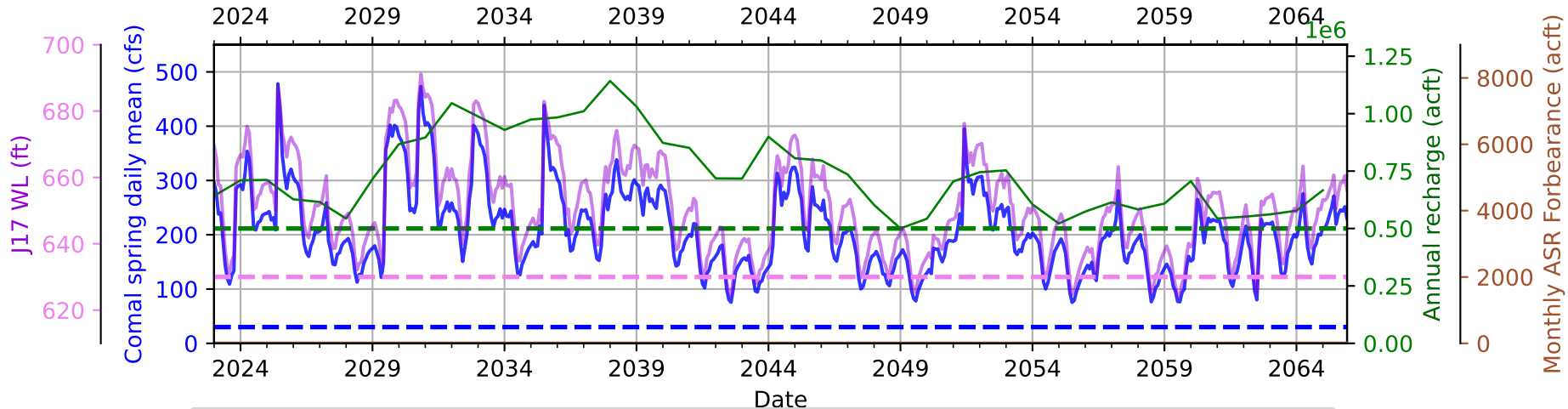
INM-CM4-8_ssp245



INM-CM4-8_ssp245

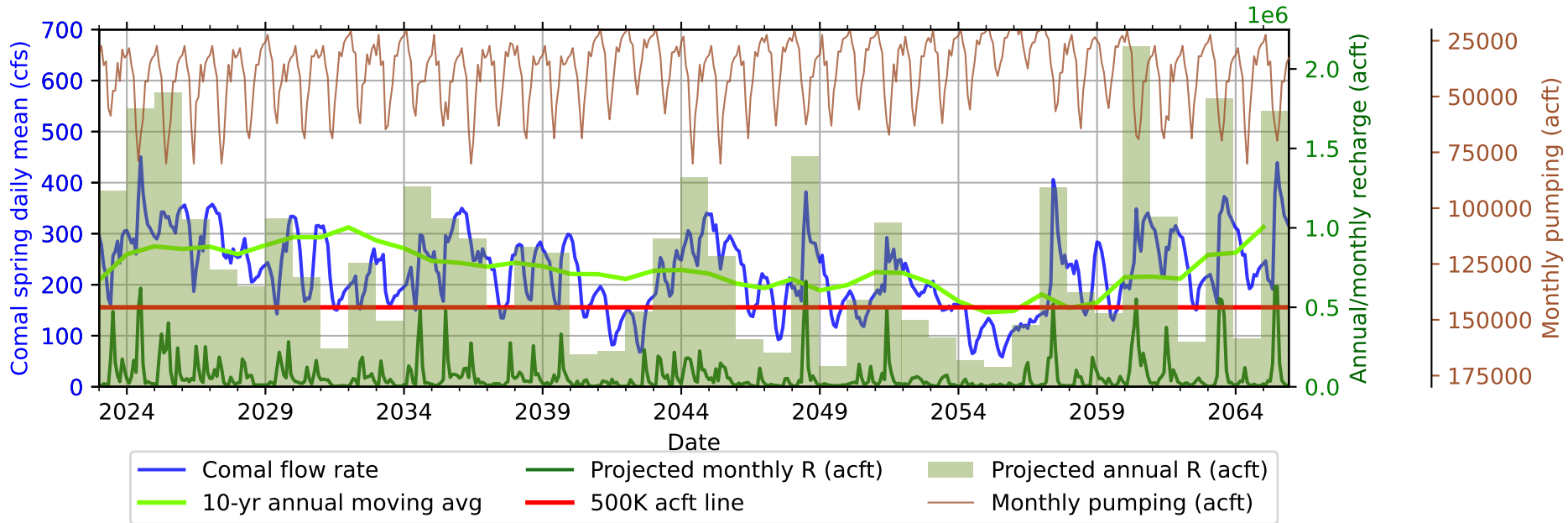


INM-CM4-8_ssp245

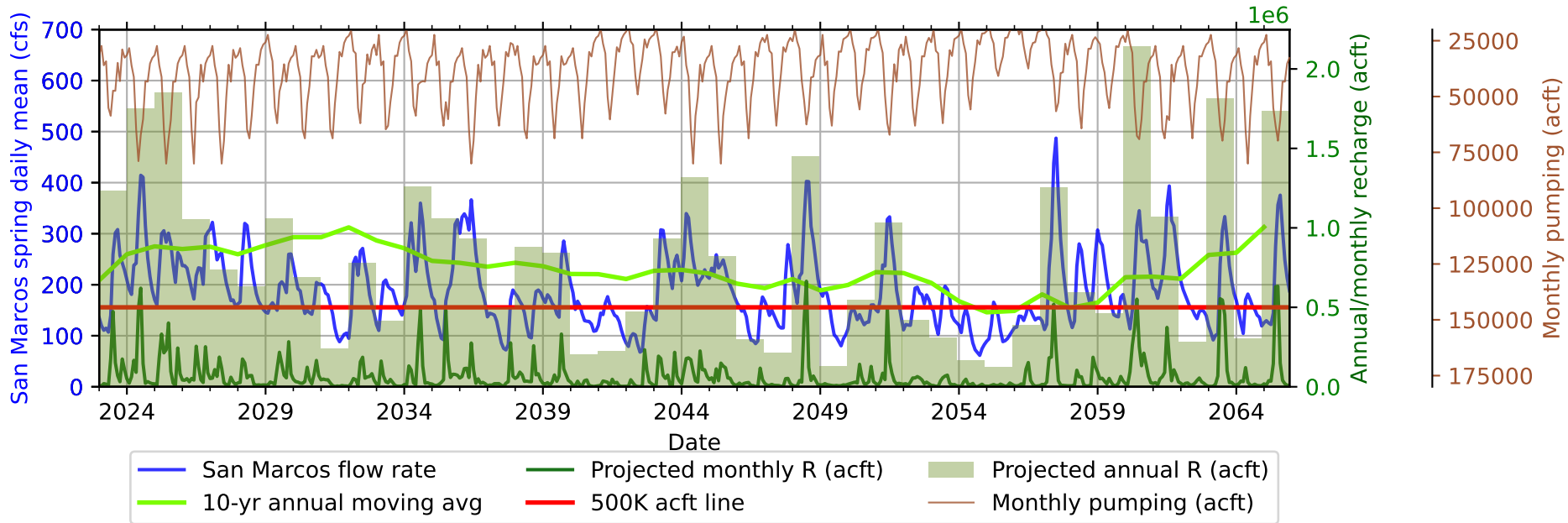


- Comal flow rate
- - - Minimumn flow rate (30 cfs)
- 10-yr annual moving avg
- - - 500K acft line
- J17 WL(ft)
- - - WL 630 ft
- ASR Forbearance monthly (acft)

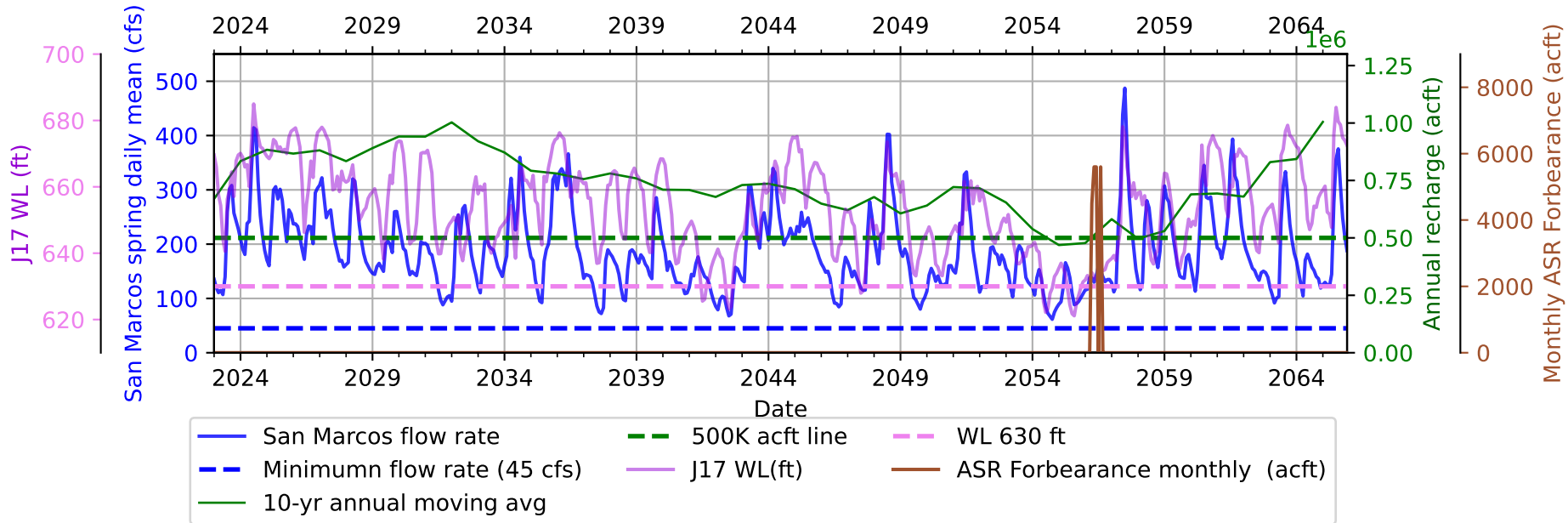
INM-CM4-8_ssp585



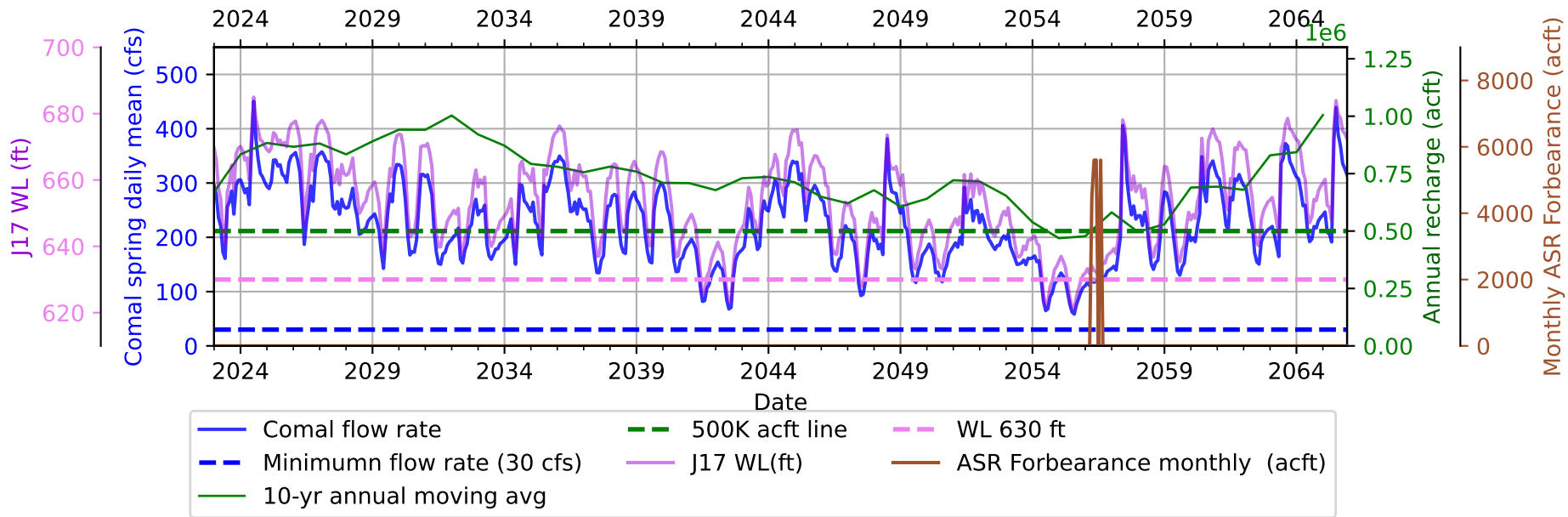
INM-CM4-8_ssp585



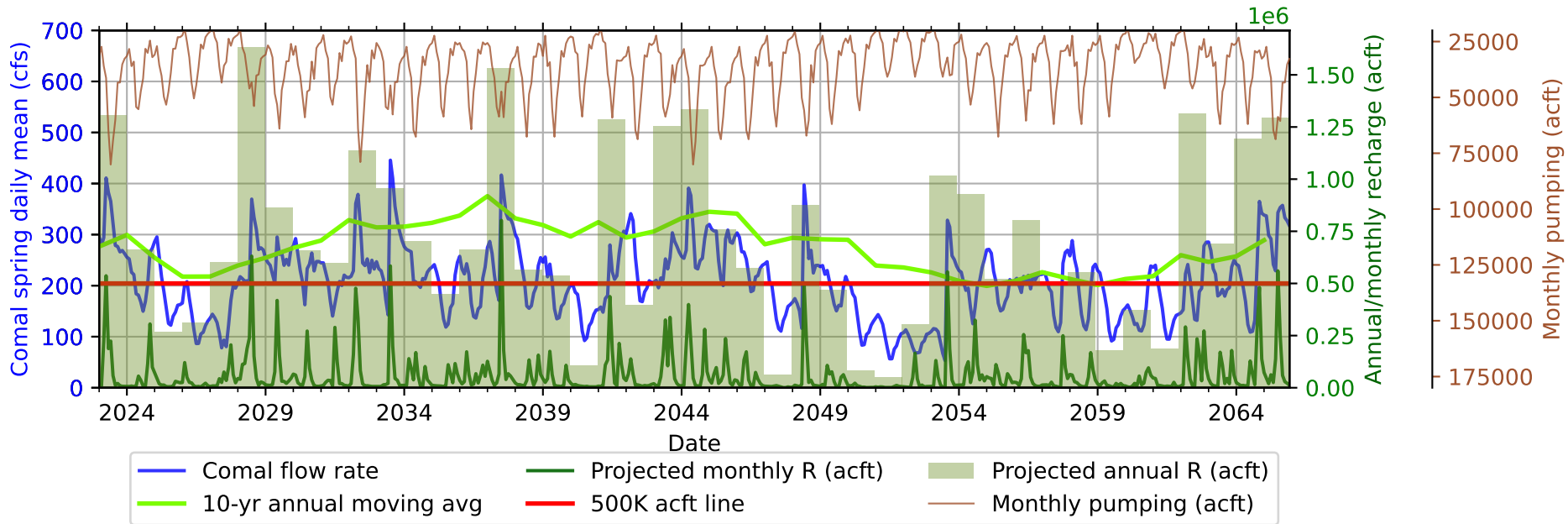
INM-CM4-8_ssp585



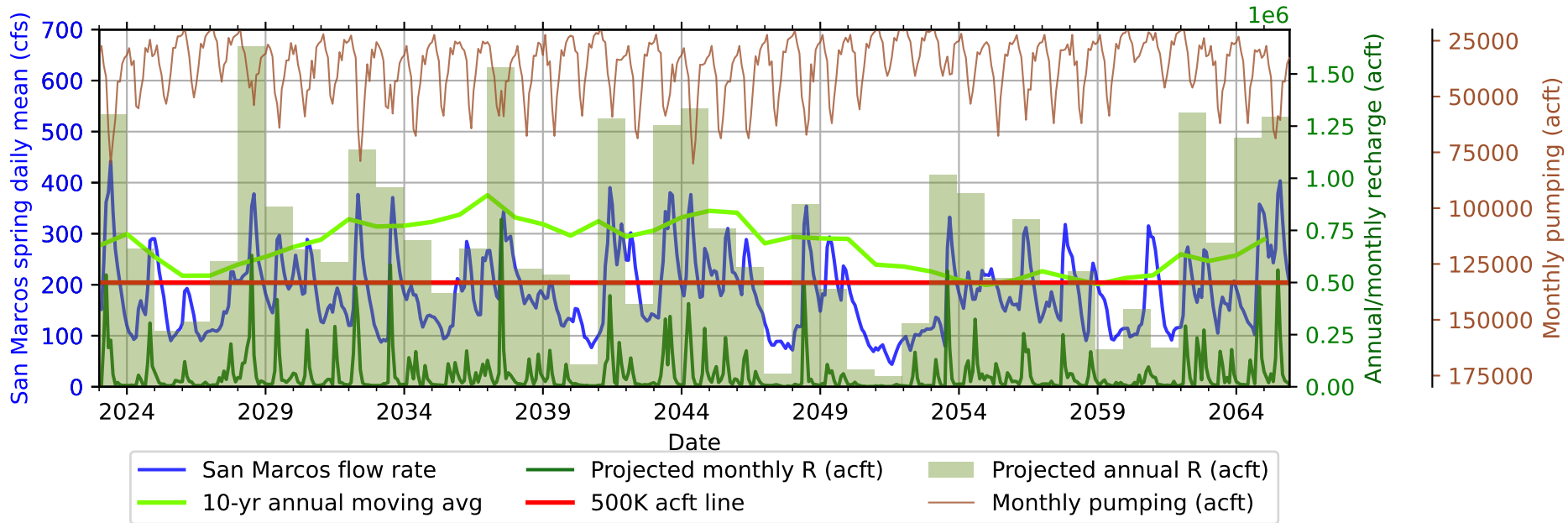
INM-CM4-8_ssp585



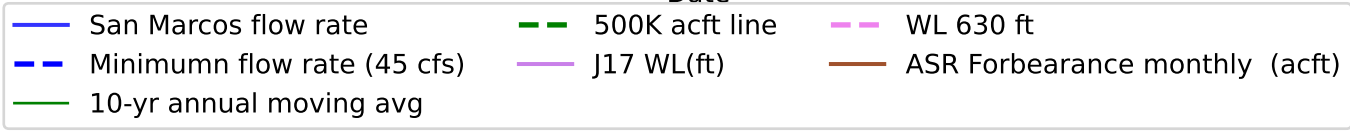
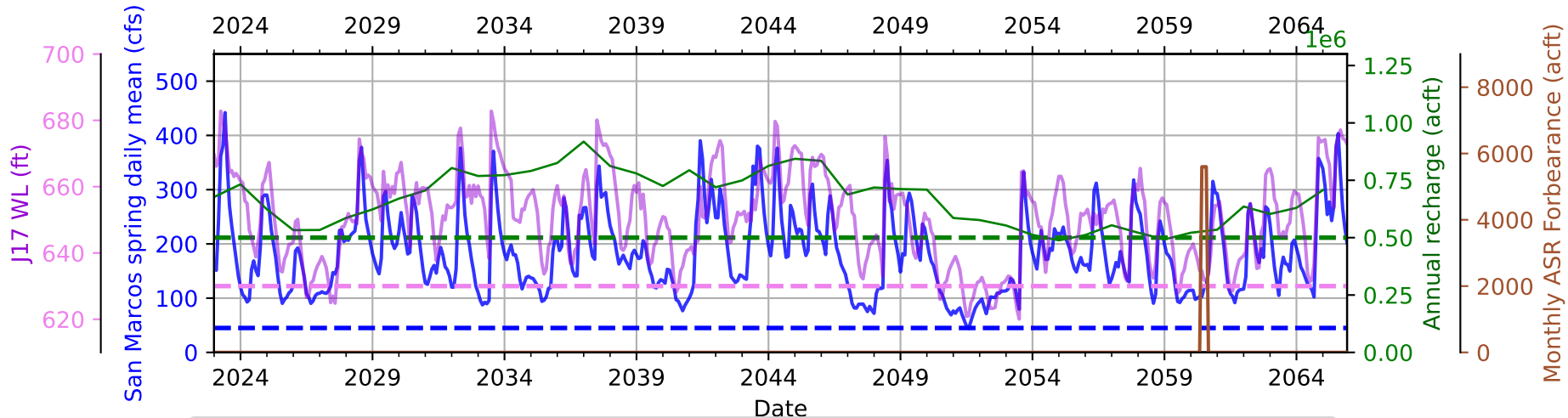
INM-CM5-0_ssp245



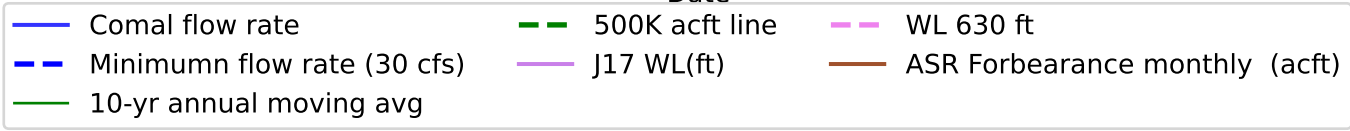
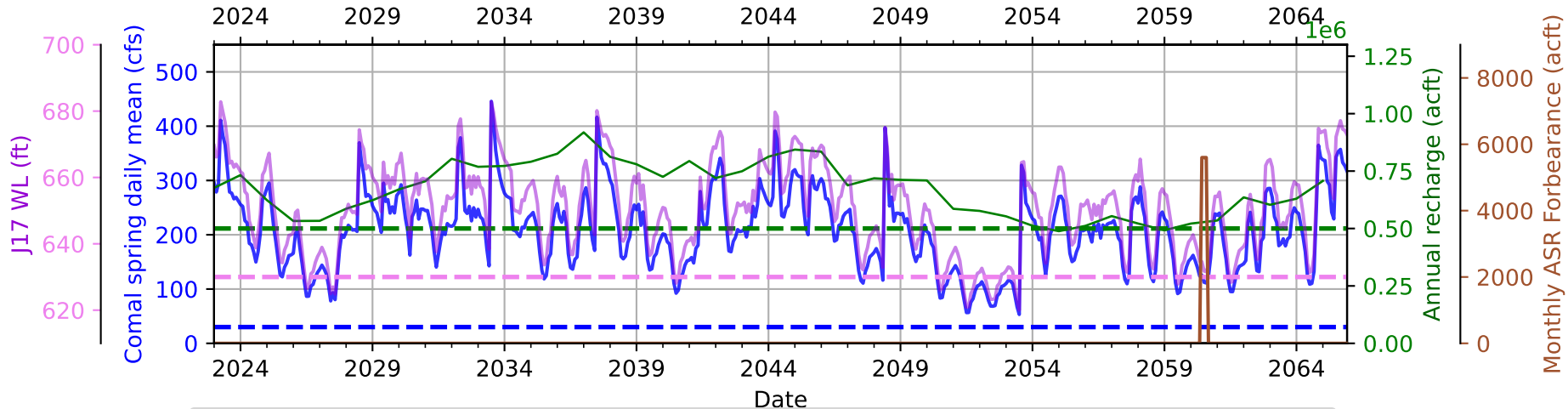
INM-CM5-0_ssp245



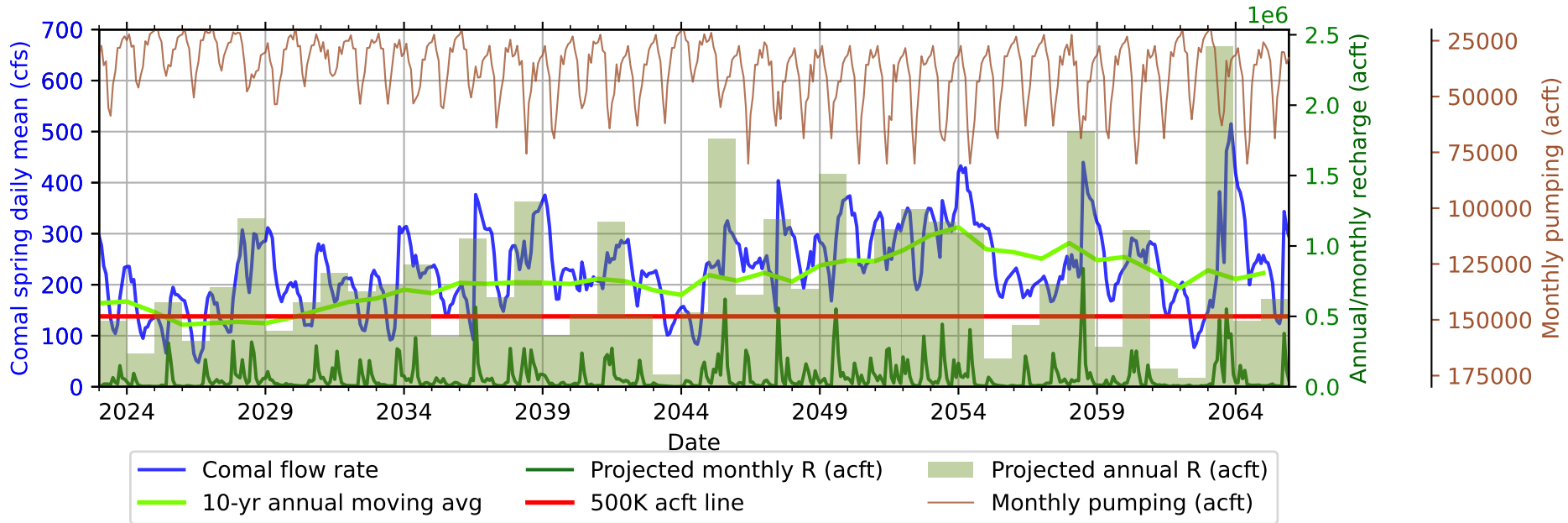
INM-CM5-0_ssp245



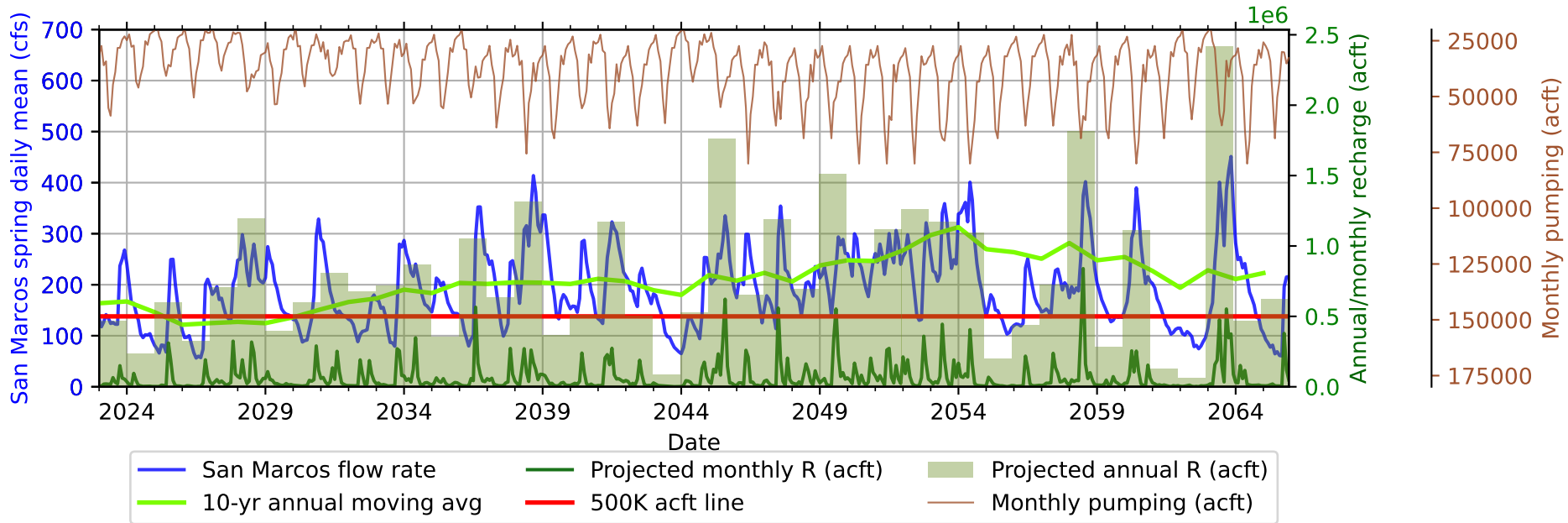
INM-CM5-0_ssp245



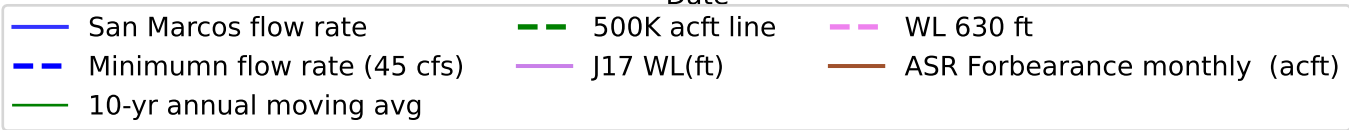
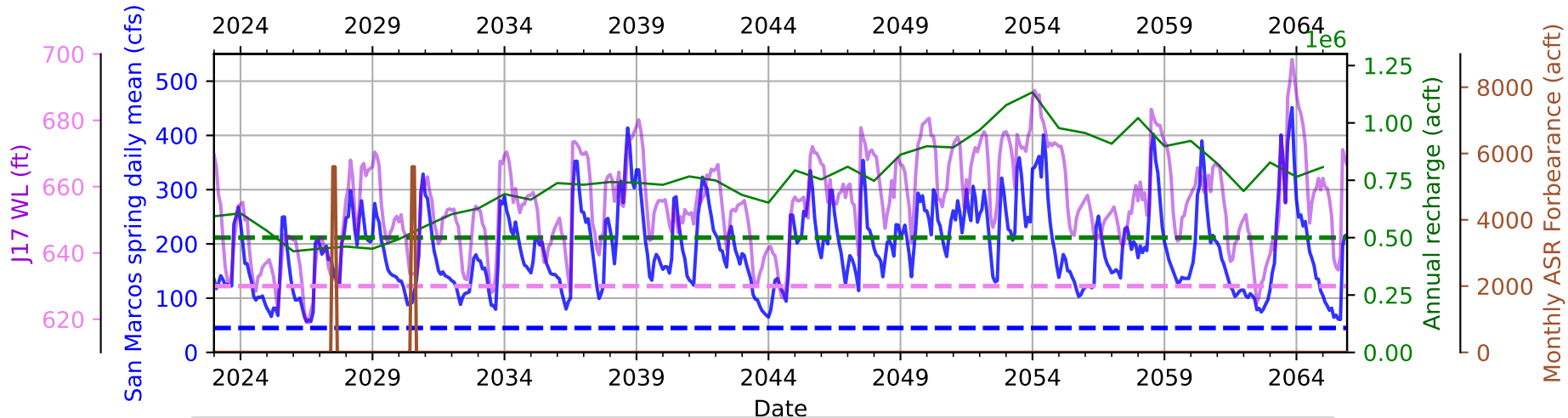
INM-CM5-0_ssp585



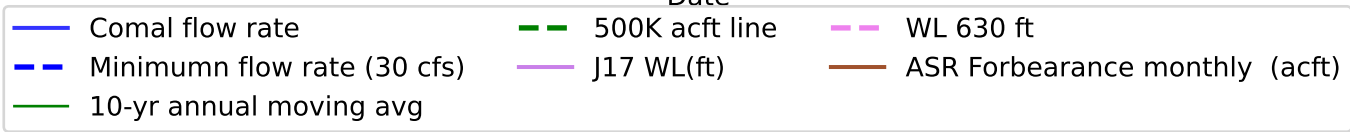
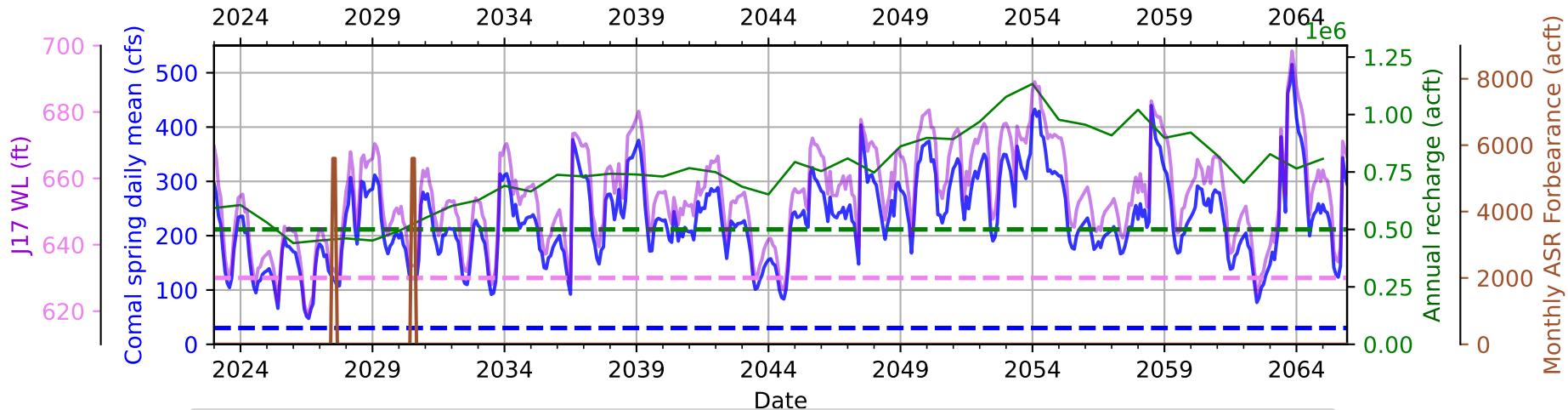
INM-CM5-0_ssp585



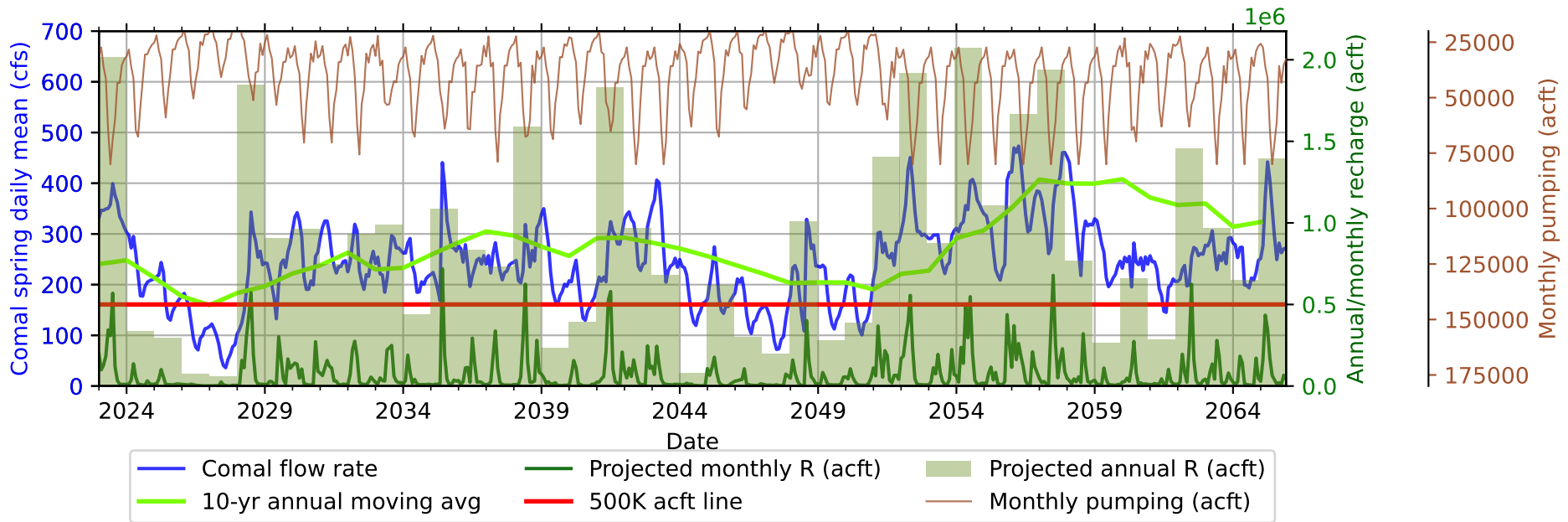
INM-CM5-0_ssp585



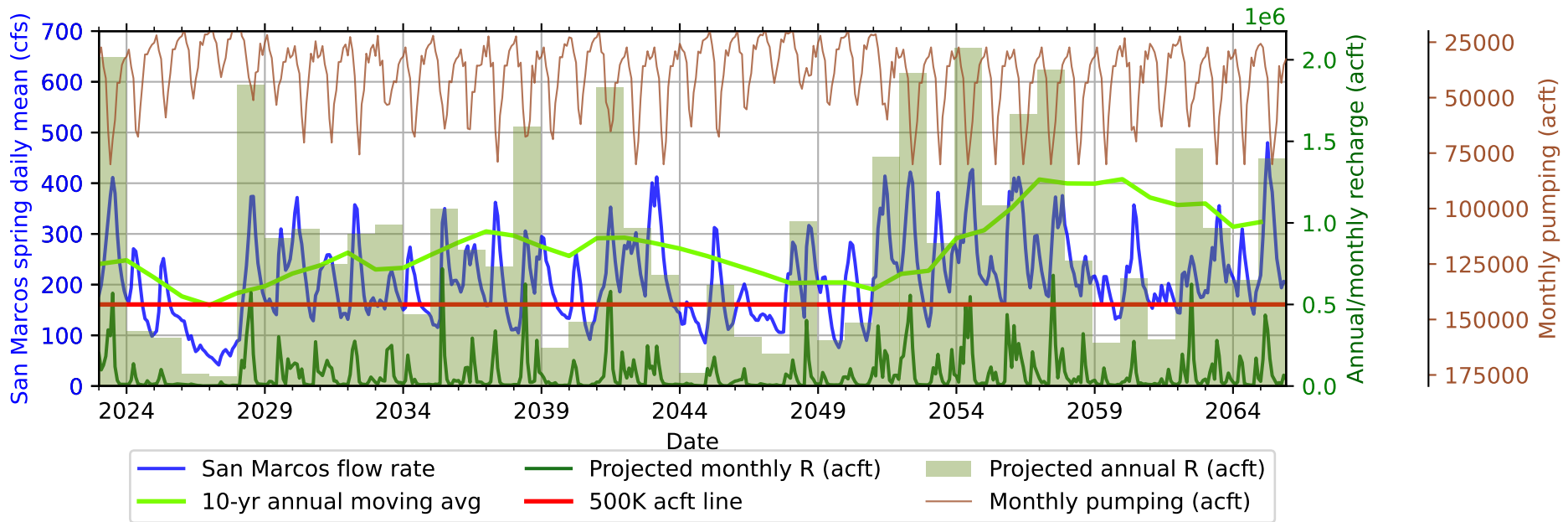
INM-CM5-0_ssp585



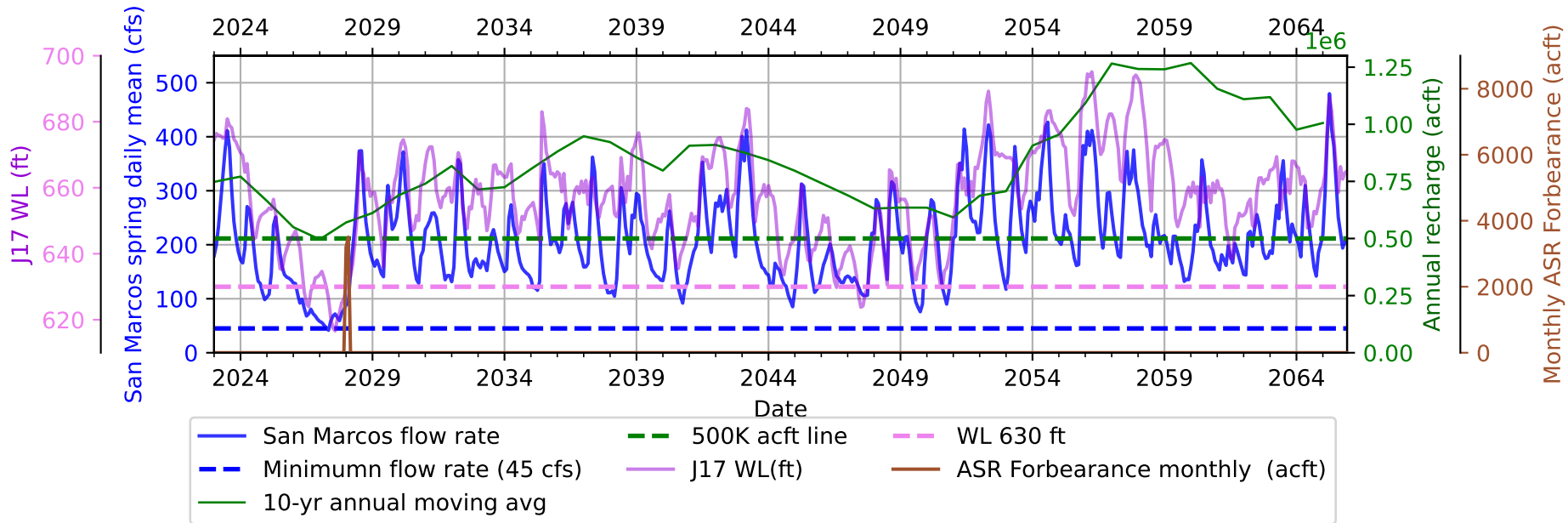
inmcm4_rcp45



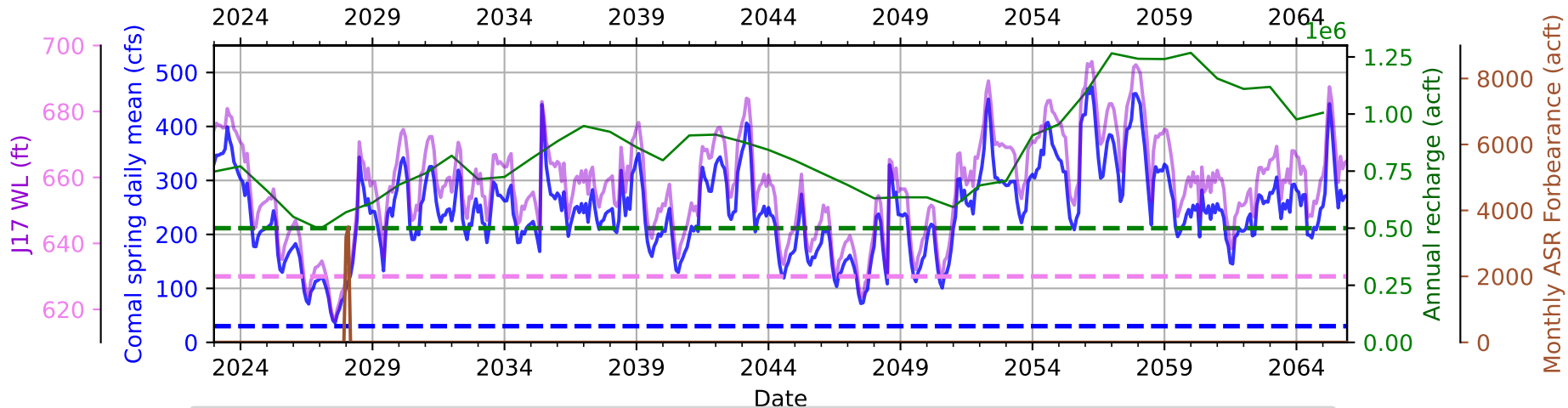
inmcm4_rcp45



inmcm4_rcp45

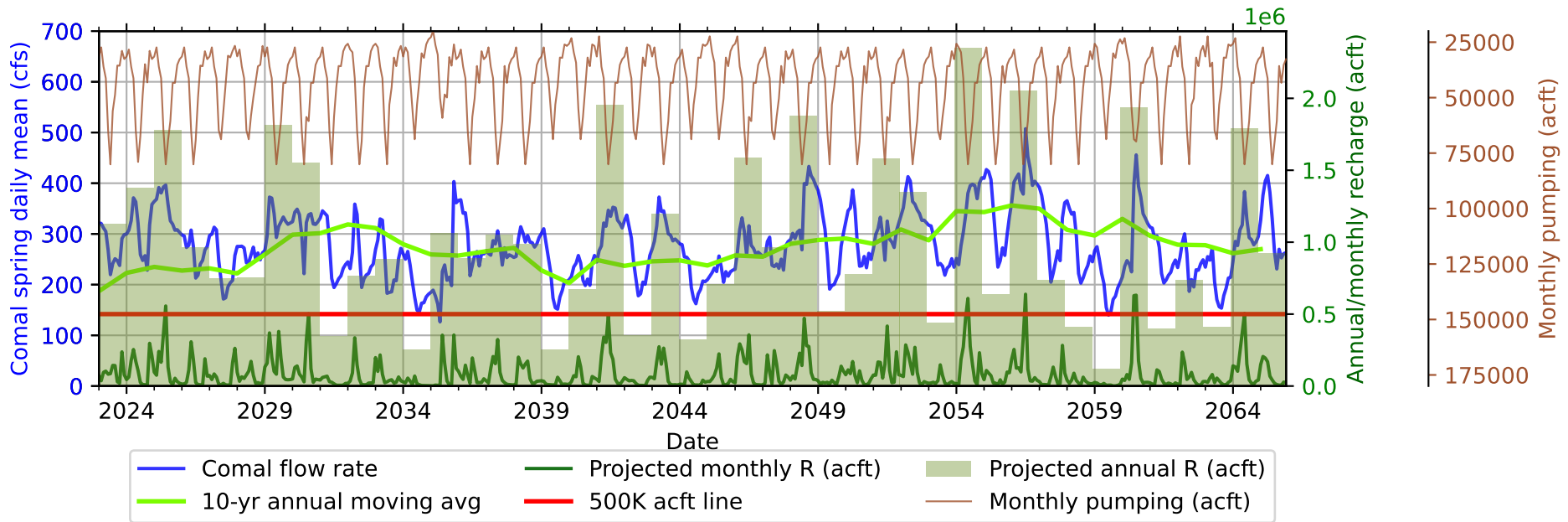


inmcm4_rcp45

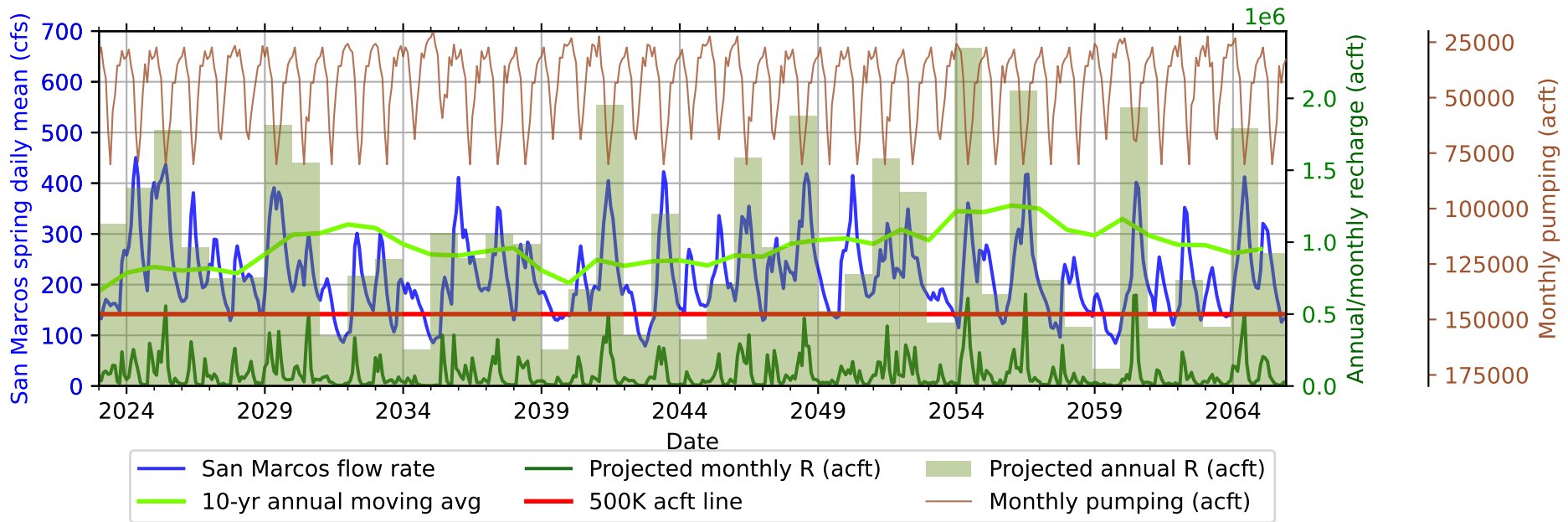


- Comal flow rate
- - - Minimumn flow rate (30 cfs)
- 10-yr annual moving avg
- - - 500K acft line
- J17 WL(ft)
- - - WL 630 ft
- ASR Forbearance monthly (acft)

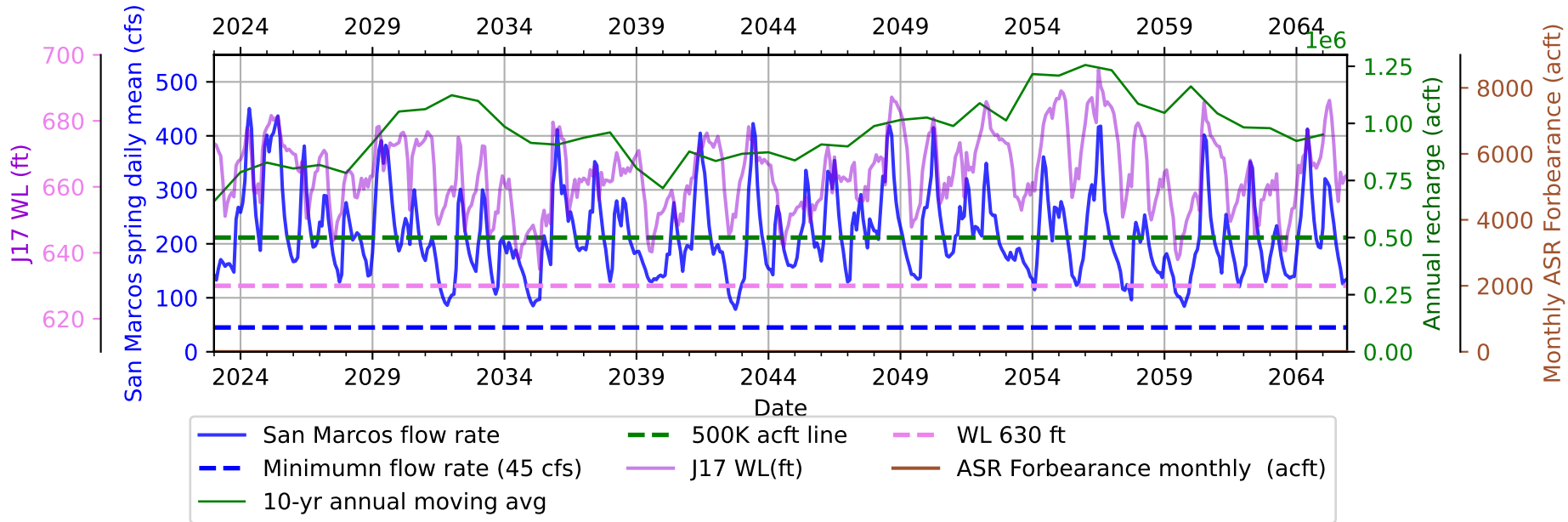
inmcm4_rcp85



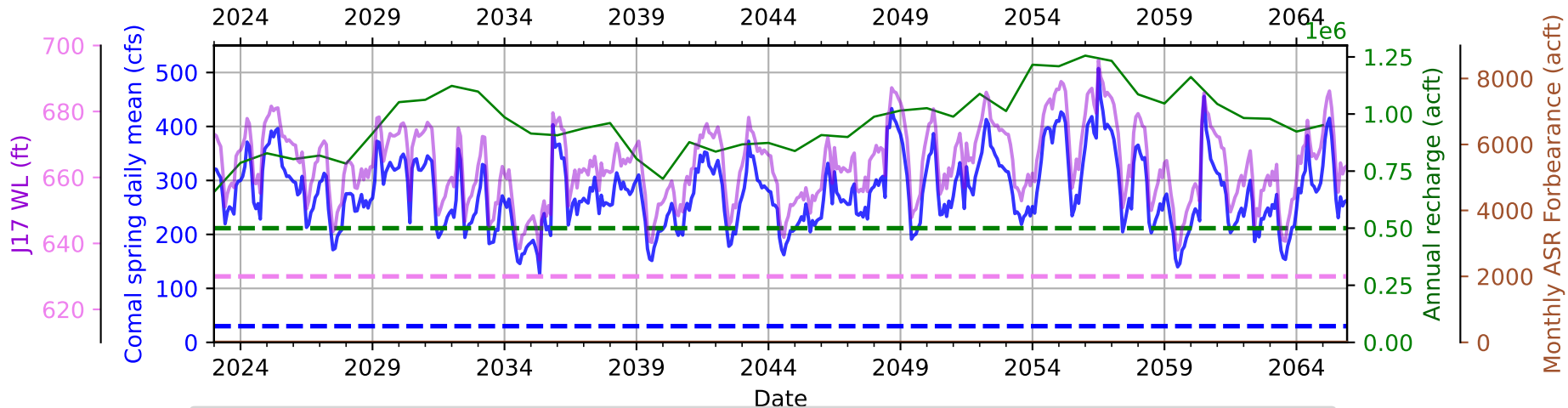
inmcm4_rcp85



inmcm4_rcp85

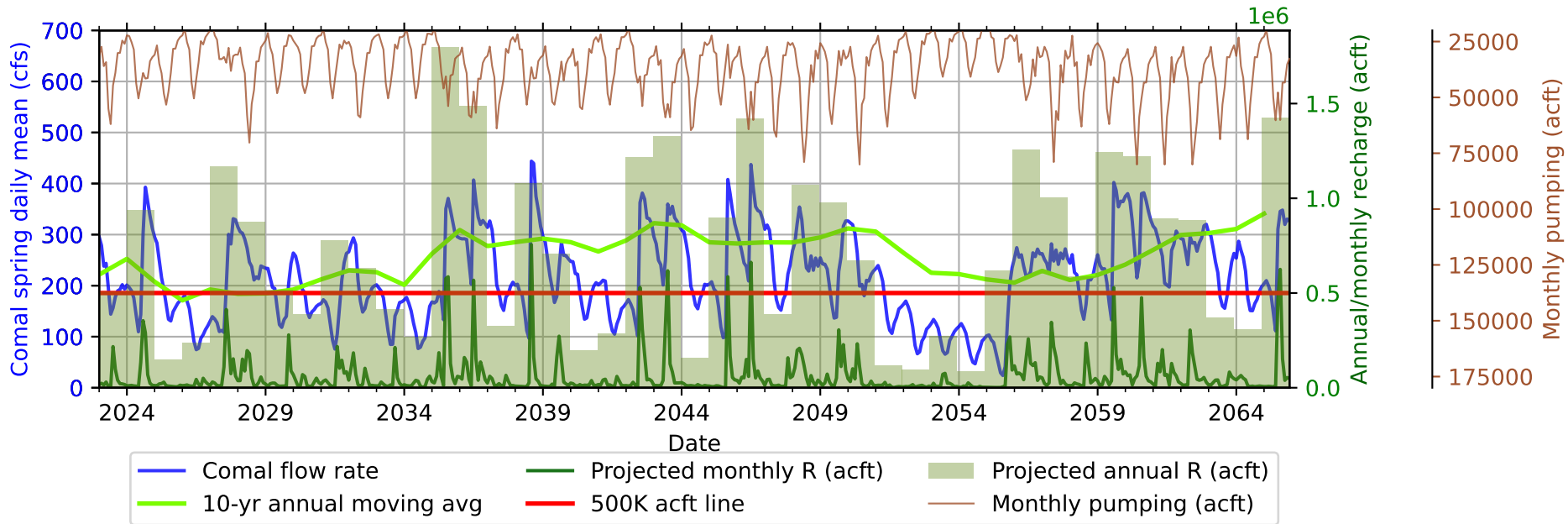


inmcm4_rcp85

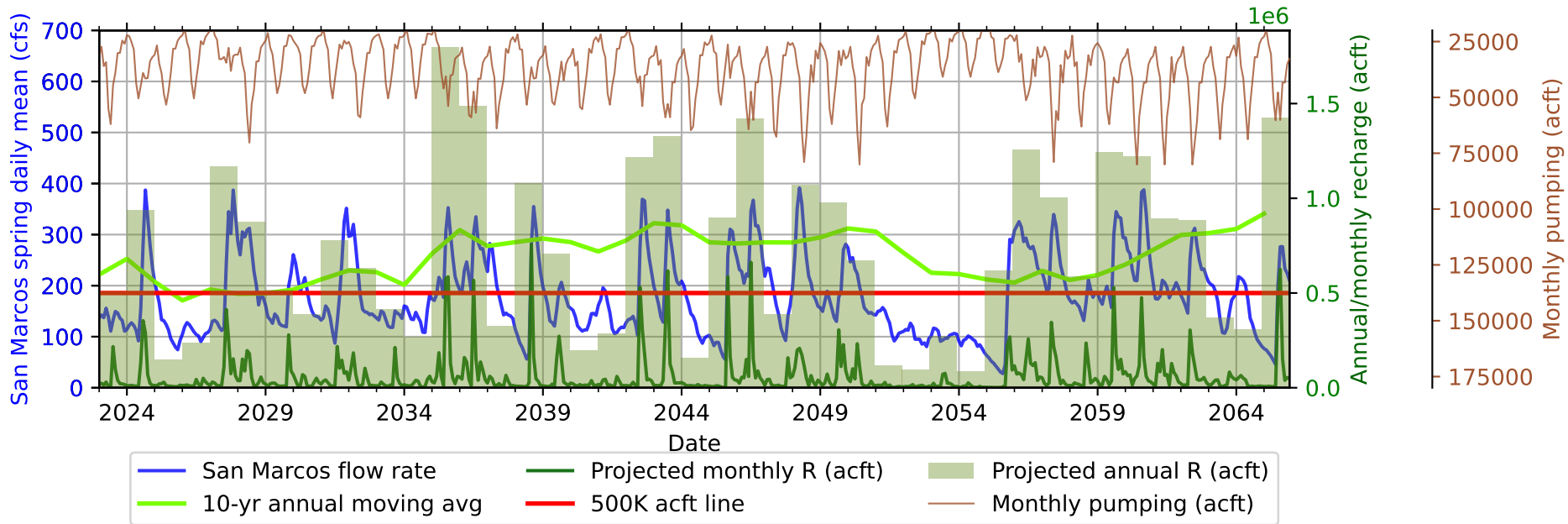


- Comal flow rate
- - - Minimumn flow rate (30 cfs)
- 10-yr annual moving avg
- - - 500K acft line
- J17 WL(ft)
- - - WL 630 ft
- ASR Forbearance monthly (acft)

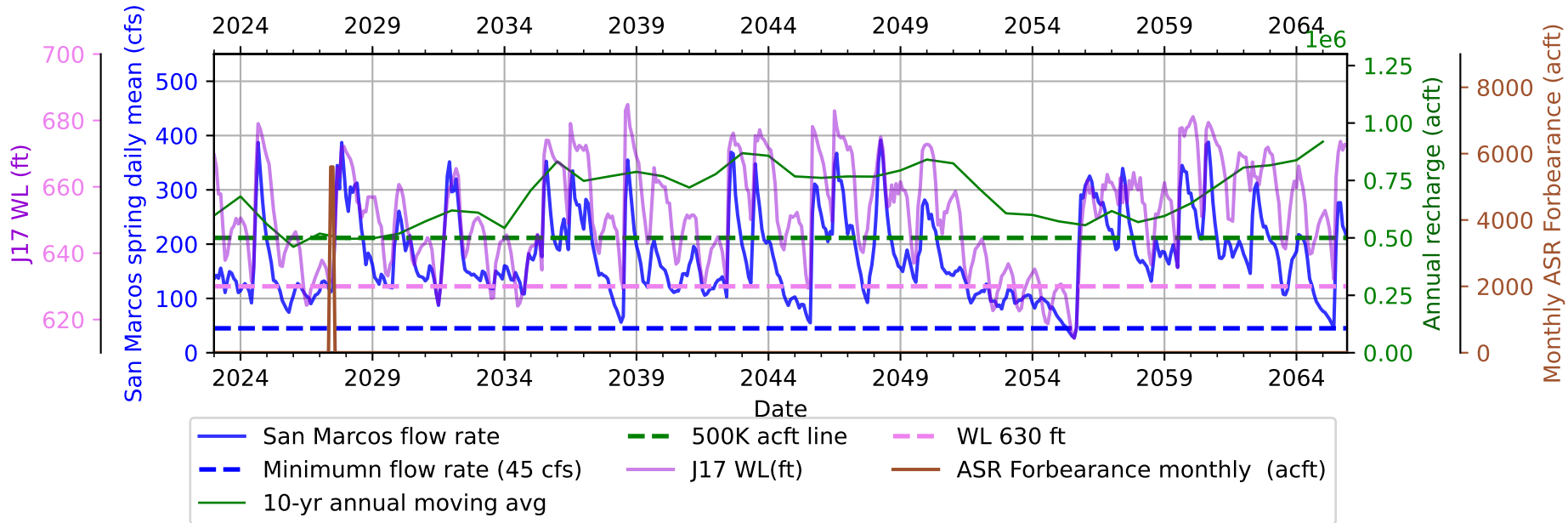
KACE-1-0-G_ssp245



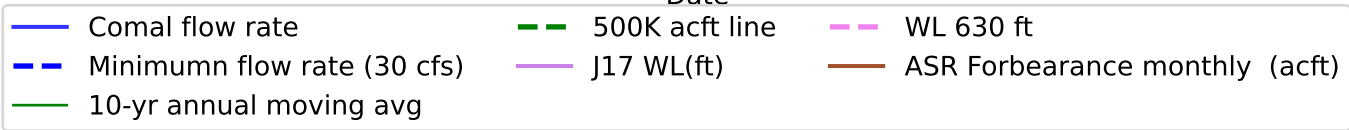
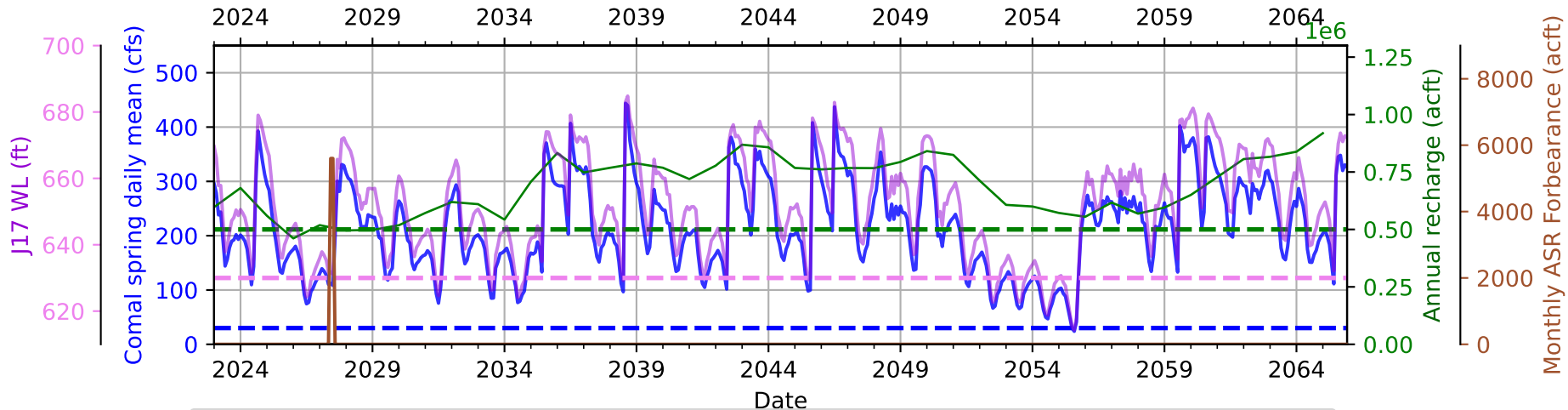
KACE-1-0-G_ssp245



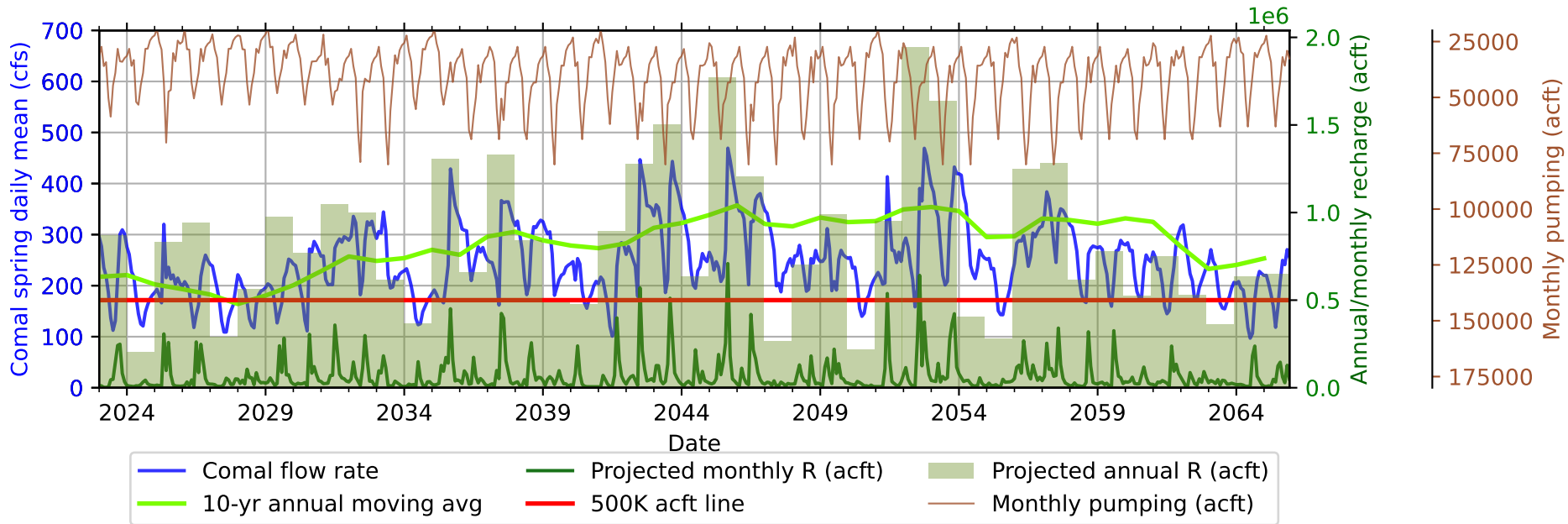
KACE-1-0-G_ssp245



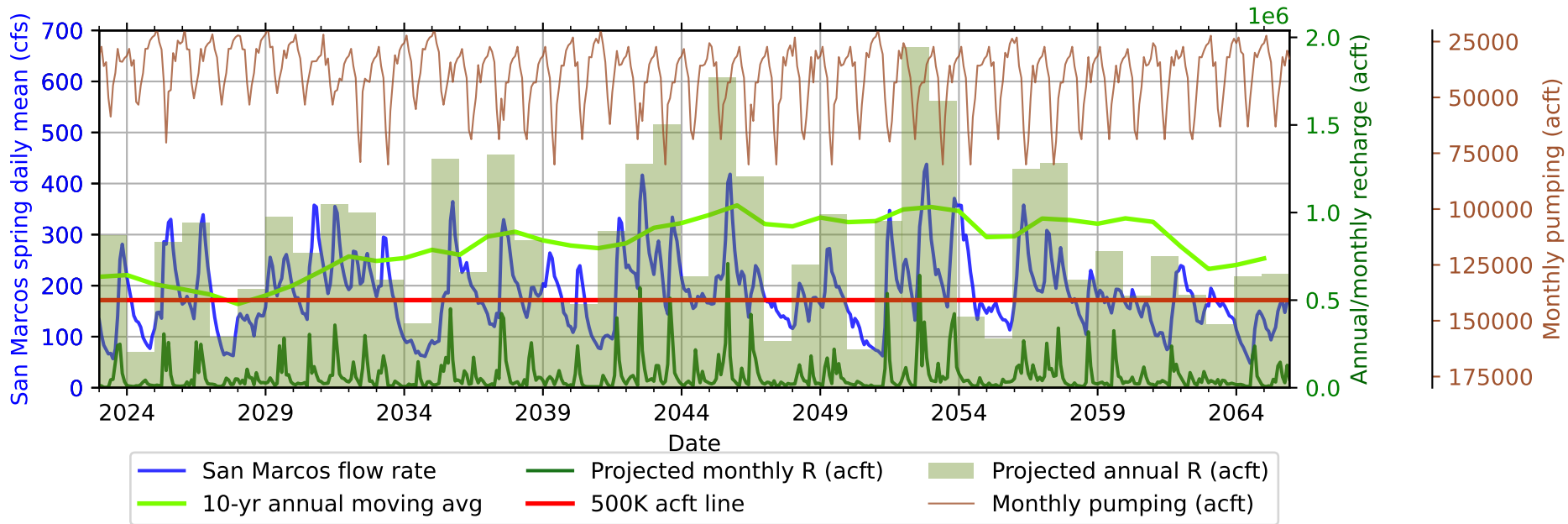
KACE-1-0-G_ssp245



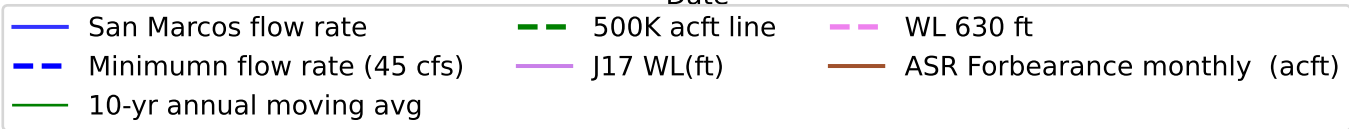
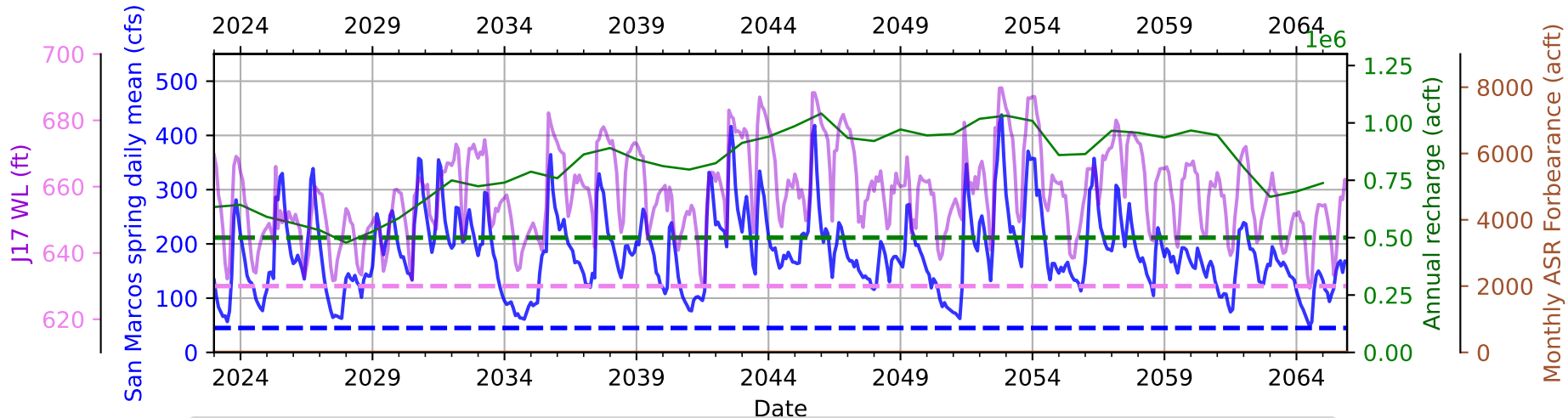
KACE-1-0-G_ssp585



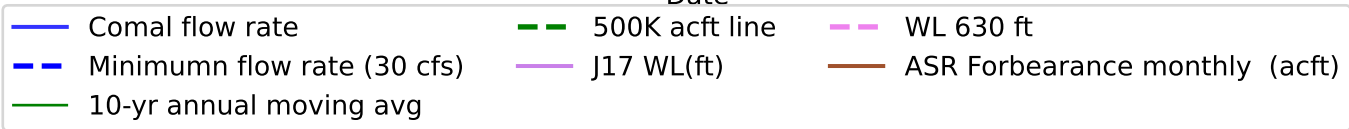
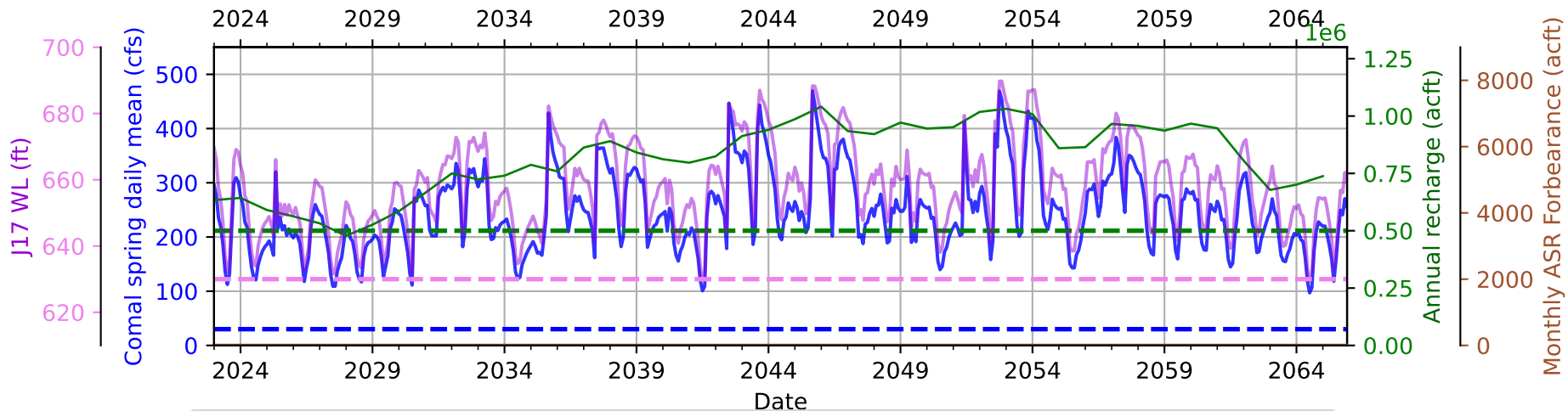
KACE-1-0-G_ssp585



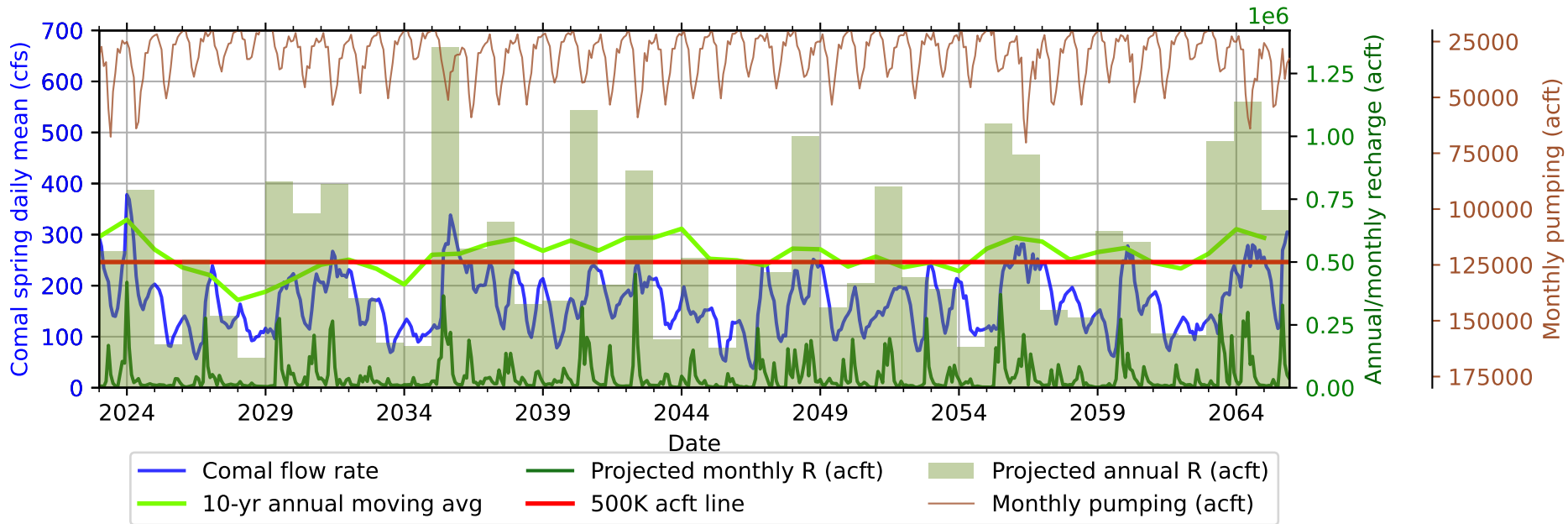
KACE-1-0-G_ssp585



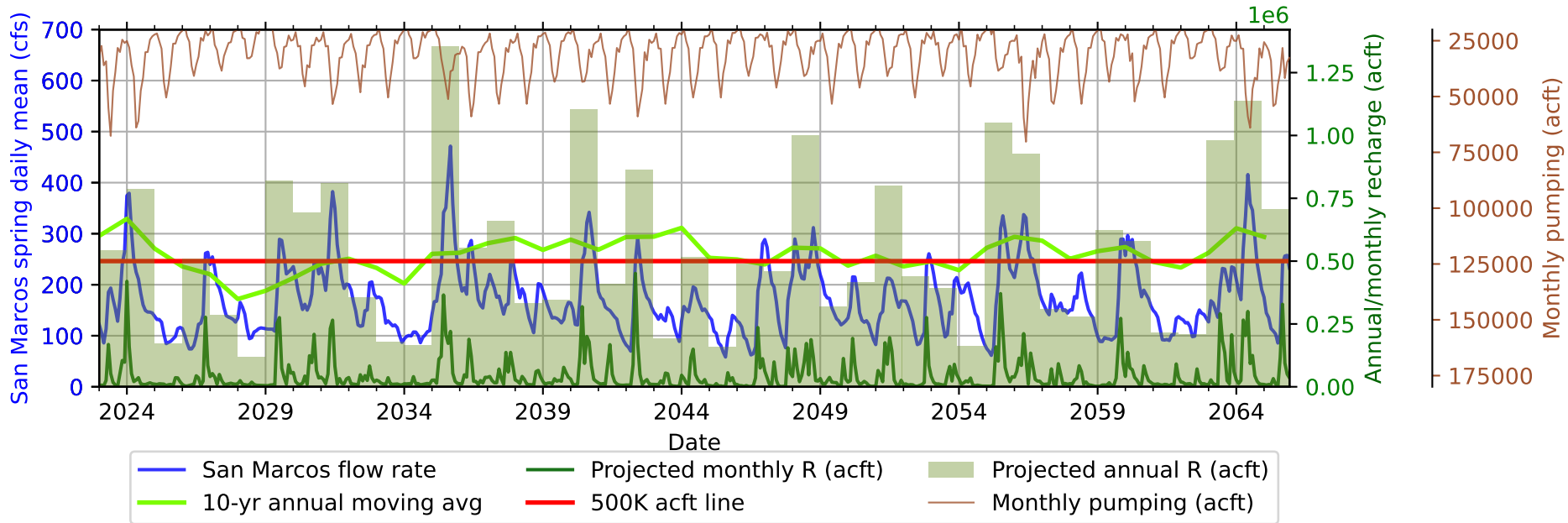
KACE-1-0-G_ssp585



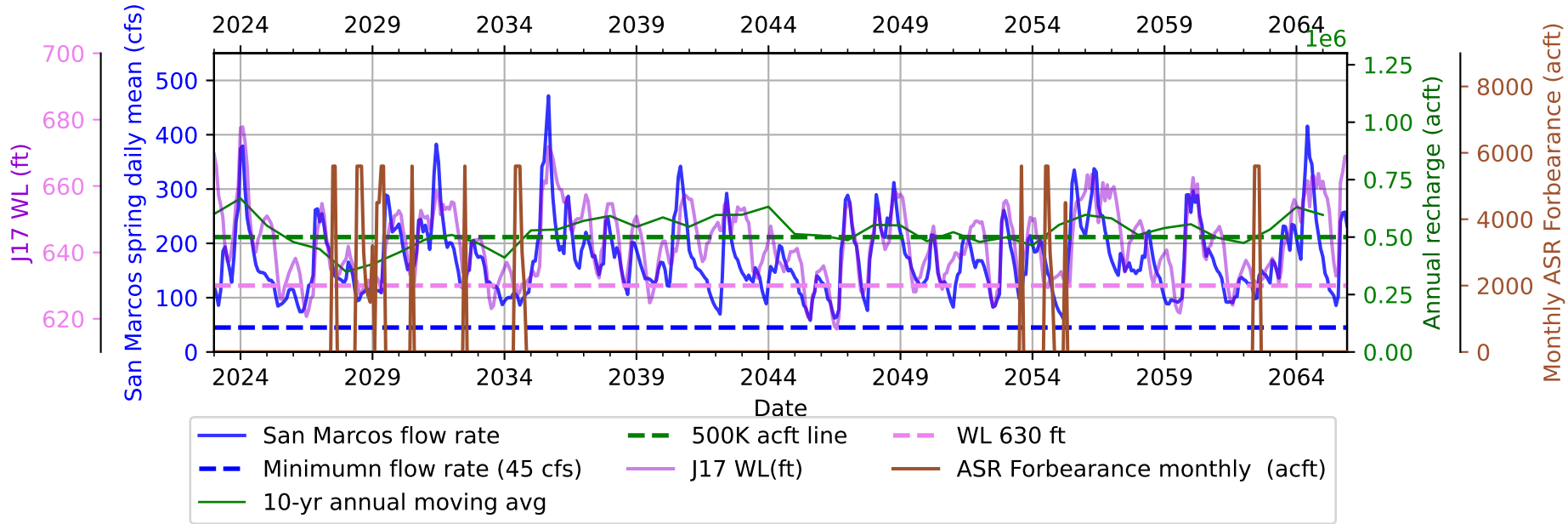
KIOST-ESM_ssp245



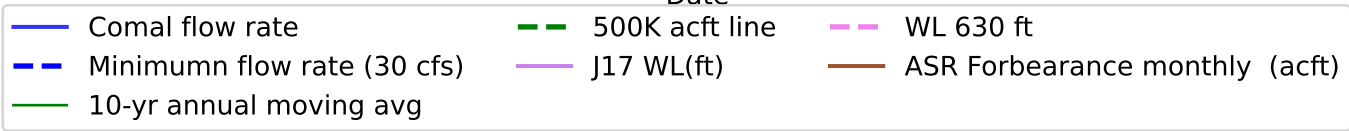
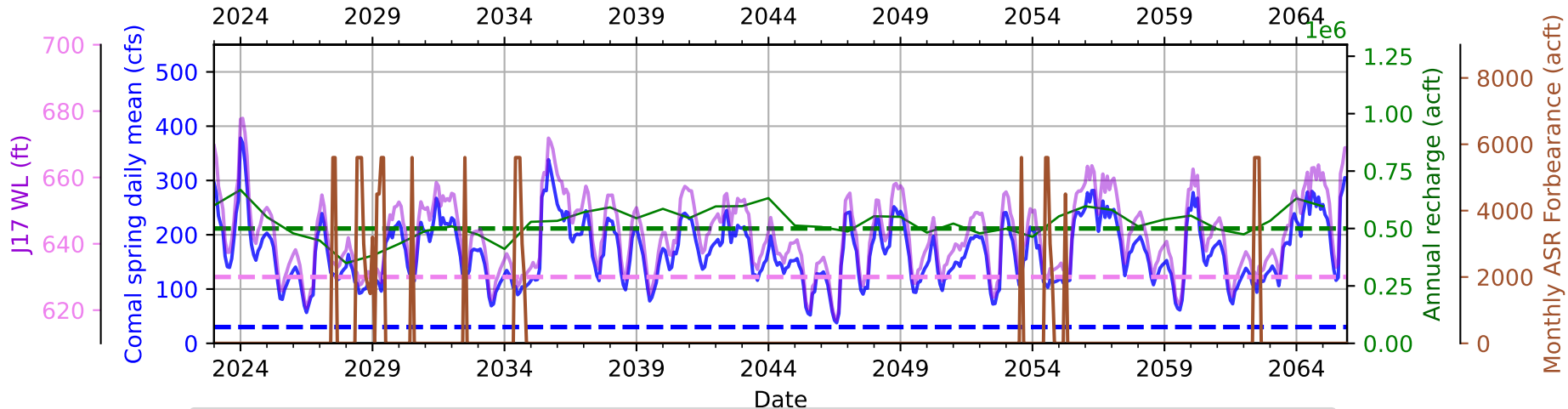
KIOST-ESM_ssp245



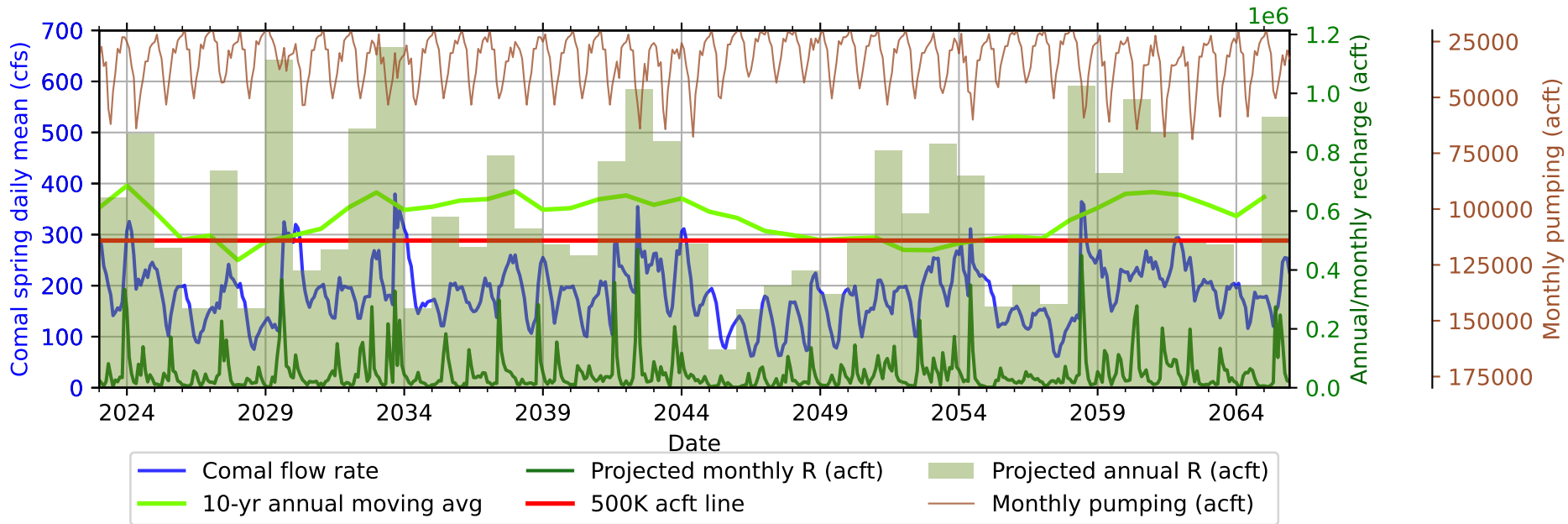
KIOST-ESM_ssp245



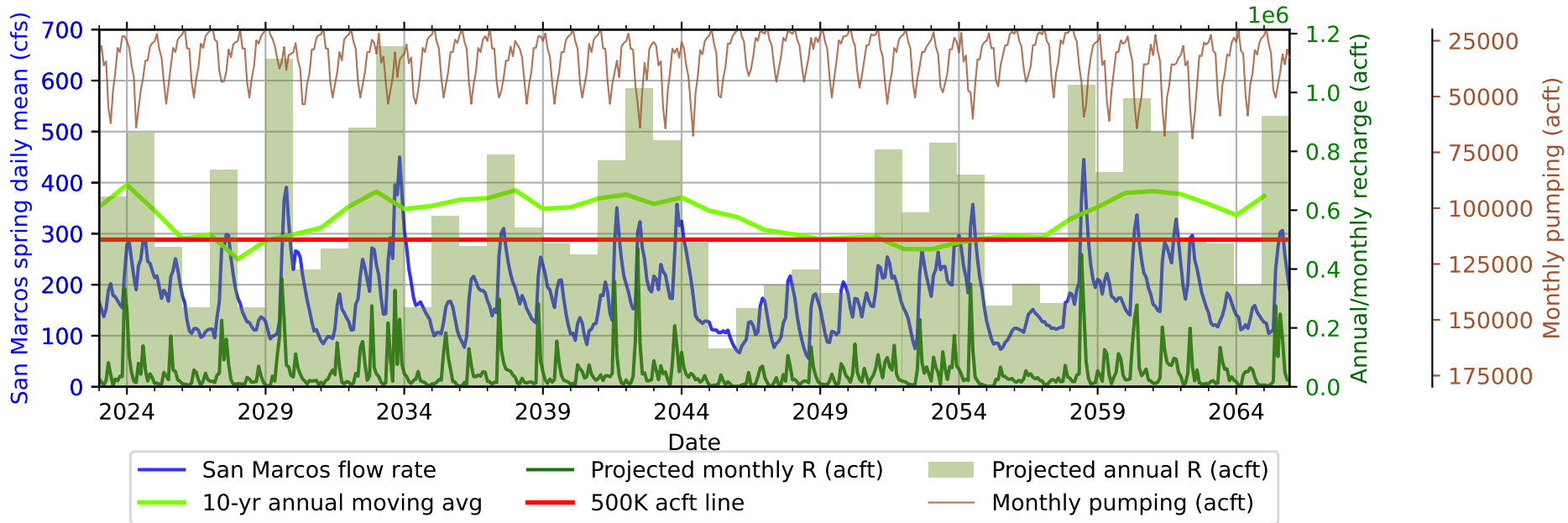
KIOST-ESM_ssp245



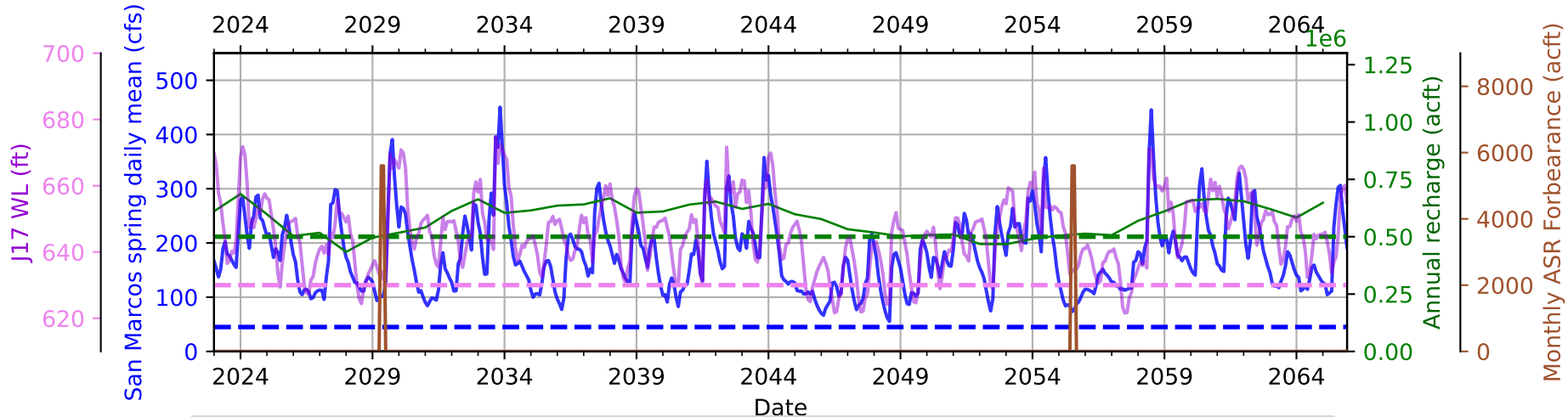
KIOST-ESM_ssp585



KIOST-ESM_ssp585

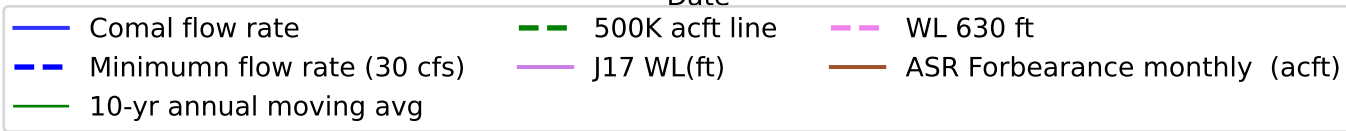
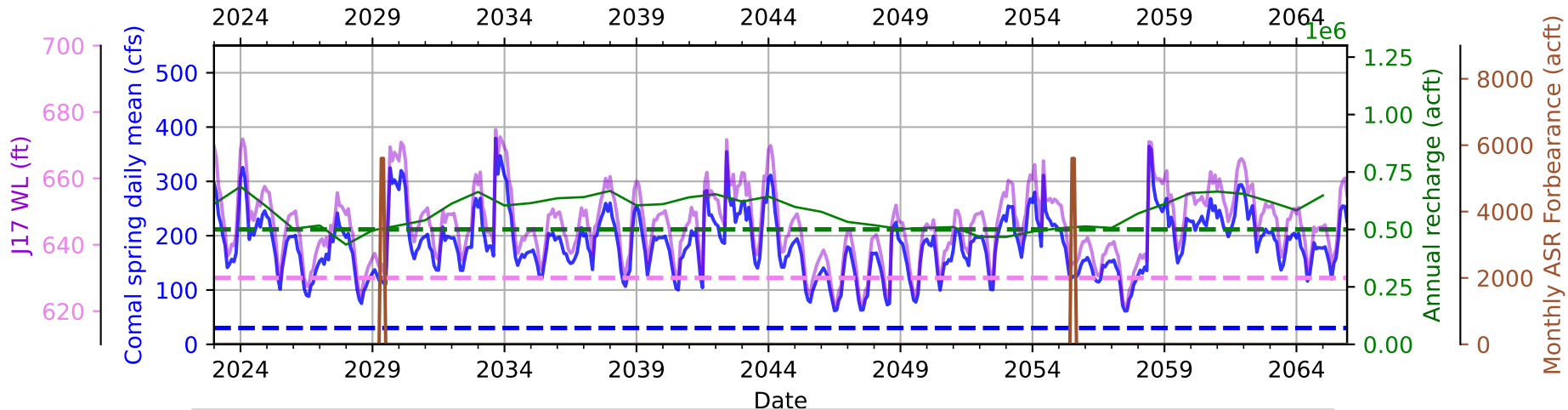


KIOST-ESM_ssp585

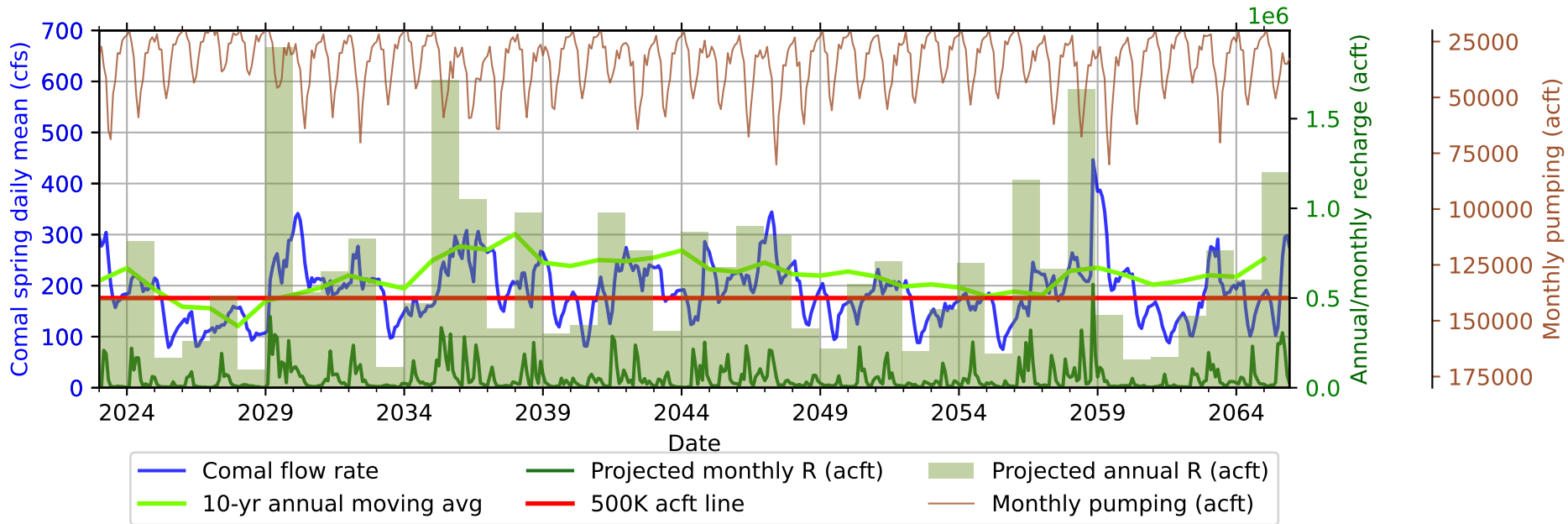


- San Marcos flow rate
- J17 WL(ft)
- 10-yr annual moving avg
- - - 500K acft line
- - - WL 630 ft
- - - Minimumn flow rate (45 cfs)
- | ASR Forbearance monthly (acft)

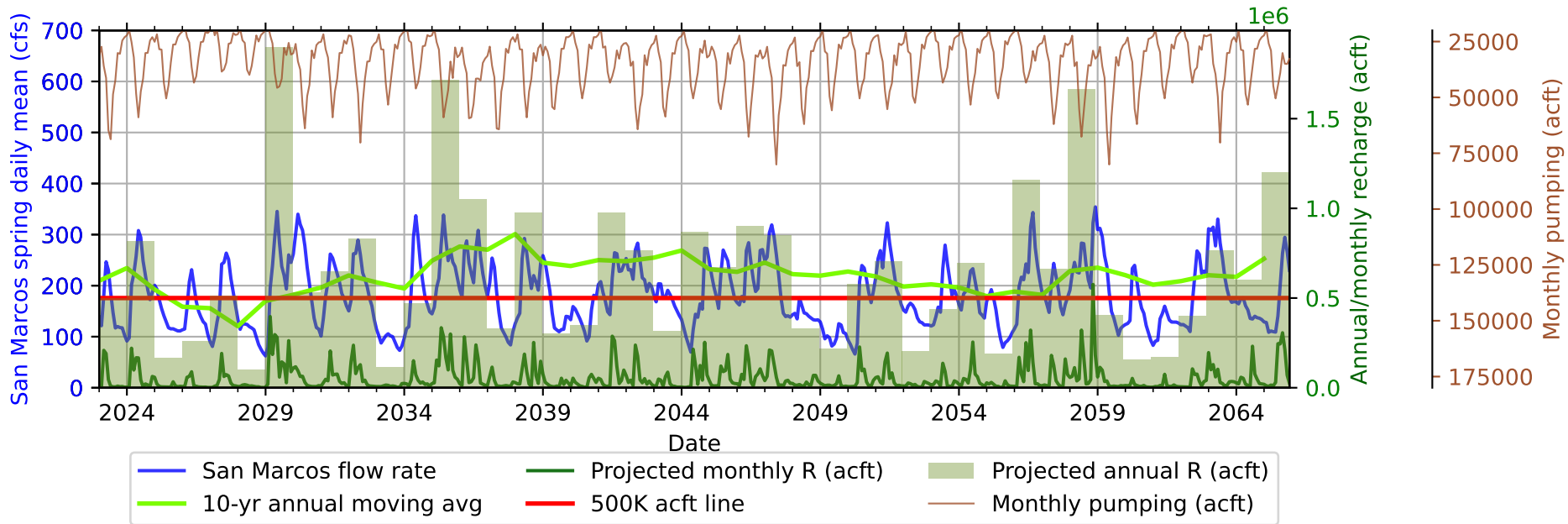
KIOST-ESM_ssp585



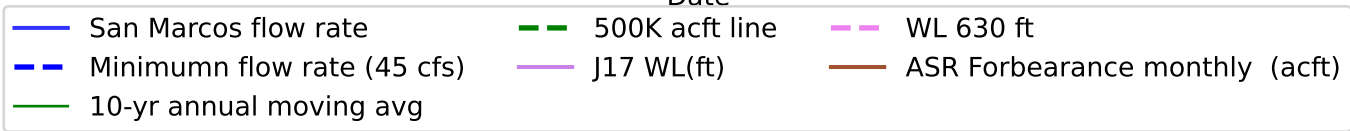
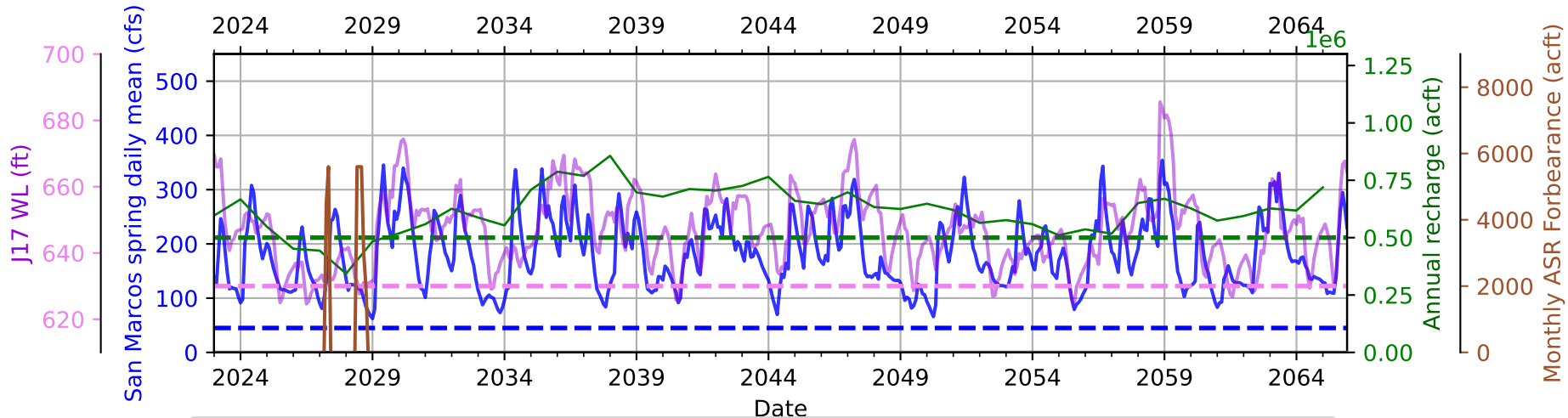
MPI-ESM1-2-HR_ssp245



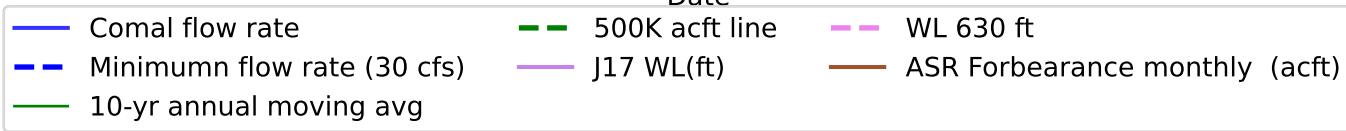
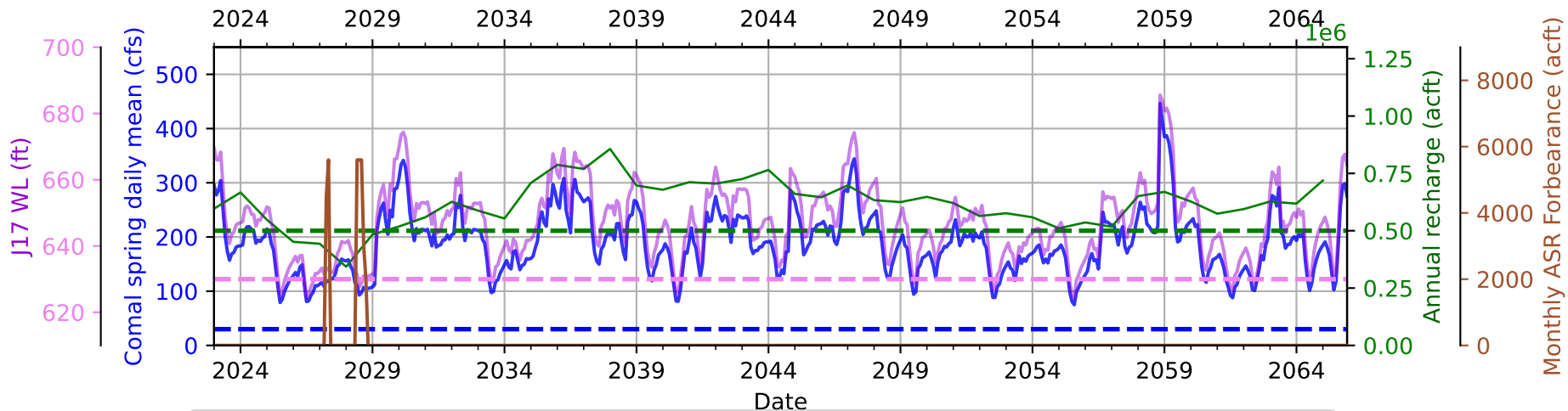
MPI-ESM1-2-HR_ssp245



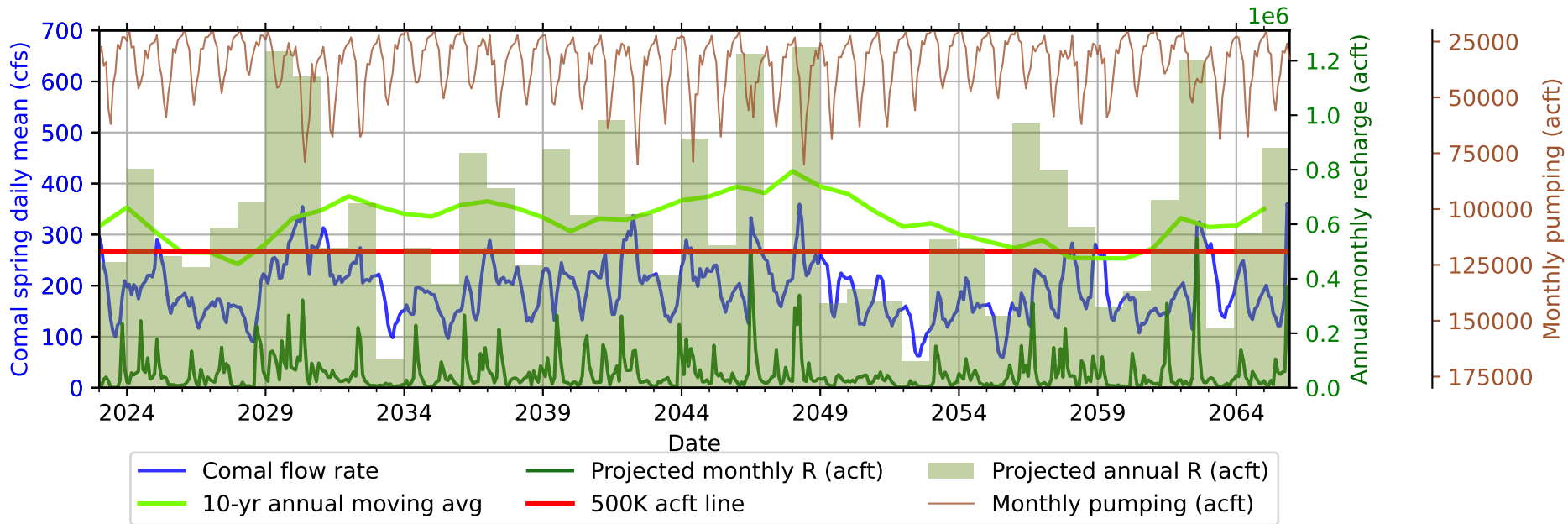
MPI-ESM1-2-HR_ssp245



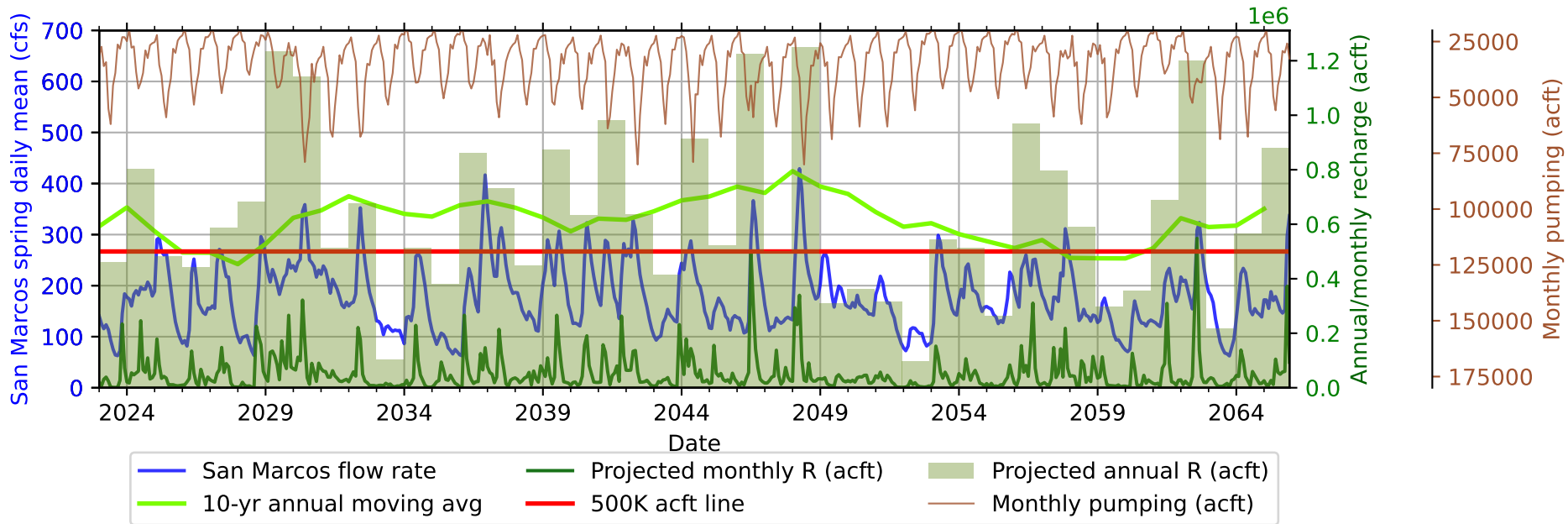
MPI-ESM1-2-HR_ssp245



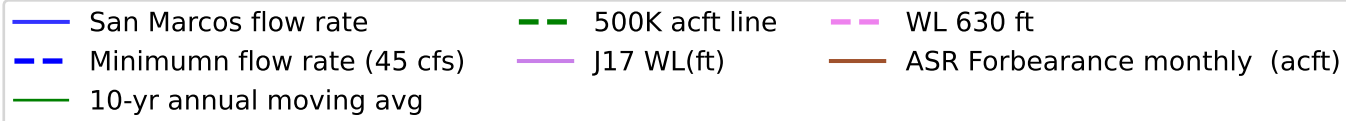
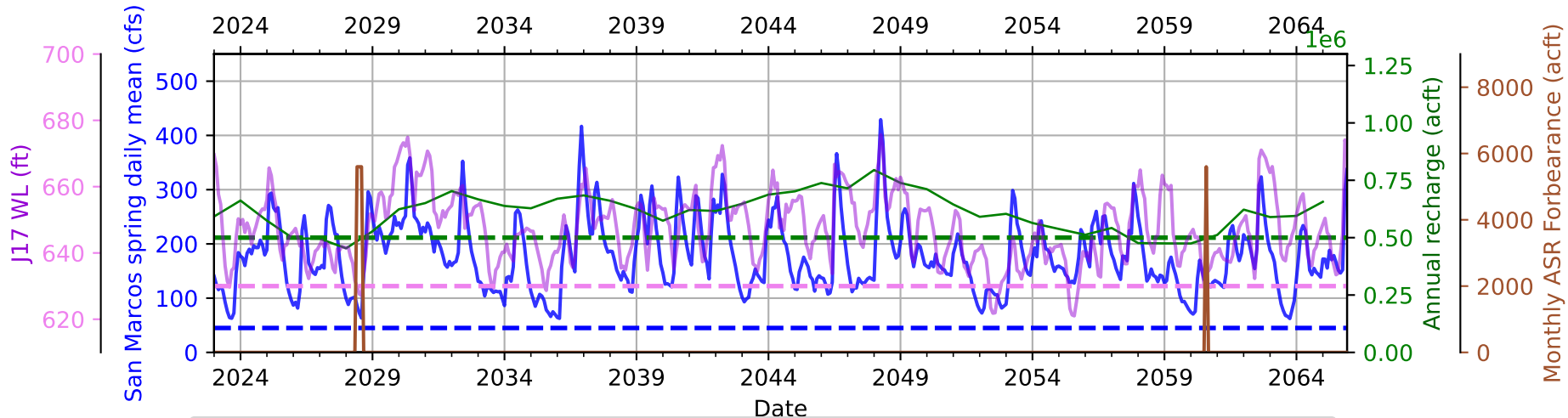
MPI-ESM1-2-HR_ssp585



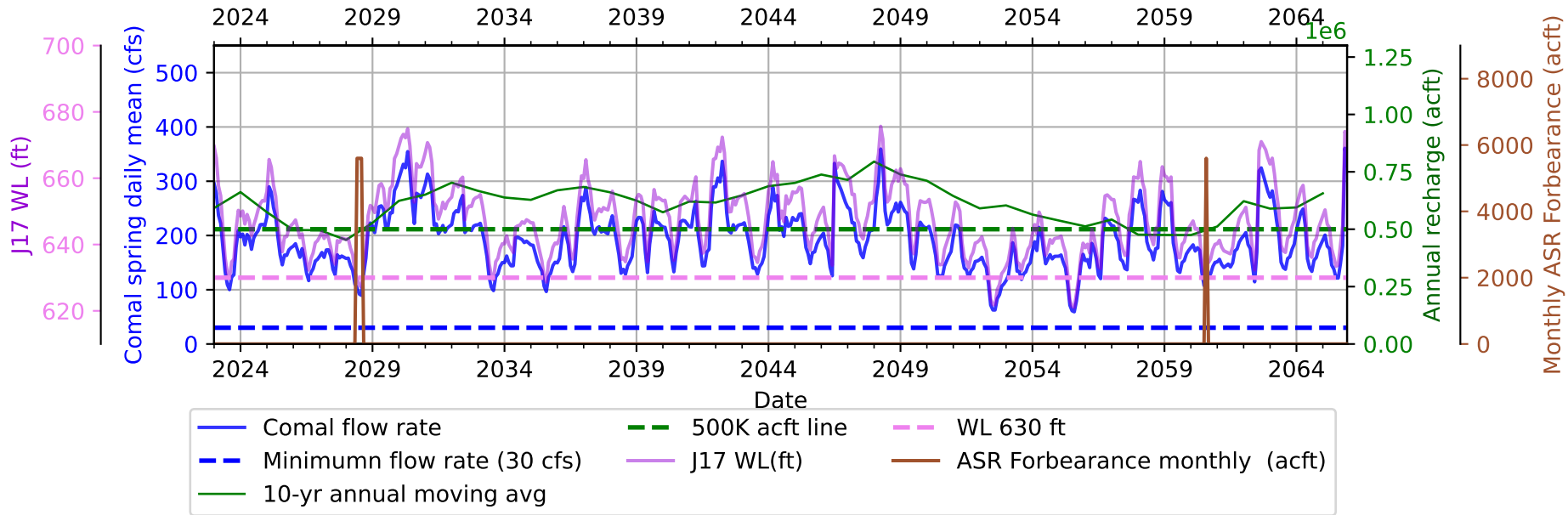
MPI-ESM1-2-HR_ssp585



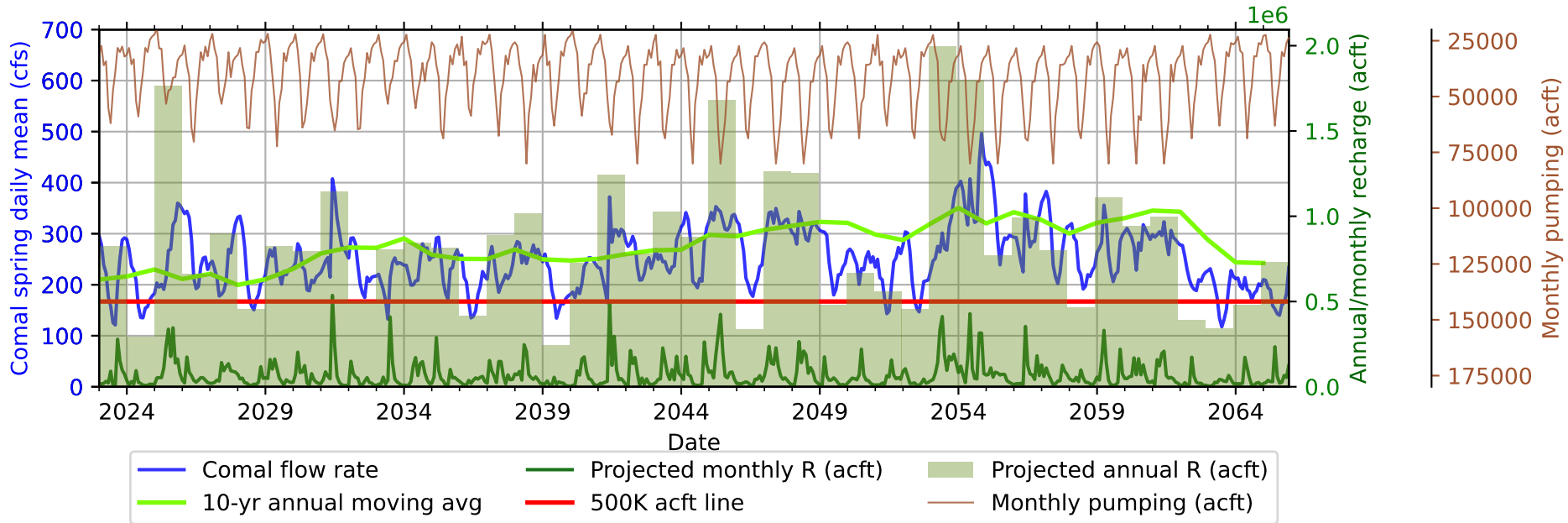
MPI-ESM1-2-HR_ssp585



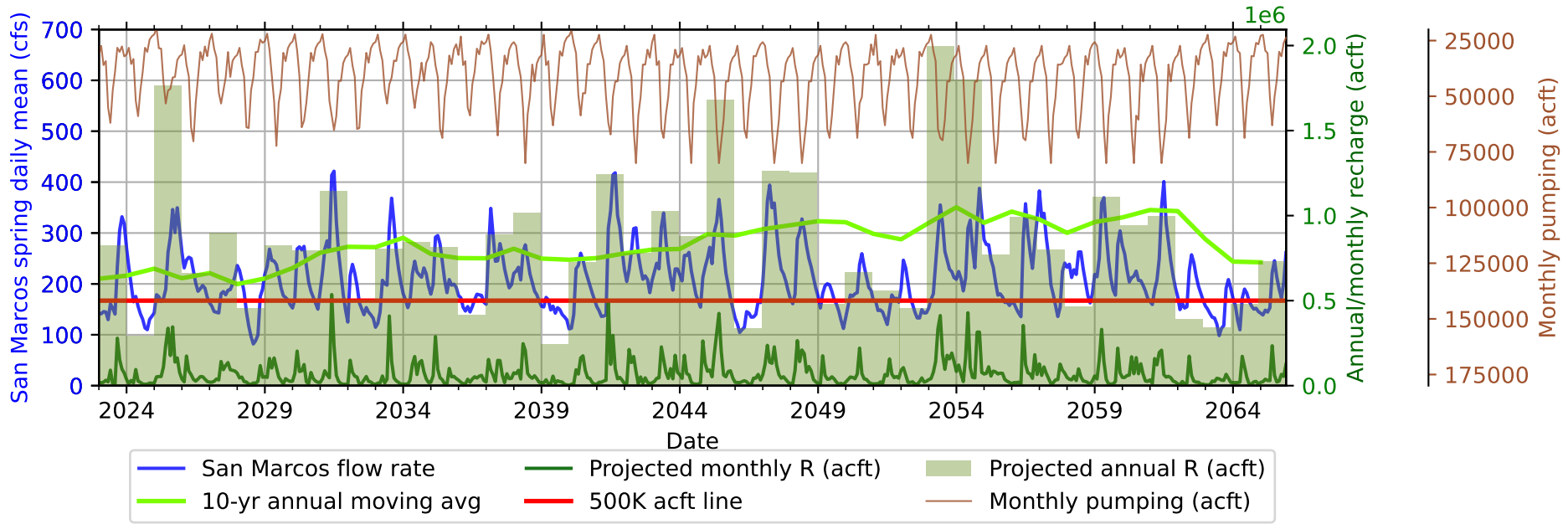
MPI-ESM1-2-HR_ssp585



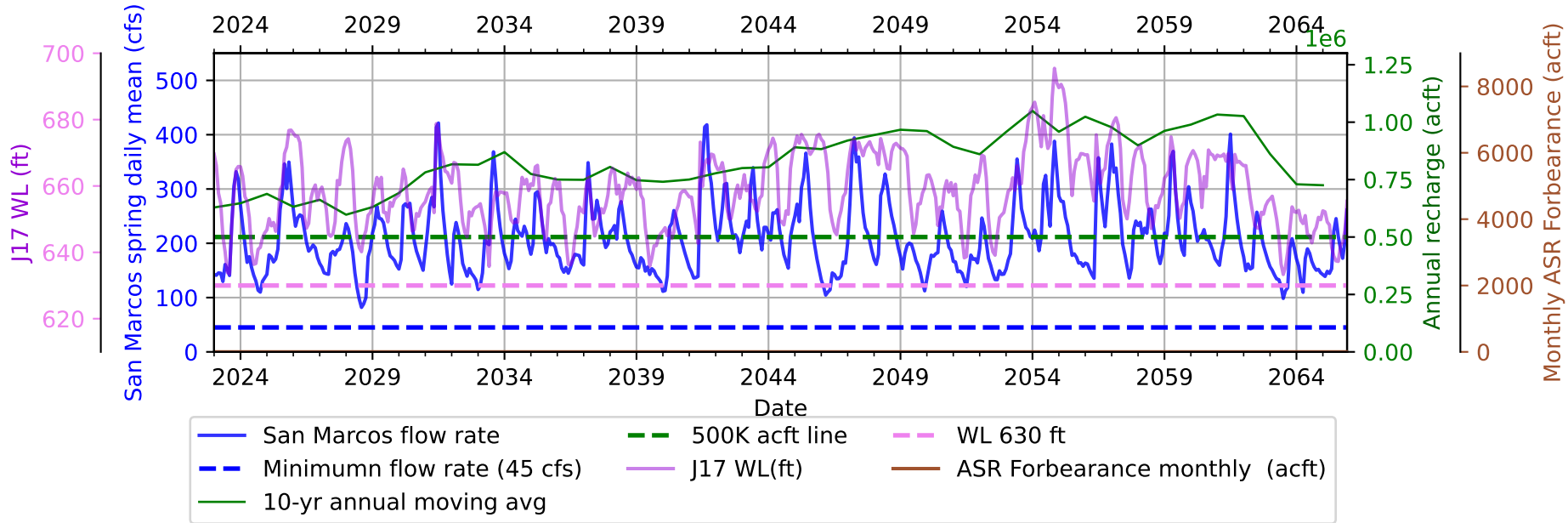
MRI-ESM1_rcp85



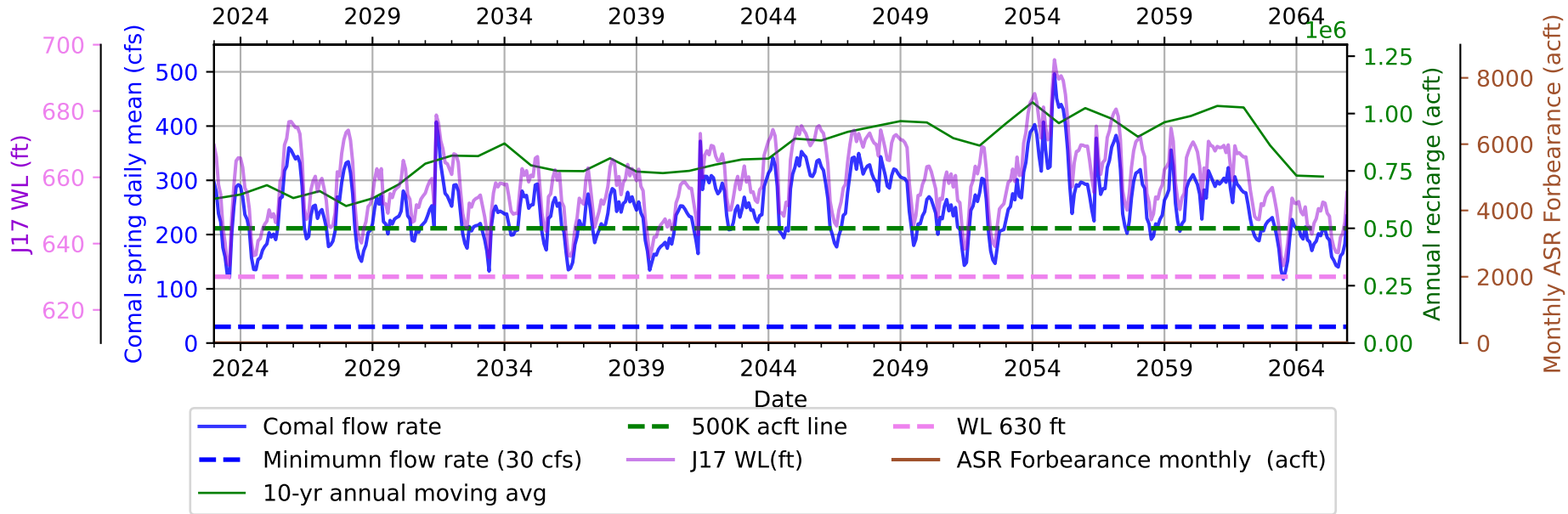
MRI-ESM1_rcp85



MRI-ESM1_rcp85



MRI-ESM1_rcp85



Appendix C

SAMP Model Runs Inputs and Assumptions

To: EAHCP Committees

From: Nathan Pence, EAHCP Program Manager

Date: June 21, 2018

Subject: SAMP Model Runs Inputs and Assumptions

The purpose of this document is to detail the modeling inputs and assumptions included in the EAHCP Phase II MODFLOW model runs. As discussed in the Strategic Adaptive Management Process (SAMP) whitepaper (Pence – June 21, 2018; herein, whitepaper), several model runs will be conducted to examine predicted springflow provided by EAHCP springflow conservation measures as implemented through a repeat of the drought of record (DOR).

HDR was tasked with the original evaluation of springflow provided by springflow conservation measures through the DOR during the EARIP planning period (HDR 2011 - EAHCP Appendix K). The HDR report identified Comal springflow shortfalls during a repeat of the DOR. In 2017, the EAA completed an update and recalibration of the MODFLOW model of the San Antonio segment of the Edwards Aquifer (Liu et al., 2017). The updated model contains significant conceptual and structural updates along with increased amounts of recent hydrologic data used to train the model. This model has been examined by a model advisory committee, the original users of the HDR EARIP model, and the National Academy of Sciences.

In addition to an updated model, the EAHCP now has empirical data on the actual implementation of springflow conservation measures from 2013 - 2018 (namely, volume and geographical distribution of enrolled water in springflow protection programs – VISPO, ASR, RWCP). Also, EAA has updated usage and pumping data related to Federal exempt use, Domestic and Livestock exempt use and the new Limited Production Well exempt use. These data can be used to improve upon the assumptions made during the original HDR hydrologic simulations.

The updated MODFLOW model will be used to conduct three types of hydrologic simulations:

Baseline Runs: Model Runs 1. and 2. These model simulations will produce daily minimum springflows (1947-1958) and long-term average springflows (1947-2000) with the updated MODFLOW model using the model inputs from the HDR model runs. The purpose of these runs is to examine whether the springflow shortfalls identified during the HDR analysis still exists using the new model with the same model inputs.

SAMP Runs: actual Model Runs 3. and 4. These model simulations will produce daily minimum springflows (1947-1958) and long-term average springflows (1947-2000) with the updated MODFLOW model using the model inputs based on the first 5 years of EAHCP implementation. The purpose of these runs is to examine whether springflow shortfalls exist using the new MODFLOW model with actual implementation of EAHCP springflow protection measures as implemented.

SAMP Runs - Expanded Phase I CMs and/or Phase II CMs: Model Run 5. These model simulations will be conducted if springflow shortfalls still exist after analysis of SAMP Runs (Runs #3 and #4). The purpose of these runs would be to examine springflows under a different set of springflow conservation measures than currently exist in Phase I of the EAHCP.

After model runs 1-5 are finalized and the specific set of additional Phase II conservation measures are determined (if any are needed), no additional modeling is anticipated until required for the rollover of the incidental take permit in 2028. This includes if the realized geographical distribution of enrollment in springflow conservation measure does not exactly match the assumptions presented in this document.

The remainder of this document details the pumping and flow protection conservation measure modeling inputs and assumptions behind each of the aforementioned MODFLOW model runs. For details regarding the construction of the HDR model or the EAA model, the reader is referred to HDR (2011) and Liu et al. (2017), respectively.

Model Runs 1 - Completed

This model run represents springflow for the period of 1947-1958 with the updated EAA model (Liu et al. 2017) using inputs from the original HDR analysis (HDR 2011). Specifically, the model run incorporates the full suite of springflow protection measures (VISPO, RWCP, ASR, STG 5) as implemented by HDR (2011). Results of this model run, in the format of estimated springflow at Comal and San Marcos springs, can be found in Appendix A. Additionally, these model runs have been presented to the Stakeholder, Implementing, and Science Committees as part of the ASR adaptive management process.

Model Run 2 – anticipated completion Fall 2018

This model run will estimate springflow from 1947-2000 and contains the same inputs as model run 1.

Model Runs 3 and 4 – anticipated completion Fall 2018 / Spring 2019

These model runs examine the same time periods as model runs 1 and 2 respectively, but use updated data gathered during implementation (2013-2018) of springflow protection measures. There are two overarching model assumptions that apply to model input for all conservation measures:

1. Forbearance measures are modeled at the county resolution, not at individual wells. The exception to this rule is for ASR forbearance at SAWS production wells during recovery (described below).
2. Uvalde County: based on the model representation of the Knippa Gap horizontal flow barrier (Liu et al. 2017), slightly more than half of the forbearance from conservation measures will be realized east of the Knippa Gap, as a majority of irrigated acreage occurs in the eastern half of Uvalde county.

Springflow Protection Assumptions for SAMP Model Runs 3 and 4:

VISPO

The VISPO program will be modeled using the 40,000 ac-ft/yr, enrollment set by the HCP (5.1.2.1). Currently, the program is fully enrolled. The modeled geographical distribution of enrolled water will be based on the geographical distribution of the current program (2018) and is shown in Table 1. The geographical distribution of water in the program is not expected to significantly change from 2018 through 2027. VISPO forbearance in any given year is simulated in the model when modeled J-17 is at or below 635 msl on October 1 of the previous year.

Table 1. SAMP model distribution of VISPO forbearance (reflective of 2013-2018 implementation).

County	Use	acft %	Total acft
Atascosa	Irrigation	0.87%	348.00
Bexar	Irrigation	6.00%	2,400.00
Hays	Irrigation	0.30%	120.00
Medina	Irrigation	27.95%	11,180.00
Uvalde	Irrigation	64.88%	25,952.00
		100.00%	40,000.00

ASR

Use of the SAWS ASR for springflow protection is divided into SAWS forbearance and injection activities and EAA forbearance activities (HCP 5.5.1).

SAWS ASR activities

The SAWS forbearance portion will be modeled by reducing pumping at 4 individual pump stations on the northeast side of the SAWS distribution system in an amount that on a monthly basis equals the amount of water available from the ASR. The SAWS forbearance and recovery of ASR water will be modeled following the same recovery schedule as used by the HDR (2011) simulations (Figure 1) and the ASR Interlocal Contract between the EAA and SAWS.

Since 2013, approximately 85,000 acft of water have been injected into the ASR on behalf of the EAHCP. The EAA anticipates filling the ASR to the 126,000 acft required (HCP 5.5.1) for recovery during a decadal DOR by 2021. HDR (2011) simulations assumed starting the DOR with 80,000 acft in storage, requiring injection over the course of the DOR (Figure 1). Model runs 3 and 4 assume beginning the DOR with 126,000 acft and no injection into ASR during the drought.

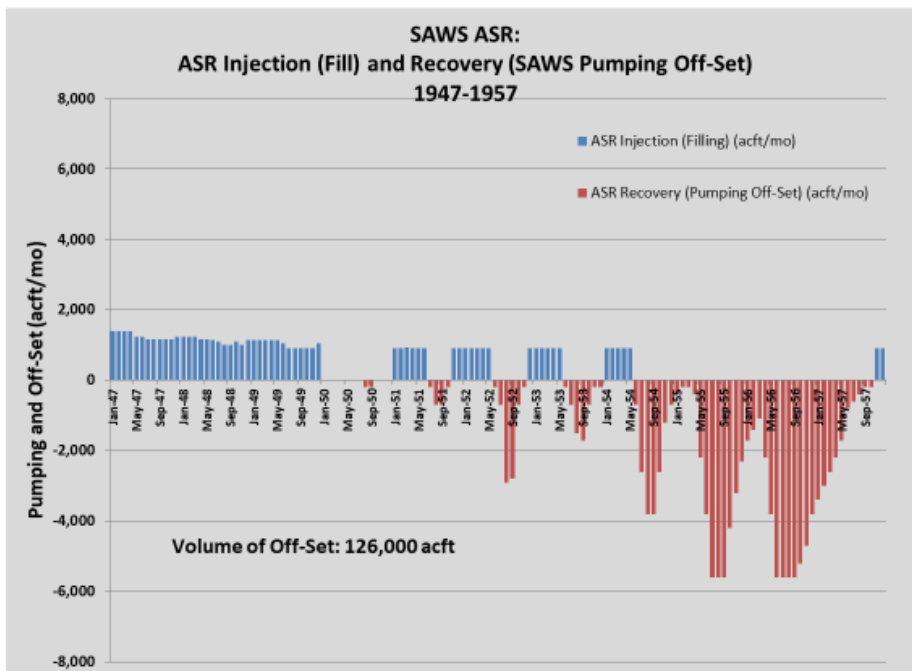


Figure 1. SAWS ASR recovery schedule during repeat of Drought of Record (taken from HDR 2011). The injection (blue bars) will not be modeled during SAMP modeling, as the ASR is full;

EAA ASR activities

The EAA forbearance portion is comprised of 50,000 acft/yr of forborne water. In 2027, 10,263.5 acft/yr will reside in long-term irrigation leases. Therefore, 50,000 ac-ft/yr included in the MODFLOW simulations is comprised of leased water (10,263.50 acft/yr) and anticipated irrigation and municipal/industrial forbearance agreements (Table 2). The geographical distribution of assumed irrigation forbearance agreements is based off the VISPO program, and the distribution of municipal/industrial leases is based on 2018 1-yr ASR leases. EAA forbearance activities are triggered in the model when the 10-year rolling recharge average is less than 500,000 acft/yr. Annual recharge estimates from the USGS are provided during the spring of the following year; forbearance activities would be initiated at the beginning of the next calendar year.

Table 2. SAMP model distribution of ASR forbearance.

Long-term leases: 10,263 acft as of 2027; actual enrollment

County	Use	acft %	Total acft
Atascosa	Irrigation	3.65%	375.00
Bexar	Irrigation	38.58%	3,959.93
Medina	Irrigation	41.88%	4,298.69
Uvalde	Irrigation	15.88%	1,629.88
		100.00%	10,263.50

Irrigation Forbearance: 29,736.50 acft; based on VISPO geographical distribution (assumed no Hays, Comal or Atascosa County enrollment)

County	Use	acft %	Total acft
Atascosa	Irrigation	0.0%	0.0
Bexar	Irrigation	6.00%	1,784.19
Hays	Irrigation	0.0%	0.0
Medina	Irrigation	28.53%	8,485.31
Uvalde	Irrigation	65.47%	19,467.00
		100.00%	29,736.50

Municipal/Industrial Forbearance: 10,000 acft – geographical distribution based on 2018 1 yr ASR leases

County	Use	acft %	Total acft
Bexar	Muni/Industrial	51.59%	5175.69
Comal	Muni/Industrial	28.00%	2784.89
Hays	Muni/Industrial	0.01%	1.4
Medina	Muni/Industrial	4.40%	439.57
Uvalde	Muni/Industrial	16.00%	1598.45
		100.00%	10,000.00

RWCP

The RWCP program will be modeled using 10,000 ac-ft/yr enrollment set by the HCP (5.1.3). Currently, the program is fully enrolled. The modeled geographical distribution of enrolled water will be based on

the geographical distribution of the current program. Table 3 displays the county level distribution of enrolled water.

Table 3. SAMP model distribution of RWCP forbearance.

County	Use	acft %	Total acft
Bexar	Irrigation	99.43%	9,943.00
Uvalde	Irrigation	0.57%	57.00
		100.00%	10,000.00

STAGE V reductions

Stage V critical period requires a 44% reduction in permitted use and applies to both the San Antonio and Uvalde pools. The critical period reductions are implemented in the model based on triggers outlined in the HCP and EAA rules.

Pumping Assumptions:

The SAMP model runs will simulate total annual pumping of 592,454 ac-ft for each year of the simulation. Annual pumping from the HDR 2011 modeling effort was 593,240 ac-ft. The distribution and timing of pumped water from all model runs will be the same as HDR runs. Pumping types in the updated model include the 572,000 ac-ft/yr permitted by the EAA Act along with Federal Exempt pumping, Limited Production Wells, and Domestic and Livestock pumping. A summary and calculations for the latter three pumping types are shown below.

Total Pumping:

- HDR EARIP Modeling = 593,240 acft
573,037 (permitted) + 6,907 (federal) + 13,296 (domestic/livestock)
- SAMP Modeling = 592,454 acft
572,000 (permitted) + 6,000 (federal) + 54 (LPW) + 14,400 (domestic/livestock)

Federal Exempt Pumping

HDR Modeling: 6,907 ac-ft/yr

SAMP pumping: 6,000 ac-ft/yr

Year	JBSA ac-ft	Hays ac-ft	Uvalde ac-ft	Total Reported
2007	6,714	193	0	6,907
2008	6,714	193	0	6,907
2009	4,483	309	169	4,961
2010	4,678	236	214	5,128
2011	5,160	195	28	5,383
2012	5,046	220	60	5,326
2013	-	195	209	404
2014	5,089	228	0	5,317
2015	-	230	0	230
2016	-	236	0	236

2017	-	254	-	254
------	---	-----	---	-----

Limited Production Wells Pumping

New EAA program in 2014
SAMP pumping: 54 ac-ft/yr (average 2015-2017)

Year	Registered Wells	ac-ft
2014	57	9.859
2015	108	47.196
2016	124	61.958
2017	128	50.622

Domestic and Livestock Pumping

HDR Modeling: 13,296 ac-ft/yr
SAMP pumping: 14,400 ac-ft/yr

Year	ac-ft
2010	13,600
2011	13,600
2012	13,700
2013	13,700
2014	13,900
2015	13,900
2016	13,900
2017	14,000

References

Liu, Angang, N Troshanov, J Winterle, A Zhang, and S Eason, 2017. Updates to the MODFLOW Groundwater Model of the San Antonio Segment of the Edwards Aquifer. 78 p. Available at: <https://www.edwardsaquifer.org/science-and-maps/research-and-scientific-reports/science-document-library>

HDR, 2011. Evaluation of Water Management Programs and Alternatives for Springflow Protection of Endangered Species at Comal and San Marcos Springs. 157 p. Available at: http://www.eahcp.org/index.php/document_library_selected?c=11&c=11

Appendix A. Model Run 1 results.

